

Relativistic jets from stellar black holes

Relativistic jets from stellar black holes

Relativistische jets van zwarte gaten
met stellaire massa

Academisch Proefschrift

ter verkrijging van de graad van doctor aan de Universiteit van Amsterdam op gezag van de Rector Magnificus prof. mr. P. F. van der Heijden ten overstaan van een door het college voor promoties ingestelde commissie, in het openbaar te verdedigen in de Aula der Universiteit

op

vrijdag 23 september 2005, te 12:00 uur

door

Elena Gallo

geboren te Rome, Italië

Promotiecommissie

Promotor	prof. dr. M. van der Klis
Overige leden	dr. A. Celotti
	prof. dr. R. P. Fender
	prof. dr. E. P. J. van den Heuvel
	dr. L. J. van den Horn
	prof. dr. G. K. Miley
	prof. dr. C. J. M. Schoutens
	prof. dr. R. A. M. J. Wijers

Faculteit der Natuurwetenschappen, Wiskunde en Informatica
Universiteit van Amsterdam

*Ho sceso, dandoti il braccio, almeno un milione di scale
e ora che non ci sei é il vuoto ad ogni gradino.
Anche cosí é stato breve il nostro lungo viaggio.
Il mio dura tuttora, nè piú mi occorrono
le coincidenze, le prenotazioni,
le trappole, gli scorni di chi crede
che la realtà sia quella che si vede.
da 'Satura', Eugenio Montale*

*A mia mamma,
per i sacrifici e le rinunce taciute.*

Contents

1	BLACK HOLES IN THE GALAXY	1
1.1	Gravity and black holes	1
1.1.1	Conceiving black holes	1
1.1.2	Observing black holes	3
1.2	X-ray states of black hole X-ray binaries	6
1.3	Accretion modes	9
1.4	Relativistic jets	11
1.5	Radio emission from black hole X-ray binaries	15
1.5.1	Steady jets	16
1.5.2	Transient jets	19
1.6	Aims of this thesis	20
2	A UNIVERSAL RADIO:X-RAY CORRELATION IN LOW/HARD STATE BLACK HOLE BINARIES	25
2.1	Introduction	26
2.2	The sample	30
2.2.1	Absorption corrections	30
2.3	Radio vs. X-ray flux densities	31
2.3.1	GX 339–4 and V 404 Cygni	31
2.3.2	Broad properties of the correlation	34
2.3.3	Jet suppression in the soft state	34
2.4	Spread to the correlation	36
2.4.1	Best–fitting	36
2.4.2	Constraining the Doppler factors	38
2.5	Beyond the hard–to–soft state transition	44
2.5.1	Discrete ejections	44
2.5.2	Other BHCs: persistent soft state and ‘extreme’ sources	44
2.6	Predicting radio fluxes at low quiescent luminosities	48
2.6.1	A 0620–00: the ideal candidate	49
2.7	Discussion	50
2.7.1	Jet–dominated ‘quiescence’	51
2.8	Summary	54

3	JET-DOMINATED STATES: AN ALTERNATIVE TO ADVECTION ACROSS BLACK HOLE EVENT HORIZON IN ‘QUIESCENT’ X-RAY BINARIES	61
3.1	Introduction	61
3.2	Jet-dominated states in black hole candidates	63
3.3	Jet-dominated states in neutron stars?	65
3.3.1	Core / crustal emission?	67
3.4	Discussion	67
3.4.1	X-ray luminosity as a function of mass accretion rate	67
3.4.2	Jets at the lowest accretion rates	69
3.4.3	X-ray jets: what if ‘hard’ X-ray binaries are already jet-dominated?	69
3.5	Conclusions	69
4	THE CONNECTION BETWEEN RADIO QUIET AGN AND THE HIGH/SOFT STATE OF X-RAY BINARIES	73
4.1	Introduction	73
4.2	Data and analysis	76
4.3	Discussion	79
5	A TRANSIENT LARGE-SCALE RELATIVISTIC RADIO JET FROM GX339-4	87
5.1	Introduction	87
5.2	ATCA observations	88
5.2.1	Outburst and optically thin core radio flare	88
5.2.2	Extended radio jet	93
5.2.3	Linear polarization	95
5.3	Summary and discussion	97
6	THE RADIO SPECTRUM OF A QUIESCENT STELLAR MASS BLACK HOLE	101
6.1	Introduction	101
6.1.1	V404 Cyg (=GS 2023+338)	102
6.2	Radio emission from V404 Cyg	103
6.2.1	WSRT observations	103
6.2.2	Results: spectrum and variability	105
6.3	Discussion	105
6.3.1	A synchrotron emitting outflow in the quiescent state of V404 Cyg	106
6.4	Summary	111

7	TOWARDS A UNIFIED MODEL FOR BLACK HOLE X-RAY BINARY JETS	115
7.1	Introduction	116
7.2	The sample: four black holes undergoing jet formation	117
7.2.1	X-ray Data analysis	117
7.2.2	Individual sources	122
7.3	Jets as a function of X-ray state: new perspectives	124
7.3.1	Persistence of the steady jet in the ‘hard VHS/IS’	124
7.3.2	Changes in the jet radio spectrum <i>prior</i> to the outburst	125
7.3.3	Association of the outburst with the soft VHS/IS peak	127
7.3.4	The variation of accretion disc radius with state	128
7.3.5	The alternative state definitions of McClintock & Remillard	129
7.4	Increasing velocity as a function of X-ray luminosity at launch	130
7.5	Radio emission and jet power	132
7.5.1	The low/hard state optically thick jet	133
7.5.2	The optically thin jets	133
7.5.3	Some caveats	135
7.5.4	A single function or a step up in jet power ?	136
7.6	Internal shocks	136
7.7	Towards a unified model	139
7.7.1	Ejected disc or ejected corona?	142
7.8	Conclusions	143
8	A DARK JET DOMINATES THE POWER OUTPUT OF THE STELLAR BLACK HOLE CYGNUS X-1	151
9	EPILOGUE	161
9.1	Relativistic jets from stellar black holes: summary	161
9.2	Future prospects	164
	SAMENVATTING IN HET NEDERLANDS	169
	RIASSUNTO IN ITALIANO	173
	PUBLICATION LIST	177
	ACKNOWLEDGMENTS	181

CHAPTER 1

BLACK HOLES IN THE GALAXY

1.1 Gravity and black holes

The gravity of a celestial body is essentially a measure of how fast a rocket must be fired in order to escape the body's attraction. Nowhere gravity is stronger than near the objects we call 'black holes': regions in space where the pull of gravity is so strong, that not even light can escape. Therefore, a black hole can never be observed *directly*; rather, its presence can be inferred by the effects of its gravitational field on nearby objects, during the collapse while it was forming, or by the light emitted by rapidly swirling matter being pulled into the black hole.

1.1.1 Conceiving black holes

The concept of a body so massive that not even light could escape from it is more than 200 years old; it was first put forward by the English geologist J. Michell, in 1783. He computed that a body 500 times the radius of the Sun and of the same density would have at its surface an escape velocity equal to the speed of light. In 1915 Einstein developed the theory of general relativity; whereas Newton described gravity as a force transmitted between bodies, Einstein postulated that gravitational fields are manifestations of the curvature of 'space-time' itself. Masses do not 'exert' gravitational pull; rather, their presence distorts space and time around them. A few months later K. Schwarzschild gave the solution for the gravitational field of a point mass, showing that something we now call a black hole could theoretically exist. The Schwarzschild radius is now known to be the characteristic horizon radius (see below) of a non-rotating black hole. In the 1920s, Chandrasekhar argued that special relativity demonstrated that a non-radiating body above a certain mass, now known as the Chandrasekhar limit, would collapse since there would be nothing that could stop the collapse. Black holes could in principle be formed in nature. Such objects for a while were called frozen stars since the collapse would be observed to rapidly slow down and become heavily red-shifted near the Schwarzschild radius. However,

these hypothetical objects were not the topic of much theoretical interest until the 1960s, thanks to the discovery of quasars and of the first pulsar. Shortly thereafter, the expression ‘black hole’ was coined by theoretical physicist J. Wheeler.

General relativity not only says that black holes can exist, but does predict that they will be formed whenever a sufficient amount of mass gets packed in a given region of space, for instance through gravitational collapse. As the mass inside that region increases, its gravity becomes stronger, the space around it becomes increasingly deformed. When the escape velocity at a certain distance from the centre reaches the speed of light, an ‘event horizon’ is formed within which matter must inevitably collapse onto a single point, forming a singularity. A quantitative analysis of this idea led to the prediction that a star remaining about three times the mass of the Sun at the end of its evolution, will almost inevitably shrink to the critical size needed to undergo a gravitational collapse. Once it starts, the collapse cannot be stopped by any physical force, and a black hole is formed. Smaller black holes can only be created if the matter is subjected to sufficient pressure from some source other than self-gravitation. Such enormous pressures are thought to have existed in the very early stages of the universe, possibly creating primordial black holes with masses smaller than that of the Sun.

According to theory, the event horizon of a black hole that is not spinning is spherical; if the black hole carries angular momentum (‘Kerr black hole’), it begins to drag space-time surrounding the event horizon. Objects can exist within this spinning ‘ergosphere’ without inevitably falling into the hole. However, because space-time itself is moving in the ergosphere, it is impossible for objects to remain in a fixed position with respect to distant flat space time. Objects grazing the ergosphere could even be ejected outwards extracting energy and angular momentum from the black hole.

Supermassive black holes containing millions to billions of solar masses could also form wherever a large number of stars are packed in a relatively small region of space, or by large amounts of mass falling into a ‘seed’ black hole, or by repeated fusion of smaller black holes. The necessary conditions are believed to exist in the centres of some – probably all – galaxies. Sagittarius A* is now agreed to be the most plausible candidate for the location of a supermassive black hole at the centre of our own Galaxy, with a mass of about 3 million of solar masses.

The interested reader is referred to *e.g.* Novikov (1990), Thorne (1994), Begelman & Rees (1998) Wheeler (1990).

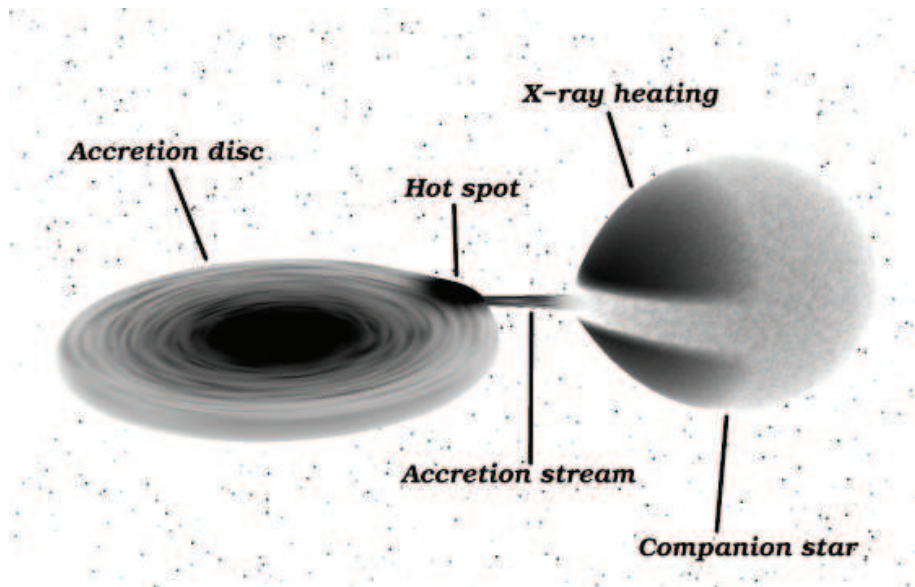


Figure 1.1: Artistic impression of a black hole X-ray binary system undergoing Roche lobe overflow. The Roche lobe is the region around a star in a binary system within which orbiting material is gravitationally bound to that star. If the star expands past its Roche lobe, then the material outside of the lobe will fall into the other star. Thus an accretion stream is created for significant mass to flow out toward the black hole for accretion. In the case of Roche-lobe overflow, the angular momentum of the accreting material will cause it to form a differentially rotating disc. Due to friction the material in this accretion disc then spirals towards the gravitational well of the black hole, heating up the inner disc to temperatures over 10^6 K (more precisely the inner disc temperature depends upon the black hole mass and the rate at which the matter accretes).

1.1.2 Observing black holes

Black holes can be inferred by observations of phenomena occurring near them. Probably the most prolific effect is that of *accretion*, i.e. the extraction of gravitational potential energy of the matter falling into the event horizon. The importance of accretion as a source of power was first recognized in the study of Galactic X-ray binary systems: a subclass of binary star systems made up of a normal star and a collapsed object, a black hole in the case of black hole X-ray binaries (BHXBs hereafter).

At some stage of their evolutionary lifetime, binary systems may start to

transfer matter under two main circumstances: i) one of the stars can increase its radius, or the binary separation shrinks, to the point where the gravitational pull of the companion can remove outer layers of its envelope; ii) at some phase one of the stars may eject much of its mass in the form of a wind, some of which will be captured gravitationally by the companion. The former case is known as Roche lobe overflow (depicted in Figure 1.1), the latter as stellar wind accretion (see Tauris & van den Heuvel, 2005, for a review on formation and evolution of stellar X-ray sources).

In the case of BHXBs, when matter starts to be transferred from the evolved star which filled its Roche lobe towards the black hole, it has rather high specific angular momentum and can not accrete directly. A continuous stream of gas tends to the orbit of lowest energy for a given angular momentum, i.e. a circular orbit. In order to fall into the gravitational potential well, such ring of gas has to loose angular momentum. Dissipative processes must be taking place (shocks, viscous dissipation, collisions etc.), which will convert some of the kinetic energy of the bulk orbital motion into internal energy, i.e. heat. Eventually, some of this energy is radiated and thus lost to the gas. As a consequence, the gas sinks deeper into the gravitational potential of the black hole, orbiting more closely. Material flowing from the companion star piles up in a dense disc orbiting the black hole: an *accretion disc* is formed (see Frank, King & Raine 2002 and references therein).

Until the early '90s, there was no clear candidate for the actual angular momentum transport mechanism in accretion discs, since e.g. normal atomic viscosity turns out to be orders of magnitude too small to drive the accretion-powered X-ray emission. Balbus & Hawley (1991; 1998) showed that the combination of a weak magnetic field and outwardly decreasing differential rotation rapidly generates magneto-hydrodynamic (MHD) turbulence via a linear instability. The result is a greatly enhanced effective viscosity. It is now widely accepted that this instability, known as the magneto-rotational instability (MRI), is responsible for the angular momentum transport in the inner regions of accretion discs.

For accretion-powered sources with a hard surface (as neutron stars) all the kinetic energy of the infalling matter is converted into radiation at the stellar surface. The maximum Newtonian value of the accretion luminosity of a body of mass M and radius R_* that accretes mass at a rate \dot{M} is given by: $L = GM\dot{M}/R_*$ (where G is the gravitational constant). For the case of accretion on to a black hole, with no hard surface, much of the accretion energy could disappear into the horizon, simply adding to its mass, rather than being radiated. This uncertainty can be parametrized by an efficiency η , such that the accretion luminos-

ity of a black hole can be expressed as $L_{\text{acc}} = \eta \dot{M} c^2$, substituting $2GM/c^2$ (the Schwarzschild radius) for R_* . In principle, accretion on to a black hole can be extremely efficient, converting up to 40 per cent of the mass energy of the infalling matter into radiation ($\eta \approx 0.42$ for a maximally rotating Kerr black hole). For comparison, $\eta = 0.007$ for nuclear burning. As noted by Frank, King & Raine (2002): ‘*For the nineteenth century physicists, gravity was the only conceivable source of energy in celestial bodies, but gravity was inadequate to power the Sun for its known lifetime. In contrast, at the beginning of the twenty-first century it is to gravity that we look at to power the most luminous objects in the Universe, for which the nuclear sources of the stars are wholly inadequate.*’.

For radiatively efficient accretion discs, the luminosity is characterized – and in general limited – by the so called Eddington luminosity: the luminosity at which the radiative momentum flux from a spherically symmetric source is balanced by the gravitational force of the accreting object: $L_{\text{Edd}} \approx 1.38 \times 10^{38}$ erg s⁻¹ per solar mass of the accretor. Correspondingly, the Eddington mass accretion rate can be defined as: $\dot{m}_{\text{Edd}} = L_{\text{Edd}}/\eta c^2$.

In order to estimate the characteristic temperature of the radiated energy, we can define a blackbody temperature T_{b} as the temperature an accretion-powered source would have if it radiated the given power as a black-body spectrum, and a thermal temperature T_{th} that the accreted material would reach if its gravitational potential energy were converted entirely into heat. In general the radiation temperature T_{rad} can be expected to vary in the range $T_{\text{b}} \lesssim T_{\text{rad}} \lesssim T_{\text{th}}$. As a result of accretion on to stellar mass black holes the upper limit gives $T_{\text{th}} \approx 5 \times 10^{11}$ K, or, in terms of energies, $kT_{\text{th}} \approx 50$ MeV (being k the Boltzmann constant). The lower limit (only weakly dependent upon L_{acc}) gives $T_{\text{b}} \approx 10^7$ K, or $kT_{\text{b}} \approx 1$ keV. Thus accreting stellar black holes are expected to be medium to hard X-ray emitters (and possibly γ -ray sources). Such compact X-ray sources were indeed discovered by the first satellite X-ray experiments, and added to by subsequent investigations.

At the time of writing, 18 black hole X-ray binaries have been identified in the Local Group (Milky Way and Magellanic Clouds), and 22 black hole candidates – for which the nature of the accretor is still uncertain – are awaiting confirmation (McClintock & Remillard 2005). These black holes are the most visible representatives of an estimated *300 million stellar mass black holes that are believed to exist in our own galaxy* (van den Heuvel 1992; Brown & Bethe 1994; Timmes et al. 1996; Agol et al. 2002). Thus the mass of this particular form of collapsed matter is about 5 per cent of the total baryonic mass of the Milky Way (Bahcall 1986; Bronfman et al. 1988).

1.2 X-ray states of black hole X-ray binaries

The spectral-energy distribution (SED) of the gravitational power released as electromagnetic radiation when matter accretes onto a black hole is far from universal. Different accretion modes are possible, and often the same initial conditions at the outer boundaries admit more than one stationary solution for the accretion flow configuration at the inner boundary, with often very different radiative properties. The main goal of accretion flow theory is to understand and distinguish all the possible different modes of accretion, and classify the different observations in terms of such modes.

The *energy* spectra of BHXBs at energies greater than 10 keV are roughly described by a power law, which may or may not have a detectable high-energy cutoff. The slope of this power-law is characterized by the photon index, Γ , where the photon number flux per unit energy (photons $\text{cm}^{-2} \text{s}^{-1} \text{keV}^{-1}$) is $F_N(E) \propto E^{-\Gamma}$, where E is the photon energy. The Fourier *power* spectra of the X-ray light curves provide an estimate of the variance as a function of Fourier frequency ν (typically in the range mHz-kHz) in terms of the power density $P_\nu(\nu)$ (see van der Klis 2005 and references therein). Broad – and hence aperiodic – structures in the power spectra are referred to as ‘noise’ while narrow features are called ‘quasi-periodic oscillations’ (QPOs).

Different X-ray states are distinguished based upon the properties of the power (strength of the noise, presence or absence of peculiar QPOs) and energy spectra (broadband luminosity, relative contribution to the X-ray luminosity of the hard power-law component with respect to a ‘soft’, quasi-thermal component which peaks around 1 keV). At luminosities close to the Eddington one, BHXBs are often in the *very high state*, where both of the two components contribute substantially to the SED. At slightly-lower luminosities, the quasi-thermal component dominates and the power-law is usually steeper ($\Gamma > 2$) and extended to the γ -ray band. This state is traditionally termed *high/soft*. At even lower luminosities the spectra are completely dominated by a hard power-law component (with $\Gamma \approx 1.7$), with the quasi-thermal component extremely weak or even absent: these are the so-called *low/hard* states. Sometimes, at luminosities intermediate between those of the soft and the hard states, an *intermediate state* is observed, with properties similar to those of the very high state. Below a few 10^{-5} Eddington, a *quiescent state* is identified, with properties similar to the low/hard state. In terms of power spectra, the low/hard, intermediate and very high state are generally characterized by the presence of strong band-limited noise (*i.e.*, that steepens towards higher frequencies) and a hard power-law component in the power spectra, whereas the high/soft state is characterized by these features

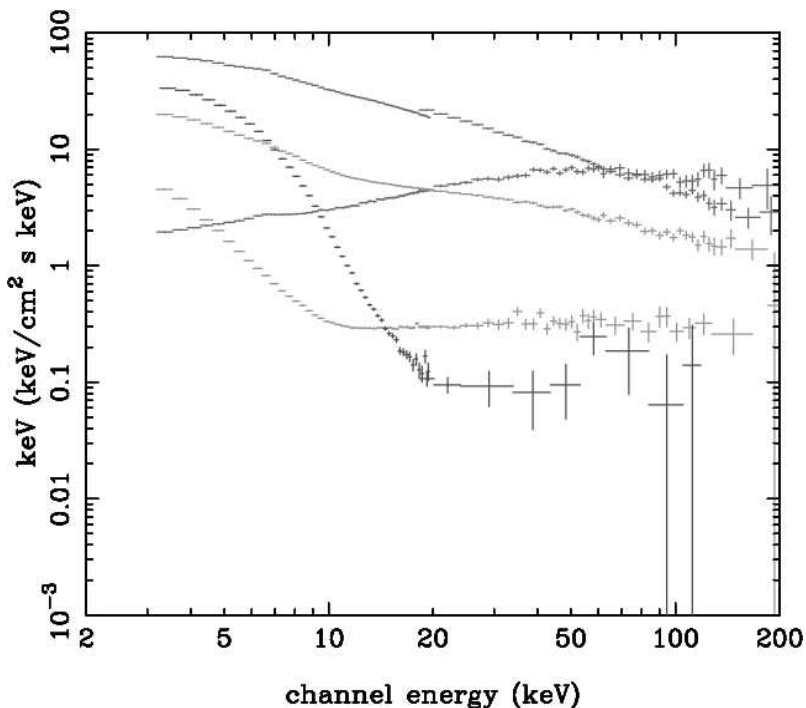


Figure 1.2: X-ray states of black hole X-ray binaries: broadly speaking, different X-ray states are distinguished based upon the integrated X-ray luminosity, the relative contribution of a ‘soft’, quasi-thermal and a ‘hard’, power-law-like spectral component, and timing properties. It is often the case that the same source, either persistent or transient, undergoes a transition between spectral states, and therefore between accretion modes. This is the case for the black hole binary XTE J1550-564 shown in this plot, where we can distinguish a low/hard state, peaking at 100 keV, and a variety of high mass accretion rate spectra, all of which peak around 1 keV: there a high/soft state (disc sharply peaking at 1 keV), an ‘ultra-soft’ high/soft state (disc showing a rounded peak at 1 keV) and two very high states (strongly Comptonized disc, giving a smooth, steep spectrum). From Done (2002).

being very weak or even absent.

It is often the case that the same source, either persistent or transient, undergoes a transition between spectral states, and therefore between accretion modes (see Figure 1.2). There are a number of reviews (with author-dependent jargon) describing in detail the properties of X-ray states of BHXBs. We refer to the reader to: Esin, McClintock & Narayan (1997); Done (2002); Homan et al. (2001); McClintock & Remillard (2005); Homan & Belloni (2005). In particular, McClintock & Remillard (2005) have recently introduced a new clas-

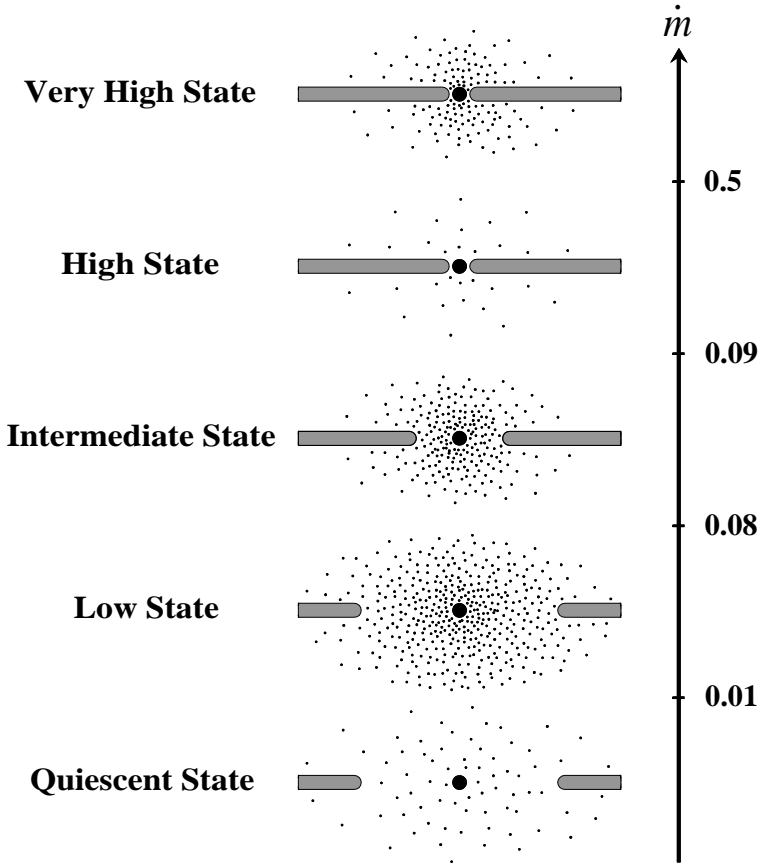


Figure 1.3: Sketch representing *possible* different accretion flow geometries over the different X-ray states (from Esin et al. 1997). It was generally believed that the main parameter driving the transition between states is disc accretion rate \dot{m} , here indicated in units of Eddington, even though it has been suggested that a second parameter may play a role (Miyamoto et al. 1995; Homan et al. 2001).

sification that is partly based on the ‘old’ scheme described above, but no longer uses luminosity as a selection criterion. They still recognize a quiescent state, hard state, soft state (renamed ‘thermal dominant’) and a very high state (renamed ‘steep power law’ state) but drop the intermediate one as a *bona fide* state.

It is generally believed that the main parameter driving the transition between states is the instantaneous accretion rate \dot{m} (see Figure 1.3) even though a second parameter may play a role (Miyamoto et al. 1995; Homan et al. 2001).

1.3 Accretion modes

The majority of spectral studies of BHXBs in the X-ray band suggest that the power-law continua of these sources are produced by thermal Comptonization (Shapiro et al. 1976; Sunyaev & Titarchuk 1980; Zdziarski 1999) in a hot, rarefied electron *corona*, which probably resides where most of the accretion energy is released, namely in the inner part of the flow. Furthermore, there is evidence that this hot, Comptonizing medium strongly interacts with the colder thermal component: such an interaction is not only required to explain the ubiquitous reflection features in the X-ray spectra (Lightman & White 1988; Matt, Perola & Piro 1991; Fabian et al. 2000), but could also provide the feedback mechanism that forces the observed values of coronal temperature and optical depth to lie in very narrow range for all the different observed sources (Haardt & Maraschi 1991). The soft quasi-thermal component is instead associated with a geometrically thin, optically thick multi-temperature accretion disc (Shakura & Sunyaev 1973; Novikov & Thorne 1973; Lynden-Bell & Pringle 1974; Pringle 1981).

It is worth mentioning that the observed hard-X-ray power laws represent a signature of a *physical process*, more than of specific accretion dynamics. This is why, if there is little doubt that the standard thin accretion disc model accounts for the basic physical properties of black holes in their soft states, the accretion mode responsible for the low-luminosity hard/quiescent states is still a matter of debate. Radiatively inefficient accretion can take place at low accretion rates if the density of the accreting gas is low enough to inhibit the energy coupling between protons and electrons.

Since their rediscovery in recent years (Narayan & Yi 1994, 1995; Narayan, Mahadevan & Quataert 1998), radiatively inefficient accretion flows (RIAFs hereafter; Ichimaru 1977; Rees et al. 1982) have been regarded as natural solutions. The key feature of RIAF solutions is that the radiative efficiency of the accreting gas is low, so that the bulk of the viscously dissipated energy is stored in the protons as thermal energy. Low-density RIAFs only exist below a critical accretion rate (which scales as the second power of the viscosity parameter). Typically, $\dot{m}_{\text{crit}} < 10^{-2} - 10^{-1} \dot{m}_{\text{Edd}}$. The optically thin gas in the flow radiates with a spectrum that is very different from the blackbody-like spectrum of a thin disc; the electrons cool via synchrotron, bremsstrahlung, and inverse Compton processes, which are responsible for producing the entire spectrum, from the radio to hard X-rays.

More importantly, the luminosity of such flows has a steep dependence on the accretion rate. The efficiency with which thermal energy is transferred from ions to electrons (to be subsequently radiated) is proportional to $\dot{m}/\dot{m}_{\text{Edd}}$, and

$L \propto (\dot{m}/\dot{m}_{\text{Edd}})^2$. In contrast, the luminosity of a Shakura-Sunyaev disc varies as $L \propto \dot{m}/\dot{m}_{\text{Edd}}$. The key difference is that whereas in a thin disc a large fraction of the released energy is radiated, in a RIAF nearly all the energy remains locked up in the gas as thermal energy. Advection dominated accretion flows (ADAFs) are popular analytical models for the dynamics of RIAFs. The structure of an ADAF is somewhat similar to the spherical Bondi accretion, despite the fact that angular momentum and viscosity are still important. ADAF solutions predict that a significant fraction of the energy stored in the protons is advected inward, and, in case of a black hole accretor, ‘disappears’ into the horizon. When tested against the best data for hard state BHXBs, though, as in the case of XTE J1118+480 (Esin et al. 2001) or Cygnus X-1 (Esin et al. 1998), ADAF models alone cannot work. A transition between an inner ADAF and an outer Shakura-Sunyaev disc is needed, as can also be inferred from studies of X-ray reflection components (Esin, McClintock & Narayan 1997; Done 2001).

There are concerns with the theoretical aspects of the aforementioned solutions, the main one being that part of the accreting gas is generically unbound and can escape freely to infinity. The reason is that the gas is likely to be supplied with sufficient angular momentum to orbit the hole and its inflow is controlled by the rate at which angular momentum is transported outward. This angular momentum transport is necessarily associated with a transport of energy. If one attempts to conserve mass, angular momentum and energy in the flow, it is found that the energy that the gas would have if it were allowed to expand adiabatically to infinity is twice the local kinetic energy.

Alternative models for the dynamics of RIAFs include e.g. convection dominated accretion flows (CDAFs, e.g. Quataert & Gruzinov 2000) and magnetically-dominated accretion flows (MDAFs; e.g. Meier 2004). In CDAFs, a significant fraction of binding energy, most of which is released in the innermost region of accretion flows, is transported outward by convection motions, whereas in MDAFs well-ordered magnetic fields play a more important role than weak, turbulent fields in the inner regions of the inflow.

Blandford & Begelman (1999) have proposed an alternative solution called adiabatic inflow outflow solution (ADIOS). Here the key notion is that the excess energy and angular momentum is lost to a wind at all radii. This mass loss makes the accretion rate on to the black hole much smaller than the rate at which mass is supplied at the outer radius. In this model the radial energy transport drives an outflow that carries away mass, angular momentum and energy, allowing the disc to remain bound to the hole. The final accretion rate into the hole may be only a tiny fraction (in extreme cases 10^{-5}) of the mass supply at large radius. This leads to a much smaller luminosity than would be observed from a standard

accretion flow.

Another possible scenario for low-luminosity black holes is that proposed by Merloni & Fabian (2002), where strong, unbound, magnetic coronae are powered by thin discs at low accretion rates. These coronal-outflow-dominated solutions are both thermally and viscously stable, as in general are all standard Shakura-Sunyaev accretion disc solutions in the gas pressure dominated regime. However, rapid and dramatic variability in the observed high-energy flux is expected, as X-rays are produced by coronal structures that are the eventual outcome of the turbulent magnetic field generation inside the disc. The geometry of these structures (open vs. closed field lines, for example) plays a very important role and may be such that, at times, parts of the corona become temporarily radiatively efficient.

Radiatively inefficient accretion can also take place at very high accretion rates, comparable to those needed to produce super-Eddington luminosities. In this case, due to the high density, the dynamical timescale of the inflow becomes shorter than the radiative timescale, causing the photons to be trapped in the accretion flow (e.g. Begelman 1979). The inability of such discs to radiate the gravitational potential energy, together with the viscous transport of energy and strong radiation pressure, is likely to drive strong outflows. The appearance of such discs is highly uncertain – it is unclear whether an X-ray emitting corona forms, and whether the atmosphere of such a disc may be capable of producing X-ray reflection spectral signatures.

It remains to be seen which, if any, of these models comes closest to reproducing the observational characteristics of accretion on to black holes at different accretion rates.

1.4 Relativistic jets

Somewhat surprisingly, part of the matter which spirals in towards the black hole can be turned around and propelled outward, in the form of narrow bipolar streams of energy and particles flowing out of the system with relativistic velocities. The origin of these relativistic *jets* remains an unsolved astrophysical problem. The effects of relativistic aberration and beaming modify their observed appearance, particularly for jets directed along our line of sight, whose emission is greatly amplified. As jets travel away from the black hole, they may decelerate and form more extended structures or lobes. Jets and lobes contain ultra-relativistic electrons and magnetic field, and thus emit synchrotron and inverse Compton radiation. They are typically visible at radio wavelengths, but in some cases the spectrum of the emission extends into the

optical, X-ray and even γ -ray bands. Although there is a general consensus that the formation and initial collimation of jets requires magnetic fields, we still do not fully understand why certain sub-classes of object produce powerful jets whilst others do not. The composition of jets is also uncertain: relativistic electrons and magnetic field must be present, but it is unclear whether the positively-charged particles are protons or positrons; the composition may also evolve as jets propagate. The parameters which characterize the jet flows such as velocity, density, pressure and magnetic-field structure have proved to be difficult to determine. We refer the reader to e.g. Hughes (1991) and Guthmann et al. (2002) for reviews of astrophysical jets.

Several mechanisms for producing bipolar outflows have been suggested but none of these seems to be able to produce outflows approaching the highly-relativistic speeds inferred for the fastest jet sources. The currently-favoured mechanism is a magneto-hydrodynamical one, somewhat similar to terrestrial accelerators of particle beams. MHD jet production was first suggested in 1976 (Blandford 1976; Lovelace 1976) and has been applied to magnetized accretion discs and rotating black holes, as outlined in the following.

The Blandford-Payne model (BP; Blandford & Payne 1982) relies on extraction of angular momentum and rotational energy from an accretion disc, by magnetic field lines that leave the disc surface (magneto-centrifugal acceleration). A centrifugally driven outflow of matter is possible if the poloidal component of the magnetic field makes an angle of less than 60° with the disc surface. At large distances from the disc, the toroidal component of the magnetic field collimates the outflow.

An outflow could also be extracted from the black hole magnetosphere through the Blandford-Znajek (BZ; Blandford & Znajek 1977) mechanism. First, the rotational energy of the black hole is extracted by large scale magnetic field lines which thread the horizon, and angular momentum is transferred along those field lines to the external plasma via magnetic tension. Such energy is then converted into Poynting flux and finally to relativistic electron/positron pairs.

Another type of (indirect) magnetic coupling is possible. This mechanism, suggested by Punsly & Coroniti (PC; 1990), has the same effect as the BZ mechanism but the field lines do not have to thread the horizon itself. Instead, they are anchored in the accreting plasma. When this plasma sinks into the ergosphere near the black hole, frame dragging causes the plasma to rotate with respect to the exterior, twisting up the field lines in a manner similar to the situation when the field is anchored in a disc.

The most important ingredient in the MHD mechanism is a magnetic field that is anchored in a rotating object and extends to large distances where the rotational speed of the field is considerably slower (see e.g. Meier, Koide & Uchida 2001; Koide et al. 2002 for reviews on MHD simulations of jet formation). Plasma trapped in the magnetic field lines is subject to the Lorentz ($\mathbf{J} \times \mathbf{B}$) force, which, under conditions of high conductivity (the MHD assumption), splits into two components: a magnetic pressure gradient ($-\nabla B^2/8\pi$) and a magnetic tension ($\mathbf{B} \cdot \nabla \mathbf{B}/4\pi$). Differential rotation between the inner and outer regions winds up the field, creating a strong toroidal component. The magnetic pressure gradient up the rotation axis accelerates plasma up and out of the system while the magnetic tension, or ‘hoop’ stress, pinches and collimates the outflow into a jet along the rotation axis (see Figure 1.4). This basic configuration of differential rotation and twisted magnetic field accelerating a collimated wind are thought to be achieved in relativistic jet sources.

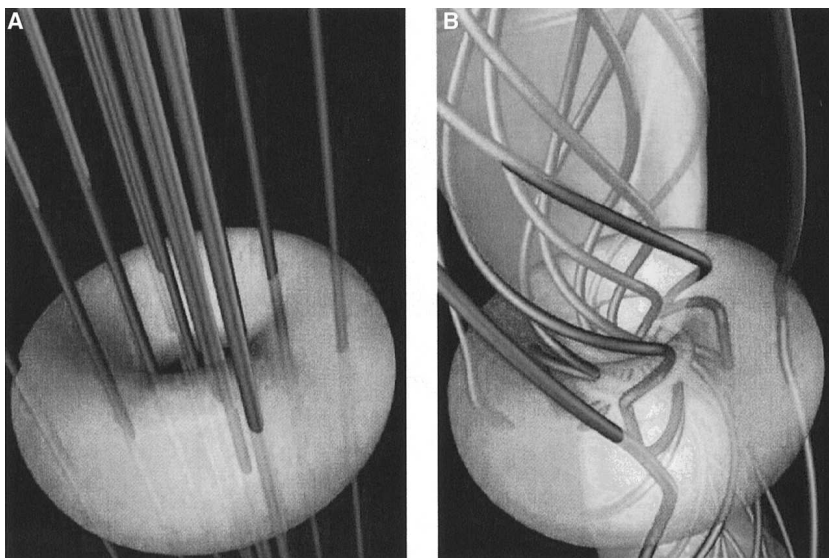


Figure 1.4: An MHD simulation of a thick magnetized disc surrounding a black hole. (A) Initial state showing the disc in rotational equilibrium with an axial magnetic field. (B) As the simulation begins, the differentially rotating torus drags the field lines in the azimuthal direction, creating a braking force that allows the material to accrete inward and gain additional rotational energy. The effect of this process is to produce a torque on the external magnetic field, generating a spinning plasma jet that carries away matter, angular momentum, and energy from the system. From Meier et al. (2001).

Alternatively, outflows can be radiatively driven. For instance, the electron/positron pairs in the corona could be accelerated by the annihilation radiation, in the so called ‘Compton rocket’ scenario (O’ Dell 1981). Radiatively driven disc winds, made of electrons and protons, have been proposed with a radiative pressure due to line emission or dust (Proga, Stone & Kallman 2000). The terminal velocities of such winds do not exceed $v \approx 0.5c$ though (Icke, 1977), thus such mechanisms are unable to explain the highest velocities, but may still be operating in mildly relativistic jet sources.

The other alternative to magnetic acceleration is thermal driving, as it is the case in the solar wind. In this case, the presence of a hot corona above the disc and/or the magnetosphere is essential for the acceleration, which is proportional to the sound speed, *i.e.* to the square root of the coronal temperature. A corona with a temperature of 10^9 K for both the ions and the electrons could result in terminal speed of 10000 km s^{-1} ; however, if 10^9 K is the electron temperature, while the protons are at 10^{12} K, a wind results with a terminal speed close to the speed of light. Thus thermal acceleration is likely to be as efficient as magnetic processes (and in fact it has been suggested that both may be at work in disc winds) for electron/protons plasmas, while the electron/positron pairs would be more likely magnetically driven from a black hole magnetosphere.

It is important to stress that there are reasons to believe that more than one jet launching mechanism may be at work in accreting black holes, and that there are definite candidates in the different cases. The following identifications are suggested by Meier (2003a; 2003b): BP-type outflows may be responsible for the lower velocity ($\sim 0.1c$) outflows, while the PC/BP mechanism inside the ergosphere may be responsible for most jets we see in active nuclei and stellar black holes. Lorentz factors $\Gamma \approx 3$ have been achieved in simulations of this process (Koide et al. 2000; Meier et al. 2001). Finally, very high Lorentz factor ($\Gamma \gtrsim 50$, inferred e.g. for the central engine of γ -ray bursts) might be identified with the BZ mechanism that couples to the black hole horizon itself.

Finally, the extreme possibility has been suggested that all types of ultra-relativistic outflows are pure electromagnetic phenomena, rather than gas dynamical (see Blandford 2002 and references therein). Electromagnetic outflows are naturally anisotropic and self-collimating; the observed jet-like emission would trace out regions of high current densities where global instabilities drive a turbulence spectrum that is responsible for the particle acceleration and the observed synchrotron and/or inverse Compton emission.

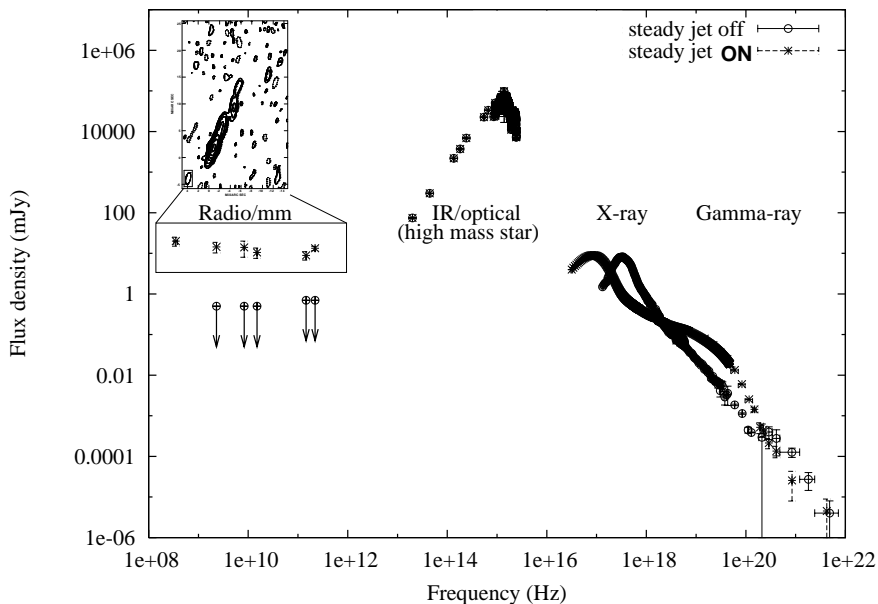


Figure 1.5: Spectral energy distribution of the prototypical 10 solar mass black hole in the high mass X-ray binary system Cygnus X-1. In the hard X-ray state the system is radio active, powering a steady jet which is resolved on VLBA scales (Stirling et al. 2001). When the system moves to higher accretion rates/X-ray luminosities, the thermal emission from the disc dominates the power output while the radio emission is quenched by a factor up to 50 with respect to the hard state. Adapted from Tigelaar et al. (2004).

1.5 Radio emission from black hole X-ray binaries

Historically, the key observational aspect of X-ray binary jets lies in their synchrotron radio emission (see Hjellming & Han 1995; Mirabel & Rodríguez 1999; Fender 2005 for reviews). The *synchrotron* nature of the radio emission from X-ray binaries in general is inferred by the high brightness temperatures, high degree of polarization and non-thermal spectra. The *outflow* nature of this relativistic (as it emits synchrotron radiation) plasma is inferred by brightness temperature arguments, leading to minimum linear sizes for the emitting region that often exceed the typical orbital separations, making it unconfined by any known

component of the binary.

Different jet properties are associated with different X-ray spectral states of BHXBs. This is illustrated schematically in Figure 1.5, which shows the spectral energy distribution, from radio to γ -ray wavelengths, of the (prototypical) stellar mass black hole in Cygnus X-1 over different accretion regimes.

1.5.1 Steady jets

BHXBs in hard states display persistent radio emission with flat radio-mm spectrum. Since we are in presence of a relativistic plasma, which is inevitably subject to expansion losses, the persistence of the emission implies the presence of a continuously replenished relativistic plasma. The flat spectral indices can only be produced by inhomogeneous sources, with a range of optical depths and apparent surface brightness, and therefore are generally interpreted in terms of synchrotron emission from a partially self-absorbed, steady jet which becomes progressively more transparent at lower frequencies as the particles travel away from the launching site (Blandford & Königl 1979; Hjellming & Johnston 1988; Falcke & Biermann 1996). We shall refer to them as *steady jets*. The observed time delays between different frequencies (*e.g.* in GRS 1915+105, Pooley & Fender 1997; Mirabel et al. 1998) rule out models in which the flat/inverted radio-mm spectrum is due to optically thin synchrotron emission from a very hard energy distribution of electrons (*e.g.* Wang et al. 1997). Confirmations of the *collimated* nature of these hard state outflows come from Very Long Baseline Array (VLBA) observations of Cyg X-1 (Stirling et al. 2001; Figure 1.6) and GRS 1915+105 (Dhawan et al. 2000; Fuchs et al. 2003), showing milliarcsecond (tens of A.U.) collimated jets.

Some authors propose a jet interpretation (rather than the standard Comptonizing corona) for the X-ray power-law which dominates the spectrum of BHXBs in the hard/quiescent state (Markoff, Falcke & Fender 2001; Markoff et al. 2003). In this model, depending on the location of the frequency above which the jet synchrotron emission becomes optically thin to self-absorption and the distribution of the emitting particles, a significant fraction – if not the whole – of the hard X-ray photons would be produced in the inner regions of the steady jet, by means of optically thin synchrotron and synchrotron self-Compton emission.

No core radio emission is detected while in the soft state: the radio fluxes are ‘quenched’ by a factor up to about 50 with respect to the hard X-ray state (Fender et al. 1999; Corbel et al. 2001), probably corresponding to the physical disappearance of the steady jet. This has been taken as strong evidence in

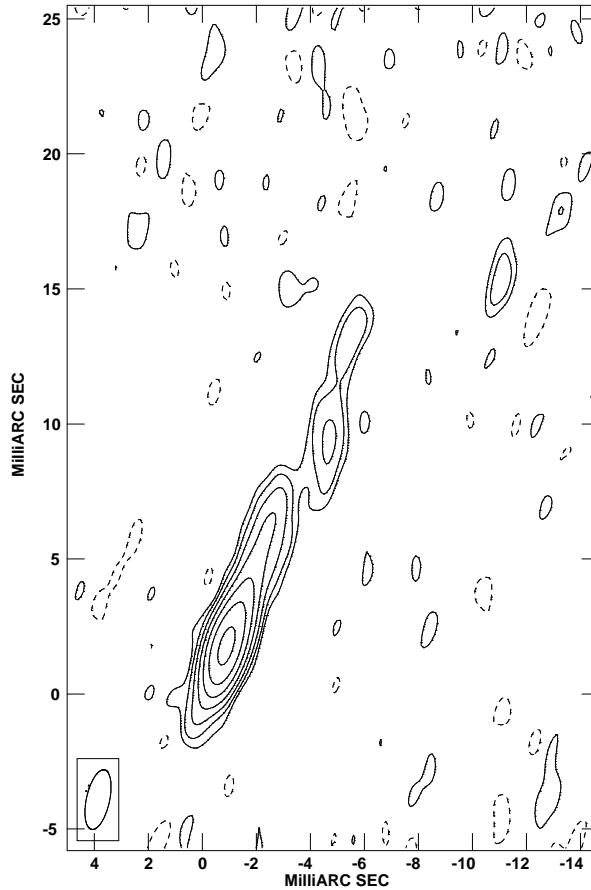


Figure 1.6: A milliarcsec scale steady jet in the hard state of Cygnus X-1. This high spatial resolution radio observations (with the Very Long Baseline Array) have confirmed the jet interpretation of the flat-spectrum radio emission in the hard state of BHXBs. From Stirling et al. (2001).

favour of MHD jet formation (Meier 2001; Meier, Koide & Uchida 2001): in this framework the jet power is proportional to the second power of the poloidal component of magnetic field, which in turn would scale as the accretion flow scale-height. Thus the steady jet would be naturally suppressed in soft state, where a geometrically thin accretion disc accounts for the observed spectrum.

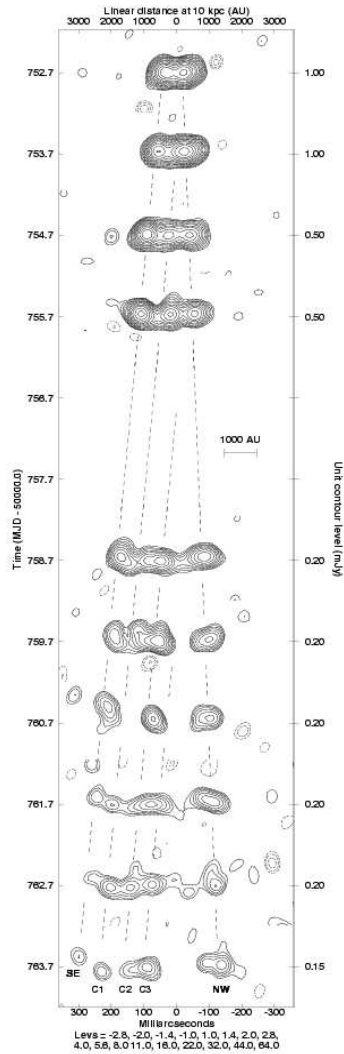


Figure 1.7: Radio observations (with the MERLIN array) of the BHXB GRS 1915+105, the first Galactic superluminal source discovered. This sequence of maps shows multiple-epoch arcsec-scale ejections of radio plasmons moving away from the binary core with highly relativistic velocities: a typical example of transient jets. From Fender et al. (1999).

1.5.2 Transient jets

Radio observations of apparent superluminal motions from GRS 1915+105, performed with the Very Large Array (VLA) back in 1994, demonstrated unequivocally that BHXBs could produce highly relativistic jets (Mirabel & Rodríguez 1994). These kind of events – after which the popular name *microquasars* was coined – have proved to be rather common among BHXBs. X-ray state transitions appear to be associated with arcsec-scale (thousands of A.U.) synchrotron-emitting plasmons moving away from the binary core with highly relativistic velocities (Mirabel & Rodríguez 1999; Fender et al. 1999; Fender 2005 and references therein). We shall refer to them as *transient jets*. Unlike milliarcsec-scale steady jets, such discrete ejection events display optically *thin* synchrotron spectra above some frequency, from which the underlying electron population can be derived. If the underlying electron distribution is a power law of the form $N(E)dE \propto E^{-p}dE$, then observations of the spectral index ($\alpha = \Delta \log S_\nu / \Delta \log \nu$, i.e. $S_\nu \propto \nu^\alpha$) in the optically thin part of the synchrotron spectrum can directly reveal the form of this electron distribution: $p = 1 - 2\alpha$. Observed optically thin spectral indices ($-0.4 \geq \alpha \geq -0.8$), indicate $1.8 \leq p \leq 2.6$. This is the same range derived for the majority of extragalactic jets powered by super-massive black holes and also for synchrotron emission observed in other astrophysical scenarios e.g. supernova remnants, and is consistent with an origin for the electron distribution in shock acceleration (e.g. Longair 1994). The monotonic flux decay observed after a few days in these transient radio ejections seems to be primarily due to adiabatic expansion losses, as the decay rate is the same at all frequencies. Significant loss of energy through the synchrotron emission process itself, or via inverse Compton scattering, would result in a more rapid decay at higher frequencies. The fact that adiabatic losses dominate indicates that the synchrotron radiation observed from such events is only a small fraction of the total energy originally input.

Association of a given synchrotron luminosity with a given volume (either by direct radio imaging or by measurement of an associated variability timescale) allows estimation of the minimum energy associated with the synchrotron-emitting plasma – for a given jet composition and filling factor – at a corresponding ‘equipartition’ magnetic field (equipartition is the condition at which the energy is nearly equally shared by the relativistic particles and the magnetic field; see Burbidge 1959).

1.6 Aims of this thesis

The largest body of observational data that pertain to relativistic jets is undoubtedly associated with active galactic nuclei. There is evidence that in some sources the jet power is a sizable fraction of the bolometric power of the accreting gas (e.g. Celotti & Fabian 1993; Di Matteo et al. 2003; Pellegrini et al. 2003) and, in general, the jet phenomenon has to be seen, on energetic grounds, as an intrinsic part of the accretion process.

Nevertheless there is still no agreement about the fundamentals of the inflow and outflow of mass around black holes; part of the problem is that there are interactions between all pairs of elements – the hole, the disc, the corona, and the jet – and most of the controversy comes about in assessing the character and strength of these interactions. Here is where stellar mass black holes may play a major role: in spite of the poorer statistics with respect to extragalactic jet sources, they are well worth studying because the duty cycles, which are thought to be set by the accretor size, and hence mass, are 10^5 up to 10^8 times shorter, and thus give far better sampled datasets for exploring time-variable accretion processes and related phenomena.

The main aim of this thesis is to provide a quantitative description of the jet-accretion coupling in black hole X-ray binary systems, and to assess the jet importance with respect to the overall accretion process in terms of energetics, and as a source of energy for the ambient interstellar medium.

In Chapter 2 evidence is presented for a quantitative scaling between the jet and the accretion power in the low/hard state of BHXBs; Chapter 3 discusses the consequences of such a correlation, extending the case to X-ray binary systems hosting neutron stars accretors, with relevant implications for the modelling of accretion flow at low luminosities. In Chapter 4 the study is extended to supermassive black holes; a possible correspondence begins to emerge between the different X-ray states and radio behaviour of BHXBs and active galactic nuclei as a function of L/L_{Edd} . Chapter 5 describes the formation and evolution of a large-scale transient radio jet from a prototypical BHXB following a major X-ray outburst. Chapter 6 discusses the nature of radio emission from BHXBs at low X-ray luminosities, in the ‘quiescent’ X-ray state. These results have contributed to the formulation of the first unified model for BHXBs jets, which is presented in Chapter 7. Chapter 8 concerns the discovery of a remarkable ring of radio emission around the ‘classical’ black hole in Cygnus X-1, and the consequences of this finding for low-luminosity black holes in general. The summary, final remarks and future prospects of this work are left to Chapter 9.

References

- Agol E. et al. , 2002, ApJ, 576, L131
Bahcall J. N., 1986, ARA&A 24, 577
Balbus S. & Hawley J. F., 1991, ApJ, 376, 214
Balbus S. & Hawley J. F., 1998, Reviews of Modern Physics, 70, 1
Begelman M. C., 1979, MNRAS 187, 237
Begelman M. C. & Rees M. J., 1998, '*Gravity's Fatal Attraction: black holes in the Universe*', Scientific American Library
Blandford R. D., 1976, MNRAS, 176, 465
Blandford R. D., 2002, in '*Relativistic flows in Astrophysics*', Springer Lecture notes in Physics, 589, 227
Blandford R. D. & Znajek R. L., 1977, MNRAS, 179, 433
Blandford R. D. & Payne D. G., 1982, MNRAS, 199, 883
Blandford R. D. & Begelman M. C., 1999, MNRAS, 303, L1
Blandford R. D. & Königl A., 1979, ApJ, 232, 34
Bronfman L. et al. , 1988, ApJ, 324, 248
Brown G. E. & Bethe H. A., 1994, ApJ, 423, 659
Burbidge G. R., 1959, ApJ, 129, 849
Celotti A. & Fabian A. C., 1993, MNRAS, 264, 228
Corbel S. et al. , 2001, ApJ, 554, 43
Dhawan V., Mirabel I. F. & Rodríguez L. F., 2000, ApJ, 543, 373
Di Matteo T. et al. , 2003, ApJ, 582, 133
Done C., 2002, Phil. Trans. Roy. Soc. Lond. A360, 1967
Done C., 2001, Advances in Space Research, 28, 255
Esin A. A., Narayan R., Cui W., Grove J. E. & Zhang S. N., 1998, ApJ, 505, 854
Esin A. A. et al. 2001, ApJ, 555, 483
Esin A. A., McClintock J. E. & Narayan R., 1997, ApJ, 489, 865
Fabian A. C. et al. 2001, PASP, 112, 1145
Falcke H. & Biermann P. L., 1996, A&A, 308, 321
Fender R. P., 2005, to appear in '*Compact Stellar X-ray Sources*', Eds. W. H. G. Lewin & M. van der Klis, Cambridge University Press (astro-ph/0303339)
Fender R. P. et al. , 1999, ApJ, 519, L165
Frank J, King A. R. & Raine D. J, 2002, '*Accretion Power in Astrophysics*', Cambridge University Press
Fuchs Y. et al. , 2003, A&A, 409, L35
Guthmann A. W. et al. , 2002, '*Relativistic Flows in Astrophysics*', Lecture Notes in Physics, Springer
Haardt F. & Maraschi L., 1991, ApJL, 380, L51

- Hawley J. F. & Balbus S. A., 2002, *ApJ*, 573, 738
- van den Heuvel E. P. J., 1992, in *'ESA, Environment Observation and Climate Modelling Through International Space Projects'*, SEE N93–23878 08
- Hjellming R. M. & Han X., 1995, in *'X-ray binaries'*, Eds. Lewin W.H.G., van Paradijs J., van der Heuvel E.P.J., Cambridge University Press
- Hjellming R. M. & Johnston K. J., 1988, *ApJ*, 328, 600
- Homan J. et al. , 2001, *ApJ*, 132, 377
- Homan J. & Belloni T., 2005, to appear in *'From X-ray Binaries to Quasars: Black Hole Accretion on All Mass Scales'*, Eds. T. J. Maccarone, R. P. Fender, L. C. Ho (astro-ph/0412597)
- Hughes P. A., 1991, *'Beams and Jets in Astrophysics'*. Cambridge Astrophysics Series, Cambridge
- Ichimaru S., 1977, *ApJ*, 241, 840
- Icke V., 1977, *Nature*, 266, 699
- Koide S., Shibata K., Kudoh T., Meier D. L., 2002, *Science*, 295, 1688
- Koide S., Meier D. L., Shibata K., Kudoh T., 2000, *ApJ*, 536, 668
- Lightman A. P. & White T. R., 1988, *ApJ*, 335, 57
- Lister M. L. & Smith P. S., 2000, *ApJ*, 541, 66
- Longair M. S., 1994, in *'High energy Astrophysics'*, Cambridge University Press, Cambridge
- Lovelace R., 1976, *Nature*, 262, 649
- Lynden-Bell D. & Pringle J. E., 1974, *MNRAS*, 168, 603
- Markoff S. Falcke H. & Fender R.P., 2001, *A&A*, 372, L25
- Markoff S. Nowak M., Corbel S., Fender R., Falcke H., 2003, *A&A*, 397, 645
- Matt G., Perola G. C. & Piro L., 1991, *A&A*, 247, 25
- McClintock J. & Remillard R.A., 2005, to appear in *'Compact Stellar X-ray Sources'*, Eds. W. Lewin & M. van der Klis, Cambridge University Press (astro-ph/0306213)
- Meier D.L., 2004, to appear in *'X-ray Binaries to Quasars: Black Hole Accretion on all Mass Scales'*, Eds. T. Maccarone & R. Fender
- Meier D. L., 2001, *ApJ*, 548, L9
- Meier D. L., 2003a, in *'New Views on Microquasars'*, Eds. P. Durouchoux, et al., Center for Space Physics: Kolkata
- Meier D. L., 2003b, *New Astron. Rev.*, 47, 667
- Meier D. L., Koide S. & Uchida Y., 2001, *Science*, 291, 84
- Merloni A. & Fabian A. C., 2002, *MNRAS*, 332, 165
- Mirabel I.F. & Rodríguez L. F., 1994, *Nature*, 371, 46
- Mirabel I. F. & Rodríguez L. F., 1999, *ARA&A*, 37, 409
- Mirabel I. F., Dhawan V., Chaty S., Rodríguez L. F., Martí J., Robinson C. R.,

- Swank J., Geballe T., 1998, A&A, 330, L9
- Miyamoto S. et al., 1995, ApJ, 442, L13
- Narayan, R. & Yi, I., 1994, ApJL, 428, L13
- Narayan, R., Mahadevan, R., & Quataert, E. 1998, in *'Theory of Black Hole Accretion Disks'*, Eds. Abramowicz, M. A., Bjornsson, G. and Pringle, J. E.
- Novikov I. D., 1990 *'Black holes and the Universe'*, Cambridge University Press
- Novikov I. D. & Thorne K. S., 1973, in *'Black Holes'*, Eds. C. De Witt and B. DeWitt, Gordon & Breach, NY
- O'Dell S. L., 1981, ApJ, 243, L147
- Pellegrini S. et al. , 2003, ApJ, 585, 677
- Pooley G. G., Fender R. P., 1997, MNRAS, 292, 925
- Pringle J. E., 1981, ARA&A, 19, 137
- Proga D., Stone J. M. & Kallman T. R., 2000, ApJ, 543, 686
- Punsly, B. & Coroniti, F., 1990, ApJ., 354, 583
- Quataert E. & Gruzinov A., 2000, ApJ, 539, 809
- Rees M. J., Phinney E. S., Begelman M. C., & Blandford R. D. 1982, Nature, 295, 17
- Shakura N. I. & Sunyaev R. A., 1973, A&A, 24, 337
- Shapiro S. L., Lightman A. P. & Eardley D. M., 1976, ApJ, 204, 187
- Spruit H. C., 1996, in *'Evolutionary Processes in Binary Stars'*, Eds. Wijers R. et al. , Kluwer, 249
- Stirling A. M., Spencer R. E., de la Force C. J., Garrett M. A., Fender R. P., Ogley R. N., 2001, MNRAS, 327, 1273
- Sunayev R. A. & Titarchuk L. G., 1980, A&A, 86, 121
- Tauris T. M. & van den Heuvel E. P. J., 2005, to appear in *'Compact Stellar X-ray sources'* Eds. W. Lewin & M. van der Klis, Cambridge University Press
- Thorne K. S., 1994, *'Black Holes and Time Warps: Einstein's Outrageous Legacy'*, New York: W. W. Norton
- Tigelaar S. P. et al. , 2004, MNRAS, 352, 1015
- Timmes F. X., Woosley S. E. & Weaver T. A., 1996, ApJ, 457, 834
- van der Klis M., 2005, to appear in *'Compact Stellar X-ray Sources'*, Eds. W. Lewin & M. van der Klis, Cambridge University Press (astro-ph/0410551)
- Wang J. et al. , 1997, ApJ, 491, 501
- Wheeler J. A., 1990, *'A Journey into Gravity and spacetime'*, Scientific American Library
- Zdziarski A. A., 1999, *'High Energy Processes in Accreting Black Holes'*, ASP Conf. Ser. 161, 16

CHAPTER 2

A UNIVERSAL RADIO:X-RAY CORRELATION IN LOW/HARD STATE BLACK HOLE BINARIES

Elena Gallo, Rob Fender & Guy Pooley

Monthly Notices of The Royal Astronomical Society 344, 60-72 (2003)

Several independent lines of evidence now point to a connection between the physical processes that govern radio (*i.e.* jet) and X-ray emission from accreting X-ray binaries. We present a comprehensive study of (quasi-)simultaneous radio:X-ray observations of stellar black hole binaries during the spectrally hard X-ray state, finding evidence for a strong correlation between these two bands over more than three orders of magnitude in X-ray luminosity. The correlation extends from the quiescent regime up to close to the soft state transition, where radio emission starts to decline, sometimes below detectable levels, probably corresponding to the physical disappearance of the jet. The X-ray transient V 404 Cygni is found to display the same functional relationship already reported for GX 339-4 between radio and X-ray flux, namely $S_{\text{radio}} \propto S_{\text{X}}^{+0.7}$. In fact the data for all low/hard state black holes is consistent with a universal relation between the radio and X-ray luminosity of the form $L_{\text{radio}} \propto L_{\text{X}}^{+0.7}$. Under the hypothesis of common physics driving the disc-jet coupling in different sources, the observed spread to the best-fit relation can be interpreted in terms of a distribution in Doppler factors and hence used to constrain the bulk Lorentz factors of both the radio and X-ray emitting regions. Monte Carlo simulations show that, assuming little or no X-ray beaming, the measured scatter in radio power is consistent with Lorentz factors $\lesssim 2$ for the outflows in the low/hard state, significantly less relativistic than the jets associated with X-ray transients. When combined radio and X-ray beaming is considered, the range of possible jet bulk velocities significantly broadens, allowing highly relativistic outflows, but implying therefore severe X-ray selection effects. If the radio luminosity scales as the total jet power raised to $x > 0.7$, then there exists an X-ray luminosity below

which most of the accretion power will be channelled into the jet, rather than in the X-rays. For $x = 1.4$, as in several optically thick jet models, the power output of ‘quiescent’ black holes may be jet-dominated below $L_X \simeq 4 \times 10^{-5} L_{\text{Edd}}$.

2.1 Introduction

There is strong observational evidence for the fact that powerful radio-emitting outflows form a key part of the accretion behaviour in some states of X-ray binary systems. Due to its high brightness temperature, ‘nonthermal’ spectrum and, in some cases, high degree of polarisation, radio emission from black hole binaries is believed to originate in synchrotron radiation from relativistic electrons ejected by the system with large bulk velocities (Hjellming & Han 1995; Mirabel & Rodríguez 1999; Fender, 2000, 2001a,b,c).

Black hole binary systems are traditionally classified by their X-ray features (see Nowak 1995; Poutanen 1998; Done 2001; Merloni 2002 for recent reviews), namely: a) the relative strength of a soft ‘black body’ component around 1 keV, b) the spectral hardness at higher energies c) X-ray luminosity and d) timing properties. Different radio properties are associated with several ‘X-ray states’, according to the following broad scheme. The *low/hard state* is dominated by a power-law spectrum, with a relatively low luminosity and an exponential cut-off above about 100 keV and little or no evidence for a soft, thermal component. It is associated with a steady, self-absorbed outflow that emits synchrotron radiation in the radio (and probably infrared) spectrum. The *quiescent/off state*, characterised by an extremely low X-ray flux, may simply be interpreted as the hard state ‘turned down’ to lower accretion rates and radiative efficiency. X-ray spectra from *high/soft state* Black Hole Candidates (BHCs) are instead dominated by thermal radiation, while the core radio emission drops below detectable levels, probably corresponding to the physical suppression of the jet. In the *very high state* both the thermal and the power law components contribute substantially to the spectral energy distribution. At a lower luminosity level an *intermediate state* is also observed, with properties similar to those of the very high state. For both the very high and the intermediate state the connection with radio behaviour is not yet clearly established. Corbel et al. (2001) show that the radio emission from XTE 1550–564 in the intermediate state was suppressed by a factor > 50 with respect to the hard state, while Homan et al. (2001) claim that intermediate and very high states can actually occur at a wide range of luminosities.

Transitions between states are often associated with multiple ejections of synchrotron emitting material, possibly with high bulk Lorentz factors (Hjellming

& Han 1995; Kuulkers et al. 1999; Fender & Kuulkers 2001).

As already mentioned, BHCs in the low/hard state, like Cygnus X-1 and GX 339-4, are characterised by a flat or slightly inverted radio spectrum ($\alpha = \Delta \log S_\nu / \Delta \log \nu \simeq 0$), interpreted as arising from a collimated, self-absorbed compact jet, in analogy to those observed in active galactic nuclei (Blandford & Königl 1979). With the direct imaging of a resolved compact radio jet from the core of Cygnus X-1 (Stirling et al. 2001), this association has been confirmed. Radio emission from X-ray binaries, especially the BHCs, is increasingly interpreted as the radiative signature of jet-like outflows.

It has been generally accepted that the soft thermal component of BH spectra originates in an optically thick, geometrically thin accretion disc (Shakura & Sunyaev 1973), whereas the power law component is produced by Comptonization of ‘seed’ photons in a hot, rarefied ‘corona’ of (quasi-) thermal electrons (Shapiro, Lightman & Eardley 1976; Sunyaev & Titarchuk 1980; Haardt & Maraschi 1991; Poutanen & Svensson 1996). Although this picture can successfully reproduce the X-ray behaviour, it can not yet address the clear correlation between radio and X-ray emission established for the persistent BHCs GX 339-4 and Cygnus X-1 while in the hard state (Hannikainen et al. 1998; Brocksopp et al. 1999; Corbel et al. 2000; Corbel et al. 2003). Moreover, some hard state sources, like XTE J1118+480 and GX 339-4, show evidence for a turnover in the infrared-optical band, where the flat-to-inverted radio spectrum seems to connect to an optically thin component extending up to the X-rays (Corbel & Fender 2002; Markoff et al. 2003a,b and references therein), suggesting again that the jet plays a role at higher frequencies.

Hence, all the evidence points to the corona in these systems being physically related to the presence of a jet: by far the simplest interpretation therefore is that the Comptonizing region is just the base of the relativistic outflow (Fender et al. 1999b; Merloni & Fabian 2002; Markoff et al. 2003a). However, joining these two previously independent scenarios is somewhat problematic because they often require different electron distributions and geometries.

Due to the fast timescales in X-ray binary systems, only simultaneous radio and X-ray observations provide the necessary tools to probe this conjecture. The following results extend and complete those presented in Gallo, Fender & Pooley (2002).

Table 2.1: System parameters for the ten hard state BHCs under consideration. Distance and N_{H} references are given in parentheses next to each value. Inclination and BH mass estimates, unless differently specified, are all taken from Orosz (2002). The last column refers to the literatures' sources from which we have obtained (quasi-) simultaneous radio and X-ray fluxes; no reference appears in case of our own observations (Cygnus X-1).

Source	Dist. (kpc)	Incl. (degree)	BH mass (M_{\odot})	N_{H} (ref) (10^{21}cm^{-2})	Data
Cygnus X-1	2.1 (1)	35±5	6.85–13.25	6.2 (16)	–
V 404 Cygni	3.5 (2)	56±4	10.06–13.38	5.0 (17)	21,22
GRS 1758–258	8.5 (3)	?	~8–9 (14)	14.0 (3)	23
XTE J1118+480	1.8 (4)	81±2	6.48–7.19	0.1 (18)	24,25
GRO J0422+32	2.4 (5)	44±2	3.66–4.97	2.0 (5)	24
GX 339–4	4.0 (6)	15–60 (13)	5.8±0.5 (15)	6.0 (6)	26
1E 1740.7–2942	8.5 (7)	?	?	118 (19)	27
XTE J1550–564	4.0 (8,9*)	72±5	8.36–10.76	8.5 (20)	20,28
GS 1354–64	10.0 (10)	?	?	32.0 (9)	29
4U 1543–47	9.0 (11)	20.7±1.5	8.45–10.39	3.5 (11)	30

References : **1:** Massey et al. 1995; **2:** Zycki, Done & Smith 1999; **3:** Main et al. 1999; **4:** McClintock et al. 2001; **5:** Shrader et al. 1997; **6:** Zdziarski et al. 1998; **7:** Sunyaev et al. 1991; **8:** Kong et al. 2002; **9:** Tomsick et al. 2001; **10:** Kitamoto et al. 1990; **11:** Orosz et al. 1998; **12:** Orosz 2002; **13:** Cowley et al. 2002; **14:** Keck et al. 2001; **15:** Hynes et al. 2003; **16:** Schulz et al. 2002; **17:** Wagner et al. 1994; **18:** Dubus et al. 2001; **19:** Gallo & Fender 2002; **20:** Tomsick et al. 2001; **21:** Han & Hjellming 1992; **22:** Hjellming et al. 2000; **23:** Lin et al. 2000; **24:** Brocksopp et al. 2003; **25:** Markoff, Falcke & Fender 2001; **26:** Corbel et al. 2000; **27:** Heindl, Prince & Grunsfeld 1994; **28:** Corbel et al. 2001; **29:** Brocksopp et al. 2001; **30:** Brocksopp, private communication.

*For XTE J1550–564 a distance of 4 kpc is assumed by both Kong et al. (2002) and Tomsick et al. (2001), as average value between 2.5 and 6 kpc, given by Sánchez-Fernández et al. (1999) and Sobczak et al. (1999) respectively.

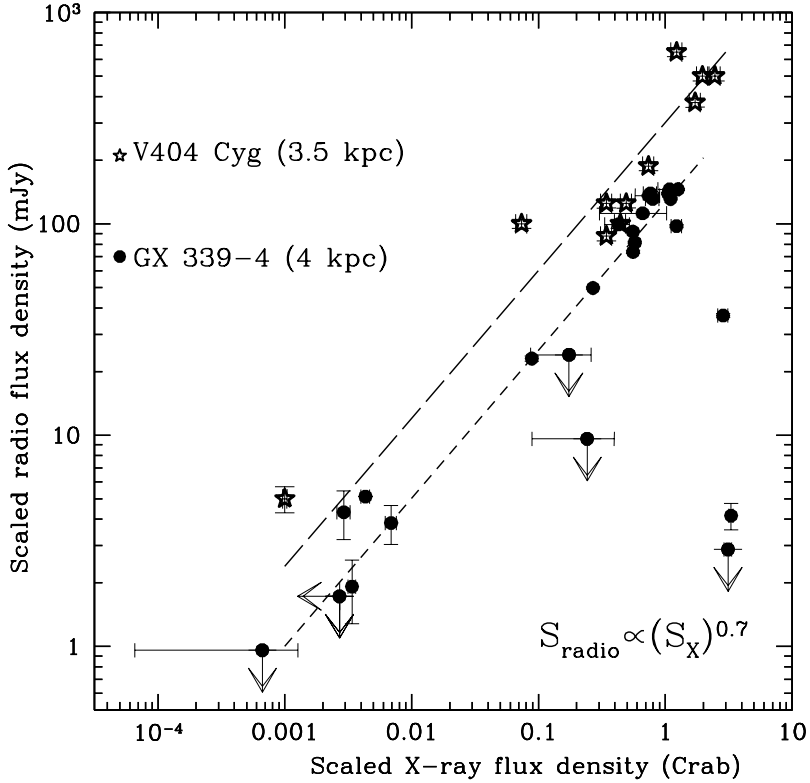


Figure 2.1: Radio against X-ray flux density, scaled to a distance of 1 kpc and absorption corrected, for V 404 Cygni and GX 339-4. Lines denote the fits to the datasets: short and long dashed for GX 339-4 and V 404 Cygni respectively. It is found that the data of V 404 Cygni are well fitted by the same functional relationship reported by Corbel et al. (2003) for the BHC GX 339-4, that is $S_{\text{radio}} \propto (S_X)^{0.7}$.

2.2 The sample

Our aim was to compile (quasi-)simultaneous radio and X-ray observations of BHCs during the low/hard state. To this purpose, we have collected all the available (to our knowledge) data from the literature and made use of our own simultaneous observations as well. These were taken with the Ryle telescope at 15 GHz (see Pooley & Fender 1997 for more details) and combined with one-day averages from RXTE ASM (this refers to Cygnus X-1, Cygnus X-3 and GRS 1915+105). Table 2.1 lists the information for the ten low/hard state BHCs for which we have at our disposal (quasi-)simultaneous radio and X-ray coverage (see Section 2.5, Table 2.3 for ‘non-canonical’ hard state sources, such as Cygnus X-3 and GRS 1915+105): distance, mass, orbital inclination, measured hydrogen column densities (see Section 2.2.1) and literature references.

Both the X-ray and the radio intensity values come from several different instruments and telescopes. Radio flux densities have been measured in different frequency bands, ranging from 4.9 up to 15 GHz; nevertheless we generically refer to ‘radio flux densities’ based on the evidence that, while in the low/hard state, black hole radio spectra are characterised by almost flat spectra ($\alpha \sim 0$) spectral index (Fender 2001a).

X-ray fluxes, taken either from spectral fits or from light curves, have been converted into Crab units in order to be easily compared with radio flux density units (1 Crab $\simeq 1060 \mu\text{Jy}$; energy range 2–11 keV). For this purpose, X-ray fluxes/luminosities in a given range have been first converted into corresponding values between 2–11 keV, and then expressed as flux density. For those sources whose X-ray flux has been derived from count rates, the conversion into Crab has been performed according to the factors provided by Brocksopp, Bandyopadhyay & Fender (2003).

2.2.1 Absorption corrections

Whenever X-ray flux density has been evaluated from count rates or absorbed fluxes, we wanted to compensate for absorption by calculating the ratio between the predicted flux from a hard state BH with a measured N_{H} value, and the predicted flux corresponding to no absorption, as follows. We have first simulated with XSPEC typical spectra of hard state BHCs as observed by *Chandra* ACIS for ten different values of hydrogen column density ranging from zero up to $12.5 \times 10^{22} \text{ cm}^{-2}$. A ‘typical’ spectrally hard BH’s spectrum is well fitted by an absorbed power law with photon index 1.5. By keeping fixed the flux corresponding to no absorption, the points turn out to be well fitted by a simple

exponential relation, which allows to express the ratio $F_{\text{abs}}/F_{\text{unabs}}$ as follows:

$$\frac{F_{\text{abs,LS}}}{F_{\text{unabs}}} = \exp \left[\frac{-(N_{\text{H}}/10^{22}\text{cm}^{-2})}{18.38} \right] \quad (2.1)$$

The procedure described has been applied to X-ray fluxes below the transition luminosity between hard and soft state. Above that value, the spectrum is not reproduced by a simple power law. In this regime, the X-ray spectrum is usually well fitted by an absorbed power law with photon index $\Gamma \simeq 2.4$ plus a disc black-body component, with a typical temperature of around 1 keV. Since in this case the 2–11 keV spectrum is almost entirely dominated by thermal emission, the previous simulations have been repeated for soft state BHCs by approximating the spectrum with a disc blackbody emission at 1 keV. We have obtained:

$$\frac{F_{\text{abs,HS}}}{F_{\text{unabs}}} = \exp \left[\frac{-(N_{\text{H}}/10^{22}\text{cm}^{-2})}{8.67} \right] \quad (2.2)$$

The latter correction has been applied to detections above the hard-to-soft state transition.

2.3 Radio vs. X-ray flux densities

2.3.1 GX 339–4 and V 404 Cygni

In Figure 2.1 we plot radio against X-ray flux densities (mJy vs.Crab), scaled to a distance of 1 kpc and absorption corrected, for GX 339–4 and V 404 Cygni, the two sources for which we have at our disposal the widest coverage in terms of X-ray luminosity.

GX 339–4 was discovered as a radio source by Sood & Campbell-Wilson (1994). When in the low/hard state, it is characterised by a flat or slightly inverted ($\alpha \gtrsim 0$) radio spectrum (see Corbel et al. 2000) and its synchrotron power has been shown to correlate with soft and hard X-ray fluxes (Hannikainen et al. 1998; Corbel et al. 2000). By means of simultaneous radio:X-ray observations of GX 339–4, Corbel et al. (2003) have recently found extremely interesting correlations between these two bands: in particular, $S_{8.6\text{ GHz}} \propto S_{3-9\text{ keV}}^{+0.71 \pm 0.01}$ (where S denotes the monochromatic flux, or ‘flux density’; slightly different slopes – within the hard state – have been found depending on the X-ray energy interval). When fitted in mJy vs. Crab (scaled to 1 kpc and absorption corrected), the relation displays the form:

$$S_{\text{radio}} = k_{\text{GX339-4}} \times (S_{\text{X}})^{+0.71 \pm 0.01} \quad (2.3)$$

$$k_{\text{GX339-4}} = 126 \pm 3$$

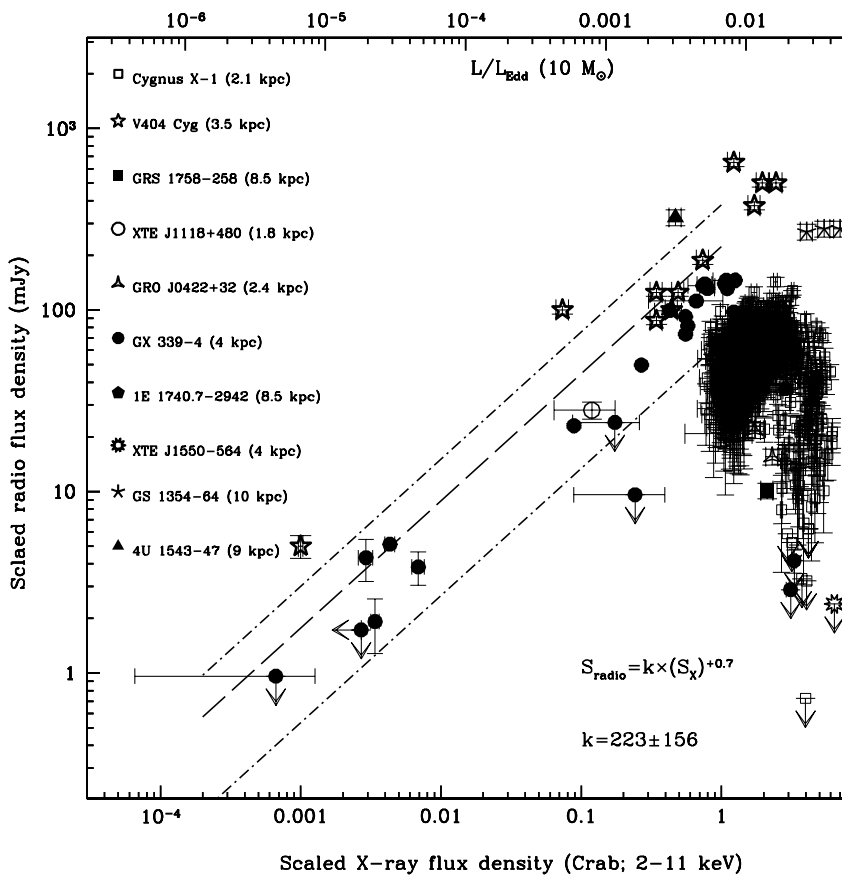


Figure 2.2: Radio flux density (mJy) is plotted against X-ray flux density (Crab) for a sample of ten hard state BHs (see Table 2.1), scaled to a distance of 1 kpc and absorption corrected (this means that the axes are proportional to *luminosities*). On the top horizontal axis we indicate luminosity, in Eddington units for a $10 M_{\odot}$ BH, corresponding to the underlying X-ray flux density. An evident correlation between these two bands appears and holds over more than three orders of magnitude in luminosity. The dashed line indicates the best-fit to the correlation, that is $S_{\text{radio}} = k \times (S_X)^{+0.7}$, with $k = 223 \pm 156$ (obtained by fixing the slope at $+0.7$, as found individually for both GX 339–4 and V 404 Cygni; see Section 2.4.1). Errors are given at $3\text{-}\sigma$ confidence level, and arrows also represent $3\text{-}\sigma$ upper limits.

The correlation appears to hold over a period of three years – 1997 and between 1999–2000 – during which the source remained almost constantly in a spectral hard state (with a transition to the high/soft state, Belloni et al. 1999, when the radio emission declined below detectable levels). Figure 2.1 shows radio against X-ray flux densities of GX 339–4 corresponding to simultaneous ATCA/RXTE observations performed between 1997 and 2000 (Corbel et al. 2000, 2003). Note that points above 1 Crab (scaled), which all correspond to RXTE-ASM detections, clearly show a sharp decreasing in the radio power (see next Section). The correlation reported by Corbel et al. (2003) actually refers to RXTE-PCA data only; it is worth mentioning that, when ASM detections below 1 Crab (*i.e.* below the radio quenching) are fitted together with PCA points, the final result is consistent, within the errors, with the fit reported by Corbel on PCA data alone (that is, a slope of 0.70 ± 0.06 is obtained in this case).

Remarkably, we have found that detections of V 404 Cygni, the source for which we have at our disposal the widest radio:X-ray coverage, are well fitted by the same functional relationship – albeit with no apparent cutoff – as GX 339–4 (see Figure 2.1).

V 404 Cygni belongs to the class of X-ray transients, sources undergoing brief episodic outbursts during which their luminosity can increase by a factor $\sim 10^6$ compared to periods of relative quiescence. All V 404 Cygni data – except for the lowest quiescent point – come from simultaneous radio (VLA; Han & Hjellming 1992) and X-ray (*Ginga*; Kitamoto et al. 1990) observations during the decay following its May 1989 outburst, during which the source, despite very high and apparently saturated luminosity, never entered a spectral soft state and always maintained a very hard X-ray spectrum (Zycki, Done & Smith 1999). According to Hjellming et al. (2000), the quiescent state of V 404 Cygni, since it ended the long decay after its 1989 outburst, has been associated with a 0.4 mJy radio source¹. Quiescent X-ray flux refers to a 1992 measurement (Wagner et al. 1994 report 0.024 ± 0.001 count s^{-1} with ROSAT-PPSPC), *i.e.* well before the onset of significant X-ray variability (see Kong et al. 2002 for details).

Denoting S_{radio} as the radio flux density in mJy and S_X as the X-ray flux density in Crab, we have obtained:

$$S_{\text{radio}} = k_{\text{V404}} \times (S_X)^{+0.70 \pm 0.20} \quad (2.4)$$

$$k_{\text{V404}} = 301 \pm 43$$

¹Starting in early 1999, VLA observations showed fluctuations ranging from 0.1 to 0.8 mJy on time scales of days; even more extreme radio fluctuations in February 2000 were accompanied by strong variability in the X-ray band as well (Hjellming et al. 2000).

The Spearman’s rank correlation coefficient is 0.91; the two sided significance of its deviation from zero equals 4.2×10^{-3} .

These results indicate that $S_{\text{radio}} \propto (S_X)^{-0.7}$ is a fundamental property of the radio:X-ray coupling in the hard state, rather than a peculiarity of GX 339–4. It is worth stressing that the fitted slopes for V 404 Cygni and GX 339–4 are identical within the errors, with the same normalisations within a factor 2.5, while detections from other sources below 1 Crab (scaled), although much narrower luminosity ranges, are all consistent with the same placing in the radio:X-ray plane, as discussed in the next Section.

2.3.2 Broad properties of the correlation

In Figure 2.2 we plot radio flux densities (mJy) against X-ray fluxes (Crab), scaled to a distance of 1 kpc and absorption corrected, for all the ten hard state BHCs listed in Table 2.1. Note that this scaling and correction means that the axes are proportional to *luminosities*.

Besides GX 339–4, Cygnus X–1 displays a positive $S_{\text{radio}} : S_X$ correlation followed by a radio turnover around 3 Crab, whereas three other sources, namely XTE J1118+480, 4U 1543–47 and GS 1354–64, lie very close to the relations inferred for GX 339–4 and V 404 Cygni. The remaining four systems (GRS 1758–258, GRO J0422+32, 1E 1740.7–2942 and XTE J1550–564) seem instead to have already undergone the radio quenching.

We can assert that these ten BH candidates display very similar behaviour in the S_{radio} vs. S_X plane. There is evidence for a positive radio:X-ray correlation over more than three orders of magnitude in terms of Eddington luminosity, as indicated in the top horizontal axis, where we show the L/L_{Edd} ratio corresponding to the underlying X-ray flux ($L_{\text{Edd}} \simeq 1.3 \times 10^{39}$ erg s⁻¹ for a 10 M_{\odot} BH). As an example, the total luminosity of Cygnus X–1 in the 0.1 to 200 keV band, while the source is in the low/hard state, is $\sim 2\%$ of the Eddington luminosity for a 10 M_{\odot} BH (di Salvo et al. 2001); that corresponds to mean flux of about 2.5 Crab (scaled to 1 kpc).

2.3.3 Jet suppression in the soft state

As already mentioned, approaching the soft state radio emission from BHCs seems to be quenched below detectable levels. Such a behaviour is well recognizable in at least two sources of our sample. As visible in Figure 2.2, both Cygnus X–1 and GX 339–4 display a clear turnover after which the radio power dramatically declines and reaches undetectable levels within a factor of two in

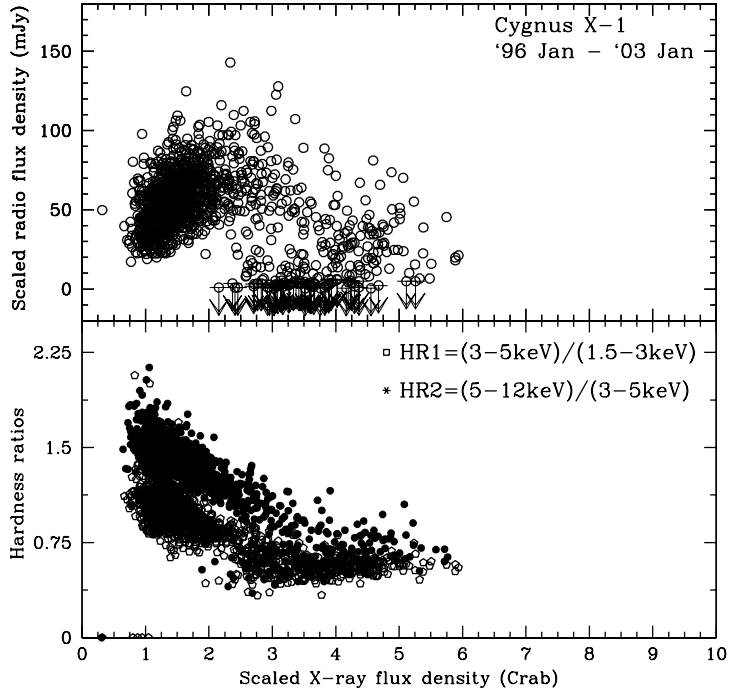


Figure 2.3: Top panel: Ryle telescope at 15 GHz and RXTE ASM daily averages for Cygnus X-1 between January 1996 and January 2003. Fluxes have been scaled to a distance of 1 kpc. Bottom panel: open squares for HR (Hardness ratio)1, defined as the ratio between the count rates at 3–5 keV and 1.5–3 keV. Filled circles for HR2, defined as the ratio between 5–12 keV and 3–5 keV. A softening of the X-ray spectrum is shown to correspond to a quenching in the radio emission.

X-ray flux (see also Fender et al. 1999b). In addition, XTE J1550–564, although suffering from poor statistics and large uncertainty in distance estimates (2.5–6 kpc), has been detected during the hard state (Corbel et al. 2001; Tomsick et al. 2001) at ‘half-quenched’ level (about 1 Crab:20 mJy scaled) while the radio emission dropped down significantly in the intermediate/very high state (about 6 Crab:<0.15 mJy scaled).

The values of the X-ray flux density (scaled) corresponding to the turnover in radio flux vary between the sources: GX 339–4, about 1 Crab; Cygnus X–1, about 3 Crab; V 404 Cygni > 1 Crab. This difference could be related to differences between the parameters that govern the powering/quenching mechanism(s) of the radio emitting jet. A discriminant parameter might be the BH mass, which is estimated to be $\sim 10 M_{\odot}$ in the case of Cygnus X–1 while it has been recently constrained around $6 M_{\odot}$ in the case of GX 339–4 (Hynes et al. 2003). If this hypothesis is correct, we would expect not to see jet quenching at X-ray luminosities below the Cygnus X–1 turnover for those systems whose BH mass has been estimated to be bigger than $10 M_{\odot}$, as, for instance, the case of V 404 Cygni, which does not appear to be quenched in radio up to about 3 Crab, and is known to possess a 10–14 M_{\odot} BH (Orosz 2002, Hjellming et al. 2000). Despite the poor statistics, this picture seems to bear out the hypothesis that the X-ray luminosity at the radio quenching might positively correlate with the BH mass, being consistent with the jet suppression occurring at a constant fraction – a few percent – of the Eddington rate.

In Figure 2.3 the quenching of the radio power in Cygnus X–1 (monitored simultaneously in radio and X-ray between January 1996 and January 2003) as a function of the X-ray flux density is shown together with X-ray hardness ratios. The 3–12 keV X-ray spectrum softens until about 5 Crab (scaled), whereas radio quenching begins around 3 Crab (scaled). While it is clear that the quenching occurs somewhere near the point of transition from low/hard to softer (intermediate or high/soft) states, pointed observations will be required to see exactly what is happening to the X-ray spectrum *at* the quenching point.

2.4 Spread to the correlation

2.4.1 Best-fitting

So far we have established two main points by looking at the distribution of low/hard state BH binaries in the radio vs. X-ray flux density plane:

- Independently of the physical interpretation, $S_{\text{radio}} \propto (S_X)^{+0.7}$ for GX

339–4 and V 404 Cygni from quiescence up to close to the hard–to–soft state transition. All other hard state BHCs lie very close to these correlations, with similar normalisations.

- At a luminosity of a few percent of the Eddington rate, close to the hard–to–soft state transition, a sharp turnover is observed in the radio:X-ray relation, that is, the radio flux density drops below detectable levels.

Bearing this in mind, our purpose is now trying to find a reliable expression for a ‘best–fit’ relationship to all hard state BHs and to estimate the spread relative to such a relation.

Assuming 0.7 as a universal slope during the low/hard state, we have determined the normalisation factor by fitting all the data – Cygnus X–1 excluded (see comments at the end of this Section) – up to 1 Crab, below which quenching does not occur for any system.

In this way we are able to provide an empirical relationship valid for all the hard state BHs, that we will call ‘best–fit’ in the following. We have obtained:

$$S_{\text{radio}} = k \times (S_X)^{+0.7}, \quad k = 223 \pm 156 \quad (2.5)$$

The best–fit and its spread are indicated in Figure 2.2 in dashed and dot–dashed lines respectively. A scatter of about one order of magnitude in radio power is particularly interesting, especially in view of comparing the observed spread to the one we expect based on beaming effects (see next Section).

The choice of excluding the whole dataset of Cygnus X–1 is related to its unusual behaviour in the radio:X-ray flux plane. In fact, a visual inspection of Figure 2.2 already suggested that the points below the radio power quenching belong to a line with a steeper slope than 0.7. In addition, despite its relatively low inclination to the line of sight (see next Section for clarity), Cygnus X–1 lies on the lower side of the correlation. It is possible that these characteristics can be explained in terms of strong wind absorption. It has been demonstrated that the wind from the donor OB star in Cygnus X–1 partially absorbs the radio emission, up to about 10% (Pooley, Fender & Brocksopp, 1999; Brocksopp, Fender & Pooley, 2002). In addition, since the jet bulk velocity during hard state is likely to be relatively low, approaching and receding jets contribute a similar amount to the total radio luminosity. However, in Cygnus X–1 only a one–sided jet has been detected (Stirling et al. 2001); this means that, possibly, a significant fraction of the receding jet is lost through wind absorption (however, since the jet structure is about 100 times bigger than the orbit, it is unlikely that the wind could absorb the entire power of the receding component). Furthermore,

because the flat–spectrum radio emission (corresponding to steady jet and generally associated with hard X-ray spectrum) is optically thick, this implies that when the jet power decreases, its size might also decrease linearly with flux. As the jet in Cygnus X–1 becomes smaller, the $S_{\text{radio}}:S_X$ relation will be subject to increasingly strong wind absorption, with the net result of steepening the correlation.

2.4.2 Constraining the Doppler factors

What kind of physical information can we deduce from the observed relation? Let us assume a very simple model, in which the same physics and jet/corona coupling hold for all hard state BHs and the observed functional relationship is intrinsic; then, one would predict the following placing in the S_{radio} vs. S_X parameter space:

1. All sources lying on a line with the same slope if neither X-ray or radio emission were significantly beamed (*i.e.* low Doppler factors).
2. Different sources lying on lines with the same slope but different normalisations if X-rays were isotropic while radio was beamed, with radio–brighter sources corresponding to higher Doppler factors.
3. As point (ii) but with higher Doppler factors sources being brighter in both radio and X-ray if both were beamed.

Despite the relatively small sample, we are able to place some constraints on these possibilities. In the first two scenarios, where X-rays are isotropically emitted while radio power is beamed, we can express the observed radio luminosity as the product of the intrinsic (rest–frame) radio power times the effective Doppler factor Δ_{radio} , defined as a function of approaching and receding Doppler factors². If $S_{\text{radio,intr}} = k \times (S_X)^{+0.7}$ for all hard state BHCs, we can write:

$$S_{\text{radio,obs}} = \Delta_{\text{radio}} \times S_{\text{radio,intr}} = \Delta_{\text{radio}} \times N \times (S_X)^{+0.7} \quad (2.6)$$

Assuming the same coupling for all sources – that means same normalisation N – the ratio $S_{\text{radio,1}}/S_{\text{radio,2}}$ between the observed radio powers from source 1 and 2, at a fixed X-ray luminosity, will correspond to the ratio between their relative effective Doppler factors.

² $\Delta_{\text{radio}} := [(\delta_{\text{app}})^2 + (\delta_{\text{rec}})^2]/2$, where: $\delta_{\text{rec/app}} = \Gamma^{-1} \times (1 \pm \beta \cos \theta)^{-1}$; $\beta = v/c$, is the bulk velocity of the radio–emitting material; $\Gamma = (1 - \beta^2)^{-0.5}$; θ is the inclination respect to the line of sight.

Returning to the case of V 404 Cygni and GX 339–4, where $S_{\text{radio,V404}}/S_{\text{radio,GX339-4}} \sim 2.5$, we are drawn to the conclusion that GX 339–4, whose inclination is poorly constrained between $15 < i < 60^\circ$ (Cowley et al. 2002), is likely to be located at a higher inclination than V 404 Cyg, well established to lie at $56 \pm 4^\circ$ (Shahbaz et al. 1994). In fact, assuming that $\Gamma_{\text{GX339-4}} \approx \Gamma_{\text{V404}}$, a ratio $S_{\text{radio,V404}}/S_{\text{radio,GX339-4}} > 1$ can be achieved only if $i_{\text{GX339-4}} > i_{\text{V404}}$.

Clearly, the previous arguments are based on the assumption that the binary system inclination to the line of sight coincides with the inclination of the jet, while recent findings (Maccarone 2002) show that this is not always the case (the misalignment of the disc and the jet has been already observed in Galactic jet sources GRO J1655–40 and SAX J1819–2525).

A recent work by Hynes et al. (2003) shows dynamical evidence for GX 339–4 being a binary system hosting a BH with mass $5.8 \pm 0.5 M_\odot$. Interestingly, based on the spectroscopic analysis by Cowley et al. (2002), see their Figure 8, this value is also consistent with a high inclination of the system to the line of sight.

Monte Carlo simulations I: radio beaming

In order to link the measured scatter in the radio:X-ray relation to the beaming effects, and possibly constraining the Doppler factors, we have performed Monte Carlo simulations according to the following scheme. We have considered the four sources (see Table 2.2) whose radio:X-ray flux densities have been utilised to obtain the best-fit relationship below 1 Crab; for each of them we have at our disposal a number n_j of simultaneous detections, with a total number of points $n = \sum_{j=1}^4 n_j = 23$. For each source j , a random inclination within the measured range has been generated and associated to an array whose dimension equals the number of detections n_j , for a total of 23 random inclinations. Then, for 15 different values of the outflow bulk velocity β , the corresponding Doppler factors $\Delta_\beta(j)$ have been calculated by running the simulation 10^4 times (*i.e.* for total of 23×10^4 values for each β). After estimating the mean Doppler factor and its relative standard deviations ($\sigma(\Delta)$) for each value of β , we have compared the simulated spread (defined as the ratio $\sigma(\Delta)/\Delta_{\text{mean}}$) to the measured spread in normalisation, that is $\sigma(k)/k = 156/223 = 0.70$.

The result is shown in Figure 2.4: in order to keep the spread in Doppler

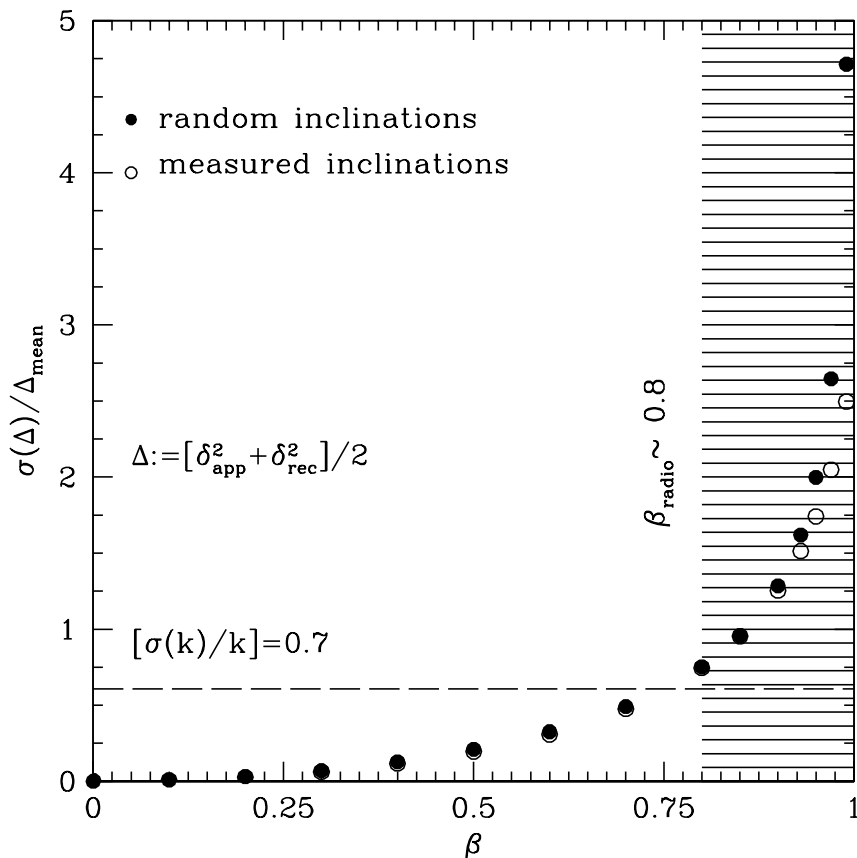


Figure 2.4: Assuming a simple model in which radio emission is beamed while X-rays are isotropic, equation 2.6 implies that the spread in radio power to the best fit can be due to the distribution in Doppler factors. The simulated spread in Δ_{radio} (defined as the ratio of standard deviation over the mean value), is plotted for 15 values of the jet bulk velocity between 0 and $0.998c$, and compared to the measured scatter in the radio:X-ray correlation. In order to maintain the spread in Doppler factors equal/smaller than observed, the outflow velocity must be smaller than 0.8 times the speed of the light, that is $\Gamma_{\text{radio}} < 1.7$. Filled circles represent Monte Carlo simulation run by allowing the inclination angles to vary between $0-90^\circ$; open circles correspond to the measured inclination angles.

Table 2.2: Observed sources for which mean Doppler factors have been simulated for 10 different values of the jet bulk velocity; measured range of inclinations and number of simultaneous radio:X-ray detections are listed.

Source	Inclination (degree)	Number of detections (n_j)
V 404 Cygni	56 ± 4^a	7
XTE J1118+480	81 ± 2^a	1*
4U 1543–47	20.7 ± 1.5^a	1
GX 339–4	$15\text{--}60^b$	14

* This single point corresponds to the average of 33 nearly simultaneous detections over a very narrow interval in X-ray luminosity.

References: **a:** Orosz 2002; **b:** Cowley et al. 2002.

factor equal/smaller ³ than observed (actually $\leq 0.77 = 0.70 + 10\%$), the bulk velocity of the radio-emitting material must be lower than $0.8c$, that is the Lorentz factor must be smaller than 1.7.

These remarks are of course valid under the basic assumptions that no beaming is affecting the X-rays. In addition we are considering a simple model in which both the bulk velocities and opening angles of the jets are constant (only under the latter assumption the probability of observing a source with a given inclination θ is uniformly distributed in $\cos \theta$).

For comparison, we ran the simulation allowing the inclination angles to vary between $0\text{--}90^\circ$ (filled circles in Figure 2.4); this is actually important in the light of what has been discussed by Maccarone (2002) about jet–disc misalignment in BH binaries, and also takes into account possible model–dependent errors in the estimation of i . The simulated spread in Doppler factors starts to significantly deviate from the previous one (calculated allowing the inclination angles for each source to vary within the measured values; open circles in Figure 2.4) only for very high bulk velocities. As expected, even if inclinations

³Smaller than measured spread are also ‘allowed’ on the ground that errors in the distance estimates are likely to influence the observed distribution, causing an additional source of scatter to the relation, which is of course not related to any boosting effect.

as 0 and 90° (*i.e.* those inclinations which translate into the highest and lowest possible values of cosine, respectively) are also taken into account, this strongly influences the mean Doppler factor only for really high values of β .

Monte Carlo simulations II: adding beamed X-rays

Following a similar approach, it is possible to constrain the Doppler factor due to the combination of beamed radio *and* X-ray radiation. As before, we assume 0.7 as an intrinsic slope which relates radio and X-ray emission. Supposing that both X-rays and radio are beamed, we will write:

$$\frac{S_{\text{radio,obs}}}{(S_{\text{X,obs}})^{0.7}} \propto \frac{\Delta_{\text{radio}}}{(\Delta_{\text{X}})^{0.7}} \quad (2.7)$$

Note that the effective Doppler factor for the X-ray radiation will be defined as $\Delta_{\text{X}} = [(\delta_{\text{rec}})^{2.5} + (\delta_{\text{app}})^{2.5}]/2$ (assuming continuous ejection and photon index 1.5 for low/hard state; see Mirabel & Rodríguez 1994, equations 8, 9).

Therefore, Monte Carlo simulations have been run by varying both radio and X-ray bulk velocities with logarithmic steps in Lorentz factors, Γ_{X} and Γ_{radio} , between 1 and 30.

The mean values of $\Delta_{\text{radio}}/(\Delta_{\text{X}})^{0.7}$ together with their standard deviations and spreads have been calculated for any combination of the two factors. The results are shown in Figure 2.5.

Filled bold circles indicate those combinations of Γ_{radio} and Γ_{X} for which the simulated spread with inclinations varying between 0–90° is smaller than/equal to 0.77. Filled-plus-open circles, instead, correspond to ‘allowed’ combinations when the inclination to the line of sight varies within the measured ranges.

In order to see why the beaming of both wavebands allows a wider spread of Γ , consider the effect on the position of a source in the flux–flux diagram: a Doppler–boosted, or deboosted, radio source moves parallel to the S_{radio} axis, while a source boosted or deboosted in both wavebands moves roughly (not exactly) parallel to the line $S_{\text{radio}} = \text{const} \times S_{\text{X}}$, and therefore roughly along the direction of the observed correlation. Consequently beaming in both wavebands disturbs the correlation less. However, if X-rays were really highly beamed, that would imply strong X-ray selection effects in detecting BH binaries.

Clearly, a possible independent estimation of the bulk velocity of the X-ray emitting material (*e.g.* Beloborodov 1999; Maccarone 2003) would naturally allow a much narrower constraint on the Doppler factor of the radio–emitting material (see discussion for further details).

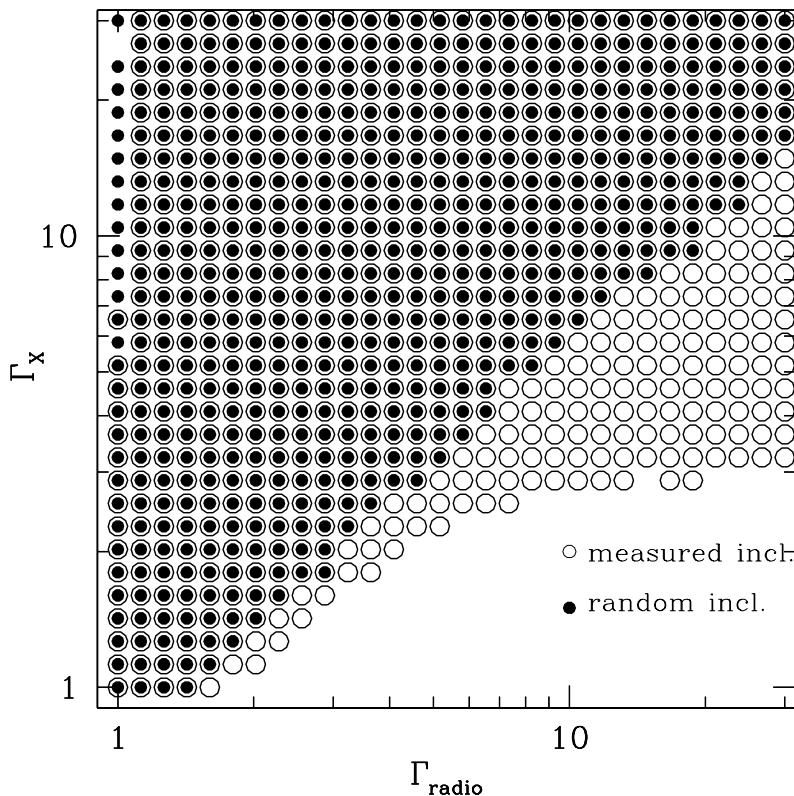


Figure 2.5: Same scheme as Figure 2.4, but assuming a model in which both radio and X-ray beaming are allowed; in this case, Monte Carlo simulations have been performed with logarithmic steps in Lorentz factors (rather than linear in β). The combination of radio plus X-ray beaming has the effect of broadening the range of allowed Γ_{radio} with respect to the case of isotropic X-ray emission. In this picture open circles indicate combinations of Γ_{radio} and Γ_X for which the simulated spread with inclinations varying within the measured ranges is smaller than/equal to 0.77. Filled circles, instead, correspond to ‘allowed’ combinations of Γ_{radio} and Γ_X when the inclination to the line of sight is randomly chosen between $0-90^\circ$. In this case the range of possible combination is smaller due to the fact that extreme inclinations, such as 0 or 90° are also taken into account.

2.5 Beyond the hard–to–soft state transition

2.5.1 Discrete ejections

So far, we only have focused on low/hard state BHs, that is, binary systems characterised by a quasi–steady state of stable accretion and whose X-ray spectrum is dominated by a hard power law.

In the following we will add to our sample radio and X-ray fluxes from transient BHCs during their episodic outbursts associated with discrete ejection events corresponding to optically thin radio emission.

All the available data, comprising of soft X-ray and radio peak fluxes with references, have been reported by Fender & Kuulkers (2001). Two points we include in this Section come from systems which have also been shown in Figure 2.2 while in the hard state, namely V 404 Cygni and GRO J0422+32. Sources under consideration, as well as their fundamental physical parameters, are listed in Table 2.3. Simultaneous radio:X-ray peak fluxes, scaled to a distance of 1 kpc are plotted in Figure 2.6 with filled squares.

Radio data are based on peak observed flux density at frequency of 5 GHz. Where measurements at 5 GHz were not available, a spectral index of $\alpha = -0.5$ was assumed in order to estimate the 5 GHz flux based on observations performed at different frequencies (see Fender & Kuulkers 2001 for details).

Most of the X-ray data are ASM detections, with the only exceptions of GRO J1655–40 and GRO J0422+32, whose outbursts have been detected by either BATSE or GRANAT. For clarity, no error bars are plotted.

2.5.2 Other BHCs: persistent soft state and ‘extreme’ sources

In between the jet quenching and the discrete ejections from transient sources, there are of course binary systems displaying a persistent soft spectrum, *i.e.* whose emission is dominated by disc blackbody photons. LMC X–1 and LMC X–3, in the Large Magellanic Clouds, are the only BHCs always observed while the soft state (actually Wilms et al. 2001; Boyd & Smale 2000 and Homan et al. 2000 reported signs that LMC X–3 entered a hard state). For both these sources, the presence of a black hole is quite well established, with a most likely mass of $9 M_{\odot}$ and $6 M_{\odot}$, respectively for LMC X–3 and LMC X–1. By means of radio and X-ray observations performed in 1997, we can place the two sources in the S_{radio} vs. S_{X} plane, in order to verify the amount of radio power from soft state BHs, which is expected to be well below the hard state correlation. LMC X–3 X-ray flux densities have been derived from Haardt et al. (2001), while LMC X–1 from Gierlinski et al. (2001). Radio upper limits for both sources are

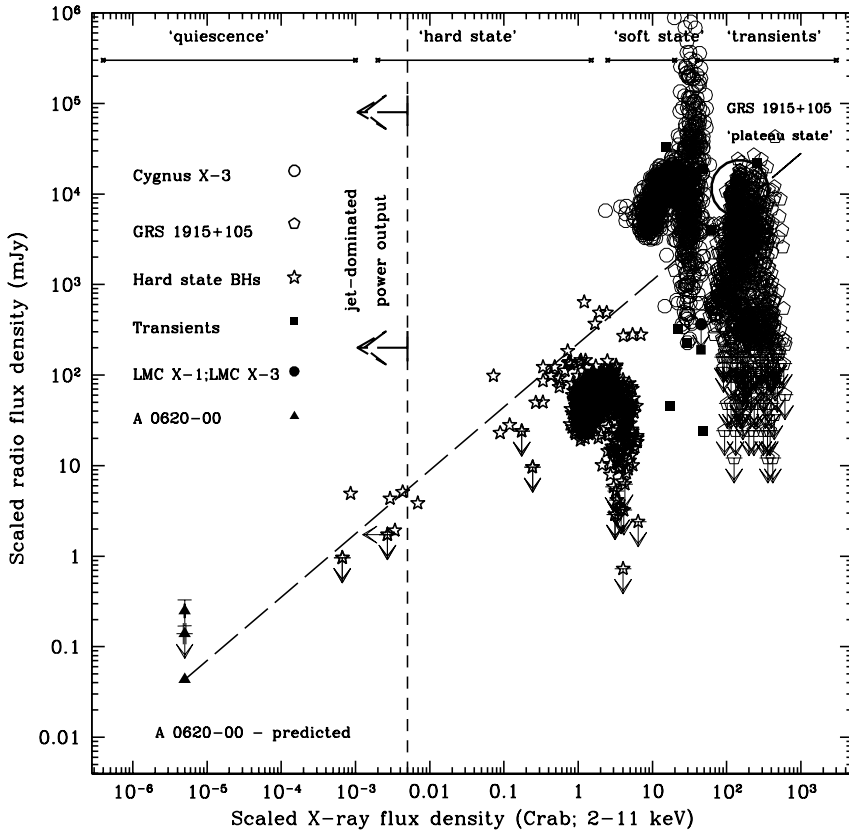


Figure 2.6: In addition to hard state BHs (open stars) we plot both single simultaneous radio:X-ray fluxes from black hole transients and detections from two canonical soft state plus somewhat ‘extreme’ sources, close to the Eddington accretion regime. Filled squares correspond to single outbursts from different sources (from Fender & Kuulkers 2001); filled circles are for persistent soft/high state sources LMC X-1 and LMC X-3, upper limits; open polygons refer to GRS 1915+105, while open circles denote Cygnus X-3 points. Based on the 0.7 correlation, and assuming that the radio luminosity scales as the total jet power raised to $x = 1.4$ (as in the Blandford & Königl, 1979, and MFF models), the radio luminosity is expected to dominate the X-rays below $L_X \approx 4 \times 10^{-5} L_{\text{Edd}}$ (about 0.005 Crab). Possible detection of the nearby SXT A 0620-00 at the predicted radio level would be capable to probe such a statement at very low X-ray level, requiring a wholly new accretion regime on to stellar BHs.

Table 2.3: Transient (plus 4 peculiar) sources whose simultaneous radio:X-ray peak fluxes associated with discrete ejections are plotted in Figure 2.6 (data from Fender & Kuulkers 2001).

Source	Distance (kpc)	N_{H} (10^{22} cm^{-2})
1A 0620–00	1 (1)	0.2 (a)
GS 2000+25	2 (2)	0.2 (b)
GS 1124–68	4.9 (3)	0.5 (c)
GRO J1655–40	3 (4)	0.7 (d)
GRS 1716–249	2.4 (5)	0.4 (e)
GRS 1739–278	8.5 (6)	2.6 (f)
4U 1630–472	10 (7)	9.4 (g)
XTE J2012+381	10 (8)	1.3 (h)
XTE J1748–288	8 (9)	7.5 (i)
XTE J1859+226	7.6 (10)	0.3 (l)
XTE J0421+560	5 (11)	0.1 (m)
GRS 1915+105	11 (12)	7.0 (n)
Cygnus X–3	9 (13)	2.7 (o)
LMC X–1	55 (14)	0.8 (14)
LMC X–3	55 (14)	0.1 (14)

References : **1:** Shahbaz et al. 1994; **2:** Callanan et al. 1996; **3:** Shahbaz et al. 1997; **4:** Kubota et al. 2001; **5:** Della Valle et al. 1994; **6:** Martí et al. 1997 ; **7:** Parmar et al. 1986; **8:** Campana et al. 2002; **9:** Kotani et al. 2000; **10:** Hynes et al. 2002; **11:** Robinson et al. 2002; **12:** Fender et al. 1999a; **13:** Predehl et al. 2000; **14:** Haardt et al. 2001.

a: Kong et al. 2002; **b:** Rutledge et al. 1999; **c:** Ebisawa et al. 1994; **d:** Ueda et al. 1998; **e:** Tanaka 1993 **f:** Greiner et al. 1996; **g:** Tomsick & Kaaret 2000; **h:** Hynes et al. 1999; **i:** Miller et al. 2001; **l:** Markwardt et al. 1999; **m:** Parmar et al. 2000; **n:** Klein–Wolt et al. 2002; **o:** Terasawa & Nakamura 1995.

taken from Fender, Southwell & Tzioumis (1998). The corresponding values, scaled to a distance of 1 kpc and corrected for absorption according to equation 2, are plotted in Figure 2.6 with filled circles (at about 150 Crab: <4540 mJy and 45 Crab: <360 mJy, LMC X-1 and LMC X-3 respectively). As expected, both points lie below the hard state relation extended to such high X-ray energies. Although we are only reporting upper limits, we can assert that fluxes from LMC X-1 and LMC X-3 do not disagree with our previous finding.

For completeness, simultaneous radio:X-ray detections of two extreme sources, namely GRS 1915+105 (open polygons) and Cygnus X-3 (open circles), have been included, corresponding to the two big ‘clouds’ at the top right region of Figure 2.6. Both systems are traditionally considered ‘exotic’ due to their timing and spectral behaviour which do not fully resemble any ‘standard’ picture generally accepted for BHCs; for instance, both these sources display either optically thin or thick radio spectra. For extensive reviews, see Bonnet-Bidaud & Chardin (1988; Cygnus X-3) and Belloni et al. (2000; GRS 1915+105). Here we note that, despite its unusually high luminosity, detections of GRS 1915+105 in the so called *plateau state* (Belloni et al. 2000) – which appears to share similar properties with the canonical low/hard state – still seem to belong to the 0.7 correlation extended up to super-Eddington regime.

Cygnus X-3 is the strongest observed persistent radio-emitting BH binary and is embedded in a dense stellar wind from the companion Wolf-Rayet star (van Kerkwijk et al. 1992; Fender, Hanson & Pooley 1999), which makes it difficult to isolate the compact object high energy spectrum. The high energy emission from the vicinity of the compact object in Cygnus X-3 is likely to be hidden by a dense stellar environment surrounding the source; as a consequence, the intrinsic X-ray luminosity might be higher than inferred, pushing the dataset closer to the 0.7 relation. Moreover, there still remains uncertainty about the nature of the accretor in this system. The neutron star hypothesis can not be ruled out with confidence.

It is interesting to note that, while the jets from GRS 1915+105 are at 60–70° (Fender et al. 1999a), those of Cygnus X-3 appear to be close to the line of sight ($\lesssim 14^\circ$, Mioduszewski et al. 2001), supporting the previous hypothesis, in which higher-than-average normalisation factors would correspond to higher Doppler factors. In addition, the behaviour of Cygnus X-3, with the apparent turnover in the radio power, is very similar to that of Cygnus X-1, except for the flaring behaviour following the jet quenching (note that points corresponding to this flaring show characteristic optically thin radio spectra; on the contrary,

Table 2.4: Five X-ray transients have been monitored in X-rays by different telescopes in different energy ranges (indicated below the table) during quiescence. Here we report the values for the maximum and the minimum luminosity, with relative references and energy ranges. For these values the corresponding predicted radio flux densities have been calculated based upon the radio:X-ray correlation we have found, that is $S_{\text{radio}} = [223 \times (S_{X,1\text{kpc}}/\text{Crab})^{0.7}]/(D/\text{kpc})^2$ mJy.

Source	L_X (10^{32} erg s^{-1})	Distance (kpc)	S_X at 1 kpc (10^{-6} Crab)	Predicted radio flux (μJy)
1A 0620–00	$0.02^1 - 0.04^2$ (a,b)	1	1–5	18–43
GRO J1655–40	$0.2^3 - 3^4$ (a,c)	3	6–82	6–34
XTE J1550–564	$< 5^5$ (d)	4	< 173	< 32
GRO J0422+32	0.08^4 (e)	2.4	~ 2	~ 4
GS 2000+25	0.02^4 (e)	2	~ 0.5	~ 2

References : **1:** 0.4–2.4 keV; **2:** 0.4–1.4 keV; **3:** 0.3–7 keV; **4:** 0.5–10 keV; **5:** 0.5–7 keV. **a:** Kong et al. 2002; **b:** Narayan et al. 1996; **c:** Asai et al. 1998; **d:** Tomsick et al. 2001; **e:** Garcia et al. 2001.

pre-flaring detections display ‘flat’ radio spectra, *i.e.* a different physical origin).

2.6 Predicting radio fluxes at low quiescent luminosities

As the same correlation appears to be maintained over many years and for different sources (like for instance Cygnus X–1, GX 339–4, V 404 Cyg), we can estimate the level of radio emission from a hard state BH by measuring its X-ray flux alone. This is particularly interesting in the case of black hole X-ray transients, whose inferred accretion rate during quiescence may be very small.

Kong et al. (2002) present *Chandra X-ray Observatory* observations of three BH transients during quiescence for which no simultaneous radio detection is available to date, namely A 0620–00, GRO J1655–40 and XTE J1550–564. In order to check for possible spectral variability, they also report results from previous X-ray observations carried out by different telescopes, such as ROSAT, ASCA and *Beppo-SAX*. According to Tomsick et al. 2001, the lowest luminosity measured for XTE J1550–564 with *Chandra* (5×10^{32} erg s^{-1} , for a distance of 4 kpc) should however be considered only as an upper limit on the quiescent luminosity

of the system. *Chandra* detections of other two transient sources, namely GRO J0422+32 and GS 2000+25, are reported by Garcia et al. 2001. In Table 2.4 we list for each of the five sources the maximum and the minimum measured X-ray luminosity in quiescence, the inferred distance and the predicted radio flux density (in μJy) based on our best-fit equation, that is $S_{\text{radio}} = 223 \times (S_X)^{+0.7}$. Given a spread of 156 over 223 in the normalisation factor, the predicted values must be considered reliable within one order of magnitude.

2.6.1 A 0620–00: the ideal candidate

The Soft X-ray Transient (SXT) A 0620–00 was discovered in outburst in 1975 (Elvis et al. 1975), while the associated radio source was at a level of 200–300 mJy (Owen et al. 1976) during the onset of the outburst. Six years later the source was detected with the VLA at level of $249 \pm 79 \mu\text{Jy}$ (Geldzahler 1983); additional VLA observations in 1986 (see McClintock et al. 1995) yielded an upper limit of 140 μJy , clearly indicating a decline in radio power (see Figure 2.6 where A 0620–00 detection/upper limit/predicted radio fluxes are marked with triangles). The 1981 detection might actually be associated to radio lobes resulting from the interaction of a relativistic–decelerating jet with the interstellar medium, as observed in the case of XTE J1550–564 about four years after the ejection of plasma from near the BH (Corbel et al. 2002).

Due to its relative proximity, A 0620–00 is the most suitable candidate to probe if our empirical radio:X-ray relation does hold down to low quiescent X-ray luminosity ($\approx 2 \times 10^{30} \text{ erg s}^{-1}$ at 1 kpc, *i.e.* about $10^{-8} L_{\text{Edd}}$; Garcia et al. 2001). In other words, if A 0620–00 was detected at the predicted radio level (a few tens of μJy , see Figure 2.6, bottom left corner), it would confirm that the mechanisms at the origin of radio and X-ray emission are correlated, if not even partly coincident, over more than six orders of magnitude in X-ray luminosity.

Moreover, if the radio:X-ray correlation were confirmed at very low X-ray luminosities (below $10^{-4} L_{\text{Edd}}$) it would strongly constrain the overall theory of accretion in quiescence. We direct the reader to the discussion for further comments.

2.7 Discussion

The presence of a coupling between radio and X-ray emission in the low/hard state of black hole binaries obviously requires a theoretical interpretation that relates somehow the powering/quenching mechanism(s) of the jet to the overall accretion pattern. Zdziarski et al. (2003) ascribe the correlation to a correspondence between the level of X-ray emission and the rate of ejection of radio-emitting blobs forming a compact jet. In this picture, there still remains the question of the condition for jet suppression. Meier (2001) interprets the steady-jet/hard-X-ray state association as strong evidence for magnetohydrodynamic (MHD) jet formation, where the most powerful jets are the product of accretion flows characterised by large scale height. The simulations show in fact that the jet is confined by the toroidal component of the magnetic field lines, coiled due to the disc differential rotation: the bigger the disc scale-height, the stronger the field. The power of the jet naturally decreases (at least 100 times weaker) in the soft/high state, associated with a standard geometrically thin disc (Shakura & Sunyaev 1973).

To date, two broad classes of geometries have been proposed for explaining X-ray emission from low/hard state BHs. The more classical picture is that of a hot, homogeneous, optically thin corona of (quasi-)thermal electrons which inverse Compton scatter ‘seed’ photons coming from the underlying accretion disc (Shapiro, Lightman & Eardley 1973 and similar later solutions). The alternative is that of a jet-synchrotron model, in which, under reasonable assumption on the input power of the jet and the location of the first acceleration zone, optically thin synchrotron emission can dominate the X-ray spectrum, traditionally thought to be a product of inverse Compton process only (see Markoff, Falcke & Fender 2001 for a detailed description of the model; hereafter MFF). This model however predicts self-synchrotron Compton up-scattering in the jet for some scenarios. Interestingly the MFF model is able to reproduce the observed slope of the radio:X-ray correlation analytically (Markoff et al. 2003a), as a function of the measured X-ray and radio-infrared spectral indices.

A revised version of the classical Comptonization model for the hard state has been proposed by Beloborodov (1999). In this case the hot coronal plasma is powered by magnetic field line reconnections (Galeev, Rosner & Vaiana 1979) and confined within several active flares with mildly relativistic bulk velocities, inferred by the relative weakness of the reflection component. Due to aberration effects in fact, the amount of X-rays as seen by the reflecting disc turns out to be reduced by a factor consistent with $\beta_X \approx 0.3$.

Maccarone (2003) draws a similar conclusion on a different ground: he has tabulated all the available measurements of X-ray luminosities at the time of the soft-to-hard state transition, for both BHC and neutron star systems. The resultant variance in state transition luminosity is also consistent with coming from material with $\beta_X \approx 0.2$; therefore $\Gamma_X \approx 1$ in both cases.

Following the approach of Section 2.4.2, this immediately implies a stringent upper limit on the beaming of radio emission as well, that is $\Gamma_{\text{radio}} \lesssim 2$ (see Figure 2.5). This is almost certainly significantly less relativistic than the jets produced during transients outbursts of sources such as GRS 1915+105 (Mirabel & Rodríguez 1994; Fender et al. 1999a) and GRO J1655–40 (Hjellming & Rupen 1995; Harmon et al. 1995; see also Fender 2003).

Therefore, if mildly relativistic beaming characterises the low/hard state, a mechanism(s) must exist which both switches the jet off – high/soft state – and produces a faster jet – discrete ejections – above $\sim 10^{-2}L_{\text{Edd}}$, where the hard-to-soft state transition occurs.

It is interesting to mention that a few percent of the Eddington rate is also close to the regime at which Ghisellini & Celotti (2001) have identified the transition line between FRI and FR II radio-galaxies, the former class being associated with slower kpc-scale jets than the latter (see Begelman 1982; Bicknell 1984; Laing 1993). This leads to a kind of correspondence between ‘extreme sources’ like GRS 1915+105, or Cyg X–3, and FR II, characterised by quite high bulk Lorentz factors, while ‘canonical’ hard state sources would be associated with FR I, with relatively low outflow bulk velocities.

2.7.1 Jet-dominated ‘quiescence’

A main task of the models remains that of reproducing the observational behaviour of accreting stellar BHs at a variety of accretion rates. An interesting prediction of this work concerns the relative power of the jet, with respect to the overall accretion power, at low quiescent luminosities.

In this regime, the BH spectral energy distribution appears very similar to that of canonical hard state sources (see Figure 2.7), although the X-ray emission in quiescence is not well reproduced by the standard accretion–corona model, requiring a much lower radiative efficiency.

Narayan et al. (1996, 1997, 2001) showed that an Advection Dominated Accretion Flow (ADAF), in which the energy released by viscous torques is ‘stored’ into the flow rather than radiated away, can adequately model the available observations at high energies. However, on the other extreme of the spectrum, in

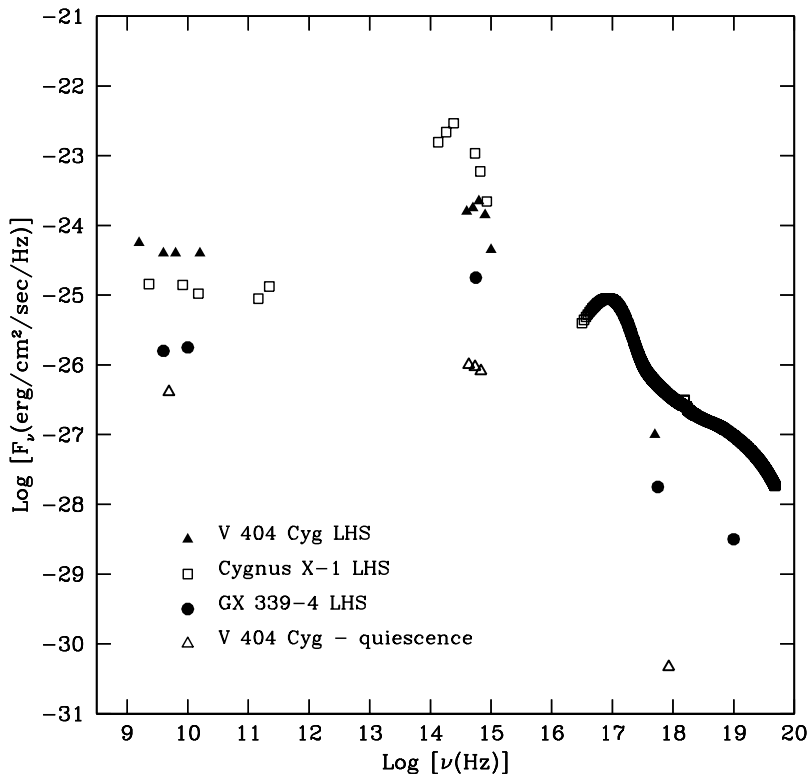


Figure 2.7: Broadband spectra of Cygnus X-1, V 404 Cygni and GX 339-4: for low/hard state (LHS) black holes, not only the behaviour in the S_{radio}/S_X plane look very similar, but even the shape of their energy spectrum, from radio wavelengths up to X-rays, suggesting either a common origin or coupling of the basic emission processes.

the radio band, the existence of a jet seriously weakens such a solution, requiring a significantly different physics to model the observed spectrum. Jet-powered radio emission is in fact several orders of magnitude brighter than expected extrapolating ADAF spectra down to radio band; moreover, the standard ADAF picture predicts highly-inverted radio spectra, instead of the observed flat ones. An alternative scenario for low-luminosity stellar black holes has been proposed by Merloni & Fabian (2002). They show that a coronal-outflow dominated accretion disc, in which the fraction of the accretion power released in the corona increases as the accretion rate decreases, would be an ideal site for

jet–launching, both MHD and thermally driven.

Based on the radio:X-ray correlation, the ratio between the observed radio and X-ray luminosities scales as:

$$\frac{L_{\text{radio}}}{L_X} \propto (L_X)^{-0.3} \quad (2.8)$$

This already implies that, as the X-ray luminosity decreases, the *radiative* jet power will become more and more important with respect to the X-rays. Moreover, because of the self-absorption effects, it has been shown that there can not be a linear relationship between the radio luminosity, L_{radio} , and the *total* jet power, L_{jet} , for any optically thick jet model which can explain the flat radio spectrum observed during the hard state. Blandford & Königl (1979), Falcke & Biermann (1996), and Markoff, Falcke & Fender (2001) obtain in fact $L_{\text{radio}} \propto (L_{\text{jet}})^{1.4}$.

If so, and in general for any relationship of the form:

$$L_{\text{radio}} \propto (L_{\text{jet}})^x \quad (2.9)$$

equation 2.8 implies the following scaling for the fractional jet power:

$$\frac{L_{\text{jet}}}{L_X} \propto (L_X)^{\left(\frac{0.7}{x}-1\right)} \quad (2.10)$$

Hence, for any $x > 0.7$, there exists an X-ray luminosity below which the jet will be the dominant output channel for the accretion power.

If $x = 1.4$, by re–scaling the numbers to XTE J1118+480 – emitting at $\sim 10^{-3} L_{\text{Edd}}$, and whose fractional jet power is at least 20% (Fender et al. 2001) – one obtains that $L_{\text{jet}} \gtrsim L_X$ for $L_X \lesssim 4 \times 10^{-5} L_{\text{Edd}}$ (*i.e.* below 0.005 Crab – scaled – see Figure 2.6). Note that observations of GX 339–4 and V 404 Cygni in quiescence already cover this regime, meaning that, if $x = 1.4$, both these sources actually *are* in a jet–dominated state.

This would be a wholly new accretion regime for X-ray binaries, requiring significant modification of existing (e.g. ADAF) models. In addition it would indicate that the overwhelming majority of ‘known’ stellar–mass black holes, which are currently in quiescence, are in fact feeding back most of their accretion energy into the interstellar medium in the form of the kinetic energy of the jets and are accreting at rather higher levels than derived based only on their X-ray luminosity.

If we do establish that accretion is taking place in quiescence, for instance through the detection of A 0620–00, and is furthermore channelling most of

its power into jet formation, then the arguments for observational evidence for black hole event horizons based upon a comparison of quiescent X-ray luminosities of black hole and neutron star binaries (e.g. Garcia et al. 2001) will need to be re-examined. In fact, assuming that $L_{\text{jet}} \propto (L_X)^{[0.7/x]}$ holds for both neutron stars and black holes, then the observed difference in ‘radio loudness’ between black hole and neutron star binaries (Fender & Kuulkers 2001) might be enough on its own to explain the discrepancy, and it may be that the event horizon plays no part. This is explored further in Fender, Gallo & Jonker (2003; see next Chapter).

2.8 Summary

In this paper we provide observational evidence for a broad empirical relation between radio and X-ray emission in Galactic black hole binaries during their spectrally hard state. The main points established throughout this work can be summarised as follows:

- In low/hard state BHCs the observed radio and X-ray fluxes are correlated over more than three orders of magnitude in accretion rate, with a spread in radio power of about one order of magnitude.
- Even at accretion rates as low as 10^{-5} Eddington a powerful jet appears to be formed; no lower limit to the relation has been found.
- V 404 Cygni is the second source to display $S_{\text{radio}} \propto (S_X)^{0.7}$, from quiescence up close to the hard-to-soft state transition.
- Assuming 0.7 as a universal slope for the low/hard state, and under the hypotheses of a) common disc-jet coupling and b) isotropic X-ray emission, the measured spread in radio flux can be interpreted in terms of a distribution in Doppler factors. Monte Carlo simulations show that the observed scatter is consistent with relatively low beaming ($\Gamma_{\text{radio}} \lesssim 2$) outflows in the low/hard state, unlike those in transient outbursts.
- When the combination of radio and X-ray beaming is taken into account, the range of possible bulk velocities in the jet significantly broadens, allowing the X-ray emitting material to be relativistic for almost any value of Γ_{radio} , but implying strong X-ray selection effects. In this case an independent estimation on Γ_X is needed to limit Γ_{radio} . Unrelated works (Beloborodov 1999; Maccarone 2003) impose stringent constraints on the

bulk velocity of the X-ray emitting material, leading to the conclusion of relatively low radio beaming ($\Gamma_{\text{radio}} \lesssim 2$) in the hard state.

- Close to the hard-to-soft state transition the jet switches off, probably in all sources. The X-ray luminosity at which the radio quenching occurs might positively correlate with the BH mass, being consistent with taking place at a constant fraction of the Eddington rate. It is worth mentioning that a similar fraction of L_{Edd} has been identified as a dividing line between FR I and FR II radio-galaxies, that is between supermassive BHs producing mildly and highly relativistic jets respectively (Ghisellini & Celotti 2001).
- Since the correlation appears to be maintained over many years and for different sources, this leads to the possibility of predicting the level of radio emission from a hard state and/or quiescent BH by measuring its X-ray flux.
- If the radio luminosity scales as the total jet power raised to x , with $x > 0.7$, this implies the existence of an X-ray luminosity below which the most of the accretion power will be channelled into the jet rather than in the X-rays. If $x = 1.4$ (e.g. Blandford & Königl 1979, Falcke & Biermann 1996; MFF), then below $L_X \approx 4 \times 10^{-5} L_{\text{Edd}}$ the jet is expected to dominate.

This work provides evidence for a physical coupling between radio and hard X-ray emitting outflows from accreting stellar BHs. A key, still unresolved issue concerns the modelling of the transition between X-ray states in a self consistent way, which could possibly account for *both* the jet suppression, when the disc dominates, *and* the transition from mildly to highly relativistic jets, as in case of transient outbursts. Including the formation of jets in the overall energetics and dynamics of the accretion process at a variety of X-ray luminosities has undoubtedly become of primary importance to address, especially based on mounting evidence for the jet power to be a significant fraction, if not the dominant output channel, of the total accretion power.

Acknowledgments

The authors wish to thank Sera Markoff, Stephane Corbel, Peter Jonker and Michiel van der Klis, for many useful suggestions and comments on the manuscript. This research has made use of data obtained through the High Energy Astrophysics Science Archive Research Center Online Service, provided

by the NASA/Goddard Space Flight Center. The Ryle telescope is supported by PPARC.

References

- Corbel S., Fender R., 2002, ApJ, 573, L35
- Corbel S., Nowak M. A., Fender R. P., Tzioumis A. K., Markoff S., 2003, A&A, 400, 1007
- Corbel S., Fender R. P., Tzioumis A. K., Nowak M., McIntyre V., Durouchoux P., Sood R., 2000, A&A 359, 251
- Corbel S. et al. , 2002, Science, 298, 196
- Corbel S. et al. , 2001, ApJ, 554, 43
- Cowley A. P., Schmidtke P. C., Hutchings J. B., Crampton D., 2002, ApJ, 123, 1741
- Della Valle M., Mirabel I. F., Rodríguez L. F., 1994, A&A, 290, 803
- Di Salvo T., Done C., Zycki P. T., Burderi L., Robba N. R., 2001, ApJ, 547, 1024
- Done C., 2001, Adv. Space Res., 28, 255
- Dubus G., Kim R. S. J., Menou K., Szkody P., Bowen D. V., 2001, ApJ, 553, 307
- Ebisawa, K. et al. , 1994, PASJ, 46, 375
- Elvis M., Page C. G., Pounds K. A., Ricketts M. J., Turner M. J. L., 1975, Nature, 257, 656
- Falcke H., Biermann P. L., 1996, A&A, 308, 321
- Fender R. P., 2003, MNRAS, 340, 1353
- Fender R. P., 2001a, MNRAS, 322, 31
- Fender R. P., 2001b, A&SS, 276, 69
- Fender R. P., 2001c, in *'Relativistic flows in Astrophysics'*, Springer Verlag Lecture Notes in Physics, Eds. A.W. Guthmann, M. Georganopoulos, K. Manolakou and A. Marcowith, Lect. Notes Phys. 589, 101
- Fender R. P., 2000, in *'Proc. of the Third Microquasar Workshop'*, Eds A. J. Castro-Tirado, J. Greiner and J. M. Paredes, A&SS 276, 69
- Fender R. P., Kuulkers E., 2001, MNRAS 324, 923
- Fender R. P., Hanson M. M., Pooley G. G., 1999, MNRAS, 308, 473
- Fender R. P., Southwell K., Tzioumis A. K., 1998, MNRAS, 298, 692
- Fender R. P., Garrington S. T., McKay D. J., Muxlow T. W. B., Pooley G. G., Spencer R. E., Stirling A. M., Waltman E. B., 1999a, MNRAS, 304, 865
- Fender R. P. et al. 1999b, ApJ, 519, L165
- Galeev A. A., Rosner R., Vaiana G. S., 1979, ApJ, 229, 318

- Gallo E., Fender R. P., 2002, *MNRAS*, 337, 869
- Gallo E., Fender R. P., Pooley G. G., 2002, in ‘*Proc. of the Fourth Microquasars Workshop*’, Eds Ph. Durouchoux, Y. Fuchs, and J. Rodriguez, Center for Space Physics: Kolkata, 201
- Geldzahler B. J., 1983, *ApJ*, 264, L49
- Ghisellini G., Celotti A., 2001, *A&A*, 379, L1
- Gierlinski M., Maciolek–Niedzwiecki A., Ebisawa K., 2001, *MNRAS*, 325, 1253
- Greiner J., Dennerl K., Predehl P., 1996, *A&A*, 314, L21
- Haardt F., Maraschi L., 1991, *ApJ*, 380, L51
- Haardt F. et al. , 2001, *ApJ*, 133, 187
- Han X., Hjellming R. M., 1992, *ApJ*, 400, 304
- Hannikainen D. C., Hunstead R. W., Campbell–Wilson D., Sood R. K., 1998, *A&A*, 337, 460
- Harmon B. A., 1995, *Nature*, 374, 703
- Heindl W. A., Prince T. A., Grunsfeld J. M., 1994, *ApJ*, 430, 829
- Hjellming R. M., Rupen M. P., 1995, *Nature*, 375, 464
- Hjellming R. M., Rupen M. P., Mioduszewski A. J., Narayan, R., 2000, *The Astronomer’s Telegram*, 54
- Hjellming R. M., Han X., 1995, in ‘*X-ray binaries*’, Eds. Lewin W. H. G., van Paradijs J., van den Heuvel E. P. J., Cambridge University Press, 308
- Homan J., Jonker P. G., van der Klis M., Kuulkers E., 2000, *IAU Circ.*, 7425, 2
- Homan J., Wijnands R., van der Klis M., Belloni T., van Paradijs J., Klein–Wolt M., Fender R., Mendez M., 2001, *ApJS*, 132, 377
- Hynes R. I., Steeghs D., Casares J., Charles P. A., O’Brien K., 2003, *ApJL*, 583, L95
- Hynes R. I., Haswell C. A., Chaty S., Shrader C. R., Cui W., 2002, *MNRAS*, 331, 169
- Hynes R. I., Roche P., Charles P. A., Coe M. J., 1999, *MNRAS*, 305, L49
- Keck J. W. et al. , 2001, *ApJ*, 563, 301
- Kitamoto S., Tsunemi H., Pedersen H., Ilovaisky S. A., van der Klis M., 1990, *ApJ*, 361, 590
- Klein–Wolt M., Fender, R. P., Pooley G. G., Belloni T., Migliari S., Morgan E. H., van der Klis M., 2002, *MNRAS*, 331, 745
- Kong A. K. H., McClintock J. E., Garcia M. R., Murray S. S., Barret D., 2002, *ApJ*, 570, 277
- Kotani T. et al. , 2000, *ApJ*, 543, L133
- Kubota A., Makishima K., Ebisawa K., 2001, *ApJ*, 560, L147
- Kuulkers E., Fender R. P., Spencer R. E., Davis R. J., Morison I., 1999,

- MNRAS, 306, 919
- Laing R. A., 1993, *'Astrophysical Jets'*, ed. D. Burgarella, M. Livio & C. O'Dea
Cambridge University Press, 95
- Lin D. et al. , 2000, ApJ, 532, 548
- Maccarone T. J., 2003, A&A, 409, 697
- Maccarone T. J., 2002, MNRAS, 336, 1371
- Main D. S., Smith D. M., Heindl W. A. Swank J., Leventhal M., Mirabel I. F.,
Rodríguez L. F., 1999, ApJ, 525, 901
- Markoff S., Falcke H., Fender R.P., 2001, A&AL, 372, L25 (MFF)
- Markoff S., Nowak M. A., Corbel S., Fender R., Falcke H., 2003a, A&A, 397,
645
- Markoff S., Nowak M., Corbel S., Fender R., Falcke H., 2003b, in Proceedings
for *'The Physics of Relativistic Jets in the Chandra and XMM Era'*, Eds. G.
Brunetti, D. E. Harris, R. M. Sambruna & G. Setti
- Markwardt C. B., Marshall F. E., Swank J. H., 1999, IAU Circ., 7274, 2
- Martí J., Mirabel I.F., Duc P.A., Rodríguez L.F., 1997, A&A, 323, 158
- Massey P., Johnson K. E., Degioia–Eastwood K., 1995, ApJ, 454, 151
- McClintock J. E., Horne K., Remillard R. A., 1995, ApJ, 442, 358
- McClintock J. E., et al. , 2001, ApJ, 555, 477
- Meier D. L., 2001, ApJ, 548, L9
- Merloni A., 2002, in *'Proc. of the Fourth Microquasars Workshop'*, Eds Ph.
Durouchoux, Y. Fuchs, and J. Rodriguez, Center for Space Physics: Kolkata,
2105.
- Merloni A., Fabian A. C., 2002, MNRAS, 332, 165
- Miller J. M., Fox D. W., Di Matteo T., Wijnands R., Belloni T., Pooley D.,
Kouveliotou C., Lewin W. H. G., 2001, ApJ, 546, 1055
- Mirabel I. F., Rodríguez L. F., Nature, 371, 46
- Mirabel I. F., Rodríguez L. F., 1999, ARA&A, 37, 409
- Mioduszewski A. J., Rupen M. P., Hjellming R. M., Pooley G. G., Waltman E.
B., 2001, ApJ, 553, 766
- Narayan R., Barret D., McClintock J. E., 1997, ApJ, 482, 448
- Narayan R., Garcia M. R., McClintock J. E., 2001, in *'Proc. of the Ninth Marcel
Grossmann Meeting'*, Eds V. Gurzadyan, R. Jantzen, R. Ruffini, Singapore:
World Scientific
- Narayan R., McClintock J. E., Yi I., 1996, ApJ, 457, 821
- Nowak M. A., 1995, PASP, 107, 1207
- Orosz, J. A., 2002, in Proc. of the IAU Symp. 212, Eds K. A. van der Hucht, A.
Herraro, & C. Esteban, San Francisco: ASP (astro-ph/0209041)
- Orosz J. A., Jain R. K., Bailyn C. D., McClintock J. E., Remillard R. A., 1998,

- ApJ, 499, 375
- Owen F. N., Balonek T. J., Dickey J., Terzian Y., Gottesman S. T., 1976, ApJ, 203, L15
- Parmar A. N., Belloni T., Orlandini M., Dal Fiume D., Orr A., Masetti N., 2000, A&A, 360, L31
- Parmar A. N., Stella L., White N. E., 1986, ApJ, 304, 664
- Pooley G. G., Fender R., Brocksopp C., 1999, MNRAS, 302, L1
- Pooley G. G., Fender R., 1997, MNRAS, 292, 925
- Poutanen J., 1998, in *'Theory of Black Hole Accretion Disks'*, Cambridge University Press, 100
- Poutanen J., Svensson R., 1996, ApJ, 470, 249
- Predehl P., Burwitz V., Paerels F., Trmper J., 2000, A&A, 357, 25
- Robinson E. L., Ivans I. I., Welsh W. F., 2002, ApJ, 565, 1169
- Rutledge R. E., Bildsten L., Brown E. F., Pavlov G. G., Zavlin V. E., 1999, ApJ, 514, 945
- Sánchez-Ferández C. et al. , 1999, A&A, 348, L9
- Schulz N. S., Cui W., Canizares C. R., Marshall H. L., Lee J. C., Miller J. M., Lewin W. H. G., 2002, ApJ, 565, 1141
- Shahbaz T., Naylor T., Charles P. A., 1994, MNRAS, 268, 756
- Shakura N. I., Sunyaev R. A., 1973, A&A 24, 337
- Shapiro S. L., Lightman A. P., Eardley D. M., 1976, ApJ, 204, 187
- Shrader C. R., Wagner R. M., Charles P. A., Harlaftis E. T., Naylor T., 1997, ApJ, 487, 858
- Sobczak G. J., McClintock J. E., Remillard R. A., Levine A. M., Morgan E. H., Bailyn C. D., Orosz J., 1999, ApJ, 517, L121
- Sood R., Campbell-Wilson D., 1994, IAU Circ., 6006, 1
- Stirling A. M., Spencer R. E., de la Force C. J., Garrett M. A., Fender R. P., Ogley R. N., 2001, MNRAS, 327, 1273
- Sunyaev R. A., Titarchk L. G., 1980, A&A, 86, 121
- Sunyaev R. A. et al. , 1991, ApJ, 383, L49
- Tanaka Y., 1993, IAU Circ., 5877, 1
- Terasawa N., Nakamura H., 1995, A&A, 294, 443
- Tomsick J. A., Kaaret P., 2000, ApJ, 537, 448
- Ueda Y., Inoue H., Tanaka Y., Ebisawa K., Nagase F., Kotani T., Gehrels N., 1998, ApJ, 492, 782; erratum ApJ, 500, 1069
- van Kerkwijk M. H. et al. , 1992, Nature, 355, 703
- Wagner R. M., Starrfield S. G., Hjellming R. M., Howell S. B., Kreidl T. J., 1994, ApJ 429, L25
- Wilms J., Nowak M. A., Pottschmidt K., Heindl W. A., Dove J. B., Begelman

M. C., 2001, MNRAS, 320, 327

Zdziarski A. A., Gilfanov M., Lubinski P., Revnivtsev M., 2003, MNRAS, 342, 372

Zdziarski A. A., Poutanen J., Mikolajewska J., Gierlinski M., Ebisawa K., Johnson W. N., 1998, MNRAS, 301, 435

Zycki P. T., Done C., Smith D. A., 1999, MNRAS, 305, 231

CHAPTER 3

JET-DOMINATED STATES: AN ALTERNATIVE TO ADVECTION ACROSS BLACK HOLE EVENT HORIZON IN 'QUIESCENT' X-RAY BINARIES

Rob Fender, Elena Gallo & Peter Jonker

Monthly Notices of the Royal Astronomical Society 343, L99-L103 (2003)

We demonstrate that at relatively low mass accretion rates, black hole X-ray binaries should enter 'jet-dominated' states, in which the majority of the liberated accretion power is in the form of a (radiatively inefficient) jet and not dissipated as X-rays in the accretion flow. This result follows from the empirically established non-linear relation between radio and X-ray power from hard state black holes, which we assume also to hold for neutron stars. Conservative estimates of the jet power indicate that all 'quiescent' black holes should be in this jet-dominated regime. In combination with an additional empirical result, namely that black hole X-ray binaries are more 'radio loud' than neutron stars, we find that quiescent neutron stars should be up to two orders of magnitude more luminous in X-rays than the black hole systems, without requiring any significant advection of energy into a black hole. This ratio is as observed, and such observations should therefore no longer be considered as direct evidence for the existence of black hole event horizons. Furthermore, even if black hole candidates do contain black holes with event horizons, this work demonstrates that there is no requirement for the advection of significant amounts of accretion energy across the horizon.

3.1 Introduction

Proving the existence of black holes remains a key goal of observational high energy astrophysics. While dynamical evidence (e.g. Charles 1998) convinc-

ingly demonstrates the existence of compact accreting objects in binary systems which have masses in excess of the highest theoretical limit for a neutron star ($\sim 3M_{\odot}$), and are therefore strong black hole candidates (BHCs), we cannot rule out the possibility that some as-yet-unconsidered state of matter may provide an alternative explanation.

As an alternative approach, in recent years much attention has been focused on finding evidence for black hole event horizons. One promising and actively pursued route has been a comparison of the X-ray luminosities of BHC and neutron star (NS) X-ray binaries (XRBs) in ‘quiescence’. In such states, black hole accretion could be advection dominated and considerably fainter than neutron stars. This is indeed what has been found observationally, with ‘quiescent’ BHCs being typically two to three orders of magnitude (in Eddington units) less luminous than their NS XRB equivalents. This has been claimed to represent some of the strongest evidence to date for the existence of black hole event horizons (Narayan, Garcia & McClintock 1997; Menou et al. 1999; Garcia et al. 2001). However, alternatives to this interpretation have also been discussed (Campana & Stella 2000; Bildsten & Rutledge 2000; Abramowicz, Kluzniak & Lasota 2002). Abramowicz et al. (2002), in particular, stress that ‘absence of evidence is not evidence of absence’, and draw attention to alternatives to black holes. Even if BHCs *do* contain black hole with event horizons, it is important to establish how much, if any, of the potential accretion energy may be being advected across their horizons.

In a series of important and related observations, in recent years it has been established that jets are an integral and relatively ubiquitous component of the process of accretion in both black hole and neutron star X-ray binaries (e.g. Mirabel & Rodríguez 1999; Fender 2002). We are now beginning to understand just how powerful these jets may be. Corbel et al. (2003) discovered that, over four orders of magnitude in X-ray luminosity, the relation between radio and X-ray luminosity for the BHC X-ray binary GX 339-4 has the form $L_{\text{radio}} \propto L_{\text{X}}^b$, where $b = 0.706 \pm 0.011$ for L_{X} in the 3–9 keV range (b increases slightly with the increasing energy of the X-ray band used for comparison). Gallo, Fender & Pooley (2003) demonstrated that the same relation holds over a comparable range in X-ray luminosity for the transient V404 Cyg (GS 2023+338), and furthermore that the data for all measured low/hard state sources is consistent with a such a Universal relation holding for all of them. This power law relation between radio and X-ray luminosity is a key observational discovery providing clues to the underlying physics of the disc–jet coupling.

Are there differences in jet power between the BHCs and NS XRBs? Fender & Kuulkers (2001) found that BHC XRBs were, in general between

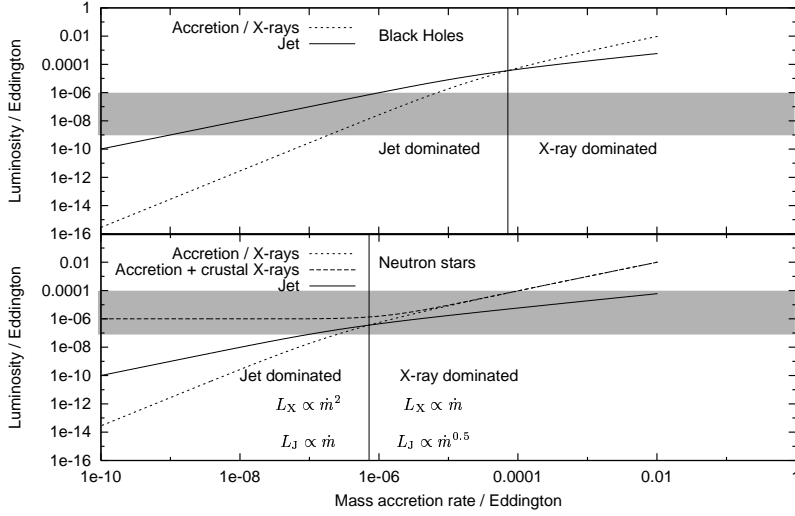


Figure 3.1: Variation of X-ray luminosity and jet power as a function of mass accretion rate, in our model, for neutron star and black hole X-ray binaries. Two regimes exist, ‘X-ray-dominated’ and ‘jet-dominated’, with the transition from the former to the latter occurring at two orders of magnitude lower accretion rate in neutron stars than in black holes, due to their lower ‘radio loudness’. In the X-ray-dominated regime, $L_X \propto \dot{m}$, but in the jet-dominated regime $L_X \propto \dot{m}^2$. The transition between the two regimes occurs at an X-ray luminosity $L_X = A^2$, where $A_{\text{BH}} \sim 6 \times 10^{-3}$ and $A_{\text{NS}} \sim 6 \times 10^{-4}$. The shaded areas indicate the range of X-ray luminosities observed in ‘quiescence’ from the two types of X-ray binary. If this model is correct, *all* of the quiescent black hole binaries are in the jet-dominated regime.

10–100 times more ‘radio loud’ (in the sense of the radio to soft X-ray ratio) than neutron star binaries. Migliari et al. (2003) compared the radio strength of the atoll-type neutron star binary 4U 1728-34 with the comparable state and X-ray luminosity of BHCs, and found a ratio of radio loudness $R_{\text{radio}} = (L_{\text{radio}}/L_X)_{\text{BH}} / (L_{\text{radio}}/L_X)_{\text{NS}} \sim 30$. The origin of this difference in radio loudness is not clear (see Fender & Kuulkers 2001 for a discussion).

3.2 Jet-dominated states in black hole candidates

In the following all luminosities and accretion rates are in Eddington units, where the Eddington luminosity is $\sim 1.3 \times 10^{38} (M/M_\odot) \text{ erg s}^{-1}$, where M is the mass

of the accreting compact star. The Eddington accretion rate, defined as that accretion rate at which the Eddington luminosity is achieved, is, for an accretion efficiency of $\sim 10\%$ (*i.e.* $\sim 0.1\dot{m}c^2$ is liberated during the accretion process) approximately $1.4 \times 10^{18}(M/M_\odot) \text{ g s}^{-1}$.

We assume that the total power output L_{total} from an X-ray binary in a ‘low/hard’ or analogous state is a combination of the radiative luminosity of the flow (L_X , directly observed as X-rays) and jet power (L_J indirectly traced by e.g. radio flux density):

$$L_{\text{total}} = L_X + L_J \quad (3.1)$$

Now we already know (Corbel et al. 2002; Gallo et al. 2003) the relation between radio (L_{radio}) and X-ray luminosity:

$$L_{\text{radio}} \propto L_X^{0.7} \quad (3.2)$$

How does observed radio flux relate to jet power; *i.e.* what is the relation between L_{radio} and L_J ? In models of optically thick jets (*e.g.* Blandford & Königl 1979; Falcke & Biermann 1996; Markoff, Falcke & Fender 2001; Heinz & Sunyaev 2003), the following scaling applies:

$$L_{\text{radio}} \propto L_J^{1.4} \quad (3.3)$$

Combining equations (2) and (3):

$$L_J \propto L_X^{0.5} \quad (3.4)$$

therefore

$$L_{\text{total}} = L_X + AL_X^{0.5} \quad (3.5)$$

which provides the relation between total power and X-ray luminosity. The normalisation A between can be estimated. Fender (2001) and Corbel & Fender (2002) conservatively estimate $L_J/L_X \geq 0.05$ for Cyg X-1 and GX 339-4 at an accretion luminosity of $L_X \sim 10^{-2}$. Fender et al. (2001) estimated that, at an accretion luminosity of $L_X \sim 10^{-3}$, the black hole transient XTE J1118+480 had $L_J/L_X \geq 0.2$ (see also Corbel & Fender 2002 for an estimate for GX 339-4). Conservatively adopting the equality for XTE J1118+480 corresponds to $A_{\text{BH}} \sim 6 \times 10^{-3}$ in Eddington units. Equivalently the relation between total power and jet power is given by:

$$L_{\text{total}} = A^{-2}L_J^2 + L_J \quad (3.6)$$

In the following we shall assume that L_{total} is proportional to the mass accretion rate \dot{m} (i.e. all the available accretion power goes either into the X-rays or the jet). In Eddington units this corresponds to

$$L_{\text{total}} = \dot{m} \quad (3.7)$$

which is the condition of no advection of accretion energy across the event horizon.

We can then plot the variation of L_X and L_J as a function of mass accretion rate. These are plotted for black holes in the top panel of Figure 3.1.

We note that there are two regimes, ‘X-ray-dominated’ at higher mass accretion rates, and ‘jet-dominated’ at lower accretion rates. In the X-ray-dominated regime, $L_X \propto \dot{m}$ and $L_J \propto \dot{m}^{0.5}$. However in the jet-dominated regime $L_X \propto \dot{m}^2$ and $L_J \propto \dot{m}$. The transition between the two regimes occurs at $L_X = A^2 \sim 4 \times 10^{-5}$ or, equivalently, $\dot{m} = 2A^2 \sim 7 \times 10^{-5}$. The shaded region in the top panel of Figure 3.1 indicates the observed range of X-ray luminosities of black hole X-ray binaries in ‘quiescence’ – if our model is correct then *all* of these systems are in the jet-dominated regime, with accretion rates $10^{-6} \lesssim \dot{m} \lesssim 10^{-5}$, and with jet powers one to two orders of magnitude greater than the observed X-ray luminosity.

3.3 Jet-dominated states in neutron stars?

A major uncertainty in knowing if the arguments outlined above apply to neutron stars is that the relation $L_{\text{radio}} \propto L_X^b$ has not yet been measured. Migliari et al. (2003) note that the relation seems steeper ($b > 1$) for the atoll-type X-ray binary 4U 1728-34, but this is over a small range in X-ray flux compared to that measured for black holes. At present we must consider that this relation remains unmeasured, due primarily to the relative faintness of atoll-type sources in the radio band compared to black holes (Fender & Hendry 2000), which results from the greater ‘radio loudness’ of black holes (Fender & Kuulkers 2001; Migliari et al. 2003). However, we will make the assumption in what follows that the same relation does indeed apply for atoll-type NS XRBs.

As already noted, the ratio of ‘radio loudness’ between BHC and NS XRBs is $R_{\text{radio}} \sim 30$. Using equation (3.3), this translates into a difference in jet power of a factor 10, i.e. $A_{\text{NS}} \sim 6 \times 10^{-4}$. The X-ray luminosity below which neutron star systems would be jet-dominated is therefore $L_X \sim 3 \times 10^{-7}$. This is comparable to the lowest X-ray luminosity measured from a neutron star in quiescence (Garcia et al. 2001) implying that, quite unlike black holes, we may have never observed

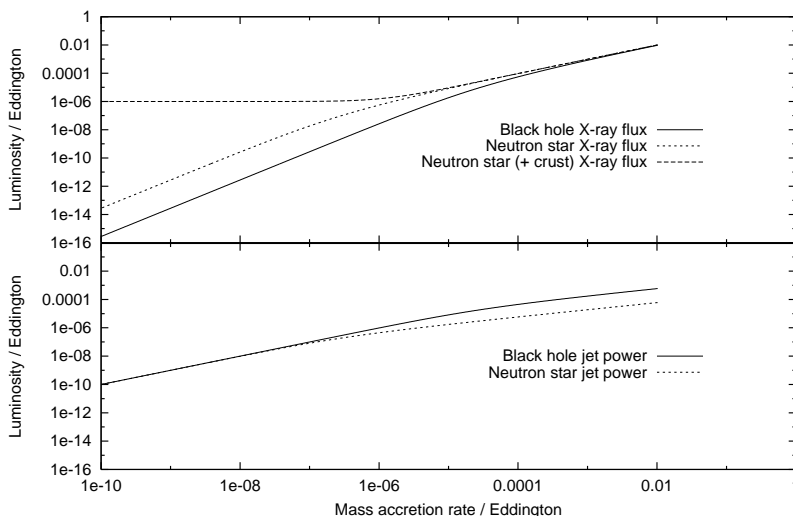


Figure 3.2: Variation of X-ray luminosity (upper panel) and jet power (lower panel) as a function of mass accretion rate for the model outlined in the text. Since black holes transit to the ‘jet-dominated’ regime at two orders of magnitude higher accretion rate than neutron stars (Figure 3.1), once both classes of system are in this regime (accretion rates corresponding to ‘quiescence’) then neutron stars will remain a factor of $Q_X \sim 130$ more luminous in X-rays. This ratio, is consistent with observations of BHCs and NS XRBs in quiescence. Furthermore note that at very low accretion rates ($\dot{m} \leq 10^{-6.5}$) the jet power from BHCs and NS XRBs is the essentially the same, despite the NS XRBs being 100 times more luminous in X-rays, and ‘quiescent’ NS and BHC XRBs may be accreting at the same rate.

a neutron star in a jet-dominated state. In the lower panel of Figure 3.1 we plot the variation of L_X and L_J as a function of mass accretion rate for neutron star binaries. As for the BHCs, the shaded region indicates the observed range of ‘quiescent’ X-ray luminosities.

In the absence of core/crustal emission (see below) which is decoupled from the accretion flow on all but the longest timescales, the observed X-ray luminosities of ‘quiescent’ NS XRBs correspond to a range in accretion rate of $10^{-6} \lesssim \dot{m} \lesssim 10^{-4}$, overlapping with the range in \dot{m} for ‘quiescent’ black holes. Therefore, in at least this respect, in the model presented here the data are consistent with both NS and BHC XRBs in ‘quiescence’ accreting at the same rate.

3.3.1 Core / crustal emission?

Brown, Bildsten & Rutledge (1998) have argued that, once accretion has halted, neutron stars will have a luminosity in the range $5 \times 10^{32} - 5 \times 10^{33} \text{ erg s}^{-1}$ from crustal emission. This model seems to be supported by observations of transient neutron star binaries in quiescence (e.g. Rutledge et al. 2001a; Rutledge et al. 2001b; Rutledge et al. 2002; see also Wijnands et al. 2001), although Garcia et al. (2001) argue that even at ‘quiescent’ levels the X-ray luminosity is dominated by accretion. Indeed, the quiescent emission of SAX J1808.4–3658 is uncomfortably low ($5 \times 10^{31} \text{ erg s}^{-1}$) and hard (power law index 1.5 with a blackbody contribution of less than 10 per cent) for the neutron star crustal emission model unless the neutron star is more massive than $1.7 M_{\odot}$ (Campana et al. 2002).

If this crustal emission does exist then it adds a new term to the total observed X-ray emission:

$$L_{X,\text{observed}} = L_X + L_{\text{crustal}} \quad (3.8)$$

In Figure 3.1 (lower panel) we also indicate the solutions with the addition of persistent ‘crustal’ emission to the observed X-ray flux from a neutron star, at a level of $10^{32} \text{ erg s}^{-1}$, approximately the lowest luminosity observed from a quiescent neutron star. This has a significant effect, since this crustal luminosity, at $\sim 10^{-6} L_{\text{Edd}}$ is above that at which neutron stars would enter the jet-dominated regime. Whereas in the case of accretion-only luminosity, while we had not observed neutron stars in jet-dominated regimes they were still possible, if such crustal luminosities are ubiquitous then neutron stars will not enter the jet-dominated regime, unless their time-averaged mass accretion rates are very low ($\dot{m} \lesssim 10^{-12} M_{\odot} \text{ yr}^{-1}$). However, note that at the lowest accretion rates neutron stars will make just as powerful jets as BHCs (see next Section).

3.4 Discussion

This work leads naturally to some interesting consequences if correct. We outline these below.

3.4.1 X-ray luminosity as a function of mass accretion rate

We have seen in the above that below a certain mass accretion rate BHC X-ray binaries probably enter a jet-dominated state. Because of their higher ‘radio loudness’, black holes make the transition to this jet-dominated state at a higher mass accretion rate than neutron stars (by a factor $(A_{\text{BH}}/A_{\text{NS}})^2$). Consequently, if

there are no other effects, once both NS and BH are in the jet-dominated regime, the NS systems will be a factor $(A_{\text{BH}}/A_{\text{NS}})^2$ brighter in X-rays than the BH systems. Since $(A_{\text{BH}}/A_{\text{NS}}) \sim 10$ then we expect a ratio of ~ 100 between quiescent X-ray luminosities at the same accretion rate. In fact, while the expressions and plots given so far are specifically for the condition in equation (3) and the estimated values of A_{BH} , A_{NS} , there is a more general expression for the ratio of X-ray luminosities when both classes of object are in the jet-dominated regime:

$$Q_X = (L_X)_{\text{NS}}/(L_X)_{\text{BH}} = R_{\text{radio}}^{1/b} \quad (3.9)$$

Since $R_{\text{radio}} \sim 30$ and $b \sim 0.7$, we expect a ratio of X-ray luminosities in quiescence of ~ 130 , when both BHCs and NS XRBs are in the jet-dominated regime, and at the same mass accretion rate. This is consistent with what is observed.

The X-ray luminosities as a function of \dot{m} are illustrated in Figure 3.2 (top panel). As already noted, the quiescent NS XRBs may not be quite in the jet-dominated regime; however, the BHC XRBs are clearly in this regime, and the difference in X-ray luminosities at the same accretion rate is already one order of magnitude at $\dot{m} \sim 10^{-5}$, increasing to Q_X at $\dot{m} \sim 10^{-6}$ (Figure 3.2, top panel). We therefore find that the observed $L_{\text{radio}} \propto L_X^{0.7}$ scaling, combined with the order of magnitude greater radio loudness of BHC XRBs, naturally results in a significant difference in the quiescent luminosities of NS and BHC XRBs, as observed.

More precisely, we expect there to be three regimes in which the ratio of X-ray luminosities, $R_X = (L_X)_{\text{BH}}/(L_X)_{\text{NS}}$ has different values:

$$\begin{aligned} \text{(a)} \quad & (L_X)_{\text{BH}} \geq A_{\text{BH}}^2 \quad (L_X)_{\text{NS}} \geq A_{\text{NS}}^2 \quad R_X = 1 \\ \text{(b)} \quad & (L_X)_{\text{BH}} \leq A_{\text{BH}}^2 \quad (L_X)_{\text{NS}} \geq A_{\text{NS}}^2 \quad 1 \leq R_X \leq Q_X \\ \text{(c)} \quad & (L_X)_{\text{BH}} \leq A_{\text{BH}}^2 \quad (L_X)_{\text{NS}} \leq A_{\text{NS}}^2 \quad R_X = Q_X \end{aligned}$$

where (a) corresponds to both classes of objects being ‘X-ray dominated’, (b) corresponds to BHCs being jet-dominated and NS not, (c) corresponds to both classes being jet-dominated. From this study it appears that $Q \sim 130$, and that observed ‘quiescence’ corresponds to regimes (a) or (b), which consistent with the observations without requiring any accretion energy to be advected across an event horizon.

It is interesting to note that in the jet-dominated regime, the scaling of X-ray luminosity with mass accretion rate, $L_X \propto \dot{m}^2$ is exactly the same as that predicted theoretically by ADAF models (e.g. Narayan et al. 1997; Mahadevan 1997).

3.4.2 Jets at the lowest accretion rates

It would be a mistake to assume that the persistent difference in X-ray luminosity will result in a difference in jet powers between NS and BHC systems at the lowest luminosities. In fact, below an accretion rate of $\dot{m} \sim 10^{-6.5}$ both NS and BHC systems are putting the same amount of power into the jet (Figure 3.2, lower panel), which dominates the power output of the system. The tiny fraction of the total power released as X-rays is insignificant whether its a BHC or a NS XRB one hundred times brighter.

It is also interesting to note that the ratio in radio loudness, R_{radio} is maintained throughout this scenario, but for somewhat different reasons in the two regimes. When ‘X-ray dominated’, BHCs are more ‘radio loud’ because they match the NS XRBs in X-rays but put out more radio power. However, at the lowest accretion rates the radio power is the same but the X-ray luminosity of the BHCs is lower, maintaining the ratio.

3.4.3 X-ray jets: what if ‘hard’ X-ray binaries are already jet-dominated ?

It has been suggested that the hard X-ray spectra observed from low/hard state BHCs may be in some, maybe all, cases optically thin synchrotron emission directly from the jet (Markoff, Falcke & Fender 2001; Markoff et al. 2003). This is at odds with the more standard view of the hard X-ray spectrum as being dominated by thermal Comptonisation from electrons with a temperature of ~ 100 keV (e.g. Sunyaev & Titarchuk 1980; Poutanen 1998, Zdziarski et al. 2003). If it is the correct interpretation, how does it affect the analysis performed here ?

Since in those models the BHCs are already completely jet dominated at $\dot{m} = 0.01$, then $L_X \propto \dot{m}^2$ (as $L_X \propto L_J^2$ [equation (4)] and $L_J \propto \dot{m}$ this is always the case for jet-dominated emission). In fact it can be shown that the same ratio of ‘quiescent’ luminosities is achieved as in the previous analysis, as long as the NS XRBs are *not* already jet-dominated at $\dot{m} \sim 0.01$ (otherwise L_X in both classes of objects would track each other). However, the transition to the jet-dominated regime would occur at a higher \dot{m} (by approximately two orders of magnitude), meaning the observed ‘quiescent’ mass accretion rates would be considerably higher than those indicated in Figure 3.1.

3.5 Conclusions

The results presented in this Letter are necessarily a subset of the possible consequences of the empirical relations and model upon which they are based. Of the

more general results, to be expanded upon in a further work, only one is given, namely that once both BHC and NS XRB are in jet dominated states the ratio of X-ray luminosities depends only upon two quantities which have already been measured, i.e. b and R_{radio} :

$$Q_X = R_{\text{radio}}^{1/b} \sim (30)^{1/0.7} \sim 130 \quad (3.9)$$

We suggest that based upon existing observational data, ‘quiescent’ BHCs are in the ‘jet-dominated’ regime and that NS XRBs are, if not jet-dominated, close to the transition to this regime. Specifically, if a similar value of b holds for NS XRBs as for BHCs (and this is the key observational uncertainty) then quiescent NS XRBs are, in the most conservative case, putting $\gtrsim 10\%$ of their power into jets. Thus the observed ratio of X-ray luminosities should be close to Q_X , consistent with what is observed. An additional core / crustal contribution to the X-ray emission from NS XRBs will only widen the discrepancy. Essentially, we find that the difference in quiescent X-ray luminosities between NS and BHC XRBs can be mostly, if not entirely, explained by a difference in the efficiency of jet production between the two types of sources (the origin of which remains unclear).

Therefore we find that the observed difference in quiescent luminosities of neutron star and black hole candidate XRBs *does not require the presence of black hole event horizons*. This should not be taken as a statement to the effect that we do not believe that black hole candidates contain black holes (see related discussion in Abramowicz et al. 2003). Certainly there are differences between the neutron star and black hole candidate XRBs, which may be naturally explained by the fact that black hole candidates do in fact contain black holes. However, since there is no requirement for significant energy to be advected into the black hole in order to explain the ratio of quiescent X-ray luminosities, these luminosities cannot in turn be taken as ‘proof’ of the existence of event horizons.

Furthermore, even if, as seems probable, the BHCs do contain black holes with event horizons, this work shows that there is no requirement for the advection of any significant quantity of accretion energy across the horizon. Rather, the relative radiative inefficiency of BHCs compared to NS XRBs at low \dot{m} is due to the low radiative efficiency of the *jets* they are powering, not the accretion flow itself.

Acknowledgements

RPF would like to thank Sera Markoff, Sebastian Heinz and Lars Bildsten for useful discussions. PGJ would like to thank Gordon Ogilvie for useful discus-

sions.

References

- Abramowicz M.A., Kluzniak W., Lasota J.-P., 2002, A&A, 396, L31
Bildsten L., Rutledge R., 2000, ApJ, 541, 908
Blandford R.D., Königl A., 1979, ApJ, 232, 34
Brown E.F., Bildsten L., Rutledge R.E., 1998, ApJ, 504, L95
Campana S., Stella L., 2000, ApJ, 541, 849
Charles P.A., 1998, in *'Theory of black hole accretion discs'*, Eds. M.A. Abramowicz, G. Björnsson, J.E. Pringle, Cambridge Contemporary Astrophysics, Cambridge University Press, p.1
Corbel S., Fender R.P., 2002, ApJ, 573, L35
Corbel S., Nowak M.A., Fender R.P., Tzioumis A.K., Markoff S., 2003, A&A, 400, 1007
Falcke H., Biermann P.L., 1996, A&A, 308, 321
Fender R.P., 2001, MNRAS, 322, 31
Fender R.P., 2002, in *'Relativistic Flows in Astrophysics'*, Eds. A.W. Guthmann, M. Georganopoulos, A. Marcowith, K. Manolakou, Springer Lecture Notes in Physics LNP 589, p. 101
Fender R.P., Kuulkers E., 2001, MNRAS, 324, 923
Fender R.P., Hjellming R.M., Tilanus R.P.J., Pooley G.G., Deane J.R., Ogley R.N., Spencer R.E., 2001, MNRAS, 322, L23
Gallo E., Fender R.P., Pooley G.G., 2003, MNRAS, 344, 60
Garcia M.R., McClintock J.E., Narayan R., Callanan P., Barret D., Murray S.S., 2001, ApJ, 553, L47
Heinz S., Sunyaev R., 2003, MNRAS, 343, L59
Kong A.K.H., Kuulkers E., Charles P.A., Homer L., 2000, MNRAS, 312, L49
Kong A.K.H., McClintock J.E., Garcia M.R., Murray S.S., Barret D., 2002, ApJ, 570, 277
Mahadevan R., 1997, ApJ, 477, 585
Markoff S., Falcke H., Fender R.P., 2001, A&A, 372, L25
Menou K., Esin A.A., Narayan R., Garcia M.R., Lasota J.-P., McClintock J.E., 1999, ApJ, 520, 276
Migliari S., Fender R.P., Rupen M., Jonker P., Klein-Wolt M., Hjellming R.M., van der Klis M., 2003, MNRAS, 342, L67
Mirabel, I.F., Rodríguez, L.F., 1999, ARA&A, 37, 409
Narayan R., Garcia M.R., McClintock J.E., 1997, ApJ, 478, L79
Poutanen, J., 1998, in *'Theory of Black Hole Accretion Disks'*, Eds. Abramow-

icz, M. A., Björnsson, G., Pringle, J. E., Cambridge Contemporary Astrophysics
Rutledge R.E., Bildsten L., Brown E.F., Pavlov G.G., Zavlin V.E., 2001a, ApJ,
551, 921

Rutledge R.E., Bildsten L., Brown E.F., Pavlov G.G., Zavlin V.E., 2001b, ApJ,
559, 1054

Rutledge R.E., Bildsten L., Brown E.F., Pavlov G.G., Zavlin V.E., Ushomirsky
G., 2002, ApJ, 580, 413

Sunyaev R.A., Titarchuk L.G., 1980, A&A, 86, 121

Wijnands R., Miller J.M., Markwardt C., Lewin W.H.G., van der Klis M., 2001,
560, L159

Zdziarski A.A., Lubinski P., Gilfanov M., Revnivtsev M., 2003, MNRAS, 342,
355

CHAPTER 4

THE CONNECTION BETWEEN RADIO QUIET AGN AND THE HIGH/SOFT STATE OF X-RAY BINARIES

Tom Maccarone, Elena Gallo & Rob Fender

Monthly Notices of the Royal Astronomical Society 345, L19-L24 (2003)

A large sample of AGN studied here shows a ‘quenching’ of the radio emission that occurs when the luminosity is from a few percent to about 10 per cent of the Eddington rate, just as is seen in the high/soft state of X-ray binaries. The result holds even when the sample of AGN includes no Narrow Line Seyfert 1 galaxies (the systems most commonly suggested to be the analog of the high/soft state). This adds substantially to the body of evidence that AGN show the same spectral state phenomenology and related disc-jet coupling as the stellar mass accreting black holes. That the power law correlation between X-ray and radio luminosity is the same in both AGN and X-ray binaries and extends below $10^{-7}L_{\text{Edd}}$ strengthens the argument that there is no fundamental difference between the low/hard state and the so-called quiescent state in X-ray binaries. We also discuss possible reasons for the scatter in the radio to X-ray luminosity correlation in the AGN.

4.1 Introduction

Accreting black holes, whether stellar mass binary systems, or active galactic nuclei, show many similarities. Both emit radiation over many decades in frequency. Many, but not all, sources in each mass range display evidence for disc accretion in the forms of thermal emission and reflection off the thin disc. Many, but not all, sources in each mass range also have relativistic jets, typically seen through radio observations (see Fender 2005 for a review of the radio properties of X-ray binaries and chapter 2 of Krolik 1999 for a brief introduction to the broadband properties of AGN). Quenching of these radio jets – defined to be a

rather sudden drop in the radio emission – has been known about for some time, both in certain classes of AGN (Epstein et al. 1982) and in certain X-ray binaries (Tananbaum et al. 1972; Waltman et al. 1996; Harmon et al. 1997; Fender et al. 1999).

X-ray binaries thought to contain black holes have at least three spectral states. The *low/hard state* shows X-ray emission well fit by either a power law with an exponential cutoff at about 200 keV or a thermal Comptonisation model with a temperature of about 70 keV, along with a weak or undetected thermal component associated with a geometrically thin accretion disc (Zdziarski 2000 and references within). A so-called ‘quiescent state’ has been suggested to exist in the black hole candidates, but in reality, the X-ray and radio properties of low luminosity black hole candidates form a continuum down to the lowest observable luminosities (Gallo, Fender & Pooley 2003 – GFP03). The spectrum of the *high/soft state* is dominated by thermal component thought to arise in a geometrically thin, optically thick accretion disc (Shakura & Sunyaev 1973; Novikov & Thorne 1973) and also exhibits a weak power law tail without an observable cutoff (e.g. Gierliński et al. 1999). The *very high state* displays the same two components, but with the steep power law, rather than the thermal component dominating the total flux (see e.g. Miyamoto et al. 1991). Steady radio emission, which can be proved by brightness temperature arguments to come from a region larger than the binary separation of the system, and hence likely from a jet, has been found in the low/hard state, and strong radio flares have been seen during the very high/flaring state (Fender 2005). Neither strong nor steady radio emission has ever been detected in the high/soft state. For a review of spectral states of X-ray binary black holes, see Nowak (1995) and references within.

Models for the hard non-thermal emission generally invoke Comptonisation in a low optical depth (i.e. $\tau \lesssim 1$ in the low/hard state and $\tau \lesssim 5$ in the very high state) geometrically thick medium (e.g. Thorne & Price 1975; Shapiro, Lightman & Eardley 1976), although it has also been suggested that the low/hard state’s X-ray emission may be optically thin synchrotron emission from a jet (Markoff, Falcke & Fender 2001 – MFF01). Nonetheless, there is general agreement that the high/soft state, the one state thought to be geometrically thin is the one state where the radio emission is suppressed substantially. Theoretical studies suggest that jet production should be suppressed in thin discs due to the lack of poloidal magnetic fields (Livio, Ogilvie & Pringle 1999; Khanna 1999; Meier, Koide & Uchida 2001).

Radio emission from active galactic nuclei is also correlated with the X-ray spectral properties of the system, and with the geometry of the inner accretion flow. Radio loud AGN typically have harder X-ray spectra than radio quiet AGN

(Elvis et al. 1994; Zdziarski et al. 1995). Double-peaked optical emission lines are more often detected in the radio loud AGN with broad lines than in their radio quiet broad line counterparts (e.g. Eracleous & Halpern 1994); it has been suggested that these lines are reprocessed flux from a large scale height X-ray emitting region (e.g. Chen, Halpern & Filippenko 1989).

More detailed evidence that AGN may follow the same spectral state behavior as the black hole binaries has been scarcer. Analogies have been drawn (1) between the Narrow Line Seyfert 1 galaxies and the high/soft state (Pounds, Done & Osborne 1995; McHardy et al. 2003), (2) among low luminosity AGN, Fanaroff-Riley (FR) I galaxies (i.e. core dominated radio galaxies – see Fanaroff & Riley 1974) and the low/hard state (Meier 2001; Falcke, K rding & Markoff 2003 – FKM03) and (3) between FR II galaxies (i.e. lobe dominated radio galaxies) and the very high state (Meier 2001). The similarities between the jet ejection events in 3C120 and GRS 1915+105 (Marscher et al. 2002) can be interpreted as evidence for an analogy between the FR II galaxies and the very high state. Finally, GFP03 found that the high luminosity ‘transient’ jets are likely to have higher velocities than the low luminosity ‘steady’ jets. This is a theoretical prediction of at least one model for explaining the FR I/II dichotomy (Meier 1999), and seems to be supported by the fact that FR I jets tend to be double sided, while FR II jets tend to be single sided (e.g. Hardcastle 1995), providing additional evidence in favor of connections between FR I jets and the low/hard state, and between FR II jets and the very high state.

One thing that has not been clear is whether the high/soft state might exist for a broad range of masses of active galactic nuclei. The Narrow Line Seyfert 1 galaxies (NLSy1’s) which represent the most convincing high/soft state analogs have generally been found to contain black holes at the low mass end of the AGN mass spectrum (i.e. typically less than about $3 \times 10^6 M_{\odot}$) and to be accreting at tens of percent of the Eddington limit. It has been suggested that the radio quiet quasars may be higher mass examples of the high/soft state (Merloni, Heinz & Di Matteo 2003 – MHD03).

If one accepts a few reasonable, albeit unproven, assumptions about the luminosities and mechanisms for state transitions in accreting black hole systems, one can show that a high/soft state might not exist above the mass limits found in the NLSy1’s; Meier (2001) suggests that the state transitions for the low/hard state to the high/soft state are caused by transitions from an advection dominated accretion flow (ADAF, see e.g. Ichimaru 1977; Esin, McClintock & Narayan 1997) to a standard thin disc, while the transitions to the very high state occur when the thin disc becomes radiation pressure dominated. Since the ADAF to thin disc transition should occur at a fraction of the Eddington luminosity

independent of mass, while the luminosity in Eddington units where the thin disc becomes radiation pressure dominated goes as $M^{-1/8}$ (Shakura & Sunyaev 1976), one might expect the thin disc state to disappear when radiation pressure domination sets in below the luminosity for the transition from ADAF to thin disc; a similar, but less detailed argument for the same effect had previously been laid out in Rozanska & Czerny (2000). The soft-to-hard state transitions for black holes in binary systems are generally found to occur at about 2% of the Eddington limit (Maccarone 2003), although the spectral states do show a hysteresis effect (Miyamoto et al. 1995; Smith, Heindl & Swank 2002; Maccarone & Coppi 2003), and the transition from the hard state to the soft state can sometimes occur at luminosities about 4 times as high. The very high state seems to set in at about 20-30% of the Eddington luminosity, and from inspection of the classification table in Miller et al. (2001), one can see that this state can also show hysteresis effects in its transition luminosities and can exist down to about 10% of the Eddington luminosity. Given a factor of five ratio for a $10 M_{\odot}$ black hole between where the very high state evolves into the high/soft state and where the high/soft state evolves into the low/hard state, one might then expect that no high/soft state systems should exist for black holes more massive than about 4×10^6 solar masses.

Other models for the state transitions invoking whether the bulk of the power in the accretion flow is dissipated as thermal energy or as magnetic reconnection events can have the same scaling with mass for both the soft/hard and the soft/very high state transitions (Merloni 2003). Searching for the high/soft state analog in higher mass AGN systems is thus a rather critical step in producing a unified understanding of accretion processes in black hole systems. In this Letter, we will show that AGN accreting in the range of 2–10% of the Eddington luminosity show a ‘quenching’ in their radio emission similar to that found in Cygnus X-1 and GX 339-4 in their high/soft states (Tananbaum et al. 1972; Fender et al. 1999; GFP), and that more generally, the presence of a hard X-ray spectral component and radio emission are well correlated (e.g. results from GRS 1915+105 in Harmon et al. 1997; Klein-Wolt et al. 2002). This similarities supports the picture where (1) the high/soft state exists for AGN of a rather wide range of masses and (2) that this high/soft state occurs at the same range of X-ray luminosities as for the Galactic stellar mass black hole candidates.

4.2 Data and analysis

The correlation between radio luminosity and broadband X-ray luminosity found in GFP03 has been generalized for black holes of all masses to be a $L_{\text{radio}} - L_X - M$

correlation, through a multi-dimensional analysis by MHD03 and through the application of a theoretically predicted mass correction by FKM03. Considerable (i.e. several orders of magnitude) scatter does remain in the AGN sample when this correlation is applied, and the difference cannot be wholly due to measurement errors – additional parameters such as the black hole spin might have a major effect on the radio luminosity.

The exact relation found by MHD03, which we have re-expressed in Eddington units, is:

$$\log \frac{L_{\text{radio}}}{L_{\text{Edd}}} = 0.60 \log \frac{L_X}{L_{\text{Edd}}} + 0.38 \log \frac{M}{M_{\odot}} - 7.33. \quad (4.1)$$

We take the data used here from the compilation of MHD03. The sample includes AGN for which there are good mass, X-ray luminosity, and radio luminosity measurements. We exclude the sources in their sample for which there is an upper limit rather than a measurement of one of the three important quantities. We then correct the radio luminosity for the mass term as in equation (1), and plot the corrected radio luminosity in Eddington units versus the broadband X-ray luminosity in Eddington units in Figure 4.1 (a figure similar to Figure 7 of MHD03 and Figure 3b of FKM03).

The X-ray luminosities have been multiplied by a factor of 4.8 as an estimated ‘broadband’ correction, assuming a $\Gamma = 1.8$ power law spectrum extending from 10 eV to 100 keV, as compared with the 2–10 keV range over which the luminosities have been tabulated. This is not quite a ‘bolometric’ correction – our goal is to make a comparison with the X-ray binaries for which RXTE’s broadband spectroscopy allows us to observe most of the X-ray emission. We thus do not wish to include the contribution from a component at wavelengths longward of the accretion disc’s peak, such as the radio jet or a far infrared bump which may be partly due to AGN induced star formation or slow reprocessing of AGN photons and may reflect the past, rather than the present luminosity. On the other hand, we do wish to correct for the fact that the thin accretion discs of bright AGN emit primarily in the optical and UV bands, and not in the X-rays. From this point on, when we refer to the ‘broadband luminosity’, we mean the emission from the disc-corona system, as estimated by the 2–10 keV X-ray luminosity with a correction factor.

Low luminosity AGN (i.e. those below about 1 per cent of the Eddington luminosity) tend not have the ‘big blue bump’ associated with the emission from a thin disc, and this broadband correction factor is well within the range generally accepted (e.g. Ho 1999), although our correction factor is a bit smaller, because we correct only for the high energy part of the spectrum associated with the disc-corona part of the accretion flow. For the brighter AGN, where the disc emission

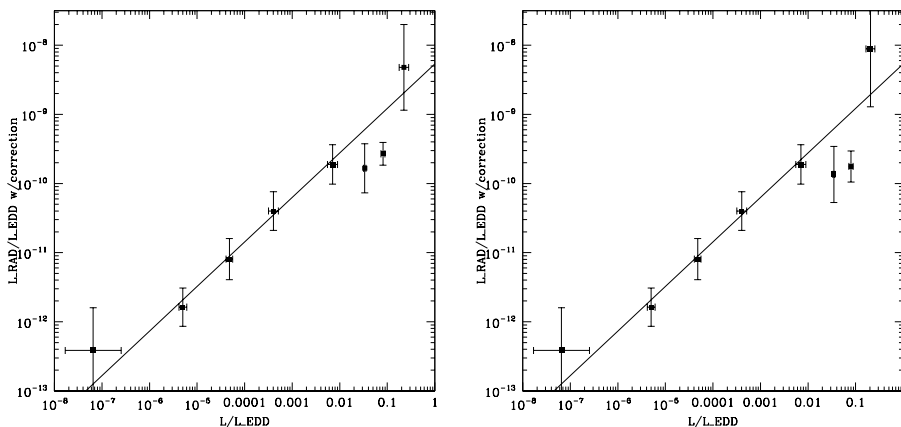


Figure 4.1: Left panel: the binned corrected AGN, including the narrow line Seyfert 1s. Right panel: the same as left, but with the NLSy1s removed from the sample. The line shows the best fit to the data (with the bins thought to represent the high/soft state excluded from the fit): $\log L_{\text{radio,corr}}/L_{\text{Edd}} = (0.64 \pm 0.09) \log L_X/L_{\text{Edd}} - (8.26 \pm 0.40)$. The different normalization from the MHD03 results comes mostly from the broadband correction.

is stronger (in agreement with the analogy to X-ray binaries), this broadband correction may be a bit too low, and instead a broadband correction of a factor of about 15–20 may be more reasonable.

We have also re-binned the available data for the X-ray binaries where simultaneous radio and X-ray points exist and where there are good mass measurements for the systems. The data set is described in GFP03, and references within; we have included data for the following low/hard state sources: GRO J0422+32, XTE J1118+480, 4U 1543-47, XTE J1550-564, Cyg X-1, V404 Cyg & GX 339-4. We have included data from GRS 1915+105 and the transient source sample of Fender & Kuulkers (2001) for the ‘very high state’. The transient source points are not based on strictly simultaneous data, and hence may have some systematic errors introduced, but ignoring these data points does not change the results substantially, because the points lie very close to the data for GRS 1915+105 and because most of the points in the high luminosity bin come from GRS 1915+105 in any case. As in the AGN case, we have excluded points where the data are upper limits (for fluxes) or lower limits (for masses), and we have applied the mass correction from MHD03 to the data. We have assumed a mass of $6 M_{\odot}$ for GX 339-4, the mass function measured by Hynes et al. (2003) and a distance of 4 kpc (Zdziarski et al. 1998), but we note that this is a lower

limit on the mass and not an actual measurement. We must include this source despite its not having an actual mass measurement because it is the only X-ray binary with simultaneous radio and X-ray data at the lowest luminosities. We have also tested the correlation assuming a mass of $9 M_{\odot}$ and have found that the results are not changed substantially.

In Figure 4.2, we have over-plotted the binned binary data with the data from the AGN. We have used the same binning ranges for the X-ray binary sample as for the AGN sample, but we note that there are no simultaneous radio and X-ray observations of X-ray binaries below about $10^{-6} L_{\text{Edd}}$ and very few in the range around $10^{-3} L_{\text{Edd}}$. Also, there are relatively few points in our X-ray binary sample very close to 10% of the Eddington luminosity because the radio data consists primarily of upper limits at this luminosity. We have also re-fit the AGN data without including the two ‘quenched’ bins in the correlation and we find that:

$$\log \frac{L_{\text{radio,corr}}}{L_{\text{Edd}}} = (0.64 \pm 0.09) \log \frac{L_X}{L_{\text{Edd}}} - (8.26 \pm 0.40), \quad (4.2)$$

values that correspond much more closely with the X-ray binary correlation found in GFP03. We note here that the low luminosity AGN and X-ray binaries show a very similar trend, and that the AGN correlation extends several orders of magnitude lower in luminosity than does the X-ray binary correlation. By analogy, this bolsters arguments that suggest that the quiescent state of X-ray binaries is merely an extension of the low/hard state, and that the jet will begin to dominate the total accretion power at very low luminosities (see e.g. Fender, Gallo & Jonker 2003). We also show in Figure 4.3 the ratio between the data points and the best fit to the non-quenched data. The AGN points with broadband luminosity at 3 per cent & 10 per cent of the Eddington luminosity are factors of ~ 5 (i.e. 1.7σ and 3.5σ , respectively) below the correlation. We note that due to the application of a broadband correction factor more appropriate to lower luminosity AGN, the 3 per cent and 10 per cent of Eddington values are likely to be underestimates by a factor of a few, and the points above a few percent of the Eddington limit in the plots should be moved a bit to the right. Sliding the points to the right would push them a bit more below the curve, so the quenching may actually be a bit stronger and more statistically significant than the factor of ~ 5 estimate.

4.3 Discussion

The high/soft state appears to exist in AGN of all masses in the sample which have broadband luminosities of order 5–10% L_{Edd} . The effect is not sensitive

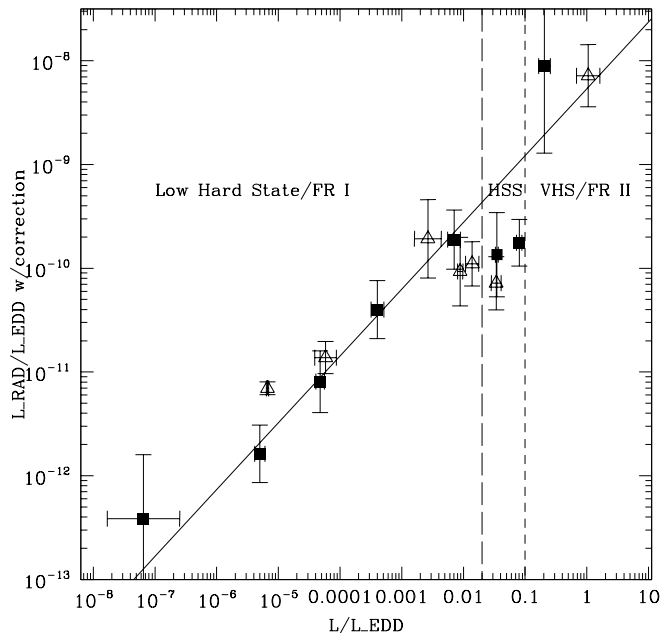


Figure 4.2: The same as Figure 4.1b, with the X-ray binaries included. The open triangles represent the X-ray binaries. The long-dashed vertical line indicates the transition luminosity between the high/soft state (HSS) and the low/hard state as measured in Maccarone (2003) and also is very close to the transition luminosity between FR I & II galaxies as determined by Ghisellini & Celotti (2001). The short-dashed vertical line indicates the estimated state transition luminosity between the high/soft state and the very high state (VHS). The fit to the data is the same as that presented in Figure 4.1.

to whether the systems classified as NLSy1's are included in the sample. The masses of the mean AGN in the bins where the downturn is seen are $5 \times 10^7 M_\odot$ and $6 \times 10^7 M_\odot$, clearly above the typical masses for the NLSy1's.

The observed correlations also help to underscore the importance of considering the radio-to-X-ray luminosity ratio as a measure of the radio loudness in addition to the more traditional radio-to-optical luminosity ratio. Such an approach does complicate comparisons with some of the historical literature on AGN and optical surveys of AGN tend to be wider and deeper than those in the X-rays. Still the optical emission in AGN sometimes is thermal emission from the accretion disc and sometimes is non-thermal emission from a jet; the relative contributions have dependences on black hole mass, redshift, viewing

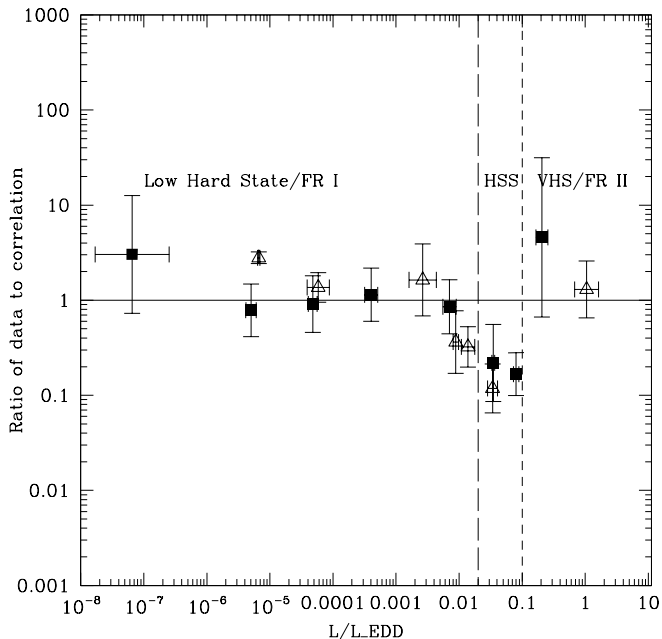


Figure 4.3: The ratio of the data in Figure 4.2 to the best fit to the data.

angle and Eddington fraction. The hard X-rays should always be dominated by emission from the Compton corona (unless one adopts an emission model such as that of MFF01 or Harris & Krawczynski 2002, in which case the hard X-ray emission should often be dominated by the jet). The greater homogeneity of emission mechanisms in the X-rays contrasted with the optical makes correlations discovered in the X-rays easier to interpret. Furthermore, correlations made in the X-ray will be easier to compare with correlations found in the stellar mass black hole candidates.

In hindsight, it is not surprising that the high/soft state exists at roughly the same luminosity for AGN as it does for X-ray binaries. The well-known work of Ledlow & Owen (1996) showed that the FR I radio galaxies lie systematically below the FR II radio galaxies in a plot of radio power versus R magnitude. Using empirical scaling relations between the radio power and bolometric luminosity, and between the R magnitudes and black hole masses, Ghisellini & Celotti (2001) found that the dividing line corresponds to about 2% of the Eddington luminosity. That the scaling relations used by Ghisellini & Celotti (2001) have considerable scatter, while there are very few sources on the ‘wrong’ side of the

dividing line between FR I and II galaxies seems may be taken as evidence that there is intrinsically a gap where there are no strong radio galaxies that would have been included in the 3C sample used in the Ledlow & Owen (1996) diagram. The gap, where the high/soft state AGN exist in reality, is then filled in by the low/hard state/FR I systems scattered upwards and very high state/FR II systems scattered downwards. Understanding where is the error in the theoretical predictions (Rozanska & Czerny 2000; Meier 2001) that soft states would not exist for such mass mass black holes remains an open question; indeed many other mechanisms for producing state transitions apart from those discussed above also predict a roughly $M^{-1/8}$ dependence of the state transition luminosities (e.g. Merloni 2003).

The quenching of the radio jets in the high/soft state range of luminosities seems not to be as extreme for the AGN as it is in the stellar mass systems; the AGN show a drop of a factor of only about 10 in the high/soft state. In the stellar mass black holes, the radio luminosity drops by a factor of at least 30–50 from the low/hard state correlation's extrapolation (Fender et al. 1999; Corbel et al. 2001). Probably this is partly from contamination of the high/soft state AGN luminosity range due to measurement errors on the masses of the black holes in the AGN and possibly also the hysteresis effects seen in the binary systems. Also, our initial broadband correction underestimates the real spectral correction factors for sources in this range, leading to an additional underestimate of the quenching effect.

The $L_X - L_{\text{radio}}$ correlation in MHD03 exhibits about 3 orders of magnitude of scatter. At least one order of magnitude is likely to come from the use of the velocity dispersion-black hole mass technique to measure most of the masses (e.g. Merritt & Ferrarese 2001), but this is unlikely to explain everything. An excellent candidate for the additional scatter would be black hole spin effects, since the black hole spin may affect jet power either directly, if the jet is the result of the extraction of black hole rotational energy (Blandford & Znajek 1977) or indirectly, if the jet is powered by the rotational energy of the inner disc, which should be larger for a rotating black hole (Blandford & Payne 1982). Given that the high mass stars which are the progenitors of stellar mass black holes have angular momenta much larger than the maximum angular momenta for black holes of the same mass, it would not seem too unreasonable for all stellar mass black holes to be rapidly rotating, as is suggested by some models for the high frequency quasi-periodic oscillations in the black hole binaries (Rezzolla et al. 2003). On the other hand, black hole-black hole mergers may contribute substantially to the spin evolution of the black holes in AGN and would tend to reduce the spins of most of the black holes produced in the mergers (Merritt

2002; Hughes & Blandford 2003). It would hence not be too surprising if the black holes in AGN show a much larger range of spins and of jet power at a given mass and luminosity. Testing this hypothesis may be possible through iron line spectroscopy with the planned Constellation-X mission, as iron lines have proved to be a powerful diagnostic of spin in AGN (see e.g. Wilms et al. 2001). It was found in MHD03 that the scatter in the correlation is reduced by eliminating sources in this range; we also find that the eliminating them makes slope of the correlation in the AGN closer to that found in the X-ray binaries.

More broadband spectroscopy should be undertaken on the putative high/soft state AGN to determine if the systems are truly identical to their lower mass counterparts; the work on NGC 4051 (McHardy et al. 2003) shows that there may be systematic spectral differences between the otherwise rather similar systems, as this system shows similar variability characteristics to the high/soft state of X-ray binaries, and a strong soft quasi-thermal component, but shows a substantially harder power law tail. This should be possible for the brightest sources with a combination of observations from INTEGRAL and from ground based optical telescopes.

A start on this investigation can be made with the existing data. Numerous studies of large samples of AGN suggest that the typical spectral index $\alpha \simeq -0.75$, where α is defined by $F(\nu) \propto \nu^\alpha$ (e.g. Wilkes & Elvis 1987; Nandra & Pounds 1994; Lawson & Turner 1997 – LT). From examining the individual spectra of the sources in the 2–10% of L_{Edd} range, we find that there are 15 sources, 3 of which are NLSy1's and hence are known to have strong soft X-ray excesses. Of the 12 non-NLSy1's, one is a Seyfert 2 galaxy in which the hypothesis of a strong soft X-ray excess is very difficult to test because of absorption, and one of the quasars, PG 0844+349 also shows evidence of rather strong absorption. One system (PG 1229+204) was rather faint and no spectral fit is available in the literature (see the discussion in LT). Of the 9 remaining systems, 5 clearly show soft excesses (Mkn 279 – see e.g. Weaver, Gelbord & Yaqoob 2001; NGC 7469 – see e.g. DeRosa, Fabian & Piro 2002; PG 0804+761 & PG 1211+143 – see e.g. George et al. 2000; Mkn 335 – see e.g. Turner & Pounds 1988), two show spectra softer than $\alpha = -0.95$ (PG 0052+251, see LT; & PG 0953+415 - George et al. 2000), one shows a fairly typical X-ray spectrum (PG 1307+085, see LT), and only one shows a spectrum harder than the typical quasar spectrum (PG 1613+658, see LT).

The sources with relatively soft spectra, but no clear soft excess have higher black hole masses than the sources with clear soft excesses (pushing their disc component's peak to lower energies since $T_{\text{disc}} \propto M_{\text{BH}}^{-1/4}$), and are at higher redshifts, so the observed soft X-rays probe a slightly higher energy in the rest

frame. One thus might expect to need to use the EUV to find their soft X-ray excesses. It is worth noting that the single truly hard X-ray spectrum belongs to a source which also shows the only flat radio spectrum among the sources (Falcke, Malkan & Biermann 1995; Ho 2002) and has an inferred luminosity just barely higher than 2% of L_{Edd} ; it may represent a source placed into the wrong bin in the correlation due to measurement errors or hysteresis. Thus while we have applied ‘mix-and-match’ criteria to discuss the spectra, there seems to be fairly suggestive anecdotal evidence that the spectra of the systems which are well below the GFP03, MHD03 & FKM03 correlation curves and which lie in the 2–10 per cent of L_{Edd} range have systematically softer X-ray spectra than the sources; the correlations between X-ray hardness and radio loudness found by Elvis et al. (1994) and by Zdziarski et al. (1995) using the classical definition of radio loudness (i.e. the radio to optical flux ratio) rather than the radio-to-bolometric luminosity ratio hold up.

Acknowledgments

TM thanks Mike Eracleous for useful discussions which helped to stimulate this work. We thank the referee, Andrea Merloni, for useful suggestions which improved this work.

References

- Blandford R. D. & Znajek R. L., 1977, MNRAS, 179, 433
Blandford R. D. & Payne D. G., 1982, MNRAS, 199, 883
Chen K., Halpern J. P. & Filippenko A. V., 1989, ApJ, 339, 742
Corbel S. et al., 2001, ApJ, 554, 43
De Rosa A., Fabian A. C. & Piro L., 2002, MNRAS, 334, L21
Elvis M., et al., 1994, ApJS, 95, 1
Epstein E. E., Fogarty W. G., Mottmann J. & Schneider E., 1982, AJ, 87, 449
Eracleous M. & Halpern J. P., 1994, ApJS, 90, 1
Esin A. A., McClintock J. E. & Narayan R., 1997, ApJ, 489, 865
Falcke H., K rding E. & Markoff S., 2003, A&A, 414, 895
Falcke H., Malkan M. A., & Biermann P. L., 1995, A&A, 298, 375
Fanaroff B. L. & Riley J. M., 1974, MNRAS, 167, 31
Fender R. P., 2005, to appear in ‘*Compact Stellar X-Ray Sources*’, Eds. W.H.G. Lewin and M. van der Klis, Cambridge University Press (astro-ph/0303339)
Fender R. P. et al., 1999, ApJL, 519, 165
Fender R. P. & Kuulkers E. 2001, MNRAS, 324, 923

- Fender R. P., Gallo E. & Jonker P., 2003, MNRAS, 343, L99
 Gallo E., Fender R. P. & Pooley G. G., 2003, MNRAS, 344, 60 (GFP03)
 George I. M. et al. , 2000, ApJ, 531, 52
 Ghisellini G. & Celotti A., 2001, A&A, 379, L1
 Gierliński M. et al. , 1999, MNRAS, 309, 496
 Hardcastle M., 1995, in *'The XXVIIth YERAC'*, Eds. D.A. Green and W. Steffen, Cambridge University Press
 Harmon B. A. et al., 1997, ApJL, 477, 85L
 Harris D. E. & Krawczynski H., 2002, ApJ, 565, 244
 Ho L., 1999, ApJ, 516, 672
 Ho L., 2002, ApJ, 564, 120
 Hughes S.A & Blandford R. D., 2003, ApJL, 585, 101
 Hynes R. I., Steeghs D., Casares J., Charles P. A. & O'Brien K., 2003, ApJL, 583, 95
 Ichimaru S., 1977, ApJ, 214, 840
 Khanna R., 1999, *'Stellar Dynamos: Nonlinearity and Chaotic Flows'*, ASP Conference Series 178, Eds. M. Nunez and A. Ferriz-Mas., ASP: San Francisco, 57
 Klein-Wolt M. et al., 2002, MNRAS, 331, 745
 Lawson A. J. & Turner M. J. L., 1997, MNRAS, 288, 920
 Ledlow M. J. & Owen F. N., 1996, AJ, 112, 9
 Livio M., Ogilvie G. I. & Pringle J. E., 1999, ApJL, 512, 100
 Maccarone T. J. & Coppi P. S., 2003, MNRAS, 336, 817
 Markoff S., Falcke H. & Fender R. P., 2001, A&A, 372, 25 (MFF01)
 Marscher A.P. et al., 2002, Nature, 417, 625
 McHardy I., Uttley P., Mason K., & Page M., 2003, in *'The Restless High Energy Universe'*, Nuclear Physics B, Eds. van den Heuvel, Wijers & in 't Zand
 Meier D. L., 2001, ApJL, 548, L9
 Meier D. L., Koide S. & Uchida Y., 2001, Science, 291, 84
 Merloni A., 2003, MNRAS, 341, 1051
 Merloni A., Heinz S. & Di Matteo T., 2003, MNRAS, 345, 1057 (MHD03)
 Merritt D., 2002, ApJ, 568, 998
 Merritt D. & Ferrarese L., 2001, ApJ, 547, 140
 Miller J. M. et al., 2001, ApJ, 546, 1055
 Miyamoto S., Kimura K., Kitamoto S., Dotani T. & Ebisawa K., 1991, ApJ, 383, 784
 Miyamoto S., Kitamoto S., Hayashida K. & Egoshi, W., 1995, ApJL, 442, 13
 Nandra K. & Pounds K. A., 1994, MNRAS, 268, 405
 Narayan R. & Yi I., 1994, ApJL, 428, L13

- Novikov I. D. & Thorne K. S., 1973, in *'Black Holes'*, Eds. C. De Witt & B. De Witt, New York:Gordon & Breach, 343
- Nowak M.A., 1995, PASP, 107, 1207
- Pounds K. A., Done, C. & Osborne, J. P., 1995, MNRAS, 277, L5
- Rezzolla L., Yoshida S., Maccarone T. J. & Zanotti O., 2003, MNRAS, 344, L37
- Rozanska A. & Czerny B., 2000, A&A, 360, 1170
- Shakura N. I. & Sunyaev R. A., 1973, A&A, 24, 337
- Shakura N. I. & Sunyaev R. A., 1976, MNRAS, 175, 613
- Shapiro S. L., Lightman A. P. & Eardley D. M., 1976, ApJ, 204, 187
- Smith D. M., Heindl W. A. & Swank J. H., 2002, ApJ, 569, 362
- Tananbaum H., Gursky H., Kellogg E., Giacconi R. & Jones C., 1972, ApJL, 177, LL
- Thorne K. S. & Price R. H., 1975, ApJL, 195, 101
- Turner T. J. & Pounds K. A., 1988, MNRAS, 232, 463
- Waltman E. B., Foster K. S., Pooley, G.G., Fender, R.P. & Ghigo, F.D., 1996, AJ, 112, 2690
- Weaver K. A., Gelbord J. & Yaqoob, T., 2001, ApJ, 550, 261
- Wilkes B. J. & Elvis, M., 1987, ApJ, 323, 243
- Wilms J., et al., 2001, MNRAS, 328L, 27
- Zdziarski A. A. et al., 1995, ApJL, 438, L63
- Zdziarski A. A., et al., 1998, MNRAS, 301, 435
- Zdziarski A. A. 2000, in *'Highly Energetic Physical Processes and Mechanisms for Emission from Astrophysical Plasmas'*, Eds. P. C. H. Martens, S. Tsuruta, & M. A. Weber, San Francisco: ASP, 153

CHAPTER 5

A TRANSIENT LARGE-SCALE RELATIVISTIC RADIO JET FROM GX339-4

Elena Gallo, Stephane Corbel, Rob Fender, Tom Maccarone & Tasso Tzioumis
Monthly Notices of the Royal Astronomical Society 347, L52-L56 (2004)

We report on the formation and evolution of a large-scale, synchrotron emitting jet from the black hole candidate and X-ray binary system GX 339–4. In 2002 May, the source moved from a low/hard to a very high X-ray state, contemporaneously exhibiting a very bright optically thin radio flare. Further observations with the Australia Telescope Compact Array have tracked the formation of a collimated structure extending to about 12 arcsec, with apparent velocity greater than $0.9c$. The luminosity of the outflow seems to be rapidly decreasing; these observations confirm that transient large-scale jets are likely to be common events triggered by X-ray state transitions in black hole X-ray binaries.

5.1 Introduction

The X-ray binary GX 339–4 comprises a compact primary which is a strong Black Hole Candidate (BHC), with mass function of $5.8 \pm 0.5 M_{\odot}$ (Hynes et al. 2003) and a secondary which is likely to be an evolved low mass star (Shahbaz, Fender & Charles 2001; Chaty et al. 2002). The system has an orbital period of 1.75 days (Hynes et al. 2003) and is located at a distance of at least 4 kpc (Zdziarski et al. 1998; see also Shahbaz, Fender & Charles 2001 and Maccarone 2003), with an orbital inclination of less than 60° to the line of sight, as inferred from the lack of eclipses (Cowley et al. 2002). GX 339–4 has been a key source in our understanding of the relation between accretion and the production of relativistic jets. It was the first BHC to reveal a positive correlation between radio and X-ray fluxes in the low/hard X-ray state (Hannikainen et al. 1998, later quantified by Corbel et al. 2003), and to demonstrate an association between the ‘quenching’ of core radio emission and the transition to a high/soft X-ray

state (Fender et al. 1999; see e.g. Done 2001, for a review on X-ray states and Fender 2005 for a comparison of radio and X-ray behaviour in Galactic BHCs). After spending almost three years in ‘quiescence’, GX 339–4 re-brightened in X-rays at the end of 2002 March (Smith et al. 2002) and changed rapidly to a soft outburst state, undergoing a dramatic state change in 2002 May. This transition was associated with a bright radio flare (Fender et al. 2002), reaching four to five times the brightest radio level ever observed from the source (see Corbel et al. 2000 for the long-term behaviour of GX 339–4). By analogy with other systems (e.g. XTE J1550–564, Corbel et al. 2001), this flare was likely to be the signature of a powerful ejection event. Repeated radio observations of GX 339–4 have indeed confirmed this association: the 2002 radio flaring has led to the formation of a large-scale relativistic radio jet, whose morphology and dynamics will be presented in the course of this Letter.

5.2 ATCA observations

The Australia Telescope Compact Array (ATCA) performed eight continuum observations of GX 339–4 at roughly regular intervals between 2002 April and August, simultaneously at 4800 MHz (6.3 cm) and 8640 MHz (3.5 cm). Three further observations were performed in 2003 January, March and May at four frequencies: 1384 MHz (21.7 cm), 2368 MHz (12.7 cm), 4800 and 8640 MHz.

The ATCA synthesis telescope is an east-west array of six 22 m antennas with baselines ranging from 31 m to 6 km; it uses orthogonal polarized feeds and records full Stokes parameters (I, Q, U, V). The target was systematically offset by about 10 arcsec from the array phase centre, in order to avoid possible artifacts due to system errors such as DC-offsets. In each observation, PKS 1934–638 was used for absolute flux and bandpass calibration, while either PMN 1603–4904, PMN 1650–5044 or PMN 1726–5529 was the phase calibrator for antenna gains and phases. The data reduction process and image analysis have been carried out with the Multichannel Image Reconstruction, Image Analysis and Display (MIRIAD) software package (Sault, Teuben & Wright 1995; Sault & Killeen 1998). Dates of ATCA observations are indicated in Figure 5.1, superimposed on the *Rossi X-ray Timing Explorer*/All Sky Monitor (RXTE/ASM) 2–12 keV light curve of the system.

5.2.1 Outburst and optically thin core radio flare

Smith et al. (2002) reported an increase in the X-ray flux from GX 339–4, which had been in quiescence for almost three years (Kong et al. 2000), on 2002 March

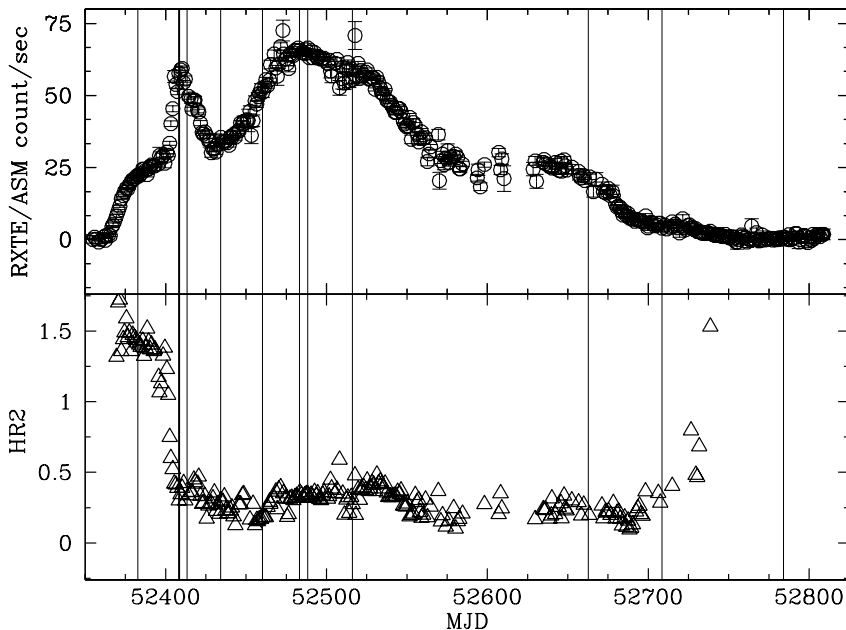


Figure 5.1: X-ray light curve and hardness ratio HR2 (5–12 keV / 3–5 keV count rate, only plotted for fractional errors < 0.25) of GX 339–4 as monitored by the *Rossi X-ray Timing Explorer*/All Sky Monitor. At the end of 2002 April, following three years of ‘quiescence’, the source re-brightened in X-rays, contemporaneously undergoing a very bright radio flare (on 2002 May 14, MJD 52408). The times of our ATCA observations are indicated with solid vertical lines; the thick line marks the peak radio level of ~ 55 mJy.

26 (MJD 52360). The source reached a peak flux (2–12 keV) of ~ 0.8 Crab on 2002 May 15 (MJD 52410), followed by a decrease to ~ 0.4 Crab, and a secondary rise to ~ 0.9 Crab around MJD 52500, after which GX 339–4 has started a slow return to ‘quiescence’ (reached by the time of writing). The hardness ratio HR2 suggests that a rapid transition from a low/hard to a softer X-ray state took place a few days before the (first) outburst peak, although colour and timing analysis of the RXTE Proportional Counter Array data indicates a smooth transition from a low/hard to a very high state in the rising phase, followed by a high/soft state (or possibly an ‘oscillating’ very-high state) after the peak (Belloni et al. 2002; Nespoli et al. 2003).

ATCA observations performed between 2002 April and June have detected the brightest radio flare ever observed by the system, which reached a peak flux

Table 5.1: Image properties of GX 339–4 as observed by ATCA at 8640 and 4800 MHz between 2002 April and August. Fluxes and positions have been derived by fitting the knots with point-like sources; position offsets are expressed in arcsec with respect to the binary core position. Flux density errors correspond to the rms noise levels in the final, naturally weighted images; upper limits are given at a 3σ confidence level.

MJD (day)	8640 MHz flux (mJy)	offset (a) α, δ (arcsec)	4800 MHz flux (mJy)	offset (a) α, δ (arcsec)	α ($S_\nu \propto \nu^\alpha$)
52382.75	13.49±0.08	-0.05, +0.07	12.97±0.07	-0.05, +0.09	+0.07±0.01
52408.48	10–40	...	10–55	...	-0.52±0.01(b)
52413.42	12.27±0.16	-0.12, +0.13	20.39±0.23	-0.12, +0.10	-0.86±0.03
52434.28	< 0.3	...	< 0.4	...	
52460.29	10.62±0.15	-0.17, -0.05	14.89±0.19	-0.22, -0.00	-0.57±0.03
52483.20	10.33±0.18	-0.25, -0.02	13.84±0.29	-0.27, -0.00	-0.50±0.04
52488.28	9.45±0.17	-0.22, -0.08	11.98±0.25	-0.30, -0.03	-0.40±0.05
52516.12	1.51±0.13	-0.63, +0.02	2.47±0.07	-0.61, +0.20	-0.83±0.14

(a) absolute positional uncertainty is of 0.26 arcsec between 2002:04:18 and 2002:06:09, 0.35 arcsec between 2002:07:05 and 2002:08:30. (b) Spectral index as measured at the peak value of 55 mJy.

density of about 55 mJy on May 14 (MJD 52408), almost contemporaneously with the (first) X-ray peak.

The radio flare light curves at 4800 and 8640 MHz are shown in Figure 5.2 together with the temporal evolution of the spectral index, which decreased from $\alpha \sim 0$ down to $\alpha \sim -0.5$ (where $\alpha = \Delta \log S_\nu / \Delta \log \nu$). As the spectral index does not significantly decrease during the last two hours prior to the flare peak, the flux rise in this time interval can not be due to decreasing optical depth, as predicted by adiabatic expansion models (*e.g.* van der Laan 1966), but instead represents a finite phase of particle acceleration.

We can derive the minimum energy associated with the emitting component during the rise, following the formulation by Longair (1994). Assuming an optimal jet viewing angle $\theta \sim 26^\circ$, for which the maximum apparent velocity of the jet is achieved (*i.e.* a jet semi-opening angle given by $\cos \theta = \beta$ with $\beta = 0.9$, see next Section), and a volume of the emitting region of about $9 \times 10^{44} \text{ cm}^3$ (given by $4/3 \pi (c \times t_{\text{rise}})^3$, with $t_{\text{rise}} = 5.5$ hours), the corresponding minimum energy

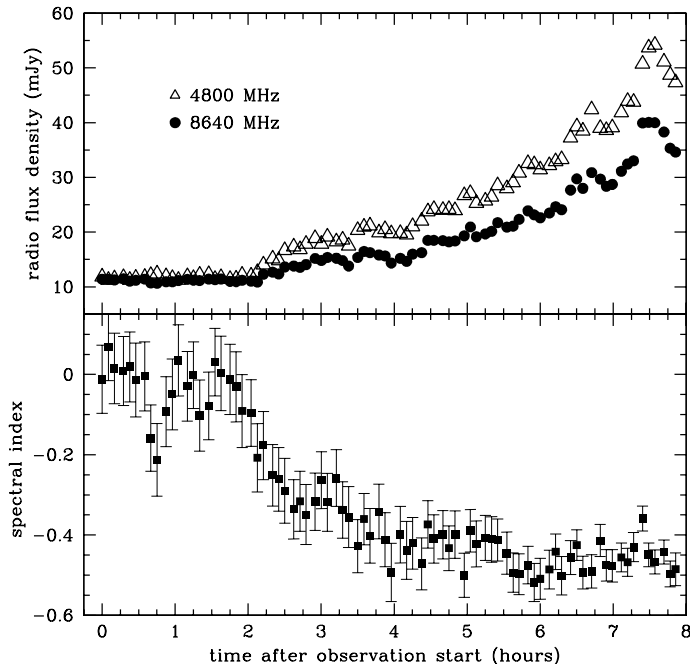


Figure 5.2: Radio light curves (5 minute averages) of GX 339-4 on 2002 May 14 (MJD 52408) at 8640 MHz and 4800 MHz are plotted on the top panel (the typical errorbar is smaller than the marker size); the flux density at 4800 MHz rose from ~ 12 to ~ 55 mJy – four to five times the brightest radio level ever observed from the source – in 5.5 hours. Temporal evolution of the spectral index α (where $S_\nu \propto \nu^\alpha$) on the bottom panel: as the flux density starts to rise, 2 hours after the beginning of the observation, the spectral index starts to decrease.

required is $E_{\min} \simeq 5 \times 10^{39}$ erg. The associated magnetic field for which the energy in relativistic particles equals the magnetic energy is of ~ 8 mG.

The kinetic energy in case of a pure e^+e^- plasma would be $E_{\text{kin}} = (\Gamma - 1) \times E_{\min} \sim 7 \times 10^{39}$ erg. If there is one (cold) proton for each electron, then $E_{\text{kin}} \sim 5 \times 10^{40}$ erg, with an associated mass of $\sim 4 \times 10^{19}$ g. In order to accumulate such mass for a $10 M_\odot$ BH accreting at a few per cent of the Eddington rate (as indicated by the X-ray luminosity), it would have taken a few minutes. The (much longer) observed rise time of 5.5 hours would be of the same order of the injection time-scale if only a few per cent of the accreted mass was loaded into the jet.

The minimum jet powers equal 3×10^{35} and 2×10^{36} erg s^{-1} , for e^+e^- and

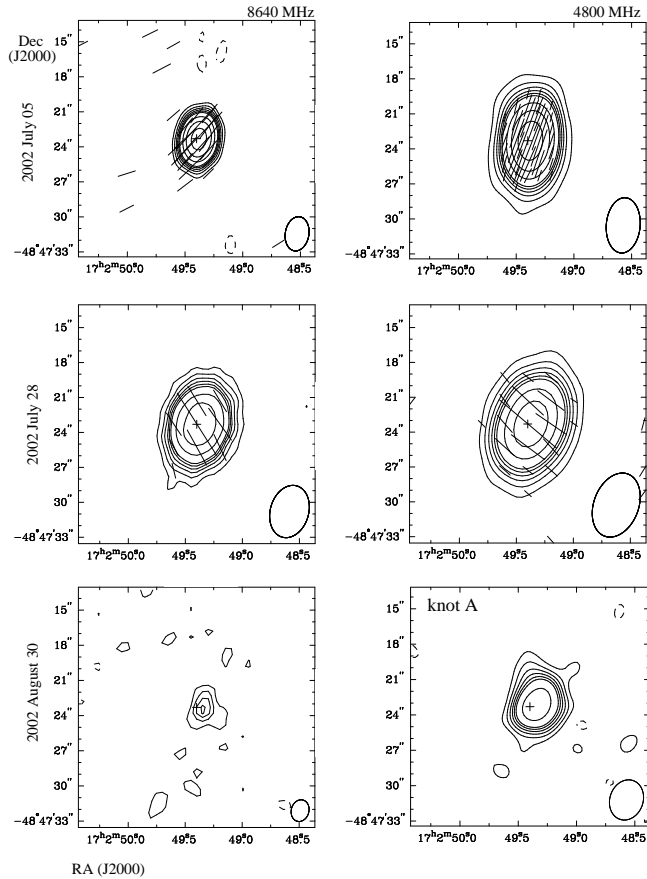


Figure 5.3: Naturally weighted ATCA images of GX 339–4 at 8640 and 4800 MHz, left and right panels; from top to bottom: 2002 July 05, July 28 and August 30. The contour interval (CI) is chosen as the rms noise in the final image and plotted contours are at $-2, 2, 4, 8, 12, 20, 32, 52, 84, 136$ times the CI. Linear polarization E vectors (when significantly detected) are superimposed upon the contour maps in the top and centre panels, showing a clear rotation in the position angles. Synthesized beams appear on the bottom right corner of each image. The cross indicates the binary core position. By 2002 August 30 the radio source is significantly displaced from the core.

baryonic plasma respectively. In the last 20 minutes of the observation, after reaching the peak level of ~ 55 mJy at 4800 MHz, the flux density decreases

linearly with time with the same slope at both frequencies, indicating that the main cooling process is adiabatic (synchrotron and Compton cooling times scale with the frequency as $\nu^{-0.5}$); the observed decline is much shallower than that predicted by adiabatic expansion models without any additional energy injection (*e.g.* $S_\nu \propto t^{-4.8}$, van der Laan 1966).

The position of the radio source on 2002 April 18, when the source was in a bright, flat-spectrum radio state prior to the outburst, is consistent with the binary centre as given by Corbel et al. (2000). Radio emission from GX 339–4 dropped to undetectable levels by 2002 June 09 (<0.4 mJy at 4800 MHz), possibly corresponding to extinction of the May 14 flare.

Although further ATCA observations are consistent with a single fading radio source (see Table 5.1), observations at 843 MHz performed with the Molonglo Observatory Synthesis Telescope (MOST) indicate more complex behaviour over the period 2002 June–July (Campbell-Wilson & Hunstead, private communication), possibly associated with multiple ejection events. A more detailed analysis of the radio variability over this period, including the MOST data, will be presented in a future paper.

Figure 5.3 shows radio maps of GX 339–4 at 8640 and 4800 MHz on 2002 July 05, July 28 and August 30. The position of the radio source as imaged by ATCA is displaced by about 0.2 arcsec to the western side (right on the maps) of the binary core on 2002 July 05, July 28 and August 02 (not shown), although, given a total positional uncertainty of 0.3 arcsec in this set of observations, these coordinates are still consistent with the binary core. By 2002 August 30, however, the displacement to the western side is of 0.6 arcsec (in position angle $PA = -72^\circ \pm 32^\circ$; PA is defined positive north–east) at both frequencies, indicating the formation of a physically separated component. If this event was powered by the May 2002 flare, that would imply a proper motion of about 6 mas/day, that is a minimum projected velocity of $0.1c$ (for the minimum distance of 4 kpc).

5.2.2 Extended radio jet

We expect the bright radio flare(s) of GX 339–4 during its 2002 outburst to be associated with powerful ejection event(s) fed by the source central engine. In fact, ATCA has been observing GX 339–4 at regular intervals again in 2003, tracking the formation of a large-scale, relativistic jet. Figure 5.4 and Table 5.2 present the result of these observations at 4800 MHz, where the most notable structures have appeared.

By 2003 January, an extended outflow composed of two separate ‘plasmons’ has developed in the same direction of the western component detected on 2002

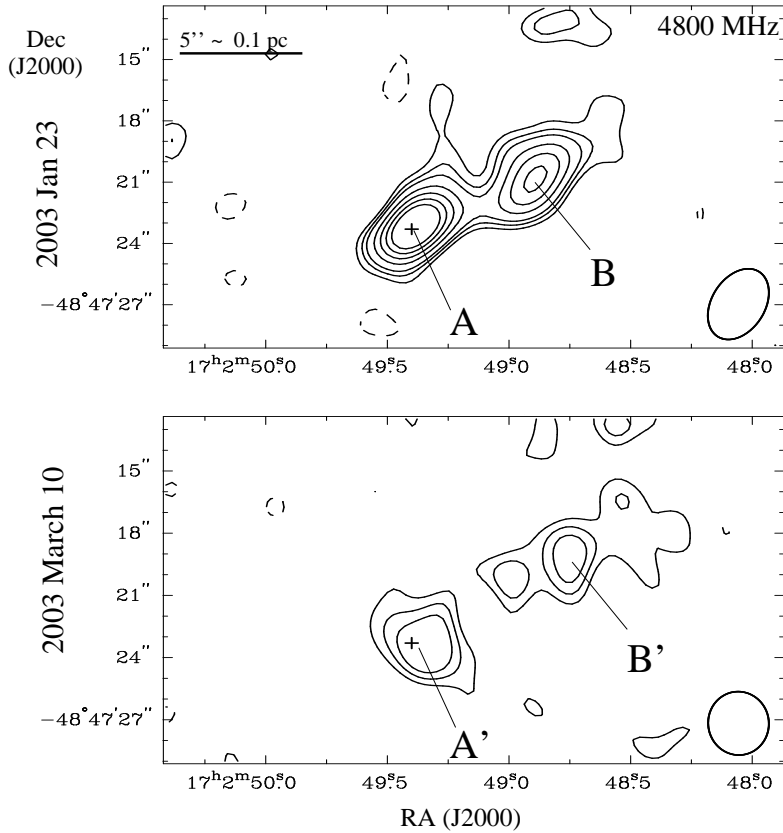


Figure 5.4: Naturally weighted 4800 MHz maps of the extended jet developed by GX 339–4. 2003 January 23 is on the top with a peak flux density of 0.66 mJy/beam and convolved with a Gaussian beam 3.62×2.24 arcsec in $PA = -22^\circ$. Contours are at $-2, 2, 4, 6, 8, 10, 12$ times the rms noise level of 0.04 mJy. March 10 2003 on the bottom panel, with a peak flux density of 0.25 mJy/beam and convolved with a Gaussian beam 3.06×2.47 arcsec in $PA = +1.7^\circ$. Contours are at $-2, 2, 4, 6, 8, 10, 12$ times the rms noise level of 0.02 mJy. Knot B' is displaced by 6.9 arcsec from the binary core: if powered by the May 2002 flare, this would correspond to a projected velocity of about 28 mas/day, that is a jet with velocity higher than $0.6c$ (for $D \gtrsim 4$ kpc).

August 30: the first structure, knot A, is displaced by 0.3 arcsec north-west from the core, while the other component, knot B, is displaced by 5.5 arcsec in $PA = -$

$62^\circ \pm 2^\circ$ with respect to the binary core, implying a minimum velocity of $\sim 0.5c$ if associated with the 2002 May flare. It is worth stressing that this value only represents a lower limit on the velocity not only because of the lower limit on the distance, but also because it is likely that the knots were energised by the outflow somewhat earlier than when they were observed (see next Section). Both knots display steep optically thin radio spectrum, with $\alpha_A = -0.98 \pm 0.03$ and $\alpha_B = -0.96 \pm 0.08$ (probably either because we are looking above the cooling break frequency, or because of resolution effects). An elongated structure is visible at 2368 MHz too.

By 2003 March 10 (MJD 52708) the outflow has faded; at least two components are distinguishable at 4800 MHz: knot A' and B', probably associated with knot A and B from January 23. They are displaced respectively by 0.5 and 6.9 arcsec (with a relative error of 0.3 arcsec), with $PA(A') = -83^\circ \pm 26^\circ$ and $PA(B') = -66^\circ \pm 2^\circ$. The spectrum remains optically thin, with $\alpha_A = -0.98 \pm 0.10$ (while knot B' is significantly detected at 4800 MHz only). Assuming again an association with the 2002 May flare, the separation between knot B' and the binary core (6.9 arcsec) corresponds to a velocity of $0.6c$ at 4 kpc. The jet *head* in the 4800 MHz map is about 12 arcsec away from the core, implying a projected extension of 0.23 pc at 4 kpc and a minimum velocity of $0.9c$. If GX 339–4 was instead at a distance of at least 5.6 kpc, as estimated from the upper limit on the magnitude of the secondary star (Shahbaz, Fender & Charles 2001), the jet would become *superluminal*, with apparent velocity higher than $1.3c$; while, given a minimum distance of 7.6 kpc, as inferred by Maccarone (2003) from the typical soft-to-hard X-ray state transition luminosity of X-ray binaries, the jet apparent velocity would be higher than $1.8c$.

By 2003 May 25 (MJD 52784), the isolated optically thin knots have faded below detectable levels at all wavelengths. Instead, a central component has re-brightened at the binary core position, with peak flux density of 0.9 mJy at 8640 MHz. Core emission at four frequencies is consistent with an inverted spectrum ($\alpha = +0.72 \pm 0.04$), characteristic of an optically thick synchrotron jet, indicating the source core return to a hard state. Table 5.3 lists core flux densities (1σ upper limits on the optically thin components of the extended jet are given by their errors, *i.e.* rms noise levels) at four frequencies. No counter-jet has been detected so far.

5.2.3 Linear polarization

Linearly polarized emission is significantly detected at three epochs: on 2002 May 14, when the powerful flare was detected, the mean polarization level is of 4% at 4800 MHz and of 9% at 8640 MHz, with mean polarization angles:

Table 5.2: Image properties of the large-scale jet developed by GX 339–4 at 4800 MHz. The absolute positional error, mainly given by the uncertainty on the phase calibrator position (here PMN 1603–4904), is of 0.26 arcsec.

Date (UT time)	MJD (day)	4800 MHz flux (mJy)	offset α, δ (arcsec)	spectral index $\alpha, (S_\nu \propto \nu^\alpha)$
2003:01:23	52662.67			
knot A		0.66±0.04	−0.25 +0.22	−0.98 ± 0.03
knot B		0.47±0.04	−4.88 +2.54	−0.96 ± 0.08
2003:03:10	52708.56			
knot A'		0.25±0.04	−0.55, −0.07	−0.98 ± 0.10
knot B'		0.21±0.04	−6.28, +2.80	(a)

(a) knot B' is significantly detected at 4800 MHz only.

PA(4800) = $-35^\circ \pm 3^\circ$ and PA(8640) = $-47^\circ \pm 2^\circ$. On 2002 July 05, about 5% of the flux is linearly polarized at both 4800 and 8640 MHz, with electric field vectors in position angle PA(4800) = $-21^\circ \pm 3^\circ$ and PA(8640) = $-56^\circ \pm 6^\circ$. A comparable polarization level is seen on 2002 July 28: position angles have switched to PA(4800) = $+56^\circ \pm 5^\circ$ and PA(8640) = $+33^\circ \pm 6^\circ$ (E vectors are plotted in Figure 5.3 superimposed upon the contour maps). The rotations Δ PA(4800 MHz) and Δ PA(8640 MHz) are consistent between 2002 July 05 and July 28, likely reflecting an overall rotation of the projected magnetic field of the emission region. The rotation angle between the two frequencies is between $24^\circ - 46^\circ$ on July 05 and between $13^\circ - 35^\circ$ on July 28, indicative of foreground Faraday rotation; if so, we get a lower limit of about 100 rad m^2 on the rotation measure. No significant linearly polarized emission is detected in any of the other 2002 observations when the source was bright enough to detect a polarized signal at a level of a few per cent (see Table 5.1 for upper limits). In particular, linear polarization is lower than 1% by 2002 April 18, when the optically thick core emission is seen ($\alpha = +0.07$); for comparison, Corbel et al. (2000) detected about 2% of linear polarization at 8704 MHz in 1997 February, with a flux of 8–9 mJy and a similar optically thick spectrum ($\alpha = 0.11-0.23$).

5.3 Summary and discussion

The main result established in this work is the formation of a large-scale relativistic radio jet powered by GX 339–4 during its 2002 outburst: this association indicates that large-scale outflows are likely to be *common* following any major radio flare triggered by a hard-to-soft(er) X-ray state transition (see *e.g.* Harmon et al. 1995; Fender & Kuulkers 2001).

How does the large-scale jet develop? The position of the radio source detected by ATCA is consistent with the binary core until the beginning of 2002 August. Observations between the end of 2002 August and 2003 March reveal the presence of at least two physically separated components: the first to appear, always brighter and closer to the binary core (knot A-A'), has a mean separation of 0.5 ± 0.1 arcsec to the western side of the core, while its density flux decreases by a factor 10 in about 220 days. The second component – always fainter – first appears in the 2003 maps (knot B-B' in Figure 5.4) and is displaced by about 7 arcsec from the binary core in $PA = -64^\circ \pm 2^\circ$. Once they have appeared, both knots decline in flux while their positions remain unchanged within uncertainties, unlike *e.g.* in GRS 1915+105, where the observed ejecta are consistent with simple ballistic bulk motions (Rodríguez & Mirabel 1999; Fender et al. 1999). The large-scale jet of GX 339-4 seems instead to be better explained in terms of *shock waves* formed within the jet itself and/or by the interaction of an underlying highly relativistic outflow with ambient matter.

Polarization analysis at three epochs shows a significant rotation of the electric vector position angle at two frequencies, indicating a change in the projection of the magnetic field on the plane of the sky. The large-scale jet position angle ($PA = -64^\circ \pm 2^\circ$) is consistent with that of the jet-like extension in the 8640 MHz map of GX 339–4 observed by ATCA in 1996 July (Fender et al. 1997). In addition, Corbel et al. (2000), analysing the persistent radio emission of GX 339–4 while in the low/hard X-ray state, found a similar PA for the electric field vector (expected to be parallel to the magnetic field vector in case of optically thick spectrum) of the linearly polarized signal, indicating a rather stable jet orientation over the years. Persistent large-scale radio jets observed in 1E 1740.7–2942 (Mirabel et al. 1992) and GRS 1758–258 (Rodríguez, Mirabel & Martí 1992) have been found to extend up to 1–3 pc; in the case of GRS 1915+105 instead, relativistic ejecta were tracked up a projected distance of 0.08 pc (Mirabel & Rodríguez 1999), while in the large-scale X-ray jet powered by XTE J1550–564 (Corbel et al. 2002), the eastern jet has been detected to a projected physical separation of 0.75 pc covered in 4 years. The large-scale radio jet of GX 339–4 displays something similar, with a projected extension of 0.23 pc (at 4 kpc) cov-

Table 5.3: Core flux densities (mJy) from GX 339–4 on 2003 May 25 (MJD 52784); the spectrum is optically thick, with $\alpha = 0.72 \pm 0.04$.

1384 MHz	2368 MHz	4800 MHz	8640 MHz
< 0.57	0.39 ± 0.08	0.60 ± 0.04	0.94 ± 0.06

ered in about 250 days (if associated with the May 2002 radio flare). Scheduled *Chandra* observation will discover if the jet is active in X-rays as well, possibly confirming the similarity with XTE J1550–564 (Corbel et al. 2002; Kaaret et al. 2003; Tomsick et al. 2003), where the X-ray jet is still capable of accelerating particles up to TeV energies four years after the main ejection event.

Acknowledgments

We thank Dick Hunstead and Duncan Campbell-Wilson for kindly providing us with preliminary results of the MOST observations. The Australia Telescope is funded by the Commonwealth of Australia for operation as a National Facility managed by CSIRO. RXTE/ASM results are provided by the ASM/XTE team at MIT.

References

- Belloni T., Nespoli E., Homan J., van der Klis M., Lewin W. H. G., Miller J. M., Mendéz M., 2002, in *New Views on Microquasars*, Proc. of the Fourth Microquasars Workshop, Ed.: Ph. Durouchoux, Y. Fuchs, and J. Rodríguez, Center for Space Physics: Kolkata (India), 75
- Chaty S., Mirabel I. F., Goldoni P., Mereghetti S., Duc P. A., Martí J., Mignani R. P., 2002, MNRAS, 331, 1065
- Corbel S. et al. , 2001, ApJ, 554, 43
- Corbel S., Nowak M. A., Fender R. P., Tzioumis A. K., Markoff S., 2003, A&A, 400, 1007
- Corbel S., Fender R. P., Tzioumis A. K., Nowak M., McIntyre V., Durouchoux P., Sood R., 2000, A&A 359, 251

- Corbel S., Fender R. P., Tzioumis A. K., Tomsick J. A., Orosz J. A., Miller J. M., Wijnands R., Kaaret P., 2002, *Science*, 298, 196
- Cowley A. P., Schmidtke P. C., Hutchings J. B., Crampton D., 2002, *ApJ*, 123, 1741
- Done C., 2001, *AdSpR*, 28, 255
- Fender R. P., 2005, to appear in '*Compact Stellar X-Ray Sources*', Eds. W. H. G. Lewin and M. van der Klis, Cambridge University Press (astro-ph/0303339)
- Fender R. P. & Kuulkers E., 2001, *MNRAS*, 324, 923
- Fender R. P., Spencer R. E., Newell S. J., Tzioumis A. K., 1997, *MNRAS*, 286, L29
- Fender R. P., Corbel S., Tzioumis A. K., Tingay S., Brocksopp C., Gallo E., 2002, *ATel* 107
- Fender R. P., Garrington S. T., McKay D. J., Muxlow T. W. B., Pooley G. G., Spencer R. E., Stirling A. M., Waltman E. B., 1999, *MNRAS*, 304, 865
- Fender R. P. et al. , 1999, *ApJ*, 519, L165
- Hannikainen D. C., Hunstead R. W., Campbell-Wilson D., Sood R. K., 1998, *A&A*, 337, 460
- Harmon B. A., 1995, *Nature*, 374, 703
- Hynes R. I., Steeghs D., Casares J., Charles P. A., O'Brien K., 2003, *ApJ*, 583L
- Kaaret P., Corbel S., Tomsick J. A., Fender R. P., Miller J. M., Orosz J. A., Tzioumis A. K., Wijnands R., 2003, *ApJ*, 582, 945
- Kong A. K. H., Kuulkers E., Charles P. A., Homer L., 2000, *MNRAS*, 312, L49
- Longair M. S., 1994, '*High Energy Astrophysics*', Cambridge University Press
- Maccarone T. J., 2003, *A&A*, 409, 697
- Mirabel I. F., Rodríguez L. F., *ARA&A*, 1999, 37, 409
- Mirabel I. F., Rodríguez L. F., Cordier B., Paul J., Lebrun F., 1992, *Nature*, 358, 215
- Nespoli E., Belloni T., Homan J., Miller J. M., Mendéz M., van der Klis M., 2003, *A&A*, 412, 325
- Rodríguez L. F., Mirabel I. F., 1999, 511, 398
- Rodríguez L. F., Mirabel I. F., Martí J., 1992, *ApJ*, 401, L15
- Sault R. J., Killeen N. E. B., 1998, '*The Miriad User's Guide*', Sydney: Australia Telescope National Facility
- Sault R. J., Teuben P. J., Wright M. C. H., 1995, '*Astronomical Data Analysis Software and Systems IV*', Ed.: R. A. Shaw, H. E. Payne, and J. J. E. Hayes, ASP Conference Series, 77, 433
- Shahbaz T., Fender R. P. & Charles P. A., 2001, *A&A*, 376, L17
- Smith D. M., Swank J. H., Heindl W. A., Remillard R. A., 2002, *ATel* 85
- Tomsick J. A., Corbel S., Fender R. P., Miller J. M., Orosz J. A., Tzioumis A.

K., Wijnands R., Kaaret P., 2003, *ApJ*, 582, 933

van der Laan H., 1966, *Nature*, 211, 1131

Zdziarski A. A., Poutanen J., Mikolajewska J., Gierlinski M., Ebisawa K.,

Johnson W. N., 1998, *MNRAS*, 301, 435

CHAPTER 6

THE RADIO SPECTRUM OF A QUIESCENT STELLAR MASS BLACK HOLE

Elena Gallo, Rob Fender & Rob Hynes

Monthly Notices of the Royal Astronomical Society 356, 1017-1021 (2005)

Observations of V404 Cyg performed with the Westerbork Synthesis Radio Telescope at four frequencies, over the interval 1.4–8.4 GHz, have provided us with the first broadband radio spectrum of a quiescent stellar mass black hole. The measured mean flux density is of 0.35 mJy, with a flat/inverted spectral index $\alpha = +0.09 \pm 0.19$ (such that $S_\nu \propto \nu^\alpha$). Synchrotron emission from an inhomogeneous optically thick relativistic outflow of plasma appears to be the most likely explanation for the flat/inverted radio spectrum, in analogy with hard state black hole X-ray binaries, indicating that a steady jet is being produced between a few 10^{-6} and a few per cent of the Eddington X-ray luminosity. The 75 per cent flux variability detected over a 5.5-hour time scale constrains the angular size of the variable emitting region to be smaller than 10 milliarcsec at 4.9 GHz (at a distance of 4 kpc).

6.1 Introduction

While accreting gas at relatively low rates, black hole candidates in X-ray binary (BHXB) systems are able to power steady, collimated outflows of energy and material, oriented roughly perpendicular to the orbital plane. The jet interpretation of the radio emission from hard state BHXBs came before the collimated structures were actually resolved with Very Long Baseline Interferometry (VLBI) techniques. In a seminal work, Blandford & Königl (1979) proposed a model to interpret the flat radio spectrum of extragalactic compact radio sources in terms of isothermal, conical outflows, or jets. A jet model for X-ray binaries was later developed by Hjellming & Johnston (1988), in order to explain both the steady radio emission with flat/inverted spectra observed in the hard state of

BHXBs, and transient outbursts with optically thin synchrotron spectra. We refer the reader to McClintock & Remillard (2005) and Fender (2005) for comprehensive reviews on X-ray states and radio properties (respectively) of BHXBs. High resolution maps of Cyg X-1 in the hard X-ray state have confirmed the jet interpretation of the flat radio-mm spectrum (Fender et al. 2001), imaging an extended, collimated structure on milliarcsec scale (Stirling et al. 2001). Further indications for the existence of collimated outflows in the hard state of BHXBs come from the stability in the orientation of the electric vector in the radio polarization maps of GX 339–4 over a two year period (Corbel et al. 2000). This constant position angle, being the same as the sky position angle of the large-scale, optically thin radio jet powered by GX 339–4 after its 2002 outburst (Gallo et al. 2004), clearly indicates a favoured ejection axis in the system. Finally, the optically thick milliarcsec scale jet of the (somewhat peculiar) BH candidate GRS 1915+105 (Dhawan, Mirabel & Rodríguez 2000) in the plateau state (Klein-Wolt et al. 2002) supports the association of hard X-ray states of BHXBs with steady, partially self-absorbed jets.

Having established this association, a natural question arises: what are the required conditions for a steady jet to exist? We wonder especially whether the jet survives in the very low luminosity, *quiescent* X-ray state. While radio emission from BHXBs in the thermal dominant (or high/soft) state is suppressed up to a factor ~ 50 with respect to the hard state (*e.g.* Fender et al. 1999; Corbel et al. 2001, and references therein), most likely corresponding to the physical disappearance of the jet, little is known about the radio behaviour of quiescent stellar mass BHs, mainly due to sensitivity limitations. Among the very few systems detected in radio is V404 Cygni, which we shall briefly introduce in the next Section.

6.1.1 V404 Cyg (=GS 2023+338)

The X-ray binary system V404 Cyg is thought to host a strong BH candidate, with a most probable mass of $\sim 12 M_{\odot}$ (Shahbaz et al. 1994), and a low mass K0IV companion star, with orbital period is of 6.5 days, and orbital inclination to the line of sight is of about 56° (Casares & Charles 1994; Shahbaz 1994). Following the decay of the 1989 outburst that led to its discovery (Makino 1989), the system entered a quiescent X-ray state, in which it has remained ever since. The relatively high quiescent X-ray luminosity of V404 Cyg (with an *average* value of about $6 \times 10^{33} \times (D/4 \text{ kpc})^2 \text{ erg s}^{-1}$ in the range 0.3 – 7.0 keV; Garcia et al. 2001; Kong et al. 2002; Hynes et al. 2004) is possibly related to the long orbital period and surely indicates that the some accretion continues to take place at $L_X \simeq 4 \times 10^{-6} L_{\text{Edd}}$, where L_{Edd} is the Eddington X-ray luminosity (for a 12

M_{\odot} BH).

As reported by Hjellming et al. (2000), since (at least) early 1999 the system has been associated with a variable radio source with flux density ranging from 0.1 to 0.8 mJy on time scales of days and it is known to vary at optical (Wagner et al. 1992; Casares et al. 1993; Pavlenko et al. 1996; Hynes et al. 2002; Shahbaz et al. 2003; Zurita et al. 2003) and X-ray wavelengths (Wagner et al. 1994; Kong et al. 2002; Hynes et al. 2004, for a coordinated variability study) as well. Yet no *broadband* radio spectrum of V404 Cyg in quiescence, nor of any other stellar mass BH below $10^{-5}L_{\text{Edd}}$, is available in the literature to date (see Corbel et al. 2000 for a 2-frequency radio spectrum of GX 339-4 at $\sim 10^{-5}L_{\text{Edd}}$). Given the quite large degree of uncertainty about the overall structure of the accretion flow in quiescence (e.g. Narayan, Mahadevan & Quataert 1999 for a review), it has even been speculated that the total power output of a quiescent BH could be dominated by a radiatively inefficient outflow (Fender, Gallo & Jonker 2003) rather than by the local dissipation of gravitational energy in the accretion flow. It is therefore of primary importance to establish the nature of radio emission from quiescent BHBs. In this brief paper we show that the radio properties of V404 Cyg closely resemble those of a canonical hard state BH, suggesting that there is no fundamental difference in terms of radio behaviour between the quiescent and the canonical hard X-ray state. A comprehensive study of the spectral energy distribution of V404 Cyg in quiescence, from radio to X-rays, will be presented elsewhere (Hynes et al., in preparation).

6.2 Radio emission from V404 Cyg

6.2.1 WSRT observations

The Westerbork Synthesis Radio Telescope (WSRT) is an aperture synthesis interferometer that consists of a linear array of 14 dish-shaped antennae arranged on a 2.7 km East-West line. V404 Cyg was observed by the WSRT at two epochs: **i**) on 2001 December 28, start time 05:28 UT (MJD 52271.3), at 4.9 GHz (6 cm) and 8.4 GHz (3 cm), for 8 hours at each frequency; observations were performed with the (old) DCB backend, using 8 channels and 4 polarizations; **ii**) on 2002 December 29, start time 06:29 UT (MJD 52637.3), at 1.4 GHz (21 cm), 2.3 GHz (13 cm), 4.9 GHz (6 cm) and 8.4 GHz (3 cm) for a total of 24 hours. Frequency switching between 8.4–2.3 GHz and 4.9–1.3 GHz was operated every 30 minutes over the two 12 hour runs, resulting in ~ 5.5 hour on the target and ~ 0.5 hour on the calibration sources (3C 286 and 3C 48) at each frequency. During this set of observations, the WSRT was equipped with the DZB

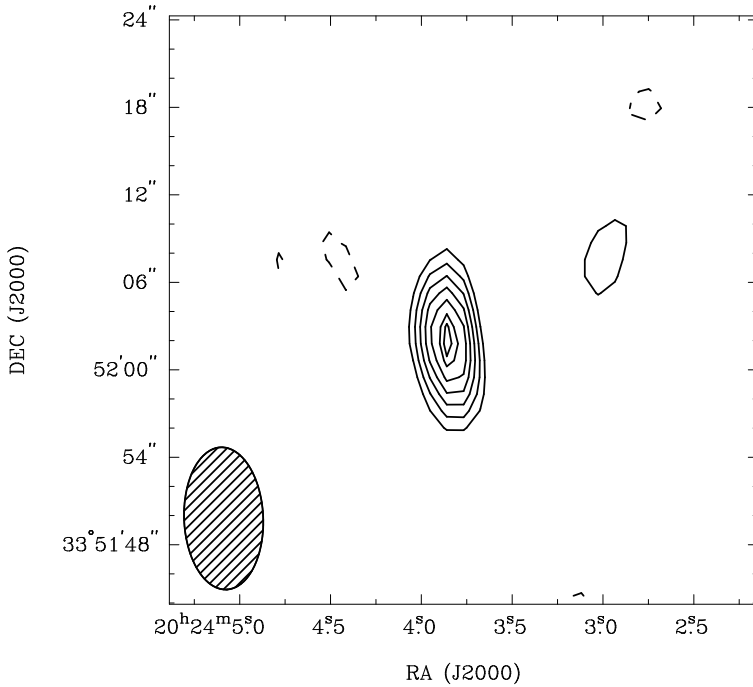


Figure 6.1: Naturally weighted contour map of V404 Cyg as observed by Westerbork at 4.9 GHz on 2002 December 29 (MJD 52637.3); contour levels are at $-3, 3, 4, 5, 6, 7, 8$ times the rms noise level of 0.05 mJy; the synthesized beam is shown on the bottom left corner.

backend using eight IVC sub-bands of 20 MHz bandwidth, 64 channels and 4 polarizations. Seven out of the eight sub-bands were employed to reconstruct the images, as the sub-band IVC-IF6 failed to detect any signal other than noise over the whole 24 hour period. The telescope operated in its *max-short* configuration, particularly well suited for observations shorter than a full 12 hour synthesis, and with a minimum baseline of 36 m (see <http://www.astron.nl/wsr/wsrGuide/> for further details). The data reduction, consisting of editing, calibrating and Fourier transforming the (u, v) -data on the image plane, has been performed with the MIRIAD (Multichannel Image Reconstruction Image Analysis and Display) software (Sault & Killeen 1998). The 1.4 and 2.3 GHz data, containing several sources with flux density well above 100 mJy, were self-calibrated in phase.

6.2.2 Results: spectrum and variability

2001 December 28 (MJD 52271.3)

An unresolved (beam size of $\sim 5.8 \times 3.0$ arcsec² at 8.4 GHz) ~ 0.50 mJy radio source was detected at both 4.9 and 8.4 GHz, at the position consistent with that of V404 Cyg ($\alpha(\text{J2000}) = 20:24:03.78$; $\delta(\text{J2000}) = +33:52:03.2$; e.g. Downers et al. 2001). Table 6.1 lists the measured flux densities with errors at each frequency; the corresponding spectral index (hereafter defined as $\alpha = \Delta \log S_\nu / \Delta \log \nu$, such that $S_\nu \propto \nu^\alpha$) is of 0.04 ± 0.68 ; such a large error bar is mainly due to the high noise in the 8.4 GHz map (see Table 6.1). The signal/noise ratios are too low to measure linearly polarized flux from the source at the expected level of a few per cent, assuming a synchrotron origin for the radio emission (see Section 6.3).

2002 December 29 (MJD 52637.3)

V404 Cyg is detected at four frequencies with a mean flux density of 0.35 mJy; flux densities at each frequency are listed in Table 6.1. The fitted four-frequency spectral index is $\alpha = 0.09 \pm 0.19$. Radio contours as measured at 4.9 GHz are plotted in Figure 6.1, while Figure 6.2 shows the radio spectra of V404 Cyg at two epochs.

Since returning to quiescence, V404 Cyg is known to vary on time scales of days, or even shorter, both in radio and in X-rays; such variability is actually detected in our 2002 WSRT observations. The low flux of V404 Cyg makes it practically impossible to subtract from the (u, v) -data all the other radio sources in the field and generate a reliable light curve of the target. We thus divided each of the two ~ 11 -hour data sets on-source in time intervals of ~ 5.5 hours (of which only ~ 2.75 hours on source per frequency, due to the frequency switching) and made maps of each time interval. Significant variability (checked against other bright sources in the field) is detected at 4.9 GHz: the flux density varied from 0.27 ± 0.07 mJy in the first half of the observation, to 0.47 ± 0.07 in the second half.

6.3 Discussion

As mentioned in the introduction, synchrotron radiation from a relativistic outflow accounts for the observed flat radio spectra of *hard* state BHXBs; we refer the interested reader to more thorough discussions in e.g. Hjellming & Han (1995), Mirabel & Rodríguez (1999) and Fender (2001; 2005). Here we shall

note that the *collimated* nature of these outflows is more debated, as it requires direct imaging to be proven. Even though confirmations come from Very Long Baseline Array (VLBA) observations of Cyg X-1 (Stirling et al. 2001) and GRS 1915+105 (Dhawan et al. 2000; Fuchs et al. 2003) in hard states, failure to image a collimated structure in the hard state of XTE J1118+480 down to a synthesized beam of $0.6 \times 1.0 \text{ mas}^2$ at 8.4 GHz (Mirabel et al. 2001) may challenge the jet interpretation (Fender et al. 2001). However, apart from GRS 1915+105, which is persistently close to the Eddington rate (see Fender & Belloni 2004 for a review), Cyg X-1 in the hard state displays a 0.1–200 keV luminosity of 2 per cent L_{Edd} (Di Salvo et al. 2001), while XTE J1118+408 was observed at roughly one order of magnitude lower level (*e.g.* Esin et al. 2001). If the jet size scaled as the radiated power, we would expect the jet of XTE J1118+408 to be roughly ten times smaller than that of Cyg X-1 (which is $2 \times 6 \text{ mas}^2$ at 9 GHz, at about the same distance), and thus still point-like in the VLBA maps presented by Mirabel et al. (2001).

Garcia et al. (2003) have pointed out that long period ($\gtrsim 1$ day) BHXBs undergoing outbursts tend to be associated with spatially resolved optically thin radio ejections, while short period systems would be associated with unresolved, and hence physically smaller, radio ejections. If a common production mechanism is at work in optically thick and optically thin BHXB jets (Fender, Belloni & Gallo 2004), the above arguments should apply to steady optically thick jets as well, providing an alternative explanation to the unresolved radio emission of XTE J1118+480, with its 4 hour orbital period, the shortest known for a BHXB. It is worth mentioning that, by analogy, a long period system, like V404 Cyg, might be expected to have a relatively larger optically thick jet.

6.3.1 A synchrotron emitting outflow in the quiescent state of V404 Cyg

Emission mechanism

The WSRT observations of V404 Cyg performed on 2002 December 29 provide us with the first broadband (1.4–8.4 GHz) radio spectrum of a stellar mass BH candidate below $10^{-5} L_{\text{Edd}}$. As we do not have direct evidence (no linear polarisation measurement, no especially high brightness temperature, see below) for the synchrotron origin of the radio emission from V404 Cyg in quiescence, we must first briefly explore different mechanisms, such as free-free emission from an ionized plasma. The donor in V404 Cyg is a K0IV star with most probable mass of $0.7 M_{\odot}$ and temperature around 4300 K (Casares & Charles 1994; Shahbaz et al. 1994), simply too cool to produce any observable free-free radio

Table 6.1: WSRT observations of V404 Cyg .

date	MJD	ν (GHz)	S_ν (mJy)	S/N
2001-12-28	52271.3	4.9	0.49 ± 0.04	12.2
		8.4	0.50 ± 0.20	2.5
2002-12-29	52637.3	1.4	0.34 ± 0.08	4.2
		2.4	0.33 ± 0.07	4.7
		4.9	0.38 ± 0.05	7.6
		8.4	0.36 ± 0.15	2.4

emission (see Wright & Barlow 1975). Alternatively, the accretion flow onto the compact object may provide the needed mass loss rates and temperatures in order to produce a flat/inverted free-free radio spectrum. In (line- and radiation-driven) disc wind models, global properties such as the total mass loss rate and wind terminal velocity depend mainly on the system luminosity (see *e.g.* Proga & Kallman 2002; Proga, Stone & Drew 1998 and references therein); very high accretion rates are required in order to sustain significant mass loss rates and hence observable wind emission, ruling out a disc wind origin for the observed radio flux from V404 Cyg. However, that mass loss via winds in sub-Eddington, radiatively inefficient accretion flows may be both dynamically crucial and quite substantial, has been pointed out by Blandford & Begelman (1999). Quataert & Narayan (1999) calculated the spectra of an advection dominated inflow (ADAF) taking into account wind losses, and found that the observations of three quiescent black holes, including V404 Cyg, are actually consistent with at least 90 per cent of the mass originating at large radii to be lost to a wind. Under the rough assumption that models developed for ionized stellar winds (*e.g.* Wright & Barlow 1975, Reynolds 1986; see Dhawan et al. 2000 for an application to the steady jet of GRS 1915+105) might provide an order of magnitude estimate of the mass loss rate even for such winds, still the required mass loss rate in order to sustain the observed radio emission for a *fully ionized* hydrogen plasma is close the Eddington accretion rate for a $12 M_\odot$ BH (assuming a 10 per cent efficiency in converting mass into light). Lower ionization parameters would

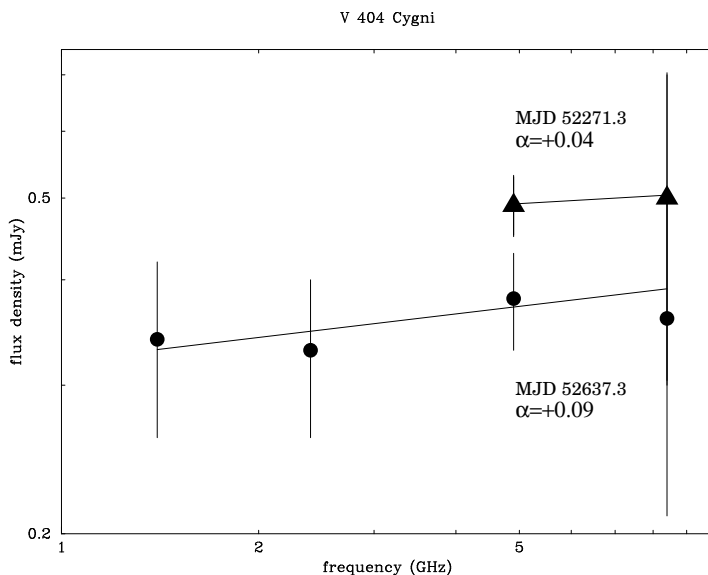


Figure 6.2: The radio spectrum of V404 Cyg as measured by the WSRT on 2001 December 28 (MJD 52271.3) and 2002 December 29 (MJD 52637.3); flux densities are listed in Table 6.1.

further increase the needed mass loss, bringing it to super-Eddington rates. Even taking into account geometrical effects, such as wind collimation and/or clumpiness, the required mass loss rates can not be more than three orders of magnitude below the spherical homogeneous wind, *i.e.* still far too high for a $\lesssim 10^{-5}$ Eddington BH to produce any observable radio emission. As free-free emission does not appear to be a viable alternative, we are led to the conclusion that *the radio spectrum of V404 Cyg in quiescence is likely to be synchrotron in origin.* This conclusion is supported by polarisation measurements during the second phase (following a bright optically thin event) of the 1989 radio outburst of V404 Cyg, when a slow-decay, optically thick component had developed (Han & Hjellming 1992). At this time, after 1989 June 1-3, V404 Cyg displayed the same flat/inverted spectrum of the present 2002 WSRT observations, but was at a few mJy level, still high enough to allow the detection of linearly polarized flux, which confirmed the synchrotron nature of the emission. In addition, the roughly constant and similar polarisation angles measured at that time, indicated that the averaged magnetic field orientation changed very little, if at all. As

Table 6.2: Constraints on the size L of the radio emission region in V404 Cyg ; a distance of 4 kpc is adopted (Jonker & Nelemans 2004).

Requirement	Frequency (GHz)	(cm)	Size (R_{\odot})	(mas)
$T_B < 10^{12}\text{K}$	1.4	$> 4.6 \times 10^{11}$	> 6.7	$\gtrsim 0.01$
$L < c \Delta t$	4.9	$< 5.9 \times 10^{14}$	< 8530	$\lesssim 10$

V404 Cyg entered a quiescent regime following the decay of that outburst (it reached the typical quiescent flux densities about 1 year after the outburst peak), it seems reasonable to assume that the present ~ 0.5 mJy radio emission with flat/inverted spectrum is of the same nature as the few mJy flat/inverted spectrum component detected in 1989, and therefore synchrotron in origin.

A further argument for the jet interpretation of this synchrotron emission is the fact that the radio and X-ray fluxes of V404 Cyg over the decline of its 1989 outburst *and* at its current quiescent X-ray and radio luminosities, display the same non-linear correlation found to hold in the whole hard state of BHXBs (Corbel et al. 2003; Gallo, Fender & Pooley 2003) and later extended to super-massive nuclei in active nuclei as well (Merloni, Heinz & Di Matteo 2003; Falcke, K rding & Markoff 2004), where there is little doubt about the jet origin of the radio emission.

Angular size

By setting a maximum brightness temperature of $\sim 10^{12}\text{K}$ (above which Compton losses become catastrophic), and assuming a distance to the system of 4 kpc (Jonker & Nelemans 2004 and references therein), we can derive a minimum linear size for the (1.4 GHz) synchrotron emitting region of $\sim 4.6 \times 10^{11}$ cm, or $\sim 6.7 R_{\odot}$. This corresponds to one fifth of the system orbital separation (Shahbaz et al. 1994), but to more than 10^5 Schwarzschild radii for a $12 M_{\odot}$ BH, *i.e.* a region more than 10 times larger than the postulated transition radius between an outer geometrically thin accretion disc and an inner advection dominated inflow (Quataert & Narayan 1999). Because of limits on the signal propagation speed, the 5.5-hour time scale variability detected at 4.9 GHz gives an upper limit to the

linear size L of the variable region: $L < 5.9 \times 10^{14}$ cm, or about $8530 R_{\odot}$. At a distance of 4 kpc, this translates into an angular extent $\theta \lesssim 10$ mas at 4.9 GHz (see Table 6.2).

In the framework of standard conical jet models (Blandford & Königl 1979; Hjellming & Johnston 1988; Falcke & Biermann 1996), flux variability could be induced by e.g. the propagation of shocks within the outflow. These shocks will not be visible until they reach the point along the outflow where it becomes optically thin at the observing frequency. The actual morphology of the radio source will depend on the ratio between the thickness Δr of the region where the variability occurs (the lower the observing frequency, the higher the thickness) and its distance R from the core. If $R \gg \Delta r$, we would expect a double radio source with flux ratios depending on Doppler boosting, while if $R \simeq \Delta r$, then we would expect to observe a continuous elongated structure. The ratio $\Delta r/R$ is unknown in the case of V404 Cyg and could only be determined by measuring *delays* between different frequencies. For comparison, the average flux rise time in the oscillations of the flat spectrum radio component in GRS 1915+105 is of about a few minutes, while the infrared-radio delays are typically of 15 min, indicating that the variable radio source should not be too distant from the core (Mirabel et al. 1998; Fender et al. 2002, and references therein). Combined with the extended core morphology of both Cyg X-1 (Stirling et al. 2001) and the core of GRS 1915+105 (Dhawan et al. 2000; Fuchs et al. 2003), this suggests that $R \simeq \Delta r$ in these two sources, but it is not clear how the outflow properties might scale with the luminosity.

The variability time scale should be roughly proportional to the observed jet scale size, which in turn scales as the inverse of the observing frequency; therefore, the lack of significant variations at frequencies lower than 4.9 GHz, where 75 per cent variability is detected, is not surprising, as lower frequency photons are thought to come from a larger emission region and hence the variability is washed out by light travel time effects.

Han & Hjellming (1992), based on the same arguments, were able to constrain the linear size of the optically *thin* ejection associated with the fast-decay phase in the radio light curve of the 1989 outburst: from the 5 min time scale variability measured on 1989 June 1st, and from brightness temperature limits, they derived $\theta \simeq 0.2$ mas. Fluctuations on time scales of tens of minutes were later measured during the slow-decay phase, when an optically thick component had developed, and interpreted as possible hot shocks propagating downstream an underlying compact jet. By analogy, this would appear a reasonable explanation for the 5-hour time scale variability detected in our WSRT observations as well.

6.4 Summary

WSRT observations of V404 Cyg performed on 2002 December 29 (MJD 52637.3) at four frequencies over the interval 1.4–8.4 GHz have provided us with the first broadband radio spectrum of a quiescent (with average L_X of a few $10^{-6}L_{\text{Edd}}$) stellar mass BHXB. We measured a mean flux density of 0.35 mJy, and a flat/inverted spectral index $\alpha = 0.09 \pm 0.19$. WSRT observations performed one year earlier, at 4.9 and 8.4 GHz, resulted in a mean flux density of 0.5 mJy, confirming the relatively stable level of radio emission from V404 Cyg on a year time-scale; even though the spectral index was not well constrained at that time, the measured value was consistent with the later one.

Synchrotron emission from an inhomogeneous, optically thick relativistic outflow of plasma seems to be the most likely explanation for the flat radio spectrum, in analogy with hard state BHXBs (Fender 2001). Optically thin free-free emission as an alternative explanation is ruled out on the basis that mass loss rates far too high would be required, either from the companion star or from the inflow of plasma to the accretor. The collimated nature of this outflow remains to be proven; based on brightness temperature arguments and the 5.5-hour time-scale variability detected at 4.9 GHz, we conclude that the angular extent of the radio source is constrained between 0.01 at 1.4 GHz and 10 mas at 4.9 GHz (at a distance of 4 kpc; Jonker & Nelemans 2004). In the context of standard self-absorbed jet models, the flux variability may be due to shocks or clouds propagating in an inhomogeneous jet.

If our interpretation is correct, a compact steady jet is being produced by BHXBs between a few 10^{-6} and $\sim 10^{-2}$ times the Eddington luminosity, supporting the notion of quiescence as a low luminosity level of the standard hard state. However, as V404 Cyg is the most luminous quiescent BHXB known to date, the existence of a steady jet in this system does not automatically extend to the whole quiescent state of stellar mass BHs. Sensitive radio observations of the nearby, truly quiescent system A0620–00 (three orders of magnitude less luminous than V404 Cyg in X-rays; e.g. Kong et al. 2002), will hopefully provide an answer about the ubiquity of compact jets from stellar mass black holes with a hard spectrum.

Acknowledgements

EG wishes to thank Raffaella Morganti for her kind assistance in the data reduction, and Alex de Koter for suggestions. RIH is supported by NASA through Hubble Fellowship grant # HF-01150.01-A awarded by STScI, which is oper-

ated by AURA, for NASA, under contract NAS 5-26555. The Westerbork Synthesis Radio Telescope is operated by the ASTRON (Netherlands Foundation for Research in Astronomy) with support from the Netherlands Foundation for Scientific Research NWO.

References

- Blandford R. D., Begelman M. C., 1999, MNRAS, 303, L1
Blandford R. D., Königl A., 1979, ApJ, 232, 34
Casares J., Charles P. A., Naylor T., Pavlenko E. P., 1993, MNRAS, 265, 834
Casares J., Charles P. A., 1994, MNRAS, 271, L5
Corbel S., Nowak M., Fender R. P., Tzioumis A. K., Markoff S., 2003, A&A, 400, 1007
Corbel S., Fender R. P., Tzioumis A. K., Nowak M., McIntyre V., Durouchoux P., Sood R., 2000, A&A, 359, 251
Corbel S. et al. , 2001, ApJ, 554, 43
Di Salvo T., Done C., Zycki P. T., Burderi L., Robba N. R., 2001, ApJ, 547, 1024
Dhawan V., Mirabel I. F., Rodríguez L. F., 2000, ApJ, 543, 373
Downes R. A., Webbink R. F., Shara M. M., Ritter H., Kolb U., Duerbeck H. W., 2001, PASP, 113, 764
Esin A. A., McClintock J. E., Drake J. J., Garcia M. R., Haswell C. A., Hynes R. I., Munro M. P., 2001, ApJ, 555, 483
Falcke H., Körding E., Markoff S., 2004, A&A, 414, 895
Falcke H., Biermann P. L., 1996, A&A, 308, 321
Fender R. P., 2005, to appear in '*Compact stellar X-ray sources*', Eds. W.H.G. Lewin and M. van der Klis, Cambridge University Press (astro-ph/0303339)
Fender R. P., 2001, MNRAS, 322, 31
Fender R. P., Belloni T., 2004, ARA&A, 42, 317
Fender R. P., Belloni T., Gallo E., 2004, 355, 1105
Fender R. P., Gallo E., Jonker P. G., 2003, MNRAS, 343, L99
Fender R. P., Rayner D., Trushkin S. A., O'Brien K., Sault R. J., Pooley G. G., Norris R. P., 2002, MNRAS, 330, 212
Fender R. P., Hjellming R. M., Tilanus R. P. J., Pooley G. G., Deane J. R., Ogle R. N., Spencer R. E., 2001, MNRAS, 322, L23
Fender R. P., Pooley G. G., Durouchoux P., Tilanus R. P. J., Brocksopp C., 2000, MNRAS, 312, 853
Fender R. P. et al. , 1999, ApJ, 519, L165
Fuchs Y. et al. , 2000, A&A, 409, L35

- Gallo E., Fender R. P., Pooley G. G., 2003, MNRAS, 344, 60
- Gallo E., Corbel S, Fender R. P., Maccarone T. J., Tzioumis A. K., 2004, MNRAS, 347, L52
- Garcia M. R., Miller J. M., McClintock J. E., King A. R., Orosz J., 2003, ApJ, 591, 388
- Han X. & Hjellming R. M., 1992, ApJ, 400, 304
- Hjellming R. M., Johnston K. J., 1988, ApJ, 328, 600
- Hjellming R. M., Han X., 1995, in 'X-ray Binaries', Eds. Lewin W. H. G., van Paradijs J., van den Heuvel E. P. J., Cambridge University Press, 308
- Hjellming R. M., Rupen M. P., Mioduszewski A. J., Narayan R., 2000, ATel 54
- Hynes R. I. et al. , 2004, ApJL, 611, L125
- Hynes R. I. et al. , 2003, MNRAS, 345, 292
- Hynes R. I., Zurita C., Haswell C. A., Casares J., Charles P. A., Pavlenko E. P., Shugarov S. Y., Lott A. D., 2002, MNRAS, 330, 1009
- Jonker P. G. & Nelemans G., MNRAS, 354, 355
- Klein-Wolt M., Fender R. P., Pooley G. G., Belloni T. M., Morgan E. H., Migliari S., van der Klis M., 2002, MNRAS, 331, 745
- Kong A. K. H., McClintock J. E., Garcia M. R., Murray S. S., Barret D., 2002, ApJ, 570, 277
- Makino F., Wagner R. M., Starrfield S., Buie M. W., Bond H. E., Johnson J., Harrison T., Gehrz R. D., 1989, IAUC, 4786
- McClintock J. E., Remillard R. A., 2005, to appear in 'Compact stellar X-ray sources', Eds. W.H.G. Lewin and M. van der Klis, Cambridge University Press (astro-ph/0306213)
- Merloni A., Heinz S., Di Matteo T., 2003, MNRAS, 345, 1057
- Mirabel I. F., Rodríguez L. F., 1999, ARA&A, 37, 409
- Mirabel I. F., Dhawan V., Mignani R. P., Rodrigues I., Guglielmetti F., 2001, Nature, 413, 139
- Mirabel I. F., Dhawan V, Chaty S., Rodríguez L. F., Martí J., Robinson C. R., Swank J., Geballe T., 1998, A&A, 330, L9
- Narayan R., Mahadevan R., Quataert E., 1998, 'Theory of Black Hole Accretion Disks', ed. M. A. Abramowicz, G. Bjornsson, and J. E. Pringle, Cambridge University Press, 148
- Pavlenko E. P., Martin A. C., Casares J., Charles P. A., Ketsaris N. A., 1996, MNRAS, 281, 1094
- Proga D., Kallman T. R., 2002, ApJ, 565, 455
- Proga D., Stone J. M., Kallman T. R., 2000, ApJ, 543, 686
- Quataert E., Narayan R., 1999, ApJ, 520, 298
- Reynolds S. P., 1986, ApJ, 304, 713

- Sault R.J., Killeen N. E. B., 1998, *'The Miriad Users Guide'*, Sydney: Australia Telescope National Facility
- Shahbaz T., Dhillon V. S., Marsh T. R., Zurita C., Haswell C. A., Charles P. A., Hynes R. I., Casares J., 2003, MNRAS, 346, 1116
- Shahbaz T., Ringwald F. A., Bunn J. C., Naylor T., Charles P. A., Casares J., 1994, MNRAS, 271, L10
- Stirling A. M., Spencer R. E., de la Force C. J., Garrett M. A., Fender R. P., Ogle R. N., 2001, MNRAS, 327, 1273
- Wagner R. M., Kreidl T. J., Howell S. B., Starrfield S. G., 1992, ApJ, 401, L97
- Wagner R. M., Starrfield S. G., Hjellming R. M., Howell S. B., Kreidl T. J., 1994, ApJ, 429, L25
- Wright A. E., Barlow M. F., 1975, MNRAS, 170, 41
- Zurita C., Casares J., Shahbaz T., 2003, ApJ, 582, 369

CHAPTER 7

TOWARDS A UNIFIED MODEL FOR BLACK HOLE X-RAY BINARY JETS

Rob Fender, Tomaso Belloni & Elena Gallo

Monthly Notices of the Royal Astronomical Society 355, 1105-1118 (2004)

We present a unified semi-quantitative model for the disc-jet coupling in black hole X-ray binary systems. In the process we have compiled observational aspects from the existing literature, as well as performing new analysis. We argue that during the rising phase of a black hole transient outburst the steady jet known to be associated with the canonical ‘low/hard’ state persists while the X-ray spectrum initially softens. Subsequently, the jet becomes unstable and an optically thin radio outburst is always associated with the soft X-ray peak at the end of this phase of softening. This peak corresponds to a ‘soft very high state’ or ‘steep power law’ state. Softer X-ray states are not associated with core radio emission. We further demonstrate quantitatively that the transient jets associated with these optically thin events are considerably more relativistic than those in the low/hard X-ray state. This in turn implies that as the disc makes its collapse inwards the jet Lorentz factor rapidly increases, resulting in an internal shock in the outflow, which is the cause of the observed optically thin radio emission. We provide simple estimates for the efficiency of such a shock in the collision of a fast jet with a previously generated outflow which is only mildly relativistic. In addition, we estimate the jet power for a number of such transient events as a function of X-ray luminosity, and find them to be comparable to an extrapolation of the functions estimated for the low/hard state jets. The normalization may be larger, however, which may suggest a contribution from some other power source such as black hole spin, for the transient jets. Finally, we attempt to fit these results together into a coherent semi-quantitative model for the disc-jet coupling in all black hole X-ray binary systems.

7.1 Introduction

Relativistic jets are a fundamental aspect of accretion onto black holes on all scales. They can carry away a large fraction of the available accretion power in collimated flows which later energise particles in the ambient medium. The removal of this accretion power and angular momentum must have a dramatic effect on the overall process of accretion. In their most spectacular form they are associated with supermassive black holes in active galactic nuclei (AGN), and with Gamma-Ray Bursts (GRBs), the most powerful and explosive engines in the Universe respectively. However, parallel processes, observable on humanly-accessible timescales, are occurring in the accretion onto black holes and neutron stars in binary systems within our own galaxy.

The current observational picture of X-ray binary jets is most simply put as follows: in the low/hard state, which exists typically below a few per cent of the Eddington luminosity L_{Edd} (e.g. Maccarone 2003; McClintock & Remillard 2005) there is a compact self-absorbed jet which manifests itself as a flat (spectral index $\alpha \sim 0$ where $\alpha = \Delta \log S_{\nu} / \Delta \log \nu$) or inverted ($\alpha \geq 0$) spectral component in the radio, millimetre and (probably) infrared bands (e.g. Fender 2001b; Corbel & Fender 2002). The radio luminosity of these jets shows a strong, non-linear correlation with X-ray luminosity (Corbel et al. 2003; Gallo, Fender & Pooley 2003) and has only been directly spatially resolved in the case of Cyg X-1 (Stirling et al. 2001), although the ‘plateau’ jet of GRS 1915+105 is phenomenologically similar and has also been resolved (Dhawan et al. 2000; Fuchs et al. 2003). The suggestion that such steady, compact jets are produced even at very low accretion rates (Gallo, Fender & Pooley 2003; Fender, Gallo & Jonker 2003) has recently received support in the flat radio spectrum observed from the ‘quiescent’ transient V404 Cyg at an average X-ray luminosity $L_X \sim 10^{-6} L_{\text{Edd}}$ (Gallo, Fender & Hynes 2005). During steady ‘soft’ X-ray states the radio emission, and probably therefore jet production, is strongly suppressed (Tanabaum et al. 1972; Fender et al. 1999b; Corbel et al. 2001; Gallo, Fender & Pooley 2003).

Additionally there are bright events associated with transient outbursts and state transitions (of which more later), which are often directly resolved into components displaying relativistic motions away from the binary core (e.g. Mirabel & Rodríguez 1994; Hjellming & Rupen 1995; Fender et al. 1999) not only in the radio but also – at least once – in the X-ray band (Corbel et al. 2002). These events typically display optically thin (synchrotron) radio spectra ($\alpha \leq -0.5$). Both kinds of jets are clearly very powerful and coupled to the accretion process. See Mirabel & Rodríguez (1999) and Fender (2005) for a more thorough review of the observational properties of X-ray binary jets.

In this paper we attempt to pin down as accurately as possible the moment at which the major radio outburst occurred and relate this to the X-ray state at the time. We subsequently compare this with the X-ray state corresponding to the lower-luminosity steady jets, to the evolution of transient outbursts, and to the velocity and power associated with each type of jet, in order to draw up a framework for a unified model of black hole X-ray binary jet production.

Several black hole systems are investigated in this paper, and in addition we compare these with the neutron star systems Cir X-1 and Sco X-1. The data relating to the radio flares, jet Lorentz factors (if measured), corresponding X-ray luminosities, estimated distances and masses, are summarised in Table 7.1.

7.2 The sample: four black holes undergoing jet formation

Is there a signature in the X-ray light curve of an outbursting source which indicates when the relativistic jet is launched? In the following we investigate radio and X-ray light curves of four black hole binaries – GRS 1915+105, GX 339-4, XTE J1859+226 and XTE J1550-564 – undergoing state transitions in order to investigate this point.

7.2.1 X-ray Data analysis

For XTE J1550-564, XTE J1859+226 and GX 339-4, we extracted the background-subtracted PCA count rate, using PCU2 only, for the each available RXTE observation relative to the first part of the outburst considered. For each observation, we also produced an X-ray colour (or hardness ratio) by dividing the background-subtracted count rates in the 6.3–10.5 keV band by those in the 3.8–6.3 keV band. For GRS 1915+105, given the much shorter time scales involved, we analyzed a single observation, producing a PCA light curve at 1 second resolution from all PCUs summed together, and an X-ray colour curve at the same time resolution. The energy bands used for the colour, 15.2–42.3 keV and 2.1–5.9 keV were different (the reason for which is that the thermal disc component in GRS 1915+105 is considerably higher than in other systems; using the same energy bands results in the harder C state having a softer colour than the softer B state. The use of a harder energy band for the numerator ensures that the thermal disc component does not strongly contaminate it).

In order to estimate in a homogeneous way the source luminosity at peak of the outburst for XTE J1550-564, XTE J1859+226 and GX 339-4, we extracted RXTE PCA+HEXTE spectra from the public archive corresponding to the peak

Table 7.1: Parameters for the X-ray binary systems and selected jet events discussed in this paper; the last two sources contain accreting neutron stars, the rest black hole candidates. The first three columns give the source name, distance and mass of the accretor. Columns 4–9 give the date, rise time, peak radio flux, constraints on bulk Lorentz factor, estimated jet power and corresponding estimated X-ray power for jet production events. The final column gives references (F99 = Fender et al. 1999; HR95 = Hjellming & Rupen 1995; B02 = Brocksopp et al. 2002; W02 = Wu et al. 2002; G04 = Gallo et al. 2004; HJ01 = Hjellming et al. 2001; Or01 = Orosz et al. 2001; P04 = Pooley 2004; B04 = Brocksopp et al. (in prep); F04 = Fender et al. 2004; F02 = Fomalont et al. 2001a,b). ^f denotes ‘flaring state’; ^o denotes ‘oscillations’

Source	d (kpc)	M M_{\odot}	Date (MJD)	Δt (s)	$S_{5\text{GHz}}$ (mJy)	Γ	L_J (L_{Edd})	$L_{\text{X,VHS}}$ (L_{Edd})	Ref
GRS 1915+105 ^f	11	14	50750	43200	320	≤ 1.4	0.6	1.1	F99
GRS 1915+105 ^o	11	14	many	300	50	≥ 2	0.05	1.1	F99
GROJ1655-40	3.5	7	49580	43200	2000	≥ 1.7	1.0	0.1	HR95
XTE J1859+226	6	7	51467	21600	50	?	0.2	0.2	B02
XTE J1550-564	6	9	51077	43200	130	≥ 2	0.3	0.5	W02
GX 339-4	8	7	52408	19800	55	≥ 2.3	0.3	0.07	G04
V4641 Sgr	8	9	51437	43200	420	≥ 9.5	0.8	4	Or01
Cyg X-1	2.5	10	53055	2000	50	?	0.02	~ 0.05	P04
XTEJ1748-288	8.5	7	50980	172800	530	≥ 2.7	1.9	~ 0.1	B04
Cir X-1	6	1.4	51837	43200	20	≥ 15	0.6	~ 0.7	F04
Sco X-1	2	1.4	many	3600	15	≥ 3.2	0.02	~ 1	F02

flux in the PCA band. Spectra were created from PCU2 data (3-25 keV) for the PCA and from cluster A data (20-200 keV) for HEXTE, using FTOOLS 5.3. The spectra were corrected for background and dead-time effects. A 0.6 per cent systematic error was added to the PCA to account for residual calibration effects. We fitted the spectra with the standard phenomenological model for these systems, consisting of a cutoff power-law (*cutoff*), a disk blackbody (*diskbb*), a Gaussian emission line between 6 and 7 keV, all modified by interstellar absorption. The actual models might be more complex, but we are interested in the determination of the flux only, so that the presence of additional components like iron absorption edges does not change significantly our results. The reduced χ^2 values were between 1.3 and 1.5. From the best fit models for each source, in order to estimate the bolometric flux, we computed the unabsorbed flux of the disc blackbody component in the 0.001-100 keV range and that of the power-law component in the 2-100 keV range. For GRS 1915+105, given the much shorter time scales involved for the short oscillations, we applied the procedure outlined above to the RXTE/PCA+HEXTE data of the observation of 1997 October 25, the last one before the launch of the major jet observed with MERLIN (Fender et al. 1999). In order to approximate the flux evolution from the count rate light curves, we applied to all preceding and following observations the count rate to flux conversion factor obtained from the peak. A comparison with published flux values for XTE J1550-564 (Sobczak et al. 2000) this proved to be a reasonable approximation for our purposes.

Much of the following discussion is based upon the association of radio emission with the X-ray states of different sources. We will use the following abbreviations throughout the paper: the low/hard state as ‘LS’; the high/soft state as ‘HS’, and the very high or intermediate states as ‘VHS/IS’. In fact, as we shall discuss further (see also Belloni et al. 1994; Homan & Belloni 2004), the VHS/IS is not a single state but has both hard (as used to describe the X-ray spectrum) and soft varieties.

Note that recently McClintock & Remillard (2005) have proposed a modification to this classification scheme in which the LS is referred to as the hard state and the HS as the ‘thermal dominant state’, while revised definitions are introduced for the VHS/IS states. While we retain the classical definitions of states, we discuss later on how these correspond to the revised state definitions of McClintock & Remillard.

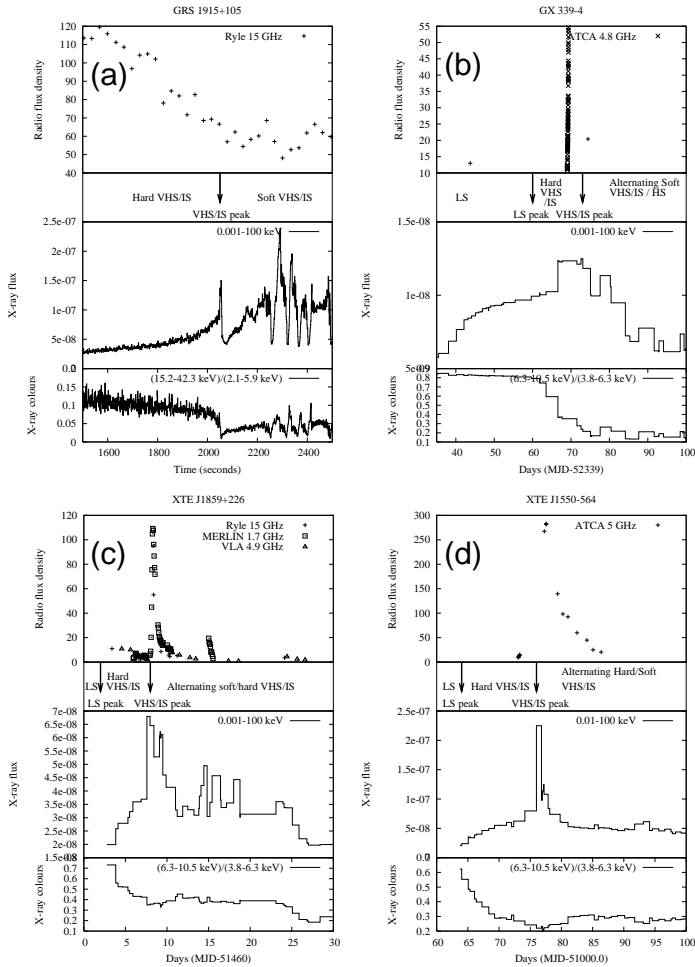


Figure 7.1: Radio and X-ray light curves, X-ray colours and X-ray state classifications during periods around transient jet formation, for four black hole (candidate) X-ray binaries. In GRS 1915+105 the canonical LS or HS are never reached; in GX 339-4, XTE J1859+226 and XTE J1550-564 the delay between the canonical LS peak and subsequent VHS/IS peak ranges from a few days to two weeks. Nevertheless, in all four cases the radio flare occurs at the time of the VHS peak, indicating a clear association between this, and not the previous LS, and the major ejection. The units of the X-ray flux are $\text{erg s}^{-1} \text{cm}^{-2}$.

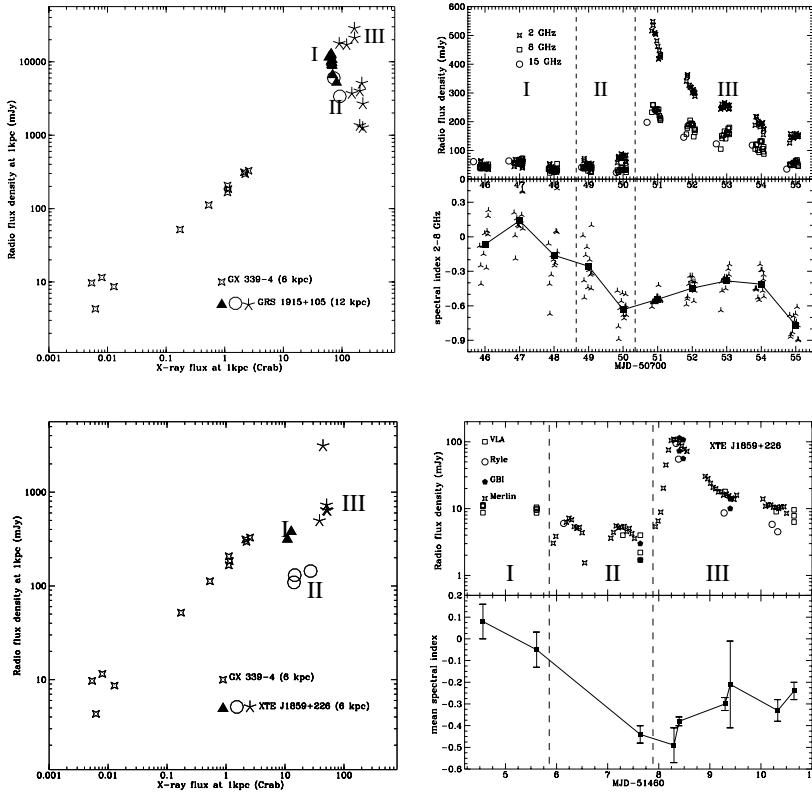


Figure 7.2: Behaviour of radio emission immediately prior to optically thin flare events. The top panel shows data for the GRS 1915+105 plateau reported in detail in Fender et al. (1999); the lower panel the outburst of XTE J1859+226 reported in Brocksopp et al. (2002) and also our Figure 7.1. The right-hand panels show in detail the radio light curves and fitted spectral indices over this period, and are separated for each source into three phases. The location of these phases in the radio luminosity : X-ray luminosity ($L_{\text{radio}}:L_X$) plane (Gallo, Fender & Pooley 2003) is indicated in the left-hand panels (the X-ray luminosity is calculated from the RXTE ASM, as in Gallo, Fender & Pooley 2003, and is therefore much less accurate than the fluxes presented in Figure 7.1). Initially, while still in a hard VHS/IS, both sources display optically thick radio emission which lies close in the ($L_{\text{radio}}:L_X$) plane to the mean relation for LS BH XRBs, as marked out by the data for GX 339-4 (Gallo, Fender & Pooley 2003). Subsequently, the radio emission seems to become more erratic and occasionally optically thin.

7.2.2 Individual sources

GRS 1915+105

GRS 1915+105 has long been a key source in our understanding of the disc-jet coupling in X-ray binary systems (see Fender & Belloni 2004 and references therein). In the context of this study it is interesting because its X-ray state never seems to reach the canonical LS or HS but instead switches between hard (state ‘C’ of Belloni et al. 2000) and soft (states ‘A’ and ‘B’) VHS/IS states (see also Reig et al. 2003). It has clearly been established in this source that phases of hard (C) X-ray emission lasting more than a few hundreds of seconds are associated with radio events, and that when the source is only in soft (A,B) states there is no radio emission (Klein-Wolt et al. 2002). In the context of this work its importance is therefore in establishing that state changes within the VHS/IS can produce radio outbursts without requiring any contact with the canonical LS or HS. Figure 7.1(a) presents the lightcurve of a typical oscillation event in which the source makes a transition from state C to state A/B. The data correspond to the RXTE observation of 1999 June 14 (class ν), time zero is 01:00:40 UT. These oscillation events can occur in very long sequences and are generally associated with sequences of synchrotron oscillations which are almost certainly from the jets (e.g. Klein-Wolt et al. 2002).

GX 339-4

GX 339-4 is also a key source in our understanding of the disc-jet coupling in X-ray binaries (Fender et al. 1999b; Corbel et al. 2000, 2003; Gallo et al. 2003; Belloni et al. 2005), albeit one which varies on timescales considerably longer than in GRS 1915+105. Recently, a clear bright optically thin radio flare was observed from this source, and subsequently found to be associated with a relativistic ejection event (Gallo et al. 2004). The light curve, corresponding to the first part of the 2002/2003 outburst (Belloni et al. 2005), presented in Figure 7.1(b) shows many similarities with that of GRS 1915+105 (Figure 7.1(a)) in the X-ray band, with a rising hard (in this case the canonical LS) state softening shortly before a soft VHS/IS peak. Subsequently both sources show a drop in the X-ray flux and then a slow recovery to even higher levels. Compared to GRS 1915+105 we see that the softening of the X-ray state began a few days *before* the radio flare, which seems to correspond to the VHS/IS peak near the *end* of the softening. However, the key thing we learn from GX 339-4 compared to GRS 1915+105 is that the major radio event is also associated with the state transition, something which is not unambiguous in GRS 1915+105. In this

context it is interesting to note that the rise and decay timescales of the radio oscillation events in GRS 1915+105 are comparable to the durations of both the hard VHS/IS and soft VHS/IS states (since the source is in general oscillating between the two). However, in GX 339-4 we see that this is clearly not the case, and that the transient radio event is associated with a specific and very limited instant in time.

XTE J1859+226

XTE J1859+226 (Figure 7.1(c)) is a more traditional transient than either GRS 1915+105 or GX 339-4, and underwent a bright outburst in 1999 (Wood et al. 1999; Markwardt et al. 1999; Brocksopp et al. 2002; Casella et al. 2004). It showed an initial LS peak during the rise to outburst, which preceded the subsequent soft peak by several days. This allows us to separate the LS and VHS/IS peaks – which was impossible for GRS 1915+105 and still difficult for GX 339-4 – and identify which is associated with the radio event. The radio data used in Figure 7.1(c) are from Brocksopp et al. (2002).

This source peaked in hard X-rays (see BATSE light curve in Brocksopp et al. 2002) about a week before the soft peak. The X-ray state between the two peaks can be formally described as a hard VHS/IS which is gradually softening. The optically thin radio event is clearly associated not with the peak of the LS, after which the X-ray spectrum starts to soften, but with the VHS/IS peak, which seems to occur just at the end of the spectral transition. Note also that some radio emission persists after the LS peak, into the VHS/IS (further discussion below).

XTE J1550-564

XTE J1550-564 (Figure 7.1(d)) is another bright transient which has undergone several outbursts in recent years. The data analysed here correspond to the brightest one, in 1998/1999 (see Sobczak et al. 2000; Homan et al. 2001; Remillard et al. 2002). This outburst was associated with a very strong optically thin radio event subsequently resolved into a radio (Hannikainen et al. 2001) and, most spectacularly, an X-ray jet moving relativistically (Corbel et al. 2002). The radio data plotted in Figure 7.1(d) are from Wu et al. (2002) and Hannikainen et al. (2005).

As in XTE J1859+226, the LS and VHS/IS peaks are clearly separated in time, in this case by approximately two weeks. cursory inspection of Figure 7.1(d) clearly indicates that the optically thin jet is launched at the time of the VHS/IS peak, which occurs, again, just at the end of the X-ray spectral transition. Once more, as in XTE J1859+226, we also note low-level radio emission

between the LS and VHS/IS peaks.

7.3 Jets as a function of X-ray state: new perspectives

Based upon the investigation we have performed, we are better able to associate the characteristics of the radio emission as a function of X-ray state, and therefore to probe the details of the jet:disc coupling. While the previously-established pattern of:

- LS = steady jet
- HS = no jet

remains valid, additional information has clearly come to light about the details of jet formation in the VHS/IS during transient outbursts.

7.3.1 Persistence of the steady jet in the ‘hard VHS/IS’

It has by now been established for several years that the canonical LS is associated with persistent flat- or inverted-spectrum radio emission which probably arises in a self-absorbed outflow (Fender 2001). This radio emission is correlated with the X-ray emission as $L_{\text{radio}} \propto L_{\text{X}}^b$ where $b \sim 0.7$ with a small apparent range in normalizations for several different systems (Corbel et al. 2003; Gallo, Fender & Pooley 2003; see also Fender, Gallo & Jonker 2003 and Jonker et al. 2004 for further discussions and implications).

While the HS was known to be associated with a dramatic decrease in the radio emission (e.g. Tananbaum et al. 1972; Fender et al. 1999b; Gallo, Fender & Pooley 2003) it was not well known how the radio emission behaved in the VHS/IS. Fender (2001a) suggested, based upon GRS 1915+105, that the VHS/IS was associated with unstable, discrete ejection events. Corbel et al. (2001) reported that the radio emission from XTE J1550-564, eleven days after a transition to the VHS/IS, was reduced (or ‘quenched’) by a factor of 50 compared to the previous LS.

However, it is clear from Figure 7.1 that some radio emission persists beyond the end of the canonical LS, before the outburst. Some of the best data available are those of XTE J1859+226 (Brocksopp et al. 2002), which are plotted in Figure 7.1(c) and Figure 7.2. For at least three days following the LS peak, while the X-ray spectrum is softening, the radio emission is persistent with an approximately flat spectrum. Furthermore, the radio luminosity remains consistent with the universal relation of Gallo, Fender & Pooley (2003); this is demonstrated in

the left panels of Figure 7.2. In fact, inspecting Figure 3 of Gallo, Fender & Pooley (2003) we can see that in the case of Cyg X-1 the turnover in the radio emission occurs *after* there has already been some softening of the X-ray emission, implying also that the compact jet persists into the hard VHS/IS. Based on a recent study of XTE J1650-500, Corbel et al. (2004) have also concluded that the steady jet may persist beyond the initial softening of the canonical LS. The importance of this is that there is clearly *not* a one-to-one relation between the behaviour of the radio emission and the X-ray states as currently defined (this will be discussed more later).

7.3.2 Changes in the jet radio spectrum *prior* to the outburst

Following the persistence of the steady LS-like radio emission into the hard VHS/IS, the data indicate that a change in the radio emission does occur prior to the radio flare. In brief, it appears that the radio emission starts to become more variable, with a peaked or (more) optically thin spectrum shortly before the radio flare. We present the evidence for this from the four key sources under study here:

GRS 1915+105

Given that in GRS 1915+105 we (i) are typically observing radio emission from the *last* state transition, (ii) the transition period between the hard and soft VHS/IS is very rapid, it is not possible to investigate this effect for the oscillation-type events in this source. However, the effect is seen in the monitoring of the plateau state and subsequent radio flares as reported in Fender et al. (1999a). As noted in that work (see also discussion in Klein-Wolt et al. 2002) major radio ejections (which were directly resolved) followed the plateau. Thus, as in the other sources, a transition from the hard to the soft VHS/IS (as GRS 1915+105 rarely, if ever, reaches the canonical LS or HS) resulted in a major ejection. However, the data also reveal that the radio spectrum started to change *prior* to the first major ejection event. This is presented in Figure 7.2.

In fact the radio spectrum is already optically thin a couple of days before the flux starts rising, reaching a mean value of -0.6 on MJD 50750, the day before the flare. The change in the radio spectrum occurs around the time that the spectrum starts to soften dramatically towards the soft VHS/IS.

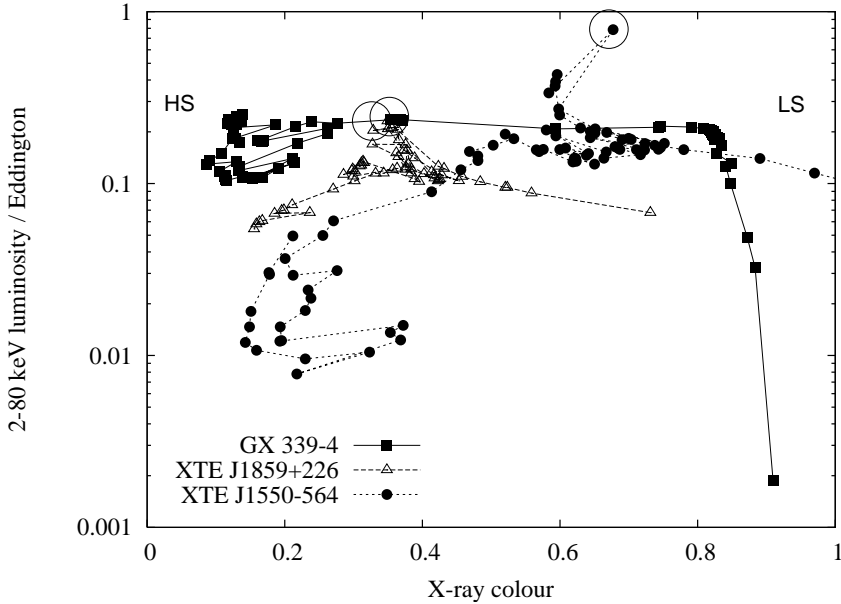


Figure 7.3: Combined X-ray hardness-intensity diagram (HID) for GX 339-4, XTE J1859+226 and XTE J1550-564. The X-ray fluxes plotted in Figure 7.1(b-d) have been scaled to Eddington-ratioed luminosities using the distance and mass estimates given in Table 7.1. Note that ejections in GX 339-4 and XTE J1859+226 occur at almost exactly the same colour and X-ray luminosity. Most of the data points correspond to varying degrees of the VHS/IS, and not the canonical LS (to the right) or HS (to the left).

GX 339-4

The detailed radio light curve of GX 339-4 around the time of the major radio flare is reported in Gallo et al. (2004). During the first 2 hours of observations on MJD 52408, immediately prior to the rise of the radio flare, the spectral index seems to vary from flat to more optically thin ($\alpha \sim -0.2$) and back to flat. Even though the error bars are relatively large, this is consistent with rapid variability of the radio spectrum outflow structure prior to the radio flare.

XTE J1859+226

In this source, over the 4 days prior to the flare on MJD 51467.5, the radio spectrum changes from flat ($0.037 \geq \alpha \geq -0.030$) to more optically thin ($\alpha = -0.237$ on MJD=51467); see Figure 7.2 (lower panels). On this date, the radio spectrum is measured over seven frequencies: Figure 5 of Brocksopp et al. (2001) shows that the actual spectrum, even though overall optically thin, is peaked around 3 GHz (i.e. flat-inverted till 3 GHz and optically thin above), indicating that a structural change in the outflow has occurred prior to the flare.

XTE J1550-564

The radio coverage of the outburst of XTE J1550-564 as presented in Figure 7.1(d) is reported in Wu et al. (2002). However, further measurements presented in Hannikainen et al. (2005) indicate that on MJD 51073, some 4.5 days prior to the flare, there was rapid spectral variability. This included a transition from a peaked to an optically thin spectrum, and back to a peaked spectrum again, on a timescale of less than half a day.

7.3.3 Association of the outburst with the soft VHS/IS peak

Many – perhaps all – sources which undergo an X-ray outburst have a bright hard state during the rising phase (e.g. Brocksopp et al. 2002; Maccarone & Coppi 2003; Yu et al. 2003; Yu, van der Klis & Fender 2004). We know that hard X-ray states correspond to phases of powerful jet production, and that the relativistic ejections tend to occur around the time of X-ray state transitions, and that soft states do not seem to produce jets (see Fender 2005 for a review).

What was difficult to tell from investigation of the most-studied sources like GRS 1915+105 and GX 339-4, was to what part of the state transition sequence the optically thin jet formation corresponded. The above examples appear to give a clear answer – the optically thin radio jet is produced at the VHS/IS peak, which occurs at or near the end of the X-ray spectral softening. We note that this is consistent with the suggestion of Mirabel et al. (1998) that the ‘spike’ in the X-ray light curve of GRS 1915+105 corresponded to the trigger point for the optically thin radio event although, as we have seen, in the case of GRS 1915+105 there are many ambiguities which cannot be resolved by studying this source in isolation.

Figure 7.3 presents the hardness-intensity diagrams (HIDs) for the three of the four sources presented in Figure 7.1, with the point corresponding most clearly to the time of the major radio flare indicated with a circle. In these HIDs

the canonical LS corresponds to a nearly vertical branch on the right hand side of the diagram, seen here only for GX 339-4; the horizontal right-to-left motion exhibited by these sources is characteristic of a transition from a hard to a soft VHS/IS (Belloni 2004; Belloni et al. 2005; Homan & Belloni 2004). Furthermore, the X-ray intensity has been converted to an Eddington-fraction luminosity, based upon the distance and mass estimates given in Table 7.1. It is clear that in all cases the radio flare occurs when the sources are in the VHS/IS, having significantly softened from the LS prior to the event, and with a X-ray luminosity in the range 10–100 per cent Eddington.

It is worth revisiting the result of Corbel et al. (2001) in which XTE J1550-564 was found to be radio-quiet while in the VHS/IS. An inspection of the X-ray data, indicates the following: the first radio observation, which resulted in an optically thin detection, was made within a day or two of the soft VHS/IS peak. The second observation, resulting in an upper limit only, was several days late, in the middle of the soft VHS/IS phase. Thus these observations are consistent with the picture presented here, namely that the optically thin radio flare occurs at the soft VHS/IS peak, and in the subsequent soft VHS/IS phase the core radio emission is suppressed.

Corbel et al. (2004) report a detailed study of the radio emission from the black hole transient XTE J1650-500 (plus a phenomenological comparison with XTE J1859+226 and XTE J1550-564) in which the canonical LS and HS, as well as various degrees of VHS/IS were observed. Specifically they conclude that the steady LS jet may persist into the hard VHS/IS, and that the optically thin radio flare is associated with the soft VHS/IS peak (although they use the state definitions of McClintock & Remillard 2005). These results seem to be consistent with the conclusions we have drawn (more quantitatively) about the association of X-ray states and jet production.

7.3.4 The variation of accretion disc radius with state

It is widely accepted that a geometrically thin, optically thick, accretion disc extends close to the black hole in soft X-ray states and is truncated at larger radii in harder X-ray states (e.g. Esin, McClintock & Narayan 1997; McClintock & Remillard 2005 and references therein). While the absolute values of the radii obtained from X-ray spectral fits may be severely underestimated (e.g. Merloni, Fabian & Ross 2000), large changes in the fitted radii are likely to be due to real changes in the location of the brightest X-ray emitting region. Specifically, for the four sources under detailed consideration here:

GRS 1915+105

The ‘dip-flare’ cycles of GRS 1915+105, such as those presented in Figure 7.11(a), are well known to be associated with apparent changes in the fitted accretion disc radius (e.g. Belloni et al. 1997; Fender & Belloni 2004 and references therein). During the soft VHS/IS (states A/B) the fitted inner disc radius reaches a stable, low, value and is considerably larger in the hard VHS (state C).

GX 339-4

Spectral fits over the period focused on in Figure 7.1(b) indicate a fitted inner disc radius which decreased dramatically at the point of spectral softening (Zdziarski et al. 2004; Nespoli 2004). This low value of the fitted inner radius remained stable for an extended period (> 100 days) until the return to the canonical LS.

XTE J1859+226

To our knowledge, detailed spectral fits over the entire outburst of XTE J1859+226 have not been published. However, both the general X-ray spectral and timing evolution and the preliminary fits reported by Markwardt (2001) indicate a similar pattern to other X-ray binaries. Note that Hynes et al. (2002) discuss the post-outburst evolution of the accretion disc in XTE J1859+226 but note that the absolute value of the inner disc radius cannot be well constrained and so it is hard to use their results to compare with earlier in the outburst.

XTE J1550-564

Sobczak et al. (2000) fitted disc radii to over 200 spectra of XTE J1550-564 during the entire 1998–1999 outburst. They found that at the peak of the outburst (soft VHS) the fitted disc radii varied a lot but were in general very (unrealistically) small. Subsequently in the canonical HS state the disc radius remained relatively small and stable over ~ 100 days.

7.3.5 The alternative state definitions of McClintock & Remillard

We can summarize these connections between X-ray state and radio emission within the framework of the revised definitions of McClintock & Remillard (2005). This is presented in Table 7.2.

Two significant points are worth noting:

Table 7.2: Comparison of the classical X-ray states, and those of McClintock & Remillard (2005), with the radio properties as discussed in detail in the text. VHS/IS corresponds to ‘Very High State/Intermediate State’ and SPL stands for ‘Steep Power Law’.

‘Classical’ states	McClintock & Remillard	Radio properties
Low/Hard state (LS)	Hard state	steady jet
Hard VHS/IS	Intermediate state	steady jet
Hard → soft VHS/IS	Intermediate → SPL	radio flare
Soft VHS/IS	Intermediate / SPL	no jet
High/Soft state (HS)	Thermal dominant	no jet

1. In the framework of McClintock & Remillard, it may be exactly at the point of the transition to the SPL that corresponds to the radio ejection event.
2. In the same framework, there appear to be both ‘jet on’ and ‘jet off’ phases associated with the same state intermediate label.

Point (i), above, was already suggested by McClintock & Remillard (2005) has been noted as likely also by Corbel et al. (2004). However, considering point (ii), it appears that the new definitions have both advantages and disadvantages.

7.4 Increasing velocity as a function of X-ray luminosity at launch

A further key component for the model towards which we are progressing is the variation of jet velocity with X-ray luminosity / state. The empirical evidence clearly points to an increase of jet velocity with X-ray luminosity, at least in the sense of a step up from mildly relativistic velocities in the LS to significantly relativistic velocities resulting from outbursts at a significant fraction of the Eddington limit. Table 7.1 presents a compilation of estimated jet Lorentz factors as a function of the X-ray luminosity at launch. In fact, with the exception of the upper limit for the LS sources (see below), these are all based upon observed

proper motions in spatially resolved radio maps and are therefore only lower limits (see Fender 2003). These data are plotted in Figure 7.4. Note that a higher Lorentz factor in transient jets associated with outbursts is further supported by the much larger scatter in the $L_{\text{radio}} : L_X$ plane compared to the LS sources (Gallo, Fender & Pooley 2003).

The measured spread to the radio/X-ray correlation in LS black hole X-ray binaries was interpreted by Gallo, Fender & Pooley (2003) in terms of a distribution in Doppler factors and used to infer an upper limit $\Gamma \lesssim 2$ to the bulk velocity of compact jets. The value of the spread as it appears in GFP03 is mainly determined by the two data sets for which the correlation extends over more than three orders of magnitude in X-ray luminosity, namely V 404 Cyg and GX 339-4. Obviously, errors in the distance estimates to these systems will introduce a further source of scatter to the correlation. While V 404 Cyg is (reasonably well) known to lie at ~ 3.5 kpc (Wagner et. al 1992), the distance to GX 339-4, and hence its luminosity, remain uncertain. Recent works (Hynes et al 2004; Zdziarski et al. 2004) have significantly revised the lower limit of 4 kpc (Zdziarski et al. 1998) adopted in GFP03, placing GX 339-4 at a distance larger than 6 kpc. In particular, Hynes et al. (2004) discuss the possibility that the system could even be located on the far side of the Galaxy, at ~ 15 kpc. In fact, any value between 6 and 15 kpc has the effect of lowering the final spread to the radio/X-ray correlation by shifting GX 339-4 closer to V 404 Cyg, resulting in a more stringent upper limit on the jet bulk Lorentz factor. A minimum distance to GX 339-4 of 6 kpc reduces the measured spread by a factor 1.6, requiring an outflow bulk velocity smaller than $0.7c$. This sets a new upper limit of $\Gamma_{\text{radio}} \lesssim 1.4$ to the average bulk Lorentz factor of LS black hole X-ray binary jets; in fact, the distance to GX 339-4 would have to be larger than 15 kpc before the spread exceeds again the value obtained for 4 kpc. As discussed in GFP03, the above arguments are formally valid in case of radio beaming combined with isotropic X-ray emission, but if X-rays are moderately beamed ($v_X \sim 0.3c$, as suggested by e.g. models of dynamical coronae, Beloborodov 1999), the conclusions remain essentially unchanged.

However, Heinz & Merloni (2004) argue that the spread around the correlation can only really be used, in the absence of additional information, to constrain the *range* in jet velocities, and not the absolute values. Based upon their arguments, it remains likely that the bulk Lorentz factor of the LS jets is $\Gamma \sim 1$ but it is not a formal requirement. Based upon an analysis of the normalizations for GX 339-4 and V404 as estimated in Gallo, Fender & Pooley (2003) they conclude that the Lorentz factors of the two sources differ by no more than a factor of two. Given the universality – within about one order of magnitude – of the

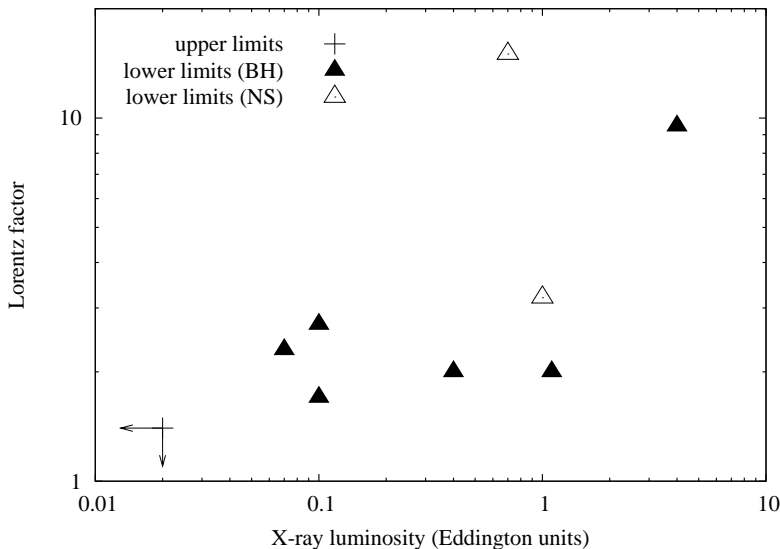


Figure 7.4: Limits on jet Lorentz factors as a function of the estimated bolometric X-ray luminosity at the time of jet launch. The arrows in the lower left of the figure indicate the condition that jets in the general LS state have $v \leq 0.8c$. The rest of the symbols are lower limits only to the Lorentz factors from individual black hole (filled symbols) and neutron star (open symbols) X-ray binaries; the data are listed in Table 7.1.

correlation presented in Gallo, Fender & Pooley (2003), this in turn implies that independent measurement of the Lorentz factor of a jet in the LS would apply to all LS sources. In the discussion that follows we shall continue to assume that the Lorentz factor of the steady jets $\Gamma \leq 2$ but note that it is not proven.

What is not clear from these data is whether the velocity is a simple ‘step’ function of the X-ray luminosity at launch, or rather a smoother function. As discussed in Fender (2003) a broad range in Γ will, in most circumstances, produce approximately the same proper motions. For the simple unified model discussed in this article either (step or smooth function) interpretation is sufficient. The key factor is that the jets associated with the VHS/IS peak are probably more relativistic than those in the LS which generally precedes it.

7.5 Radio emission and jet power

It is also crucial to estimate the jet power as a function of X-ray luminosity / state. In the following we present simplified expressions for the power in both optically

thick and optically thin jets, in Eddington units, as a function of observable radio and X-ray emission.

7.5.1 The low/hard state optically thick jet

In Fender, Gallo & Jonker (2003) it was argued that the total jet power L_J , in the absence of significant advection, was related to the accretion luminosity L_X as follows:

$$L_J = A_{\text{steady}} L_X^{0.5}$$

where $A_{\text{steady}} \geq 6 \times 10^{-3}$ (the normalization is referred to simply as A in Fender, Gallo & Jonker 2003).

Studies of the rapid variability from the hard transient XTE J1118+480, which remained in the LS throughout its outburst, have supported the idea that the optical emission may originate in an outflow and not reprocessed emission from the disc (Merloni, di Matteo & Fabian 2000; Kanbach et al. 2001; Spruit & Kanbach 2002; Malzac et al. 2004). Detailed modelling of the correlated variability by Malzac, Merloni & Fabian (2004) has resulted in a normalization of the jet/outflow power which corresponds to $A_{\text{steady}} \sim 0.3$ in the above formalization, which would imply that all LS sources are jet-dominated. For now we shall take this as the largest likely value of A_{steady} (see also Yuan, Cui & Narayan 2004 who estimate a value for the radiative efficiency for the jet in XTE J1118+480 which lies between the lower limit of Fender, Gallo & Jonker 2003 and the estimate of Malzac, Merloni & Fabian 2004).

7.5.2 The optically thin jets

The power associated with the production of optically thin jets can be calculated from the peak luminosity and rise time of the event, adapting the minimum energy arguments of Burbidge (1956, 1959), as follows:

$$L_J = 20 \Delta t^{2/7} L_{\text{radio}}^{4/7} M^{-3/7} = 2 \times 10^{-5} \Delta t^{2/7} d^{8/7} S_{5\text{GHz}}^{4/7} M^{-1}$$

where L_J is the mean power into jet production (in Eddington units), Δt is the rise time of the event, in seconds, L_{radio} is the peak radio luminosity of the event at 5 GHz (in Eddington units), d is the distance in kpc, $S_{5\text{GHz}}$ is the peak radio flux density at 5 GHz (in mJy), and M is the black hole mass in solar units. The equation assumes an emitting plasma with volume corresponding to $4\pi(\Delta t c)^3$, a filling factor of unity, negligible energy in protons and a spectral index of $\alpha = -0.75$. See Longair (1994) for a fuller discussion.

In addition, since we have argued above that the bulk Lorentz factor is considerably higher for the transient jets underlying these optically thin outbursts, we need to compensate for the resultant Doppler effects. Fender (2001b) demonstrated that it is much more likely, for significantly relativistic jets, that the jet power is underestimated than overestimated, and introduced a correction factor $F(\Gamma, i) = \Gamma\delta^{-3}$ where δ is the relativistic Doppler factor associated with bulk Lorentz factor Γ (the correction includes the kinetic energy of bulk flow). For $2 \leq \Gamma \leq 5$ the mean value of $F(\Gamma, i)$ averaged over $\cos(i)$ is ~ 50 . We adopt this value as an additional (upward) correction to the power of the optically thin jets. Comparison of the formula given above with specific examples more carefully considered, e.g. the 1997 ejections from GRS 1915+105 reported by Fender et al. (1999), indicate this to be a reasonable correction. As discussed earlier, however, we have no clear upper limit on Γ associated with these events, and the correction could be much larger. For example, for $2 \leq \Gamma \leq 7$ the mean value of $F(\Gamma, i)$ is ~ 160 , and for $2 \leq \Gamma \leq 10$ is it ~ 575 .

In Table 7.1 we list in columns eight and nine the estimated optically thin radio powers during the flare events, L_J , and the corresponding peak soft VHS/IS X-ray luminosity, $L_{X,VHS}$, both expressed as Eddington fractions. These values are plotted against each other in Figure 7.5, and compared with the functions for the steady / LS jets as outlined above, for both the Fender, Gallo & Jonker (2003) lower limit and the Malzac, Merloni & Fabian (2004) estimate.

A best-fit power-law to the data for the transient events is of the form

$$L_{\text{jet}} = A_{\text{trans}} L_X^{0.5 \pm 0.2}$$

where the fitted value is $A_{\text{trans}} = (0.4 \pm 0.1)$. Note that since for the transient jets $L_X \sim 1$ this indicates near equipartition of L_X and L_J around the time of such events.

The index of the fit, 0.5 ± 0.2 is comparable to that derived for the LS, namely $L_{\text{jet}} \propto L_X^{0.5}$ (Fender, Gallo & Jonker 2003). The value of the normalization, A_{trans} , is much larger than the conservative value for the steady jet normalization A_{steady} estimated in Fender, Gallo & Jonker (2003; see above). However, it is only ~ 50 per cent larger than the value of A_{steady} implied by the results of Malzac, Merloni & Fabian (2004). Were such a large value to be valid for the LS it would imply that black hole X-ray binaries are likely to be jet-dominated below $L_X = A_{\text{steady}}^2 \sim 0.1 L_{\text{Edd}}$. Since most sources do not strongly exceed this Eddington ratio while in a hard X-ray state (see e.g. Figures 7.3 and 7.5), it implies that *only* in the HS and soft VHS/IS and states, when the jet is suppressed, is the X-ray luminosity dominant over the jet (see also discussion in Malzac et al. 2004). Put another way, for such a large normalization, whenever the jet is on, it is the

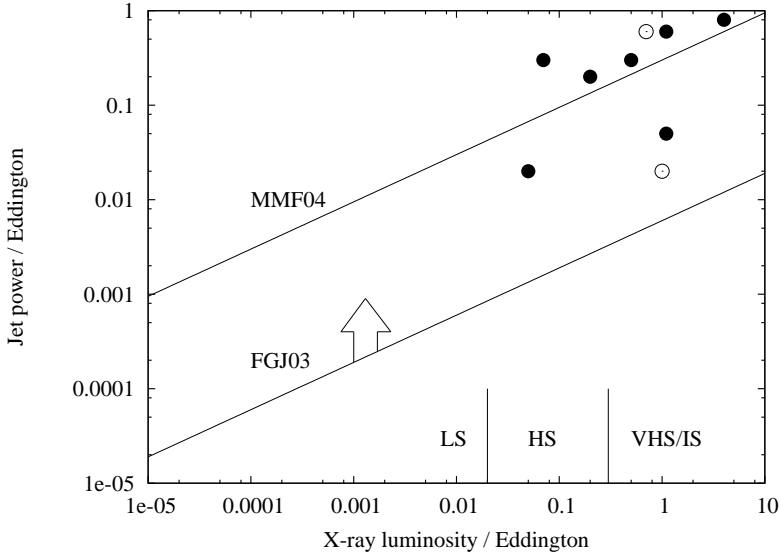


Figure 7.5: Comparing estimated jet power in the steady / LS and transients / VHS/IS states. Note that the uncertainties on the estimated jet powers are large, *at least* one order of magnitude. The solid line marked FGJ03 indicates the lower limit to the steady jet power in the LS as estimated by Fender, Gallo & Jonker (2003). The line marked MMF04 indicates the same function with the larger normalization as calculated by Malzac, Merloni & Fabian (2004). The (solid) points indicate the estimates of jet power for the transient events listed in Table 7.1. It is interesting to note that the data are therefore compatible with the MMF04 relation at all X-ray luminosities. If the steady LS jet power is lower, nearer to the lower limit indicated by the FGJ03 function, then there may be a step up in jet power for the transient events. A very approximate indication of the regimes typically corresponding to the different X-ray states is indicated at the bottom of the figure. The power estimates for the two neutron star sources, Sco X-1 and Cir X-1, are indicated by open symbols.

dominant power output channel.

7.5.3 Some caveats

Note that there are very large uncertainties remaining in the estimation of both A_{steady} and A_{trans} . The functions used for the power of the steady jets are based upon essentially one detailed example – XTE J1118+480 – and extrapolated to other sources via the universal $L_{\text{radio}} \propto L_{\text{X}}^{0.7}$ relation (although estimates from a handful of other sources are also compatible). While this approach may well

be appropriate, spectral changes – in particular the location of the optically thin break in the synchrotron spectrum – could strongly affect the variation of L_J as a function of L_X and more work needs to be done in the future.

In the case of the power function for the transient jets, we have in fact more independent measurements, but those measurements themselves probably have a greater associated uncertainty. Underestimation of L_J can clearly arise due to deviations from equipartition, a lack of knowledge of the high-frequency extension of the synchrotron spectrum and a possible underestimate of the bulk Lorentz factor. Overestimation of L_J could arise due to overestimation of the synchrotron-emitting volume (ie. a filling factor $f < 1$ or injection/acceleration of particles into a confined jet).

7.5.4 A single function or a step up in jet power ?

Nevertheless, it is noticeable that a single power-law relation could be plotted through both the steady LS and transient VHS/IS functions, and that the normalization of such a single function would be close to that estimated by Malzac, Merloni & Fabian (2004), i.e. $A_{\text{steady}} \simeq A_{\text{trans}} \simeq 0.3$.

If there is not a single function then it seems that the transient VHS/IS jets are somewhat more powerful as a function of L_X than an extrapolation of the steady LS jets function. This suggestion is strengthened by our argument, below, that the optically thin events are likely to arise in internal shocks which do not dissipate 100 per cent of the available kinetic energy. If real, this effect may be due to temporarily increased efficiency of jet production in the inner disc, or the transient addition of a new power source, namely the black hole spin (e.g. Blandford & Znajek 1977; Punsly & Coroniti 1991; Livio, Ogilvie & Pringle 1999; Meier 1999, 2001, 2003; Koide et al. 2002). Nevertheless, we consider the similarity in both gradient and normalization of the two jet functions to be remarkable. We note that for the model outlined in this paper to be tested against higher-mass (intermediate or supermassive) black holes, a further mass term would be required for both expressions (see Heinz & Sunyaev 2003; Merloni, Heinz & di Matteo 2003; Falcke, K rding & Markoff 2004). However, for the X-ray binaries where the range in mass is likely to be ≤ 2 this is not important at the current level of accuracy.

7.6 Internal shocks

The arguments given above clearly indicate that as the X-ray luminosity of the accreting source increases, then so does the velocity of the outflow (although

whether this is in the form of a step, or other functional form, is as yet unclear). Since most, probably all, outbursting sources have followed a path in which they have become monotonically brighter in a hard state before making a transition to a soft state, this tells us that a shock should form in the previously-generated steady jet as the faster-moving VHS/IS jet catches up and interacts with it. This internal shock is therefore a natural origin for the optically thin events observed at the beginning of X-ray transient outbursts. Internal shocks have previously been proposed for AGN (e.g. Rees 1978; Marscher & Gear 1985; Ghisellini 1999; Spada et al. 2001) and gamma-ray bursts (GRBs) (e.g. Rees & Meszaros 1994; van Paradijs, Kouveliotou & Wijers 2000 and references therein). Indeed in the context of X-ray binaries an internal-shock scenario has already been discussed previously for GRS 1915+105 by Kaiser, Sunyaev & Spruit (2000), Vadawale et al. (2003) and Turler et al. (2004), and their ideas have significantly inspired this work.

Rees & Meszaros (1994) spelled out the basis for such internal shocks in the context of GRBs. They assumed two shells of equal mass but differing Lorentz factors were ejected such that the later ejection had the higher Lorentz factor. This component, if moving along precisely the same trajectory as the original component, will collide with it. Assuming conservation of energy and momentum it was shown that up to 40 per cent of the total kinetic energy could be released in this shock.

The formulation for the efficiency of energy release, ϵ , as presented in Rees & Meszaros corresponds to the case in which both blobs have Lorentz factors $\Gamma_{1,2} \gg 1$. We have repeated their approach, but considered instead the case in which the first blob is at most only mildly relativistic ($\Gamma_1 < 2$).

In Figure 7.6 we plot the internal shock efficiency for two cases:

- **(a)** The blobs have the same total energy, fulfilling the criterion that $\Gamma_1 M_1 = \Gamma_2 M_2$ (where M is the mass of the blob). This corresponds to the situation in which the jet power does not increase significantly, while the Lorentz factor does.
- **(b)** The blobs have equal mass. This corresponds to a genuine increase in jet power by a factor $\Gamma_2 - \Gamma_1 \sim \Gamma_2$. This corresponds to the maximum efficiency for the internal shock (e.g. Spada et al. 2001).

For the kind of values estimated for transient jets, efficiencies in the range 5–40 per cent are expected. For a total jet power of P_J , the power in the shock (i.e. available for particle acceleration) will be $P_{\text{shock}} \leq \epsilon P_J$. The remaining jet power $(\epsilon - 1)P_J$ is associated with the kinetic energy of the merged shells and should eventually be dissipated via interactions with the ambient medium.

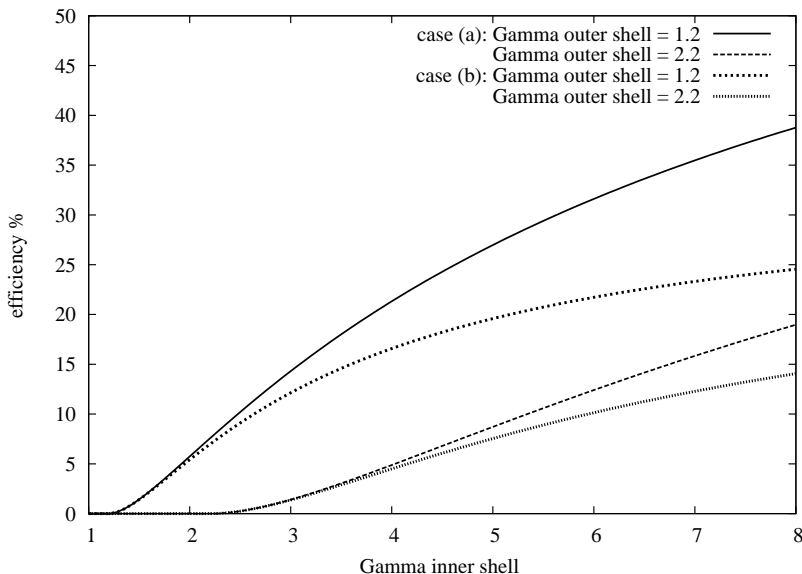


Figure 7.6: Efficiency of energy release for the collision of two shells, where the outer shell is only mildly relativistic (bulk Lorentz factor [BLF] $\Gamma < 2$), under the assumption of conservation of momentum and energy. Case (a) corresponds to the case of two blobs with equal total energy (i.e. $\Gamma_1 M_1 = \Gamma_2 M_2$) in which case the jet power has not increased. Case (b) corresponds to the case of the same mass but increased Lorentz factor, i.e. an increase in jet power by a factor $\Gamma_2 - \Gamma_1$. This can be considered a (high oversimplified) approximation to the collision of a relativistic VHS/IS jet (inner shell) with the preceding steady LS jet (outer shell).

Of course this is a highly oversimplified approximation of the true circumstances as the jet increases in velocity. Nevertheless, it illustrates that the internal shock produced by a transient (as it is subsequently shut down in the soft state) acceleration of the jet from $\Gamma \sim 1$ to $\Gamma \lesssim 10$ could produce dissipation in an internal shock with an observed energy release comparable (within the order or magnitude uncertainty) to that estimated for the steady jet prior to the acceleration. If, as seems likely, $A_{\text{trans}} \geq A_{\text{steady}}$ then the more efficient shock scenario (b) (Figure 7.6) is more likely, and the total jet power, and not just velocity, has significantly increased. Beloborodov (2000) discusses in further detail the high radiative efficiencies which may be obtained in the internal shock model.

The internal shock scenario is also attractive as an explanation for why the same radio flux at a given radio frequency for a given source can be sometimes optically thin and sometimes optically thick. Consider GRS 1915+105, where in the plateau states a flux density of ~ 40 mJy at 15 GHz may be associated with

an optically thick spectrum, and later a comparable flux density with optically thin rising phases of oscillation events (e.g. Fender et al. 1999). If the particle acceleration all occurred at the base of a jet with an approximately fixed structure, this is hard to explain. However, it follows naturally from a scenario where the optically thin events are associated with internal shocks occurring at a much larger distance from the dense inner jet.

Note that it is the radiation resulting from the energy liberated by the internal shock, which we have measured in order to estimate the jet power in the section above. However, since our estimates of the bulk Lorentz factor must be based upon observations of the post-shock plasma, then the true jet power must be larger by a factor ϵ^{-1} . Since $0.05 \lesssim \epsilon \lesssim 0.45$ in the above simplification, this may imply that the underlying jet power is actually a further order of magnitude larger for the transient jets. In this case a single function corresponding to both the LS and VHS/IS jets seems less likely.

As discussed in Vadawale et al. (2003) the strength of the shock is likely to be related to the amount of material lying in the path of the faster VHS/IS jet. They discussed this in the context of GRS 1915+105, where the strength of post-plateau jets (Klein-Wolt et al. 2002) is shown to be correlated with the total X-ray fluency of the preceding plateau (which was presumably a phase of slower jet production). Generalising this phenomenon to other X-ray transients, it provides a natural explanation for why, although there are often multiple radio flaring events, the first is invariably the strongest.

7.7 Towards a unified model

Based upon the key generic observational details assembled above, we have attempted to construct a unified, semi-quantitative, model for the disc-jet coupling in black hole X-ray binaries. A simplified version of the model specific to GRS 1915+105 has been presented in Fender & Belloni (2004). The model is summarised in Figure 7.7, which we describe in detail below. The diagram consists of a schematic X-ray hardness-intensity diagram (HID) above a schematic indicating the bulk Lorentz factor of the jet and inner accretion disc radius as a function of X-ray hardness. The four sketches around the outside of the schematics indicate our suggestions as to the state of the source at the various phases **i–iv**. The path of a typical X-ray transient is as indicated by the solid arrows.

- **Phase i:** Sources are in the low-luminosity LS, producing a steady jet whose power correlates as $L_{\text{jet}} \propto L_{\text{X}}^{0.5}$ (ignoring any mass term). This phase probably extends down to very low luminosities (quiescence).

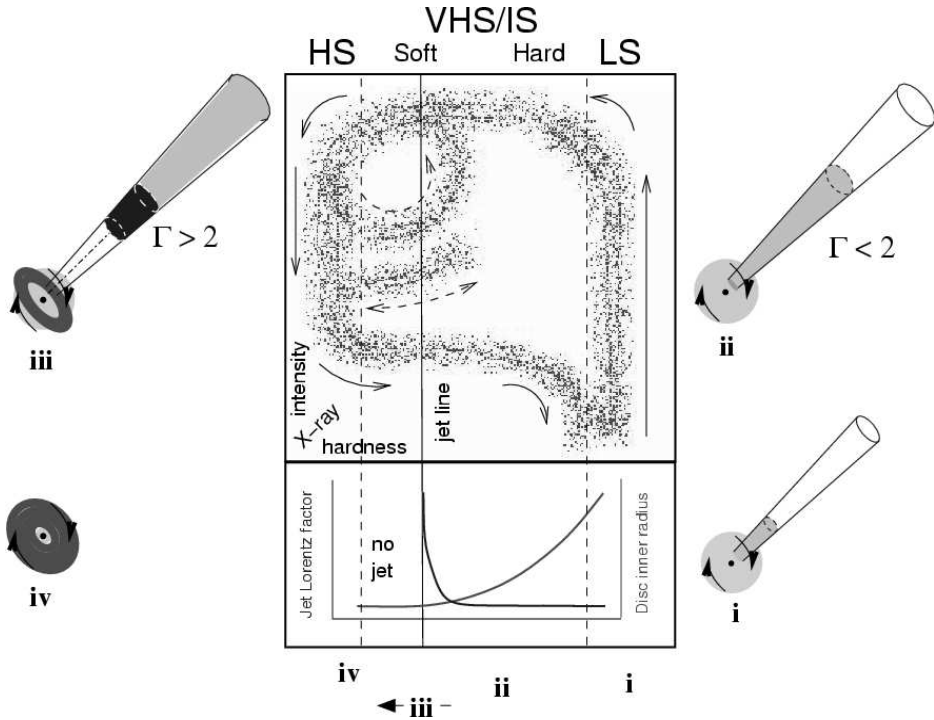


Figure 7.7: A schematic of our simplified model for the jet-disc coupling in black hole binaries. The central box panel represents an X-ray hardness-intensity diagram (HID); HS indicates the ‘high/soft state’, VHS/IS indicates the ‘very high/intermediate state’ and LS the ‘low/hard state’. In this diagram, X-ray hardness increases to the right and intensity upwards. The lower panel indicates the variation of the bulk Lorentz factor of the outflow with hardness – in the LS and hard-VHS/IS the jet is steady with an almost constant bulk Lorentz factor $\Gamma < 2$, progressing from state **i** to state **ii** as the luminosity increases. At some point – usually corresponding to the peak of the VHS/IS – Γ increases rapidly producing an internal shock in the outflow (**iii**) followed in general by cessation of jet production in a disc-dominated HS (**iv**). At this stage fading optically thin radio emission is only associated with a jet/shock which is now physically decoupled from the central engine. As a result the solid arrows indicate the track of a simple X-ray transient outburst with a single optically thin jet production episode. The dashed loop and dotted track indicate the paths that GRS 1915+105 and some other transients take in repeatedly hardening and then crossing zone **iii** – the *jet line* – from left to right, producing further optically thin radio outbursts. Sketches around the outside illustrate our concept of the relative contributions of jet, corona and accretion disc at these different stages.

- **Phase ii:** The motion in the HID, for a typical outburst, has been nearly vertical. There is a peak in the LS after which the motion in the HID becomes more horizontal (to the left) and the source moves into the hard VHS/IS. Despite this softening of the X-ray spectrum the steady jet persists, with a very similar coupling, quantitatively, to that seen in the LS.
- **Phase iii:** The source approaches the *jet line* (the solid vertical line in the schematic HID) in the HID between jet-producing and jet-free states. As the boundary is approached the jet properties change, most notably its velocity. The final, most powerful, jet, has the highest Lorentz factor, causing the propagation of an internal shock through the slower-moving outflow in front of it.
- **Phase iv:** The source is in the soft VHS/IS or the canonical HS, and no jet is produced. For a while following the peak of phase iii fading optically thin emission is observed from the optically thin shock.

Following phase **iv**, most sources drop in intensity in the canonical HS until a (horizontal) transition back, via the VHS/IS, to the LS. Some sources will make repeated excursions, such as the loops and branches indicated with dashed lines in Figure 7.7, back across the jet line. However, with the exception of GRS 1915+105, the number of such excursions is generally ≤ 10 . When crossing the jet line from right to left, the jet is re-activated but there is (generally) no slower-moving jet in front of it for a shock to be formed; only motion from left to right produces an optically thin flare (this is a prediction). Subsequently the motion back towards quiescence is almost vertically downwards in the HID.

The model as outlined above has many similarities with the scenarios described by Meier (1999, 2001, 2003) who has approached the problem from a more theoretical point of view. Meier (2001) has suggested that in low-luminosity states the jet is powered by a modification of the Blandford & Payne (BP) (1982) mechanism taking into account frame-dragging near a rotating black hole (Punsly & Coroniti 1990). This BP/PC mechanism can extract black hole spin by the coupling of magnetic field lines extending from within the ergosphere to outside of it. Meier (2001) further suggests that during phases of very high accretion the Blandford & Znajek (BZ) (1977) mechanism may work briefly. This may be associated with a ‘spine jet’ which is considerably more relativistic than the ‘sheath jet’ produced by the BP/PC mechanism. Note that the power of the jets as given in Meier (2001, 2003) is about linearly proportional to the accretion rate; in the formulation of Fender, Gallo & Jonker (2003) this corresponds to the jet-dominated state (see also Falcke, Körding & Markoff 2004).

We can revisit the scenarios of Meier in the light of our compilation of observational results and steps toward a unified model. In the faint LS (phase **i** in Figure 7.7) is the jet formed by the BP or BP/PC mechanisms? Given that the jet may be formed at relatively large distances from the black hole in such states, there may not be any significant influence of the black hole spin on the jet formation process. However, it is also likely that in such states the jet-formation process is not occurring within thin discs, as is the basis of the BP mechanism, but rather in a geometrically thick flow (see also e.g. Blandford & Begelman 1999; Meier 2001; Merloni & Fabian 2002)

As the accretion rate increases the power of this disc-jet will increase and the geometrically thin accretion disc will propagate inwards. During this phase the jet formation process may migrate from BP→BP/PC. However, the suggestion that the most relativistic jets are formed by the BZ process seems at odds with the observation of significantly relativistic outflows from two neutron star systems (Fomalont et al. 2001a,b; Fender et al. 2004). In a related work, the results of Yu, van der Klis & Fender (2004) indicate that the subsequent evolution of X-ray transient outbursts is approximately determined *before* the soft VHS/IS peak, in both neutron star and black hole systems. This suggests that already by the time of the LS peak we can estimate the size of the ejection even which is to follow, and is a further indication that the study of neutron stars will shed important light on the physics of jet formation in black hole systems.

7.7.1 Ejected disc or ejected corona?

It is interesting to compare the sequence of events we have outlined as being responsible for ejection events with the interpretation most commonly put forward when the disc-jet coupling in GRS 1915+105 was first observed. In this source oscillations, on timescales of tens of minutes, between hard (state C \equiv hard VHS/IS) and soft (states A and B \equiv soft VHS/IS – see Figure 7.1(a)) were associated with cycles of disc emptying and refill (e.g. Belloni et al. 1997b). When the relation to ejection events (Pooley & Fender 1997; Eikenberry et al. 1998; Mirabel et al. 1998) was discovered, it was suggested that the disappearance of the inner disc was directly related to its (partial) ejection (see also Feroci et al. 1999; Nandi et al. 2001). The following sequence of events was envisaged:

1. Thin disc extends close to black hole (soft state)
2. Inner disc is ejected, resulting in:
 - Disappearance of inner disc \rightarrow transition to hard state

- Synchrotron event

3. Refill of disc \rightarrow return to soft state

However, Vadawale et al. (2003) argued that it was the corona which was subsequently ejected as the disc moved in, again specifically for the case of GRS 1915+105. Rodríguez, Corbel & Tomsick (2003) have also suggested, in the case of XTE J1550-564, that it is coronal, and not disc, material which is ejected prior to radio outburst

It is clear that if the model we have outlined in this paper is correct, the disc-ejection scenario is unlikely to be, for any black hole X-ray binary. Specifically, it is the transition *towards* the soft state (that is, the refill of the inner disc) which causes the ejection event. Therefore, if we are to consider the ejection of mass, it is more likely the corona (or whatever form the accretion flow has in the harder states) and not the disc which is ejected.

7.8 Conclusions

We have examined the observational properties of the jets associated with black hole X-ray binary systems. The key observations can be summarised as:

1. **The radio:X-ray coupling:** we have established that the steady radio emission associated with the canonical LS persists beyond the softening of the X-ray spectrum in the hard VHS/IS. At the end of the transition from hard to soft VHS/IS, usually associated with a local maximum in the X-ray light curve, a transient radio outburst occurs. The radio emission is subsequently suppressed until the source X-ray spectrum hardens once more. Some source may repeatedly make the transition from hard to soft VHS/IS and back again, undergoing repeated episodes of steady and transient jet formation.
2. **Jet velocities:** we have argued that the measured velocities for the transient jets, being relativistic with $\Gamma \gtrsim 2$ are significantly larger than those of the steady jets in the LS, which probably have $\Gamma \lesssim 1.4$.
3. **Jet power:** we have furthermore established that our best estimates of the power associated with the transient jets are compatible with extrapolations of the functions used to estimate the power in the LS (albeit with a relatively large normalization).

Essentially equivalent conclusions about the radio:X-ray coupling have been drawn by Corbel et al. (2004). Putting these observational aspects together we have arrived at a semi-quantitative model for jet production in black hole XRBs. We argue that for X-ray spectra harder than some value (which may be universal or vary slightly from source to source) a steady jet is produced. The power of this jet correlates in a non-linear way (approximately given as $L_J \propto L_X^{0.5}$) with the X-ray luminosity. As the X-ray luminosity increases above ~ 1 per cent of the Eddington rate the X-ray spectrum begins to soften. Physically this probably corresponds to the heating of the inner edge of the accretion disc as it propagates inwards with increasing accretion rate. Initially the jet production is not affected. As the disc progresses inwards the jet velocity increases. As it moves through the last few gravitational radii before the inner stable orbit, the Lorentz factor of the jet rises sharply, before the jet is suppressed in a soft disc-dominated state. The rapid increase in jet velocity in the final moments of its existence results in a powerful, optically thin, internal shock in the previously existing slower moving outflow.

The inner disc may subsequently recede, in which case a steady jet is reformed, but with decreasing velocity and therefore no internal shocks. If the disc once more moves inwards and reaches the ‘fast jet’ zone, then once more an internal shock is formed. In fact while jets are generally considered as ‘symptoms’ of the underlying accretion flow, we consider it possible that the reverse may be true. For example, it may be the growth of the steady jet (via e.g. build up of magnetic field near the black hole) which results in the hardening of the X-ray spectrum, perhaps via pressure it exerts on the disc to push it back, or simply via Comptonization of the inner disc as it spreads (for further discussions see e.g. Nandi et al. 2001; Tagger et al. 2004).

In the context of the nature and classification of black hole states, these states, whether classical or as redefined by McClintock & Remillard (2005) do not have a one-to-one relation with the radio properties of the source. It seems that as far as the jet is concerned, it is on – albeit with a varying velocity – if the disc does not reach ‘all the way in’, which probably means as far as the innermost stable orbit. The dividing jet line (Figure 7.7) HID, may also correspond, at least approximately, to a singular switch in X-ray timing properties (Belloni et al. 2005; Homan & Belloni 2004; see also once more discussion in McClintock & Remillard 2005) and may be the single most important transition in the accretion process. Further study of the uniqueness of the spectral and variability properties of sources at this transition point should be undertaken to test and refine our model.

Finally, given that Merloni, Heinz & di Matteo (2003) and Falcke, Körding & Markoff (2004) (see also Heinz & Sunyaev 2003; Maccarone, Gallo & Fender 2003) have recently demonstrated quantitatively the scaling of radio:X-ray coupling across a range of $\gtrsim 10^7$ in black hole mass, it is obviously of great interest to see if the model we are working towards for the coupling of accretion and jet formation in black hole binaries may also be applied to AGN. In addition, detailed modelling of the internal shock scenario is required to see if the coupling, as outlined above, really could allow us to predict radio light curves from X-ray, and vice versa. These two areas should be the next steps forward.

Acknowledgements

RPF would like to thank many people for useful discussions related to the ideas presented here, including Catherine Brocksopp, Annalisa Celotti, Stephane Corbel, Jeroen Homan, Peter Jonker, Marc Klein-Wolt, Tom Maccarone, Dave Meier, Simone Migliari, Jon Miller and Felix Mirabel. We thank the referee, Andrea Merloni, for thoughtful and detailed comments on the paper.

References

- Beloborodov A. M., 1999, ApJ, 510, 123
Beloborodov A. M., 2000, ApJ, 539, L25
Belloni T., 2004, in *'The restless High-Energy Universe'*, Nuclear Physics B, Eds. van den Heuvel E.P.J., in 't Zand J.J.M. and Wijers R.A.M.J.
Belloni T., Mendez M., van der Klis M., Hasinger G., Lewin W.H.G., van Paradijs J., 1996, ApJ, 472, L107
Belloni T., Mendez M., King A.R., van der Klis M., van Paradijs J., 1997, ApJ, 488, L109
Belloni T., Klein-Wolt M., Mendez M., van der Klis M., van Paradijs J., 2000, A&A, 355, 271
Belloni, T., Homan, J., Nespoli, E., Casella, P., van der Klis, M., Lewin, W.H.G., Miller, J.M., Méndez, M., 2005, A&A, in press (astro-ph/0504577)
Blandford R., Znajek R.L., 1977, MNRAS, 179, 433
Blandford R., Königl A., 1979, ApJ, 232, 34
Blandford R.D., Begelman M.C., 1999, MNRAS, 303, L1
Brocksopp C. et al., 2002, 331, 765
Burbidge G.R., 1956, Phys. Rev., 103, 264

- Burbidge G.R., 1959, ApJ, 129, 849
- Corbel S., Fender R.P., 2002, ApJ, 573, L35
- Corbel S., Fender R.P., Tzioumis A.K., Nowak M., McIntyre V., Durouchoux P., Sood R., 2000, A&A, 359, 251
- Corbel S. et al., 2001, ApJ, 554, 43
- Corbel S., Fender R.P., Tzioumis A.K., Tomsick J.A., Orosz J.A., Miller J.M., Wijnands R., Kaaret P., 2002, Science, 298, 196
- Corbel S., Nowak M.A., Fender R.P., Tzioumis A.K., Markoff S., 2003, A&A, 400, 1007
- Corbel S., Fender R., Tomsick J.A., Tzioumis A.K., Tingay S., 2004, ApJ, 617, 1272
- Dhawan V., Mirabel I.F., Rodríguez L.F., 2000, ApJ, 543, 373
- Esin A.E., McClintock J.E., Narayan R., 1997, ApJ, 489, 865
- Falcke H., Biermann P.L., 1996, A&A, 308, 321
- Falcke H., Körding E., Markoff S., 2004, A&A, 414, 895
- Fender R.P., 2001a, in *'Black Holes in Binaries and Galactic Nuclei'*, Proceedings of the ESO Workshop held at Garching, Germany, 6-8 September 1999. Eds. Lex Kaper, Edward P. J. van den Heuvel, Patrick A. Woudt, Springer, 193
- Fender R.P., 2001b, MNRAS, 322, 31
- Fender R.P., 2003, MNRAS, 340, 1353
- Fender R.P., 2005, to appear in *'Compact Stellar X-ray Sources'*, Eds. W.H.G. Lewin and M. van der Klis (astro-ph/0303339)
- Fender R., Belloni T., 2004, ARA&A, 42, 317
- Fender R.P., Gallo E., Jonker P., 2003, MNRAS, 343, L99
- Fender R.P., Garrington S.T., McKay D.J., Muxlow T.W.B., Pooley G.G., Spencer R.E., Stirling A.M., Waltman E.B., 1999a, MNRAS, 304, 865
- Fender R. et al., 1999b, ApJ, 519, L165
- Fender R., Wu K., Johnston H., Tzioumis T., Jonker P., Spencer R., van der Klis M., 2004, Nature, 427, 222
- Feroci M., Matt G., Pooley G., Costa E., Tavani M., Belloni T., 1999, A&A, 351, 985
- Fomalont E.B., Geldzahler B.J., Bradshaw C.F., 2001a, ApJ, 553, L27
- Fomalont E.B., Geldzahler B.J., Bradshaw C.F., 2001b, ApJ, 558, 283
- Fuchs Y. et al., 2003, A&A, 409, L35
- Gallo E., Fender R.P., Pooley G.G., 2003, MNRAS, 344, 60
- Gallo E., Corbel S., Fender R.P., Maccarone T.J., Tzioumis A.K., 2004, MNRAS, 347, L52
- Gallo E., Fender R.P., Hynes R.I., 2005, MNRAS, 356, 1017
- Ghisellini G., 1999, *'Astronomische Nachrichten'*, 320, 232

- Hannikainen D.C., Campbell-Wilson D., Hunstead R., McIntyre V., Lovell J., Reynolds J., Tzioumis T., Wu, K., 2001, *ApSSS*, 276, 45
- Hannikainen D.C. et al., 2005, in prep.
- Harmon B.A. et al., 1995, *Nature*, 374, 703
- Harmon B.A., Deal K.J., Paciesas W.S., Zhang S.N., Robinson C.R., Gerard E., Rodríguez L.F., Mirabel I.F., 1997, *ApJ*, 477, L85
- Heinz S., Sunyaev R.A., 2003, *MNRAS*, 343, L59
- Heinz S., Merloni A., 2004, *MNRAS*, 355, L1
- Hjellming R.M., Johnston K.J., 1988, *ApJ*, 328, 600
- Hjellming R.M., Rupen M.P., 1995, *Nature*, 375, 464
- Hjellming R.M., Rupen M.P., Mioduszewski A.J., Smith D.A., Harmon B.A., Waltman E.B., Ghigo F.D., Pooley G.G., 1998, *BAAS*, 30, 1405
- Homan J., Belloni T., 2004, to appear in *'From X-ray Binaries to Quasars: Black Hole Accretion on All Mass Scales'*, ed. T. J. Maccarone, R. P. Fender, L. C. Ho (Kluwer)
- Homan J., Wijnands R., van der Klis M., Belloni T., van Paradijs J., Klein-Wolt M., Fender R., Mèndez M., 2001, *ApJS*, 132, 377
- Hynes R.I., Haswell C.A., Chaty S., Shrader C.R., Cui W., 2002, *MNRAS*, 331, 169
- Hynes R. I., Steeghs D., Casares J., Charles P. A., O'Brien K., 2004, *ApJ*, 583, L95
- Jonker P.G., Gallo E., Dhawan V., Rupen M., Fender R.P., Dubus G., 2004, *MNRAS*, 351, 1359
- Kaiser C.R., Sunyaev R., Spruit H.C., 2000, *A&A*, 356, 975
- Kanbach G., Straubmeier C., Spruit H.C., Belloni T., 2001, *Nature*, 414, 180
- Klein-Wolt M., Fender R.P., Pooley G.G., Belloni T., Migliari S., Morgan E.H., van der Klis M., 2002, *MNRAS*, 331, 745
- Koide S., Shibata K., Kudoh T., Meier D.L., 2002, *Science*, 295, 1688
- Levine A.M., Bradt H., Cui W., Jernigan J.G., Morgan E.H., Remillard R.A., Shirey R., Smith D., 1996, *ApJ*, 469, L33
- Livio M., Ogilvie G.I., Pringle J.E., 1999, *ApJ*, 512, 100
- McClintock J.E., Remillard R.A., 2005, to appear in *'Compact Stellar X-ray Sources'*, Eds. W.H.G. Lewin and M. van der Klis (astro-ph/0306213)
- Maccarone T., 2003, *A&A*, 409, 697
- Maccarone T.J., Coppi P.S., 2003, *MNRAS*, 338, 189
- Maccarone T., Gallo E., Fender R.P., 2003, *MNRAS*, 345, L19
- Malzac J., Merloni A., Fabian A.C., 2004, *MNRAS*, 351, 253
- Malzac J., Belloni T., Spruit H.C., Kanbach G., 2003, *A&A*, 407, 335
- Markwardt C., 2001, *ApSSS*, 276, 209

- Markwardt, C.B., Marshall, F.E., Swank, J.H., 1999, IAUC, 7274
- Marscher A.P., Gear W.K., 1985, ApJ, 298, 114
- Marscher A.P., Jorstad S.G., Gomez J-L., Aller M.F., Terasranta H., Lister M.L., Stirling A.M., 2002, Nature, 417, 625
- Meier D.L., 1999, ApJ, 522, 753
- Meier D.L., 2001, ApJ, 548, L9
- Meier D.L., 2003, New Astronomy Reviews, 47, 667
- Meier D.L., Koide S., Uchida Y., 2001, Science, 291, 84
- Merloni A., Fabian A.C., 2002, 332, 165
- Merloni A., Fabian A.C., Ross R.R., 2000, MNRAS, 313, 193
- Merloni A., Di Matteo T., Fabian A.C., 2000, MNRAS, 318, L15
- Merloni A., Heinz S., di Matteo T., 2003, MNRAS, 345, 1057
- Miller J.M. et al., 2002, ApJ, 578, 348
- Mirabel, I.F., Rodríguez, L.F., 1994, Nature, 371, 46
- Mirabel, I.F., Rodríguez, L.F., 1999, ARA&A, 37, 409
- Nandi A., Chakrabarti S.K., Vadawale S.V., Rao A.R., 2001, A&A, 380, 245
- Orosz J.A. et al., 2001, ApJ, 555, 489
- Paredes J.M., Marti J., Peracaula M., Pooley G., Mirabel I.F., 2000, A&A, 357, 507
- Pooley G.G., 2004, ATel # 242
- Punsly B., Coroniti F.V., 1990, ApJ, 354, 583
- Rees M.J., 1978, MNRAS, 184, 61
- Rees M.J., Meszaros P., 1994, ApJ, 430, L93
- Reig P., Belloni T., van der Klis M., 2003, A&A, 412, 229
- Remillard, R.A., Sobczak, G.J., Munro, M.P., McClintock, J.E., 2002, 564, 962
- Rodríguez J., Corbel S., Tomsick J.A., 2003, ApJ, 595, 1032
- Sobczak G.J., McClintock J.E., Remillard R.A., Cui W., Levine A.M., Morgan E.H., Orosz J.A., Bailyn C.D., 2000, ApJ, 533, 993
- Spada M., Ghisellini G., Lazzati D., Celotti A., 2001, MNRAS, 325, 1559
- Spruit H.C., Kanbach G., 2002, A&A, 391, 225
- Stirling A.M., Spencer R.E., de la Force C.J., Garrett M.A., Fender R.P., Ogle R.N., 2001, MNRAS, 327, 1273
- Tagger M., Varniere P., Rodríguez J., Pellat R., 2004, ApJ, 607, 410
- Tanabbaum H., Gursky H., Kellogg E., Giacconi R., Jones C., 1972, ApJ, 177, L5
- Turler M., Courvoisier T.J.-L., Chaty S., Fuchs Y., 2004, A&A, 415, L35
- Vadawale S.V., Rao A.R., Naik S., Yadav J.S., Ishwara-Chandra C.H., Pramesh Rao A., Pooley G.G., 2003, ApJ, 597, 1023
- Van Paradijs J., Kouveliotou C., Wijers R.A.M.J., 2000, ARA&A, 38, 379

- Wagner R. M., Kreidl T. J., Howell S. B., Starrfield S. G., 1992, ApJ, 401, L97
Wang X.Y., Dai Z.G., Lu T., 2003, ApJ, 592, 347
Wood, A., Smith, D.A., Marhsall, F.E., Swank, J.H., 1999, IAUC 7274
Wu K., Soria R., Campbell-Wilson D., Hannikainen D., Harmon B.A., Hunstead R., Johnston H., McCollough M., McIntyre V., 2002, ApJ, 565, 1161
Yu W., Klein-Wolt M., Fender R., van der Klis M., 2003, ApJ, 589, L33
Yu W., van der Klis M., Fender R., 2004, ApJ, 611, L121
Yuan F., Cui W., Narayan R., 2005, ApJ, 620, 905
Zdziarski A. A., Poutanen J., Mikolajewska J., Gierlinski M., Ebisawa K., Johnson W. N., 1998, MNRAS, 301, 435
Zdziarski A. A., Gierlinski M., Mikolajewska J., Wardzinski G., Smith D. M., Harmon A. B., Kitamoto S., 2004, MNRAS, 351, 791

CHAPTER 8

A DARK JET DOMINATES THE POWER OUTPUT OF THE STELLAR BLACK HOLE CYGNUS X-1

Elena Gallo, Rob Fender, Christian Kaiser, David Russell
Raffaella Morganti, Tom Oosterloo & Sebastian Heinz
Nature 436, 819-821 (2005)

Accreting black holes are thought to emit the bulk of their power in the X-ray band by releasing the gravitational potential energy of the infalling matter (Frank, King & Raine 2002). At the same time, they are capable of producing highly collimated jets of energy and particles flowing out of the system with relativistic velocities (Hughes 1991). Here we show that the 10 solar mass black hole in the X-ray binary Cygnus X-1 (Bowyer et al. 1965, Gies & Bolton 1986, Herrero et al. 1995) is surrounded by a large-scale (~ 5 pc in diameter) ring-like structure that appears to be inflated by the inner radio jet (Stirling et al. 2001). We estimate that in order to sustain the observed emission of the ring the jet of Cygnus X-1 has to carry a kinetic power that can be as high as the bolometric X-ray luminosity of the binary system. This result may imply that low-luminosity stellar mass black holes as a whole dissipate the bulk of the liberated accretion power in the form of ‘dark’, radiatively inefficient relativistic outflows, rather than locally in the X-ray emitting inflow.

Relativistic jets are a common feature of accreting black holes on all mass scales, from super-massive black holes at the centres of active galactic nuclei (Urry & Padovani 1995; Blandford 2001) to stellar mass black holes in X-ray binary systems within our own Galaxy (Mirabel & Rodríguez 1994, 1999; Fender 2005). While the inflow of hot gas can be very efficient in producing light (up to ~ 40 per cent of the accreted material may be transformed into energy and radiated away in the form of optical/UV/X-ray photons) the same is not true for the synchrotron-emitting outflow, whose efficiency might be lower than a

few per cent. Estimating the *total* – radiated plus kinetic – power content of the jets, and hence their importance with respect to the accretion process in terms of energetics, is a primary aim of high energy astrophysics.

We observed the field of the 10 solar mass black hole and Galactic jet source Cygnus X-1 at 1.4 GHz for 60 hours with the Westerbork Synthesis Radio Telescope (WSRT), yielding the deepest low frequency radio observation of that region to date (Martí et al. 1996). A ring of radio emission – with a diameter of ~ 1 million AU – appears northeast of Cygnus X-1 (Figure 8.1), and seems to draw an edge between the tail of the nearby HII nebula Sh2-101 (Sharpless 1959; whose distance is consistent with that to Cygnus X-1; Hunter & Massey 1990) and the direction of the radio jet powered by Cygnus X-1. Since Cygnus X-1 moves in the sky along a trajectory which is roughly perpendicular to the jet (Lestrade et al. 1999; Stirling et al. 2001; Mirabel & Rodrigues 2003) and thus can not possibly be traced back to the ring centre, this rules out that the ring might be the low-luminosity remnant of the natal supernova of the black hole. In analogy with extragalactic jet sources, the ring of Cygnus X-1 could be the result of a strong shock that develops at the location where the collimated jet impacts on the ambient interstellar medium (Figure 8.2). The jet particles inflate a radio lobe which is over-pressured with respect to the surroundings, thus the lobe expands sideways forming a spherical bubble of shock-compressed ISM, which we observe as a ring because of limb brightening effects. The collisionally ionized gas behind the bow shock would produce the observed bremsstrahlung radiation; in addition, if the shock is radiative, significant line emission is expected from hotter gas at the bow shock front. Structures similar to the ring of Cygnus X-1 have been found at the edges of the radio lobes of powerful radio galaxies hosting super-massive black holes (Smith et al. 2002), where the much higher temperatures of the intra-cluster medium compared to the ISM shift the bremsstrahlung emission to X-ray frequencies. Striking confirmation of this interpretation comes from follow-up optical observations of the field of Cygnus X-1 with the Isaac Newton Telescope Wide Field Camera: the ring is clearly detected using a $H\alpha$ filter in an exposure of only 1200 sec (Figure 8.3). The estimated flux of the ring at $H\alpha$ frequencies exceeds the measured radio flux by a factor $\gtrsim 20$, indicating that the collisionally ionized gas in the ring is indeed emitting bremsstrahlung radiation and also that a significant amount of the measured $H\alpha$ flux is due to line emission, as expected in the case of a radiative shock.

Acting as an effective jet calorimeter, the ISM allows an estimate of the jet's *power* \times *lifetime* product (Burbidge 1959) that is, in principle, independent of the uncertainties associated with the jet spectrum and radiative efficiency. Following a self-similar fluid model developed for extragalactic jet sources (Castor &

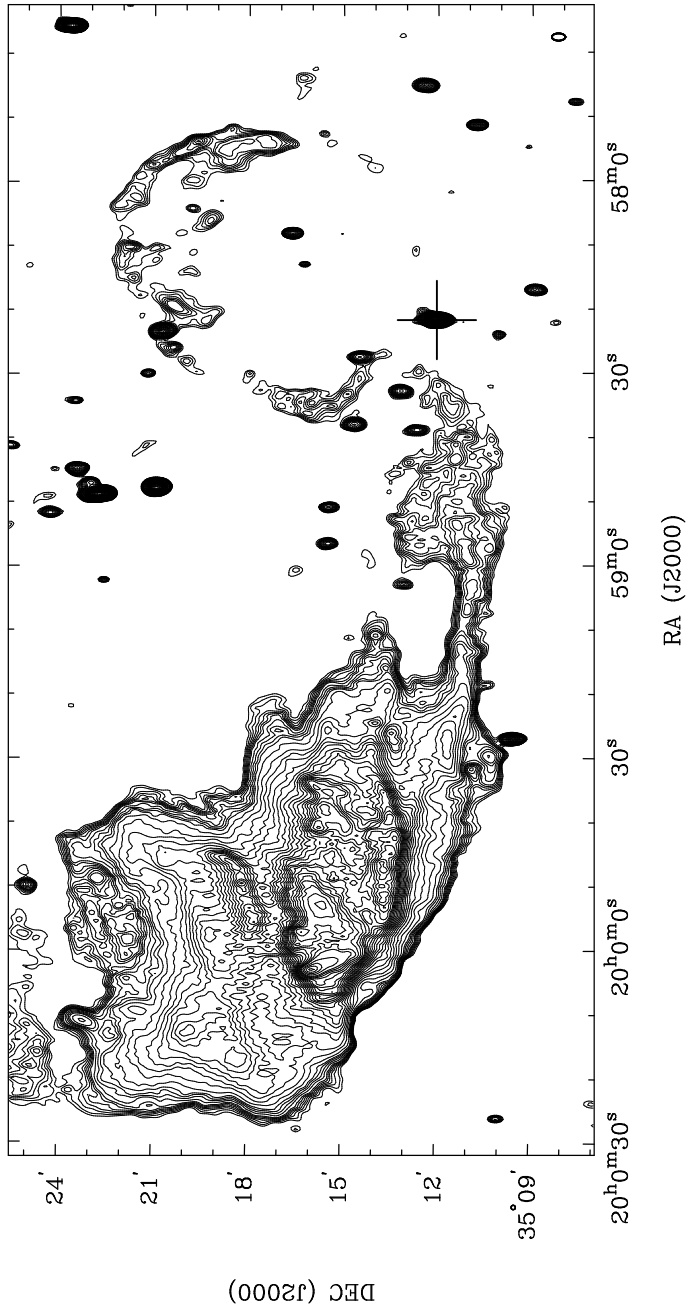


Figure 8.1: The interstellar gas around a Galactic stellar black hole is stirred by the pressure of a ‘dark’, highly collimated relativistic jet of energy and particles, resulting in a 15 light-years wide ring of radio emission. The field of view of the 10 solar mass black hole in Cygnus X-1 (marked by a cross) was observed by the Westerbork Synthesis Radio Telescope for 60 hours at 1.4 GHz: the ring appears to draw an edge between the tail of Sh2-101, the nearby HII nebula on the left hand side, and the direction of the inner radio jet of Cygnus X-1 (Figure 8.2). The spatial resolution in this map is 25×14 arcsec². The average ring monochromatic flux is $0.2 \text{ mJy beam}^{-1}$, vs. a map rms noise value of about $0.05 \text{ mJy beam}^{-1}$. At a distance of 2.1 kpc, the separation L between Cygnus X-1 (coincident with the jet base) and the ring’s outermost point is $1.9 \times 10^{19} \times \sin(\theta)^{-1} \text{ cm}$, where θ is the jet inclination to the line of sight ($\theta \simeq 35^\circ$, Herrero et al. 1995). Because of limb-brightening, we observe a ring whose thickness ΔR in the plane of the sky equals the effective length we are looking through into the bubble. At 2.1 kpc, $\Delta R \simeq 1.6 \times 10^{18} \text{ cm}$.

McCray 1975; Kaiser & Alexander 1997, Heinz et al. 1998), we assume that the jet of Cygnus X-1 is supplying energy at a constant rate P_{jet} , and is expanding in a medium of constant density. We set the minimum temperature of the thermal gas to $T_{\text{shock}} \gtrsim 10^4 \text{ K}$, a typical temperature above which the cooling time becomes critically short, and below which the ionization fraction becomes too low for the ring to emit observable bremsstrahlung radiation. Given the average ring monochromatic luminosity, we are able to estimate a density of about 1300 cm^{-3} for the shock-compressed particles in the ring from the expression of the bremsstrahlung emissivity (Longair 1992; Lotz 1967). By balancing the interior pressure exerted by the lobe and the ram pressure of the shocked ISM, it can be shown (Kaiser & Alexander 1997) that the jet length within the lobe grows with the time t in such a way that: $t \simeq (L/2)^{(5/3)} \times (\rho_0/P_{\text{jet}})^{(1/3)}$, being L the separation between Cygnus X-1 and the ring’s outermost point, and ρ_0 the mass density of the un-shocked gas. By writing the time derivative of this equation, there follows a simple relation between the jet lifetime, its length within the lobe, and the ring velocity: $t = \frac{3}{5}(L/v_{\text{ring}})$.

For a strong shock in a mono-atomic gas, the expansion velocity is set by the temperature of the shocked gas. If the shock is radiative, then the initial post-shock temperature can be higher than that of the thermalized, bremsstrahlung-emitting gas. A stringent constraint comes from X-ray observations: from the non-detection of soft X-ray emission in a 12 ksec observation of Cygnus X-1 taken with the Chandra X-ray Observatory, we can place an upper limit of $T_{\text{shock}} \lesssim 3 \times 10^6 \text{ K}$ by modelling the emission as a radiative shock. This, combined with the lower limit of 10^4 K , gives a ring velocity $v_{\text{ring}} \simeq 20 - 360 \text{ km}$

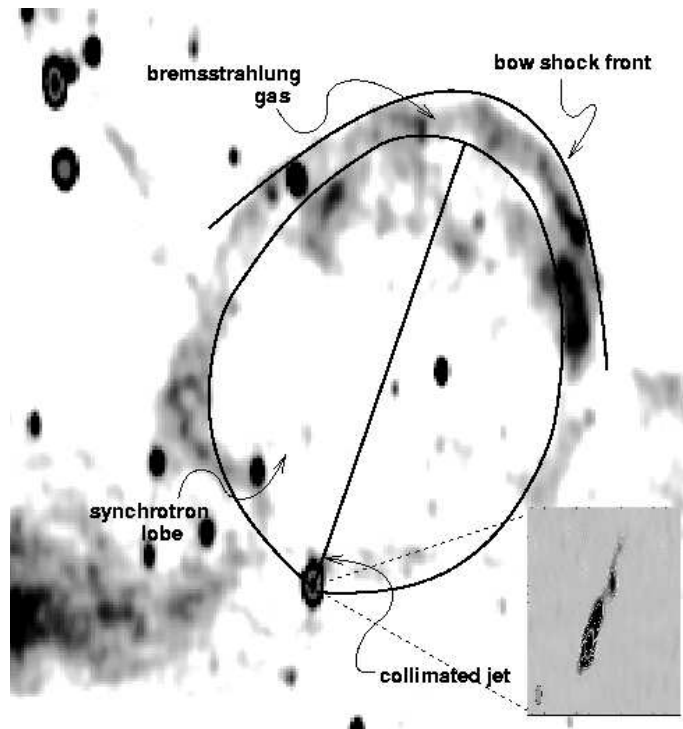


Figure 8.2: The ring of Cygnus X-1 is the result of a strong shock that develops at the location where the pressure exerted by the collimated milliarcsec-scale jet is balanced by the interstellar medium. Inset jet map from Stirling et al. (2001). The jet particles start to inflate a synchrotron-emitting lobe which is over-pressured with respect to the surrounding gas, thus the lobe expands sideways forming a spherical bubble of shock-compressed bremsstrahlung-emitting gas. The monochromatic luminosity of the ring, $L_{1.4 \text{ GHz}} \approx 10^{18} \text{ erg sec}^{-1} \text{ Hz}^{-1}$, equals the product ($\epsilon_\nu \times V$), where the source unit volume V is given by the beam area times the measured ring thickness: $V \approx 4 \times 10^{53} \text{ cm}^3$, and ϵ_ν is the expression for the bremsstrahlung emissivity for a pure hydrogen gas emitting at a temperature T : $\epsilon_\nu = 6.8 \times 10^{-38} g(\nu, T) T^{(-1/2)} n_e^2 \exp(h\nu/k_B T) \text{ erg cm}^{-3} \text{ sec}^{-1} \text{ Hz}^{-1}$ (being h and k_B the Plank and Boltzmann's constant, respectively). For $T \approx 10^4 \text{ K}$ and a Gaunt factor $g \approx 6$, the density n_e of the ionized particles in the ring is $n_e \approx 25 \text{ cm}^{-3}$. The ionization fraction at 10^4 K is $x \approx 0.02$ (Lotz 1967), resulting in a total particle density $n_t \approx 1300 \text{ cm}^{-3}$. The minimum pressure inside the lobe predicted by the model is $\approx 5 \times 10^{-11} \text{ erg cm}^{-3}$. If this pressure is solely due to a magnetized relativistic pair plasma in equipartition, then the strength of the magnetic field is about $40 \mu\text{G}$.

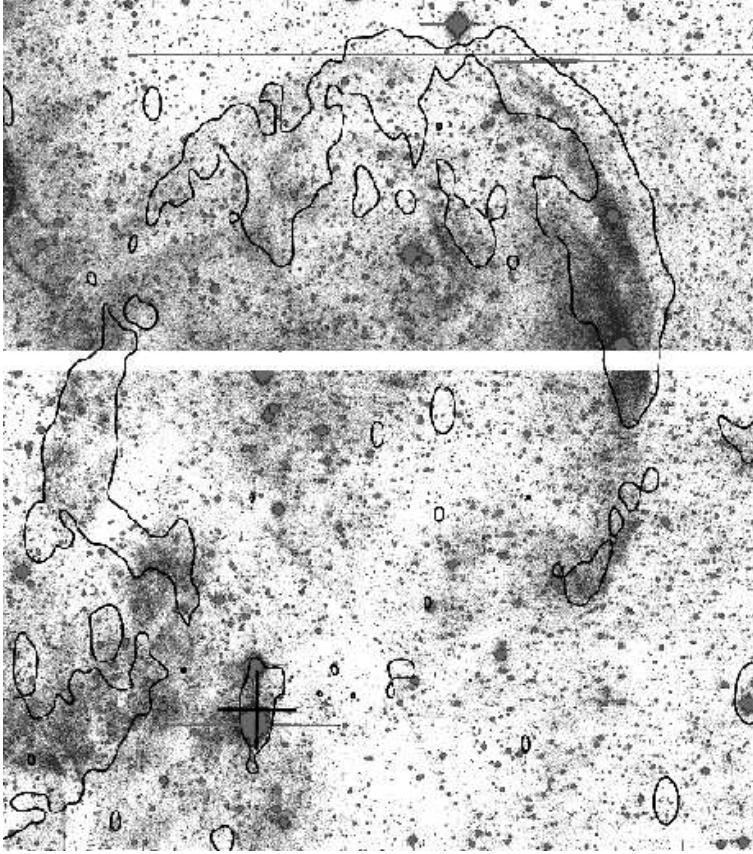


Figure 8.3: Optical counter-part of the radio ring of Cygnus X-1. The optical image, taken with the Isaac Newton Telescope Wide Field Camera using an $H\alpha$ filter, is shown with the 3σ radio contours over-plotted in black. As no calibration was taken during the observation, an absolute flux scale can not be set; however, given that the ring is clearly detected in a 1200 sec exposure, and taking into account the atmospheric and sky conditions during the observation, this translates into a minimum unabsorbed $H\alpha$ flux of $0.02 \text{ mJy arcsec}^{-2}$. The corresponding radio-optical spectral index a (defined such that $F_\nu \propto \nu^a$) is greater than 0.2. This implies an emission mechanism with flat spectrum, such as bremsstrahlung, plus excess flux possibly due to line emission, as expected in the case of radiative shock. For comparison, if the ring emitted optically thin synchrotron radiation with a spectral index $a = -0.7$, the expected flux at $H\alpha$ frequencies would be $1.2 \cdot 10^{-7} \text{ mJy arcsec}^{-2}$, by no means detectable by the INT WFC in 1200 sec.

sec^{-1} . The resulting jet lifetime is $t \simeq 0.02 - 0.32 \text{ Myr}$, to be compared with the estimated age of the progenitor of the black hole in Cygnus X-1, of a few Myr

(Mirabel & Rodrigues 2003).

Adopting a mass density of the un-shocked gas that is 4 times lower than the initial post-shock density, we infer a *time-averaged* energy rate between 8×10^{35} and 10^{37} erg sec⁻¹ by the jet. Based upon daily X-ray and radio monitoring of Cygnus X-1 over the last 10 years, we know that Cygnus X-1 is in a hard X-ray state (McClintock & Remillard 2005) – and hence powers a collimated jet (Fender 2005) – for about 90 per cent of its lifetime. Taking this duty cycle into account, the total power carried by the jet of Cygnus X-1 is: $9 \times 10^{35} \lesssim P_{\text{jet}} \lesssim 10^{37}$ erg sec⁻¹, up to two orders of magnitude higher than the existing estimate based on the flat radio spectrum (Fender et al. 2001). The fact that the jet of Cygnus X-1 switches off for short periods of times (typically for a few months over timescales of years) does not violate the model assumptions: the condition of constant power supply is met as long as the jet is intermittent over timescales that are short compared to its lifetime. The total power carried by the jet is a significant fraction $f \approx 0.03 - 0.5$ of the bolometric (0.1-200 keV) X-ray luminosity of Cygnus X-1 while in the hard state (Di Salvo et al. 2001); the total energy deposited by the jet into the surrounding ISM over its lifetime is $\approx 7 \times 10^{48}$ erg.

Assuming minimum energy conditions (Longair 1992), the expected lobe synchrotron surface brightness would be more than 150 times higher than the ring itself; the fact that we do not detect radio emission from the lobe means that either the system is far from equipartition, or the energy stored in the non-radiating particles (presumably baryons) is at least 20 times higher than the energy density shared by the electrons and the magnetic field. The particle density of the ISM through which the ring is expanding is constrained between a few and about 300 cm⁻³, at most three orders of magnitude higher than the average ISM density in the Galaxy. The lack of a ‘counter-ring’ can be explained in terms of a much lower particle density in the opposite direction to Cygnus X-1. Such large density inhomogeneities are not unusual for dense star forming regions, such as the Cygnus association, and would support the hypothesis that the ring is the result of the interaction between the radio lobe and the tail of the HII nebula. If so, the counter-jet of Cygnus X-1 is travelling undisturbed to much larger distances, gradually expanding and releasing its enormous kinetic energy. This could mean that the ring of Cygnus X-1 is a rather exceptional detection for this class of objects, made possible by its proximity to the HII nebula. Taking into account the contribution of the counter-jet as well, the total power dissipated by the jets of Cygnus X-1 in the form of kinetic energy can be as high as the bolometric X-ray luminosity of the system ($f \approx 0.06 - 1$).

The results presented here have important consequences for low-luminosity

stellar mass black holes as a whole: several works (Gallo, Fender & Pooley 2003; Livio, Pringle & King 2003; Malzac, Merloni & Fabian 2004) have suggested that hard state stellar black holes below a critical X-ray luminosity dissipate most of the liberated gravitational power in the form of radiatively inefficient outflows, rather than locally in the accretion flow. This is because in hard state black hole binaries the total jet power and the observed X-ray luminosity follow a non-linear relation (Fender, Gallo & Jonker 2003) of the form $P_{\text{jet}} \propto L_X^{0.5}$ (in Eddington units). Using the ring of Cygnus X-1 as an effective calorimeter for the jet power, we have constrained the normalization factor of the above equation, showing that $P_{\text{jet}} = fL_X$, with $f \simeq 0.06 - 1$, when $L_X \simeq 0.02$. Thus the critical X-ray luminosity below which $P_{\text{jet}} > L_X$ is *no lower* than a few 10^{-5} Eddington, and could even be as high as the peak luminosity of the hard X-ray state. This radically alters our concepts of the accretion process and of the feedback of accretion power into the surroundings. Via the new observations presented here we have strong evidence that the power output of low-luminosity – i.e. the overwhelming majority – stellar black holes is dominated by the kinetic energy of ‘dark’ outflows, whose key signature is the eventual energisation of the ambient medium.

Acknowledgements

We are grateful to Dimitris Mislis and Romano Corradi for the H α observation presented in this work. The Westerbork Synthesis Radio Telescope is operated by the ASTRON (Netherlands Foundation for Research in Astronomy) with support from the Netherlands Foundation for Scientific Research (NWO).

References

- Blandford R. D., 2001, *Prog. Theor. Phys. Suppl.*, 143, 182
Bowyer S., Byram E. T., Chubb T. A. & Friedman H., 1965, *Science*, 147, 394
Burbidge G. R., 1959, *ApJ*, 129, 849
Castor J., McCray R. & Weaver R., 1975, *ApJ*, 200, L107
Di Salvo T., Done C., Zycki P. T., Burderi L. & Robba N. R., 2001, *ApJ*, 547, 1024
Fender R. P., 2005, to appear in ‘*Compact Stellar X-Ray Sources*’, Eds. W. Lewin and M. van der Klis, Cambridge University Press
Fender R. P., Gallo E. & Jonker P. G., 2003, *MNRAS*, 343, L99
Fender R. P., Pooley G. G., Durouchoux P., Tilanus R. P. J. & Brocksopp C., 2000, *MNRAS*, 312, 853

- Frank J., King A. R. & Raine D. J., 2002, *'Accretion Power in Astrophysics'*, Cambridge University Press
- Gallo E., Fender R. P. & Pooley G. G., 2003, MNRAS, 344, 60
- Gies D. R. & Bolton C. T., 1986, ApJ, 304, 371
- Heinz S., Reynolds C. S. & Begelman M. C., 1998, ApJ, 501, 126
- Herrero A., Kudritzki R. P., Gabler R., Vilchez J. M., Gabler A., 1995, A&A, 297, 556
- Hughes P. A., 1991, *'Beams and Jets in Astrophysics'*, Cambridge Astrophysics Series
- Hunter D. A. & Massey P., 1990, Astron. J., 99, 846
- Kaiser C. R. & Alexander P., 1997, MNRAS, 286, 215
- Lestrade J.-F. *et al.*, 1999, A&A, 344, 1014
- Livio M., Pringle J. E. & King A. R., 2003, ApJ, 593, 184
- Longair M. S., 1992, *'High Energy Astrophysics'*, Cambridge University Press
- Lotz W., 1967, ApJSS, 14, 207
- Malzac J., Merloni A. & Fabian A. C., 2004, MNRAS, 351, 253
- Martí J., Rodríguez L. F., Mirabel I. F. & Paredes J. M., 1996, A&A, 306, 449
- McClintock J. E. & Remillard R. A., 2005, to appear in *'Compact Stellar X-Ray Sources'*, Eds. W. Lewin and M. van der Klis, Cambridge University Press
- Mirabel I. F. & Rodrigues I., 2003, Science, 300, 1119
- Mirabel I. F. & Rodríguez L. F., 1999, ARA&A, 37, 409
- Mirabel I. F. & Rodríguez L. F., 1994, Nature, 371, 46
- Stirling, A. M. *et al.*, 2001, MNRAS, 327, 1273
- Urry C. M. & Radovani P., 1995, PASP, 107, 803
- Sharpless S., 1959, ApJSS, 4, 257
- Smith D. A., Wilson A. S., Arnaud K. A., Terashima Y. & Young A. J., 2002, ApJ, 565, 195

CHAPTER 9

EPILOGUE

9.1 Relativistic jets from stellar black holes: summary

The work presented in this thesis deals with relativistic jets powered by stellar mass black holes in X-ray binary systems, with the primary aim of quantifying the jet importance for the overall energetics of the accretion process and as a source of energy input into the interstellar medium.

The key observational aspect of BHXB jets lies in their synchrotron radio emission. Such jets appear to come in two types: milliarcsec-scale continuous jets with flat radio-mm spectra, and arcsec-scale optically thin jets resolved into discrete plasmons moving away from the binary core with relativistic velocities. The former type – referred to as ‘steady’ – is persistently detected when the source X-ray spectrum is dominated by a hard power-law component and shows little or no evidence for a disc contribution (in the hard X-ray state). The latter type – referred to as ‘transient’ – is only observed after major X-ray outbursts.

In Chapter 2 we demonstrate the existence of a fundamental coupling between accretion and the production of steady jets in hard state BHXBs, in terms of a tight non-linear radio/X-ray correlation of the form $L_{\text{radio}} \propto L_{\text{X}}^{0.7 \pm 0.1}$. The correlation extends over more than three orders of magnitude in L_{X} and breaks down around a few per cent of the Eddington X-ray luminosity for a 10 solar mass black hole, above which the sources enter the ‘soft’ X-ray state, with some 90 per cent of the X-ray luminosity ascribed to a thin accretion disc. In this regime the radio emission drops below detectable levels, probably due to the physical disappearance of the jet. The observed spread to the best-fit relation can be interpreted in terms of a distribution in Doppler factors and hence used to constrain the bulk Lorentz factors Γ of the steady jet (assuming random inclinations). Employing Monte Carlo techniques, we have shown that in case of little or no X-ray beaming, the measured scatter in radio power implies $\Gamma \lesssim 1.7$ for the steady jets (for which no upper limits were available in the literature). When combined radio and X-ray beaming is considered, the range of possible jet bulk velocities significantly broadens, allowing highly relativistic outflows, but implying there-

fore severe X-ray selection effects. Probably the most notable implication of this non-linear relation is the predicted existence of ‘*jet-dominated states*’, i.e. accretion modes in which most of the liberated accretion power would be carried away by the radiatively inefficient outflow, rather than being dissipated locally by the inflow of matter.

In Chapter 3 we argue that the transition from an accretion- to a jet-dominated regime should occur at L_X/L_{Edd} no lower than a few 10^{-5} , thereby encompassing the whole ‘quiescent’ state – i.e. the overwhelming *majority* – of BHXBs. In addition, we show that if the same empirical radio/X-ray correlation holds for neutron star (NS) X-ray binaries too, in combination with the fact that BHXBs are more ‘radio-loud’ NS X-ray binaries, then quiescent NSs should be up to two orders of magnitude more luminous in X-rays than quiescent BHXBs (this is because they would enter the jet-dominated regime at two orders of magnitude lower accretion rates). Such L_X/L_{Edd} ratio is indeed observed; as a consequence, the relative dimness of quiescent BHXBs compared to NSs should no longer be interpreted as evidence for the existence of black hole event horizons.

Remarkably, the same radio/X-ray scaling found for BHXBs holds for supermassive black holes in active galactic nuclei (AGN) when a mass term is included in the analysis: Merloni, Heinz, Di Matteo (2003) and Falcke, Körding & Markoff (2004), have proved that accreting black holes (the binaries plus a sample of some 100 AGN) form a fundamental plane (FP) in the $\log(L_{\text{radio}}, L_X, M)$ domain (see Figure 9.1). In Chapter 4 we show that when the AGN FP is projected in terms of ‘mass-corrected’ L_{radio} vs. broadband L_X , a downturn in the radio is visible in the same Eddington range where the radio emission from BHXBs is suppressed, suggesting the presence of a critical regime for the jet formation, and also pointing towards a mass-independent description of the jet-accretion coupling.

The FP, for AGN, extends to Eddington ratios as low as $\sim 10^{-7}$, where the very existence of BHXBs jets remains to be proven, mainly because of sensitivity limitations on the existing radio telescopes. In Chapter 6 we argue that the broadband radio spectrum of a ‘quiescent’ stellar mass black hole closely resembles that of ‘canonical’ hard state sources emitting at $\sim 10^4$ times higher X-ray levels (and where the jets are actually resolved), suggesting that a steady jet is being formed down to at least a few $10^{-6}L_{\text{Edd}}$.

In Chapter 5 we provide definitive evidence for an association between the transient jets and X-ray outbursts associated with hard-to-soft X-ray state transitions in BHXBs. Tight radio monitoring of the prototypical system GX339-4 during its 2002 outburst led to the detection of a bright radio flare simultaneous

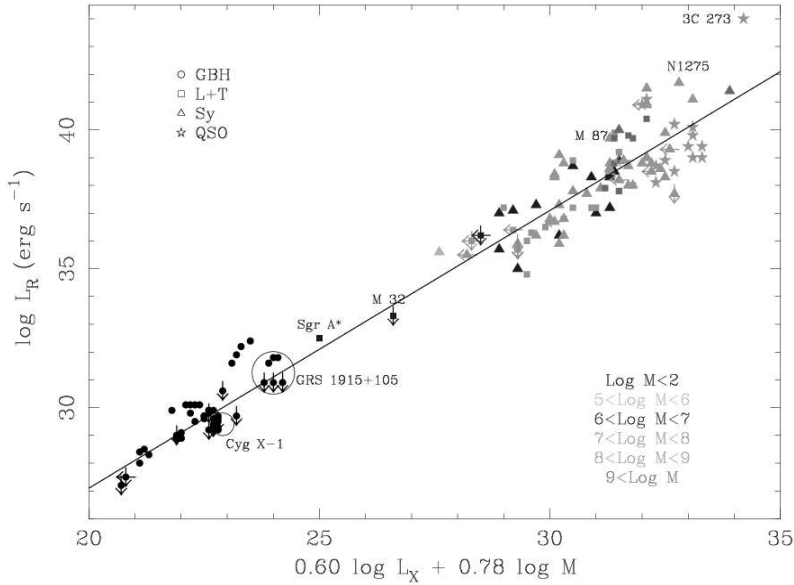


Figure 9.1: An edge-on view of the ‘Fundamental Plane of black hole activity’ (FP; from Merloni, Heinz & Di Matteo 2003; see also Falcke, Körding & Markoff 2004). The same correlation (within the errors) found to hold in BHXBs (Chapter 2) has been proven to apply in supermassive black holes when a mass term is included in the analysis.

with the X-ray peak, followed by the formation of a large-scale optically thin relativistic jet. From minimum energy arguments, we estimate that the power content in the transient jet was comparable to that inferred for the steady jet.

In Chapter 7 we address the issue whether the steady and transient jets of BHXBs have a different origin or are somewhat different manifestations of the same phenomenon, showing that: i) the power content of the steady and transient jets are consistent with a monotonically increasing function of L_X ; ii) the measured bulk Lorentz factors of the transient jets are systematically higher than those inferred for the steady jets. Based upon these arguments, the *first* unified model for the jet/accretion coupling in BHXBs has been put forward. The key idea is that, as the disc inner boundary moves closer to the hole (hard-to-soft state transition), the escape velocity from the inner regions increases. As a consequence, the steady jet bulk Lorentz factor rises sharply, causing the propagation of an internal shock through the slower-moving outflow in front of it.

Eventually, the result of this shock is what we observe as a post-outburst, optically thin radio plasmon. No emission from the steady jet is detected until the inner disc recedes once more, in which case a new cycle begins.

Finally, in Chapter 8 we report on the discovery of a jet-blown ring of radio and optical emission in the field of the 10 solar mass black hole in Cygnus X-1. The ring provides us with the unprecedented possibility to perform accurate calorimetry of a stellar black hole jet. Applying a fluid model developed for extragalactic jet sources, we estimate that in order to sustain the observed ring emission the jet of Cygnus X-1 has to carry a kinetic power that is a sizable fraction of the bolometric X-ray luminosity of the binary system while in a hard X-ray state. This finding has important consequences for low-luminosity stellar black holes as a whole. As discussed in Chapters 2 and 3, the jet power of hard state BHXBs scales with the X-ray luminosity in a non-linear fashion, implying the existence of a critical X-ray luminosity L_X below which the power output from accreting stellar black holes would be jet-dominated. By finding and measuring the ring of Cygnus X-1, we have established the normalization of such scaling, confirming that the power output from ‘quiescent’ black holes (if not the entire hard state) would be dominated by the kinetic power of radiatively inefficient jets, rather than by the X-ray emitting inflow.

9.2 Future prospects

A number of questions remains open; among others:

- How are jets formed? Specifically: are different jet production mechanisms at work in different types of sources? What is the role of the black hole spin?

There are reasons to believe that more than one MHD jet launching process may occur in galactic and extragalactic jet sources. Meier (2003) suggests that the Blandford-Payne (BP) mechanism may be responsible for mildly relativistic outflows, e.g. for steady jets in the hard state of BHXBs, whereas highly relativistic jets, likely powered by the Blandford-Znajek (BZ) mechanism, would only be produced at high accretion rate states, when rapid accretion can press the magnetic field onto the black hole, e.g. during the very high state or even the high/soft state. The fact that no core radio emission has ever been detected in the soft state of BHXBs does not automatically rule out the possibility of an intrinsically weaker, or an ultra-relativistic (and thus Doppler-dimmed) outflow. Deep radio observations of soft state BHXBs are needed in order to address this

issue observationally.

This also brings up the important point of the black hole spin. The efficiency of the Blandford-Znajek mechanism has been put into question by several authors (e.g. Livio, Ogilvie & Pringle 1999); the main argument is that the extraction of energy from the black hole through this process would be at most as efficient as the extraction of energy from the disc itself. This could be in favour of a ‘spine-sheath’ structure, i.e. a BZ-driven leptonic jet embedded in a hadronic BP-driven wind/jet. As a matter of fact though black holes with similar (inferred) mass and accretion rate can differ in radio power by large amounts. Jet production mechanisms that depend upon extraction of black hole rotational energy, therefore, provide a third parameter that lifts the mass/accretion rate degeneracy and potentially can explain why some sources are radio loud and some are radio quiet. From an observational point of view, comparing the radio emission of neutron star X-ray binaries – whose specific angular momenta are necessarily lower compared to the black holes’ – and BHXBs appears as a mandatory task (even though the neutron stars’ magnetic field could ‘poison’ the comparison).

- What is the causal connection between the presence/absence of jets and X-ray state transitions in BHXBs?

This is a ‘chicken and egg’ problem; as pointed out in Chapter 7, while jets are generally considered as ‘symptoms’ of the underlying accretion flow, it is possible that the reverse may be true; it may be the growth of the steady jet (via e.g. build up of magnetic field near the black hole) which results in the hardening of the X-ray spectrum, perhaps via pressure it exerts on the disc to push it back, or simply via Comptonization of the inner disc as it spreads. Sparse radio observations of outbursting BHXBs already indicate that in the phase prior to the outburst peak the jet radio spectral index seems to ‘oscillate’ in an odd fashion, as if the jet was experiencing some kind of instability as the X-ray spectrum softens. One possibility is that, as the disc moves in, the hot Comptonizing region responsible for producing the hard X-rays is evacuated and loaded in to the jet itself.

Livio, Pringle & King (2003) have recently proposed a model for the disc-jet connection, in which the inner part of the accretion disc switches between two states: in one state, the accretion energy is dissipated locally (some within the disc some within the corona) to produce the observed disc luminosity. In the second state, the accretion energy is deposited into the bulk flow of a relativistic jet. The transition between the two states is

associated with the onset of a global, poloidal magnetic field generated via a dynamo process (e.g. Tout & Pringle 1996).

Simultaneous radio/X-ray and possibly γ -ray observations of the phase immediately prior to the luminosity peak during a state transition will possibly establish a causal connection, if any, between the jet and the hard X-ray region.

- How ‘fundamental’ is the Fundamental Plane of black hole activity?

The FP of black hole activity (Merloni et al. 2003; Falcke et al. 2004) appears to tell us that accreting black holes are a three parameter family, defined by their mass, radio and X-ray luminosity, tracing respectively the hole size, the jet power output and the accretion flow power output. The plane unites accreting BHs over nine orders of magnitude in accretion rate and eight orders of magnitude in BH mass. Thus it can be used as a ‘mass-gauge’ to address the natural of the putative intermediate mass black holes by means of radio and X-ray observations.

Testing the plane beyond its current range is the next step to be taken: this can be done by probing the low luminosity, low-mass corner of the distribution, i.e. by simultaneous radio/X-ray observations of very dim nearby black holes. Failure to detect their radio (flying X-ray mission are typically two orders of magnitude more sensitive than the existing radio telescopes) counterparts at the predicted levels would indicate that the jet formation process at low accretion rates may not be scale invariant, in fact cutting off for some physical reason in relatively low mass black holes at very low accretion rates, with important consequences for the energisation of the interstellar medium from BHXB jets (see Fender et al. 2005).

- Is there a relation between the different states of BHXBs and the different observational appearance of supermassive black holes in AGN?

Theoretically, there should be fundamental similarities between the behaviour of accretion flows on to black holes. Typically, BHXB state transitions occur on timescales of a few days: this translates into timescales of a few $100 - 10^5$ years when scaled to supermassive black holes. The one (known) exception is the stellar black hole in GRS 1915+105, where state transitions occur on timescales of seconds (Belloni et al. 2000), implying 10-1000 days in an active nucleus. Indeed Marscher et al. (2002) have presented evidence for an association between spectrally hard dips in the X-ray light curve and subsequent superluminal ejection events in the AGN 3C120, just as observed in GRS 1915+105 (Klein-Wolt et al.

2002). Thus it should be really possible to build up a comprehensive, mass-independent description of the jet/accretion coupling in accreting black holes on all mass scales, testing whether the different accretion regimes/radio behaviour of stellar mass objects may correspond to different morphologies in AGN, as if supermassive black holes were ‘snapshots’ of stellar black holes, frozen in a given accretion mode for millions of years. This requires careful estimates of the duty cycles of Galactic BHXBs, combined with with high resolution X-ray spectra in different accretion regimes. The comparison shall be extended to X-ray binary systems in external galaxies.

It is obviously easier to raise such issues than to tackle them.

References

- Belloni T. M. et al. , 2000, *A&A*, 355, 271
Falcke H., K rding E. & Markoff S., 2004, *A&A*, 414, 895
Fender R. P., Maccarone T. J. & van Kesteren Z., 2005, *MNRAS*, 360, 1077
Klein-Wolt M. et al., 2002, *MNRAS*, 331, 745
Livio M., Pringle J. E. & King A. R., 2003, *ApJ*, 593, 184
Livio M., Ogilvie G. I. & Pringle J. E., 1999, *ApJ*, 512, 100
Marscher A. P. et al. , 2002, *Nature*, 417, 625
Meier D. L., 2003, *New Astronomy Reviews*, 47, 667
Merloni A., Heinz S. & di Matteo T., 2003, *MNRAS* 345, 1057
Tout C. A. & Pringle J. E., 1996, *MNRAS*, 281, 219



SAMENVATTING IN HET NEDERLANDS

Zwarte gaten en relativistische jets

De ontsnappingsnelheid van een hemellichaam is in wezen een maatstaf voor hoe snel een raket moet worden afgevuurd om aan de zwaartekracht te ontsnappen. Zo is de ontsnappingsnelheid vanaf aarde ongeveer tien kilometer per seconde. Nergens is de zwaartekracht sterker dan bij objecten die we 'zwarte gaten' noemen. Materie dat richting een zwart gat valt kan extreem heet worden en oplichten, dit maakt het voor ons mogelijk de aanwezigheid hiervan op te maken. Nog verrassender is dat deel van de invallende materie naar buiten gedreven kan worden in de vorm van zeer smalle dubbelpolige stromen. Omdat de ontsnappingsnelheid vlakbij een zwart gat dicht bij dat van licht ligt, moeten deze uitvloeiende stromen ongelooflijk snel zijn, wel twee honderd duizend kilometer per seconde, of nog sneller. Deze verschijnselen, 'relativistische jets' genoemd, zijn een van meest spectaculaire objecten van het heelal. Ondanks tientallen jaren van onderzoek moeten deze mechanismen van 'jet productie' nog verder onderzocht worden ten einde ze beter te kunnen begrijpen.

Dit proefschrift gaat over relativistische jets, opgewekt bij zwarte gaten in onze eigen melkweg. 'Stellaire zwarte gaten' – met massa's in de orde van een zonsmassa – worden gevormd zodra een zware ster, zo'n tien maal zwaarder dan onze zon, sterft. Als ze haar brandstof heeft uitgeput kan de kern van een zware ster de zwaartekracht niet langer weerstaan. Ze stort in en vormt een zwart gat. Omdat de meeste sterren in ons melkwegstelsel dubbelsterren zijn, blijft dit zwarte gat over met een begeleidende ster en begint hier massa van op te slokken. Dit verschijnsel heet 'accretie'. Tegelijkertijd lukt het een deel van de invallende materie te ontsnappen in de vorm van een relativistische jet.

Hoe kunnen we deze objecten bestuderen, die zich op honderden lichtjaren afstand bevinden? Dit doen we met behulp van telescopen, zowel op aarde als in de ruimte. We nemen de invallende materie waar in de vorm van röntgenstraling, en de relativistische jet in de de vorm van radiostraling. Omdat röntgenstraling niet door de atmosfeer heen komt hebben we satellieten in de ruimte nodig om de röntgenstraling te kunnen detecteren. Radiostraling kan zonder problemen de atmosfeer door. We kunnen daarom radiotelescopen op aarde gebruiken om de radiostraling waar te nemen. Op dit moment zijn er ongeveer twintig stellaire zwarte gaten die mogelijk radio-jets produceren, maar we denken dat er wel 300000 van deze objecten moeten bestaan.

In mijn onderzoek kijk ik naar hoe deze jets gerelateerd zijn aan het materiaal

dat stellaire zwarte gaten invalt. Ik doe dit door naar de energiehuishouding te kijken, in relatie tot de hoeveelheid uitgestraalde röntgenstraling. Mijn onderzoek richt zich ook op het effect dat deze jets hebben op het omringende interstellaire gas. In het bijzonder geeft dit proefschrift het observationele bewijs dat de radiostraling van de jets slechts een klein deel van totale energieproductie is; het is als de rook die afkomt van een veel grotere machine.

Dit proefschrift

In Hoofdstuk 2 wordt de kwalitatieve verhouding beschreven tussen de jet en de accretie-energie in stellaire zwarte gaten. De relatie tussen deze twee grootheden impliceert dat als de röntgenlichtkracht (d.w.z. de lichtkracht veroorzaakt door de influx van gas) van een stellair zwart gat afneemt, de relatieve hoeveelheid energie die in de jet terechtkomt, toeneemt. In andere woorden, er bestaat een kritieke röntgenlichtkracht, beneden welke stellaire zwarte gaten het overgrote deel van hun lichtkracht uitstralen in de vorm van ‘donkere’ jets.

Hoofdstuk 3 beschrijft deze ‘jet-gedomineerde’ toestand. In dit hoofdstuk worden dubbelsterren beschreven, waarvan het centrale object een neutronenster is, in plaats van een zwart gat. Als dezelfde relatie tussen jet en accretie-energie bestaat voor neutronensterren, dan kan dit een verklaring zijn voor het waargenomen verschil in röntgenlichtkracht voor ‘stille’ (d.w.z. met een lage lichtkracht) zwarte gaten en neutronensterren. ‘Stille’ neutronensterren zijn over het algemeen 100 keer helderder in het röntgen dan ‘stille’ zwarte gaten. Dit kan worden verklaard doordat neutronensterren een ‘jet-gedomineerde’ toestand hebben voor veel lagere accretie-snelheden dan zwarte gaten dat hebben.

In Hoofdstuk 4 gaan we verder in op super-zware zwarte gaten in het centrum van andere melkwegstelsels; een mogelijke overeenkomst wordt duidelijk in het röntgen- en het radiogedrag tussen de stellaire zwarte gaten en de super-zware zwarte gaten – met massa’s zwaarder dan een miljoen keer de massa van de zon. In het bijzonder wordt er een kritisch röntgenhelderheidsinterval gevonden waarbinnen het jet- mechanisme wordt geactiveerd. Dit suggereert een massa-onafhankelijke beschrijving van de jet-accretie koppeling.

Hoofdstuk 5 beschrijft de formatie en evolutie van radio-jets bij uitbarstingen in de röntgenhelderheid van prototypische stellaire zwarte gaten. Dit werk bevestigt eerdere suggesties dat het ontstaan van dergelijke ‘transient’ (veranderlijke) radio-jets gedreven wordt door plotselinge veranderingen in de röntgenhelderheid.

In Hoofdstuk 6 bestuderen we de radio-emissie die afkomstig is van de stellaire zwarte gaten met lage röntgenhelderheid, tijdens de ‘stille state’, en we

suggereren dat een stabiele jet nog steeds gevormd kan worden in deze toestand.

Deze resultaten hebben bijgedragen aan de formatie van het eerste jetmodel voor stellaire zwarte gaten, dat wordt gepresenteerd in Hoofdstuk 7. Het idee achter dit model is dat de twee belangrijkste vormen van radio-jets bij stellaire zwarte gaten, de kleine schaal-stabiele jets en de grote schaal-‘transient’ jets, twee verschillende manifestaties zijn van hetzelfde fenomeen. Daarbij worden de waargenomen verschillen tussen de twee vormen toegeschreven aan een plotselinge verandering van de snelheid van het geejecteerde materiaal dat in de jet beweegt.

Hoofdstuk 8 is geheel gewijd aan de ontdekking van een bijzondere ring-vormige emissie met een diameter van 15 lichtjaar rond het prototypische zwarte gat Cygnus X-1, dat lijkt te worden gevoed door de radio-jets van dit systeem. Er wordt aangetoond dat om een dergelijke ring-vormige emissie in stand te houden, de radio-jets een vermogen moeten produceren (waarvan dan maar een klein deel als radiostraling wordt uitgezonden) die in dezelfde orde van grootte is als het vermogen dat wordt opgewekt in het röntgen. Deze ontdekking stelt ons in staat een bovengrens te stellen aan de hoeveelheid waargenomen röntgenstraling waarbinnen de jet het totale vermogen van lichte zwarte gaten domineert, en het suggereert dat een grote meerderheid van dergelijke systemen het meeste vermogen vrijgeven in de vorm van ‘donkere’ jets.



RIASSUNTO IN ITALIANO

Buchi neri e getti relativistici

La gravità di un corpo celeste è essenzialmente una misura della velocità con cui un razzo deve essere lanciato per vincere l'attrazione di quel corpo. Ad esempio, la velocità di fuga della terra è di circa dieci chilometri al secondo. Non c'è oggetto la cui forza di gravità superi quella di un 'buco nero'. Una volta superata una distanza critica dal buco nero (distanza che dipende dalla massa del buco nero stesso) nulla può vincere la sua attrazione gravitazionale, neppure la luce. Tuttavia la materia in caduta verso un buco nero, prima di venire risucchiata, diventa estremamente calda e luminosa, permettendoci di osservare indirettamente e quindi di dedurre, la presenza di un buco nero. In aggiunta, una piccola parte della materia in caduta viene espulsa sotto forma di getti altamente collimati. Poiché la velocità di fuga in prossimità di un buco nero è prossima a quella della luce, i getti devono essere incredibilmente veloci, centinaia di migliaia di chilometri al secondo. Questi 'getti relativistici' sono fra i fenomeni più spettacolari dell'Universo. Eppure, malgrado decenni di studi, i meccanismi di produzione ed accelerazione dei getti non sono ancora pienamente compresi.

Questa tesi tratta di getti relativistici prodotti da buchi neri di massa stellare nella Via Lattea, la nostra galassia; oggetti che si formano quando una stella massiva, qualche decina di volte più massiva del nostro sole, muore. Dopo aver esaurito gli elementi per sostenere reazioni nucleari al suo interno, il cuore di una stella massiva non può più contro-bilanciare la propria gravità e crolla in un buco nero. Poiché la maggioranza delle stelle nella galassia fanno parte di sistemi binari, il buco nero comincia a risucchiare materia dalla sua stella compagna: un fenomeno noto col termine di 'accrescimento'. Allo stesso tempo, parte della materia in accrescimento viene incanalata in getti collimati ed accelerata a velocità relativistiche, tali da sfuggire alla gravità del buco nero.

Come possiamo studiare oggetti del genere, a centinaia di anni luce da noi? Osserviamo la materia calda che accresce tramite la radiazione X che emette ed i getti relativistici in forma di onde radio. La radiazione X è bloccata dall'atmosfera terrestre, per cui sono necessari telescopi X in orbita intorno alla terra per dettarla. Le onde radio al contrario passano attraverso l'atmosfera indisturbate, e vengono dettate da telescopi radio terrestri.

A tutt'oggi conosciamo circa venti sistemi galattici contenenti un buco nero di massa stellare in accrescimento, ma molti altri sono in attesa di conferma e si pensa che ce ne possano essere decine di migliaia. Lo scopo di questa ricerca è

quello di quantificare il ruolo dei getti relativistici da buchi neri di massa stellare, ed in particolare di quantificarne la potenza rispetto a quella liberata sotto forma di radiazione X dalla materia in accrescimento. Specificamente, questa tesi dimostra che il segnale radio è solo una piccolissima frazione della potenza totale incanalata nei getti relativistici. Nonostante i getti siano poco efficienti nel convertire la propria energia in onde radio, essi trasportano un contenuto di potenza pari a quello liberato dalla materia in accrescimento, contrariamente a quanto generalmente assunto.

Contenuto della tesi

Il Capitolo 2 presenta e discute una correlazione quantitativa tra la potenza dei getti (i.e. la luminosità radio) e quella della materia in accrescimento (i.e. la luminosità X) in buchi neri di massa stellare. La forma della correlazione implica che, al decrescere della luminosità X, la frazione relativa di potenza che viene incanalata nel getto aumenta. In altre parole esiste una luminosità X critica al di sotto della quale i buchi neri di massa stellare emettono la maggior parte della propria potenza in forma di getti relativistici.

Il Capitolo 3 discute le conseguenze di questi ‘jet-dominated states’ (stati dominati del getto), estendendo lo studio a sistemi binari in cui l’oggetto ad alta gravità è una stella di neutroni invece di un buco nero. In particolare, se la stessa relazione radio-X è valida per sistemi contenenti stelle di neutroni, questo potrebbe spiegare perché tali sistemi siano sistematicamente più luminosi in X dei buchi neri.

Nel Capitolo 4 lo studio è esteso a buchi neri super-massivi (con masse di milioni di masse solari) al centro di altre galassie: sembra esistere un particolare valore della luminosità X intorno al quale il meccanismo di produzione del getto è inibito sia in buchi neri stellari che super-massivi. Questo risultato suggerisce la possibilità di descrivere i fenomeni che avvengono intorno ad un buco nero in modo indipendente dalla massa del buco nero stesso.

Il Capitolo 5 descrive l’evoluzione di un getto osservato intorno ad un buco nero galattico a seguito di un ‘burst’ (esplosione) di luminosità X e conferma l’associazione di getti transienti (che appaiono e scompaiono su tempi scala dell’anno) e variazioni sostanziali della luminosità X.

Il Capitolo 6 discute la natura e l’origine dell’emissione di onde radio da buchi neri galattici ‘quiescenti’, ovvero di bassissima luminosità X, suggerendo che un getto stazionario è ancora presente anche in questo regime.

Questi risultati hanno contribuito alla formulazione del primo modello unificato per getti di buchi neri galattici di massa stellare, presentato nel Capitolo 7.

L'idea chiave è che i due diversi tipi di getti in questi sistemi – getti stazionari e getti transienti – siano di fatto diverse manifestazioni dello stesso fenomeno e che la diversa morfologia sia causata da un repentino cambiamento di velocità nel getto.

Il Capitolo 8 riguarda la scoperta di uno stupefacente ‘anello’ di emissione – con un diametro di 15 anni luce – intorno ad un buco nero galattico nella costellazione del Cigno. L’anello sembra essere dovuto alla pressione esercitata dal getto relativistico del buco nero sul gas interstellare, e di conseguenza rappresenta un calorimetro ideale per misurare la potenza del getto stesso. Questa scoperta suggerisce che la maggioranza dei buchi neri di massa stellare nella nostra galassia stiano incanalando la maggior parte della loro energia in getti relativistici, la cui emissione di onde radio non rappresenta che una piccolissima frazione della potenza totale.



PUBLICATION LIST

Refereed journal papers

- Gallo, E.; Fender, R. P.; Kaiser, C.; Russell, D.; Morganti, R.; Oosterloo, T.; Heinz, S., 2005, *Nature*, Volume 436, pp. 819-821
'A dark jet dominates the power output of the stellar black hole Cygnus X-1'
- Gallo, E.; Fender, R. P.; Hynes, R. I., 2004, *Monthly Notices of the Royal Astronomical Society*, Volume 356, Issue 3, pp. 1017-1021
'The radio spectrum of a quiescent stellar mass black hole'
- Fender, R. P.; Belloni, T.; Gallo, E., 2004, *Monthly Notices of the Royal Astronomical Society*, Volume 355, Issue 4, pp. 1105-1118
'Towards a unified model for black hole X-ray binary jets'
- Tigelaar, S. P.; Fender, R. P.; Tilanus R. P.; Gallo, E.; Pooley G. G., 2004, *Monthly Notices of the Royal Astronomical Society*, Volume 352, Issue 3, pp. 1015-1018
'Quenched millimetre emission from Cygnus X-1 in a soft X-ray state'
- Jonker, P. G.; Gallo, E.; Dhawan, V.; Rupen, M.; Fender, R. P.; Dubus, G., 2004, *Monthly Notices of the Royal Astronomical Society*, Volume 351, Issue 4, pp. 1359-1364
'Radio and X-ray observations during the outburst decay of the black hole candidate XTE J1908+094'
- Hynes, R. I.; Charles, P. A.; Garcia, M. R.; Robinson, E. L.; Casares, J.; Haswell, C. A.; Kong, A. K. H.; Rupen, M.; Fender, R. P.; Wagner, R. M.; Gallo, E.; Eves, B. A. C.; Shahbaz, T.; Zurita, C., 2004, *The Astrophysical Journal*, Volume 611, Issue 2, pp. L125-L128
'Correlated X-ray and optical variability in V404 Cygni in quiescence'
- Gallo, E.; Corbel, S.; Fender, R. P.; Maccarone, T. J.; Tzioumis, A. K., 2004, *Monthly Notices of the Royal Astronomical Society*, Volume 347, Issue 3, pp. L52-L56
'A transient large scale relativistic jet from GX 339-4'
- Maccarone, T. J.; Gallo, E.; Fender, R. P., 2003, *Monthly Notices of the Royal Astronomical Society*, Volume 345, Issue , pp. L19-L24

'The connection between radio quiet AGN and the high/soft state of X-ray binaries'

- Gallo, E.; Fender, R. P.; Pooley, G. G., 2003, Monthly Notices of the Royal Astronomical Society, Volume 344, Issue 1, pp. 60-72
'A universal radio-X-ray correlation in low/hard state black hole binaries'
- Fender, R. P.; Gallo, E.; Jonker, P. G., 2003, Monthly Notices of the Royal Astronomical Society, Volume 343, Issue 4, pp. L99-L103
'Jet-dominated states: an alternative to advection across black hole event horizons in quiescent X-ray binaries'
- Gallo, E.; Fender, R. P., 2003, Monthly Notices of the Royal Astronomical Society, Volume 337, Issue 3, pp. 869-874
'Chandra imaging spectroscopy of 1E 1740.7-2942'
- Petrucci, P. O.; Merloni, A.; Fabian, A.; Haardt, F.; Gallo, E., 2001, Monthly Notices of the Royal Astronomical Society, Volume 328, Issue 2, pp. 501-510
'The effects of a Comptonizing corona on the appearance of the reflection components in accreting black hole spectra'

Proceedings

- Gallo, E.; Fender, R. P., 2005, Proceedings of the 'Stellar end products' workshop (Granada, April 2005), edited by M.A. Perez-Torres. To appear in Vol. 77 of MmSAI.
'Accretion modes and jet production in black hole X-ray binaries'
- Fender, R. P.; Belloni, T. M.; Gallo, E., 2005, Proceedings of 'From X-ray Binaries to Quasars: Black Hole Accretion on All Mass Scales' (Amsterdam, July 2004), edited by T. J. Maccarone, R. P. Fender & L. C. Ho (Kluwer)
'A unified model for black hole X-ray binary jets?'
- Gallo, E.; Fender, R. P.; Kaiser, C., 2005, Proceedings of 'Interacting Binaries: Accretion, Evolution and Outcomes' (Cefalu', July 2004), edited by A. Antonelli et al.
'Black hole X-ray binary jets'
- Fender, R. P.; Gallo, E.; Jonker P. G., 2004, Proceedings of the II BeppoSAX meeting 'The Restless High-Energy Universe' (Amsterdam, May

2003), edited by E. van den Heuvel, R. Wijers and J. in 't Zand
'Jet dominated states in X-ray binaries'

- Gallo, E.; Fender, R. P.; Maccarone, T. J., Jonker, P. J., Proceedings of 'Stellar-mass, Intermediate-mass and Supermassive black Holes' (Kyoto, October 2003), edited by K. Makishima and S. Mineshige
'Towards a unified description of the jet-accretion coupling in stellar and super-massive black holes'
- Gallo, E.; Fender, R. P.; Pooley, G. G., 2004, Proceedings of the II Bep-poSAX meeting 'The Restless High-Energy Universe' (Amsterdam, May 2003), edited by E. van den Heuvel, R. Wijers and J. in 't Zand
'Jet-accretion coupling in low/hard state Galactic black hole candidates'
- Gallo, E.; Fender, R. P.; Pooley, G. G., 2003, Proceedings of 'The Fourth Microquasar Workshop' (Cargese, May 2002), edited by P. Durouchoux, Y. Fuchs and J. Rodriguez
'On the correlation between radio and X-ray flux in low/hard state black hole candidates'
- Petrucci, P. O.; Merloni, A.; Fabian, A.; Haardt, F.; Gallo, E. Malzac, J., 2001, Proceedings of 'Gamma 2001: Gamma-Ray Astrophysics' (Baltimore, April 2001), edited by S. Ritz, N. Gehrels, and C. R. Shrader.
'The effects of a Comptonizing corona on the appearance of the reflection components in accreting black hole spectra'

Other publications

- Migliari, S.; Sault, R.; Gallo, E.; Fender, R.; Wijnands, R.; van der Klis, M., 2005, Astronomer Telegram 513
'Radio upper limits for SAX J1808.4-3658'
- Gallo E., Fender R. P., Hynes R., ASTRON Newsletters 2004
'The radio spectrum of a quiescent stellar mass black hole'
- Buxton, M.; Gallo, E.; Fender, R. P.; Bailyn, C., 2004, Astronomer Telegram 230
'Increased radio and optical activity in GX 339-4'
- Gallo, E.; Fender, R. P.; Corbel S., 2003, Astronomer Telegram 196
'GX 339-4 in a very low luminosity state'

-
- Fender, R. P.; Corbel, S.; Tzioumis, A. K.; Tingay, S.; Brocksopp, C.; Gallo, E., 2002, Astronomer Telegram 107
'The recent evolution of radio emission from GX 339-4'

ACKNOWLEDGMENTS

Coming to Amsterdam to do a Ph.D. represented a real adventure for me, and a big challenge at the same time. If today I feel at home here, it is thanks to many special people I have met on the journey.

The first to be mentioned is Rob Fender, my supervisor. I owe him much for his guidance and for the energy and enthusiasm he put into this project. He taught me the way to approach astronomical problems, and the way to communicate our findings. Above all, I have appreciated his honesty and unbiased view towards others' opinions, in science as in any other matter.

Being part of the X-ray group at the 'Anton Pannekoek' Institute, I benefited from interactions with many brilliant minds working in this field, such as my promoter Michiel van der Klis, Ed van den Heuvel, Mariano Méndez and Ralph Wijers. I have learned a lot from them, and for this opportunity I'm very grateful.

It is a pleasure to thank Francesco Haardt and Monica Colpi, whose example inspired me to commence a Ph.D.; Raffaella Morganti and Tom Oosterloo for their extensive help with WSRT data reduction and for the warm hospitality at ASTRON; Christian Kaiser and Annalisa Celotti, for patiently initiating me to the theoretical aspects of jet physics. I'm indebted to all those who deserve co-authorship on this thesis, for their valuable teachings and constructive criticisms.

I also wish to express my gratitude to the members of the reading committee for investing considerable time and effort to provide detailed comments, as well as to Marc, Thijs and Minou for translating the summary into Dutch, and to Gabriele for inspiring suggestions about the cover illustration.

Thanks to Jane, Fieke, Minou, Annemiek and Lide for their kind assistance with administrative issues and travel organization over these four years. The Leids Kerkhoven-Bosscha Fonds is acknowledged for financial support.

There are indeed lots of things brushed under the carpet of this thesis. There's chatting with Martin, which I liked so much because of that rare talent of his for giving the right weight to things, and for making me see them from a different perspective. Oops, that wasn't quite low-profile..

Marc, whom I wish to say thanks to once more, for always being helpful and generous and for his contagious good humor. I can not forget how kind Margriet and he were to me since my very first day in Amsterdam, when I could barely speak English, and I sincerely hope that we'll be keeping in touch, even on the other side of the Ocean.

Sora Nanda, who trained her dog to kill me, burst my eardrums, stole my

kitchenware and even made me speak *romanesco* (te possino..). And who helped me when I was really down, once upon a time.

The coffee/gossip-breaks with Diego, and watching Diego courting new girls: sei bellissimo! Manu and Stefano, looking dreamy while there are playing music; Peter, waving his hands in flawless Italian style. Arjen, undoubtedly my favourite Dutch singer; the laughs with Andrea and Steve; Luciano's barbecues and his exhilarating anecdotes; Gabriele, churning out amazing ideas as how to become a billionaire – and frankly I think he'll make it.

Carsten: I very much enjoyed being his office mate for four years. I guess that, contrary to common expectations, we have proven to be a quite successful Italo-German alliance (I thought you would appreciate this kind of humor).

And yet again there are Rohied, Alex, Tom, Alexander, Arjan, Annique, Thijs, Alessandro, along with all the students and staff at the Institute, whom I wish to say thanks to for making it such a unique place to work. I have got very happy memories of the time I spent with them: the long evenings at the East, the outings, the Sinterklaas parties.

A special thought goes to Jasinta: I know few people as gentle and brave as her; our continued friendship and correspondence is very precious to me.

I will miss each one of them. And with them I'll miss Amsterdam, as still I find myself stopped cycling in the middle of a bridge, watching its colours, the houses and lights reflected in the water.

Then there are the old, everlasting friends: Valentina, Nene, Claudia, Paola, Miriam, Miriam Z and Gianluca: every time I'm back in Novara it's as if nothing has changed, and that makes me feel good, and cherished.

Finally those who have mattered most over these four years: Simone, and Anna, and Tizi; to them, just a simple, heartfelt thank-you, for it is especially difficult to talk and to write about loved ones.

The last words are for my mother: without her support, and unspoken sacrifices, all this wouldn't have been possible.

Elena Gallo
Amsterdam, 5 August 2005